

**Bioaccumulation, biological effects and trophic transfer of
metal (oxide) nanoparticles in marine invertebrates**

Submitted by **Antony James Baker** to the University of Exeter
as a thesis for the degree of
Doctor of Philosophy in Biological Sciences
in May 2017

This thesis is available for Library use on the understanding that it is copyright material and that no quotation from the thesis may be published without proper acknowledgement.

I certify that all material in this thesis which is not my own work has been identified and that no material has previously been submitted and approved for the award of a degree by this or any other University.

Signature:

Abstract

The production and use of manufactured metal (oxide) nanoparticles has exploded in recent years as they are exploited for their novel physical and chemical properties. Cerium oxide NPs (CeO₂NPs) help increase combustion in diesel engines and their reported ability to scavenge free radicals has been exploited in therapeutic treatments. Silver NPs (AgNPs) are now used in consumer products such as socks and sticking plasters due to their antibacterial properties. Once released into the environment, their ultimate fate is predicted to be the oceans

The aims of this thesis are to investigate the bioaccumulation and biological effects (oxidative stress and lipid peroxidation) of CeO₂NPs and AgNPs on the mussel *Mytilus edulis*, and to understand the potential for trophic transfer of CeO₂NPs to the crab *Carcinus maenas*, and subsequent induced biological effects.

It was found in acute exposures that, at the suggested regulatory limit of 3mg/l, less than 5% of a CeO₂NP dose will be accumulated by the digestive gland of *M. edulis* within 4 hours, before being depurated over at least 56 hours. There were no significant biological effects of CeO₂NPs, yet larger, micron-size particles had significant anti-oxidant effects. Most effects were transitory, returning to normal levels after 24 hours.

In uptake comparisons between AgNPs and Ag-nanorods (AgNRs) at 10µg/l (towards the regulatory limit of 1.9µg/l), AgNRs were accumulated in the digestive gland within 2 hours, but were depurated by 4 hours. Similarity in accumulation between AgNPs and ionic Ag – including continuous accumulation in the gills over 48 hours – suggested dissolution was mostly responsible for this. Both nanoforms instigated isolated oxidative stress responses over 4-24 hours, yet none were significantly worse than AgNO₃, which instigated the greatest suite of significant oxidative stress responses.

In trophic transfer experiments *C. maenas* accumulated CeO₂NPs in the hepatopancreas at less than 1% of the fed dose. Stomach accumulation was high but transitory, with most particles removed in the faeces. Gills were also a

site of accumulation and it was thought that the haemolymph provided a route of transit between the digestive organs and the respiratory organs. This novel experiment used NPs crafted from ^{140}Ce ; changes in isotopic ratios of Ce in the crab following trophic transfer could therefore be used to determine absolute increases in concentration against high, and highly variable, background concentrations. There were no significant biological effects following trophic transfer of these $^{140}\text{CeO}_2\text{NPs}$.

It was found that the current regulatory limits are predicted to be sufficient to protect *M. edulis* and *C. maenas* from acute exposure to CeO_2NPs and AgNPs , yet chronic exposures should be investigated since the relationship between the uptake and elimination rate of NPs will determine the extent of bioaccumulation and biological effects.

CONTENTS

Abstract	3
Commonly Used Acronyms	8
List of Tables and Figures	9
Author's Declaration	19
Chapter 1: General Introduction	21
1.1 Introduction.....	23
1.2 Some Relevant Characteristics of Me(O)NPs	27
1.2.1 Size and Shape.....	28
1.2.2. Aggregation, Dissolution or Both?	30
1.2.3 Quantifying Anthropogenic Release	36
1.2.4 Propensity to Cause Biological Effects	39
1.3 Specific Effects of Me(O)NPs on Marine Invertebrates and Bacteria	41
1.3.1 Annelida	42
1.3.2 Arthropoda	43
1.3.3 Bacteria	45
1.3.4 Echinodermata	47
1.3.5 Mollusca	47
1.4 Trophic Transfer	56
1.5 Conclusion	58
1.6 Aims and Objectives	62
Chapter 2: Materials and Methods	58
2.1 Choice of Me(O)NPs and Me(O)NP Properties	67
2.1.1 JRC Cerium Oxide NPs	67
2.1.2 Isotopically-Enriched ¹⁴⁰ Cerium Oxide NPs	71
2.1.3 JRC Silver NPs	73
2.1.4 Silver Dissolution	78
2.2 Sample Processing for Metal Analysis and Assessing Biological Effects	80
2.2.1 Dissection of <i>M. edulis</i> and <i>C. maenas</i>	80
2.2.2 Acid Digestion for Metal Analysis.....	80
2.2.3 Assays for Biological Effects (Lipid Peroxidation and Oxidative Stress)	81
2.2.4 Data Analysis	85
2.3 The Blue Mussel <i>Mytilus edulis</i>	86
2.3.1. Pertinent Physiology	86

2.3.2 Method Development: Exposure of <i>M. edulis</i> to Me(O)NPs	89
2.3.3 Final Apparatus for Exposure of Me(O)NPs to <i>M. edulis</i>	101
2.4 The Shore Crab <i>Carcinus maenas</i>	104
2.4.1 Pertinent Physiology	104
2.4.2 Method Development for Feeding Exposed <i>M. edulis</i> to <i>C. Maenas</i>	106
Chapter 3: Bioaccumulation and biological effects of CeO ₂ NPs in <i>M. edulis</i>	58
3.1 Abstract	113
3.2 General Introduction.....	115
3.3 Time Series Uptake of 10nm CeO ₂ NPs by <i>M. edulis</i>	118
3.3.1 Introduction.....	118
3.3.2 Method.....	119
3.3.3 Results & Discussion.....	120
3.4 CeO ₂ NP Uptake as a Factor of Size and Concentration.....	125
3.4.1 Introduction.....	125
3.4.2 Method.....	127
3.4.3 Results & Discussion.....	127
3.5 Examining Biological Effects – Oxidative Stress and Lipid Peroxidation	133
3.5.1 Introduction.....	133
3.5.2 Method.....	137
3.5.3 Results & Discussion.....	138
3.6 Conclusion	144
Chapter 4: Uptake of CeO ₂ NPs by <i>C. maenas</i> through Immersed Exposure and Emerged Trophic Transfer, and their Biological Effects	147
4.1 Abstract	149
4.2 General Introduction.....	151
4.3 Trophic Transfer of 28nm CeO ₂ NPs from <i>M. edulis</i> to <i>C. maenas</i> through Emerged Feeding.....	154
4.3.1 Introduction.....	154
4.3.2 Method.....	155
4.3.3 Results and Discussion	157
4.4 Immersed Uptake and Depuration of 10nm and 600nm JRC CeO ₂ NPs by <i>C. maenas</i>	163
4.4.1 Introduction.....	163
4.4.2 Method.....	165
4.4.3 Results	166
4.5 Trophic Transfer of 10nm JRC CeO ₂ NPs from <i>M. edulis</i> to <i>C. maenas</i> whilst Emerged ..	179

4.5.1 Introduction.....	179
4.5.2 Method.....	180
4.5.3 Results and Discussion	181
4.6 Conclusion	189
Chapter 5: Use of Isotopically-labelled $^{140}\text{CeO}_2\text{NPs}$ in Trophic Transfer Experiments.....	191
5.1 Abstract	193
5.2 Introduction.....	195
5.3 Method.....	199
5.4 Results and Discussion	200
5.4.1 Accumulation of $^{140}\text{CeO}_2\text{NPs}$ in <i>M. edulis</i> and subsequent Biological Effects.....	200
5.4.2 Trophic Transfer of $^{140}\text{CeO}_2\text{NPs}$ from <i>M. edulis</i> to <i>C. maenas</i> , and subsequent Biological Effects	206
5.5 Conclusion	210
Chapter 6: Comparisons in the Uptake Efficiency between Silver Nanoparticles and Silver Nanorods by <i>M. edulis</i> , and subsequent Biological Effects	213
6.1 Abstract	215
6.2 General Introduction.....	217
6.3. Time Series Uptake of Ag Nanorods and Nanoparticles by <i>M. edulis</i> and Differences in Biological Effects following 4 and 8 hours Exposure.....	221
6.3.1 Introduction.....	221
6.3.2 Method.....	223
6.3.3 Results and Discussion	224
6.4. Comparing AgNPs to AgNRs, their Dispersants, and Ionic Silver: Accumulation and Biological Effects in <i>M. edulis</i> following 24 Hours Exposure	234
6.4.1 Introduction.....	234
6.4.2 Method.....	235
6.4.3 Results and Discussion	236
6.5 Conclusion	251
Chapter 7: Conclusion	253
Appendix A: Conferences, Publications & Grants	266
References.....	267

Commonly Used Acronyms

• AgNP	Silver Nanoparticle
• AgNR	Silver Nanorod
• CAT	Catalase
• CeO ₂ NP	Cerium Oxide Nanoparticle
• GSH	Glutathione (reduced)
• GSSG	Glutathione (oxidised)
• GST	Glutathione-s-transferase
• LPx	Lipid Peroxidation
• Me(O)NP	Metal (or Metal Oxide) Nanoparticle
• MDA	Malondialdehyde
• MW	Mann-Whitney U-Test
• NP	Nanoparticle
• OS	Oxidative Stress
• ROS	Reactive Oxygen Species
• SOD	Superoxide Dismutase
• TBARS	Thiobarbituric Acid Reactive Substances
• TEM	Transmission Electron Microscopy
• TTF	Trophic Transfer Factor

List of Tables and Figures

Chapter 1

Table 1.1: Properties of reference metal and metal oxide nanomaterials (the NM-series) carried by the OECD/Joint Research Council (JRC 2011).

Table 1.2: US EPA Aquatic Life Criteria Water Quality Standards (EPA 2009), and UK Environmental Quality Standards (SEPA 2005) for certain metal ions in fresh and/or salt waters

Fig 1.1: Stages of interactions of NPs with organisms with regards to uptake, accumulation and depuration [Mollusc Image from Biodidac (Livingstone 1995)]

Fig 1.2: Interactions of nanoparticles with cell membranes

Fig 1.3: A Simple Phylogenetic Tree for Marine Organisms. (X) denotes number of studies (published prior to 2013) concerning marine phyla where some metal or metal oxide nanoparticle toxicity testing has occurred in marine media

Table 1.3: Examples of well-characterised zinc oxide (JRC-IRMM 2011) and cerium oxide micro- and nanoparticles, highlighting size variation between characterisation methods, and behavioural differences in differing media (CAS = Chemical Abstracts Service, EINECS = European Inventory of Existing Commercial Chemical Substances, XRD = X-Ray Diffraction, SEM = Scanning Electron Microscopy, CPS = CPS Disc centrifuge, BET SSA = Braun Emmet Teller Specific Surface Area, XPS = X-ray Photoelectron Spectroscopy , DI = Deionised Water, SW = Sea Water).

Table 1.4: A summary of potential uptake methods and effects of nanoparticles on various marine organisms

Fig 1.4: Sources of Nanoparticle release, their behaviour, and potential uptake routes for organisms in the marine environment

Table 1.4: A summary of potential uptake methods and effects of nanoparticles on various marine organisms

Chapter 2

Table 2.1: Properties of the JRC NM-Series of CeO₂NPs (CAS = Chemical Abstracts Service; EINECS = European Inventory of Existing Commercial Chemical Substances; XRD = x-ray diffraction; SEM = scanning electron microscope; CPS = disc centrifuge; BET = Brunauer-Emmett-Teller; mv = millivolts; DI = deionised water; SW = saltwater; XPS = X-ray Photoelectron Spectroscopy (Singh *et al.* 2014)

Fig 2.1: TEM images (x400,000) of NM-211 (10nm) CeO₂NPs

Fig 2.2: TEM images (x400,000) of NM-212 (28nm) CeO₂NPs

Fig 2.3: TEM image (x400,000) of ¹⁴⁰CeO₂NPs. Arrows highlight some of the particles, here shown as extremely dense black dots.

Table 2.2 Percentage of AgNPs (NM-300K) falling within a defined size range, following measurement using TEM images (x400,000) analysed with Image-J software (n = 320)

Fig 2.4: TEM images (x400,000) of silver nanoparticles (NM-300K)

Fig 2.5: TEM images (x400,000) of silver nanorods (NM-302)

Fig 2.6: Scatterplot showing length and width of silver nanorods (NM-302) following measurement using TEM images (x400,000) and analysed using Image-J software (n = 52). Red box = nominal size range

Fig 2.7: Percentage dissolution of silver from NM-300K (9.23µg/l) and NM-302 nanorods (3.75µg/l) following 4, 24 and 48 hours in 330ml artificial seawater (n=1 per timepoint per treatment, pooled from n=2)

Fig 2.8 The mussel *M. edulis* covered in barnacles (left) and cleaned of epibionts (right)

Fig 2.9: Internal anatomy of *M. edulis*. dg = digestive gland, f = foot, g = gills, ih = inhalant siphon, m = mantle, p = palps

Fig 2.10: Marine snow manufacture (left) and *M. edulis* exposure technique (right)

Fig 2.11: Cerium accumulation ($\mu\text{g/g}$ dry weight) following uptake of 28nm CeO_2NPs [10 mg/l, with and without marine snow] for 72 hours by *M. edulis* into the Digestive Gland, Gill and Mantle. Note that y-axis for stomach content is a log scale. Samples pooled to $n=1$ per treatment.

Table 2.3: Percentage of total cerium uptake found in each tissue ($n=1$)

Fig 2.12: Methodology for exposure of *M. edulis* to CeO_2NPs singularly (left) and in a group (right)

Fig 2.13: Mean cerium concentrations ($\mu\text{g/g}$ d.w.) in *M. edulis* when exposed to 3 mg/l CeO_2NPs either singularly ($n=7$) or in groups of 4 ($n=8$). (6) = Outlier

Fig 2.14: Exposure technique to compare oxygen consumption by *M. edulis* under low bubble (left) and high bubble (right) conditions

Fig 2.15: Mean percentage oxygen in water following mussels exposed to CeO_2NPs (1mg/l) for 3 hours under low bubble ($n=5$) and high bubble ($n=6$) conditions (with std. dev.). (*) denotes significant difference ($p < 0.005$, t -test)

Fig 2.16: Mean Seawater oxygen concentration following exposure of *M. edulis* to algae, and to algal feed in combination with 1, 3 and 5 mg/l CeO_2NPs ($n=6$ per treatment).

Fig 2.17: Seawater sample (34ppt) NH_3 content following exposure of *M. edulis* to 28nm CeO_2NPs (3mg/l) over 56 hours at 14°C . Control mussels were unexposed. Results pooled to $n=1$, hence no statistical analysis performed.

Fig 2.18: Mean pH (with error bars) over 23 hours (1380) mins of exposure water for *M. edulis* ($n=6$) left unfed, fed algae at 5,000 cells/ml, and fed algae with 1mg/l CeO_2NPs (NM-212, 28nm)

Fig 2.19: Standardised equipment set-up for the exposure of *M. edulis* to Me(O)NPs

Fig 2.20: The Shore Crab *Carcinus maenas*

Fig 2.21 Top: Simplified internal anatomy of the main digestive features of *C. maenas* [adapted from (McLaughlin 1980)], and Bottom: potential routes taken by

ingested materials through the stomach (dotted lines = solid food, solid lines = fluid). [adapted from: (Dall and Moriarty 1983)]

Fig 2.22: Tank set-up for feeding exposed *M. edulis* to immersed *C. maenas*

Fig 2.23: Mean Cerium content ($\mu\text{g/g}$ d.w.) of the stomach, hepatopancreas and gills of crabs fed unexposed (control) *M. edulis* and those fed *M. edulis* exposed to 20mg/l CeO_2NPs . (*) = significant difference ($p < 0.05$, *t*-test). Control $n = 4$, Exposed $n = 6$.

Chapter 3

Fig 3.1: Cerium concentrations found in the digestive gland, mantle and gill (μg Ce/g dry weight) of *M. edulis* following exposure to 10nm (NM-211) CeO_2NPs at 1mg/l for 56 hours (samples pooled to $n=1$ from $n=7$ per timepoint)

Table 3.1: Percentage accumulation of cerium by the gill, digestive gland, or mantle, and whole body of *M. edulis* following exposure to 330 μg (1mg/l) of 10nm CeO_2NPs at for 4, 8 24 or 32 hours (■ = timepoint with highest percentage uptake). Figures are calculated by subtracting cerium background (control, = 0 hr) concentration from tissue concentration at each timepoint, and then dividing by the dose of cerium received (NB: CeO_2 contains 81.4% cerium).

Table 3.2: Properties of the JRC NM-Series of CeO_2NPs (XRD = x-ray diffraction; SEM = scanning electron microscope; DI = deionised water; mv = millivolts; SW = saltwater (Singh *et al.* 2014)

Fig 3.2: Cerium concentrations found in the digestive gland (μg Ce/g dry weight) of *M. edulis* following 24 hours exposure to 10nm (NM-211), 28nm (NM-212) and 600nm (NM-213) CeO_2 at 1 and 5 mg/l (samples pooled from $n=7$ to $n=1$). C= Control

Fig 3.3: Cerium concentrations found in the gill (μg Ce/g dry weight) of *M. edulis* following 24 hours exposure to 10nm (NM-211), 28nm (NM-212) and 600nm (NM-213) CeO_2 at 1 and 5 mg/l (samples pooled from $n=7$ to $n=1$). C= Control

Fig 3.4: Cerium concentrations found in the mantle (μg Ce/g dry weight) of *M. edulis* following 24 hours exposure to 10nm (NM-211), 28nm (NM-212) and

600nm (NM-213) CeO₂ at 1 and 5 mg/l (samples pooled from $n=7$ to $n=1$). C= Control

Fig 3.5: Cerium concentrations found in the haemolymph ($\mu\text{g Ce/ml}$) of *M. edulis* following 24 hours exposure to 10nm (NM-211), 28nm (NM-212) and 600nm (NM-213) CeO₂NPs at 1 and 5 mg/l (pooled samples). C= Control

Table 3.3: Percentage uptake of cerium in the tissues of *M. edulis* following exposure to various sizes and concentrations of CeO₂ for 24 hours (**bold** = maximum uptake)

Table 3.4: Percentage of an accumulated dose of CeO₂NPs [10, 28 or 600nm, at concentrations of (1) or (5) mg/l) found in different tissues of *M. edulis* following 24 hours exposure

Fig 3.6: Simplified pathway for methods of cellular free radical detoxification. **Red** = Damaging Component, **Blue** = Conjugating Enzyme, **Green** = Stable End Product

Table 3.5: Properties of Properties of the JRC NM-Series of CeO₂NPs. XRD = x-ray diffraction; SEM = scanning electron microscope; XPS = X-ray Photoelectron Spectroscopy; BET = Brunauer-Emmett-Teller; SW = Seawater (Singh *et al.* 2014)

Fig 3.7a: Significantly different effects from biological assays (TBARS, GST, SOD, CAT) performed on the gill, digestive gland and mantle of *M. edulis* following exposure to Nano (10nm) or Micro (600nm) CeO₂NPs at 3 mg/l for **8 hours**. ■ = Control, ■ = Nano, ■ = Micro. $n = 8$. * = significantly lower than control, † = significantly lower size-related effect ($p < 0.05$).

Fig 3.7b: Significantly different effects from biological assays (TBARS, GST, SOD, CAT) performed on the gill, digestive gland and mantle of *M. edulis* following exposure to Nano (10nm) or Micro (600nm) CeO₂NPs at 3 mg/l for **24 hours**. ■ = Control, ■ = Nano, ■ = Micro. $n = 8$. * = significantly lower than control, † = significantly lower size-related effect ($p < 0.05$).

Chapter 4

Fig 4.1: Set-up for feeding *M. edulis* to *C. maenas* out of water

Fig 4.2: Average cerium concentrations ($\mu\text{g Ce/g d.w.}$) found in *C. maenas* tissues following consumption in air of exposed *M. edulis*. Please note the log scale axis used on the y-axis. $n=4$ per treatment. No significance recorded.

Table 4.1: Actual total cerium content (μg) of the stomach, hepatopancreas, gills and faeces of the crabs used in this experiment ($n=4$ per treatment). NB: *Total Not Eaten values based upon weight of mussel not eaten. **Total Ingested value = Average Mussel Burden – Total Not Eaten

Fig 4.3: Correlation between accumulation of cerium in the stomach and faeces of *C. maenas* following consumption of *M. edulis* exposed to CeO_2NPs . Relationship is significant ($p = 0.032$, Linear Regression)

Fig 4.4: Set-up for aqueous exposure of *C. maenas* to CeO_2

Fig 4.5: Cerium concentrations ($\mu\text{g/g dry weight}$) found in the ionic gill, non-ionic gill, hepatopancreas and stomach of *C. maenas* following exposure to 10nm (NM-211) and 600nm (NM-213) CeO_2NPs at 3 mg/l (C = Control/unexposed, M = 'Micro- CeO_2 ' [600nm], N = Nano- CeO_2 [10nm]) for 4 hours, 8 hours, or following 12 hours' depuration (NB: samples were pooled from $n=6$ to $n=1$, hence no statistical analysis could be performed).

Table 4.2: Total μg Cerium found in the various organs of *C. maenas* following exposure to 27mg of 600nm Micro- CeO_2 or 10nm CeO_2NPs (3 mg/l) for 4 hours, 8 hours, and following 12 hours' depuration. % Accumulation derived from (Total Extra μg Cerium/Ce dose of 7.33mg)

Fig 4.6: Oxidative stress and lipid peroxidation in the **Respiratory Gill** of *C. maenas* following aqueous exposure to 3mg/l 600nm Micro- CeO_2 (NM-213) and 10nm CeO_2NPs (NM-211). $n=6$. No significant difference recorded.

Fig 4.7: Oxidative stress and lipid peroxidation in the **Ionic Gill** of *C. maenas* following aqueous exposure to 3mg/l 600nm Micro- CeO_2 (NM-213) and 10nm CeO_2NPs (NM-211). Significant difference ($p<0.01$, one-way ANOVA with Tukey post-hoc) from unexposed control (*) or between particle types (†). $n=6$

Fig 4.8: Oxidative stress and lipid peroxidation in the **Stomach** of *C. maenas* following aqueous exposure to 3mg/l 600nm Micro- CeO_2 (NM-213) and 10nm

CeO₂NPs (NM-211). Significant difference ($p < 0.05$) from unexposed control (*) or between particle types (†). n=6

Fig 4.9: Oxidative stress and lipid peroxidation in the **Hepatopancreas** of *C. maenas* following aqueous exposure to 3mg/l 600nm Micro-CeO₂ (NM-213) and 10nm CeO₂NPs (NM-211). Significant difference ($p < 0.05$, Mann-Whitney U-test) from unexposed control (*). n=6

Fig 4.10: Mean Cerium content in the stomach and hepatopancreas of *C. maenas* having been allowed to feed for 24 hours on *M. edulis* exposed to 20mg 10nm CeO₂NPs/l. Control organisms fed unexposed mussels (* = significantly different to control, $p < 0.05$, *t*-test, control n=4, exposed n=6) NB: Y-axis on a log-scale for clarity.

Fig 4.11: Mean Cerium content in the haemolymph of *C. maenas* having been allowed to feed for 24 hours on *M. edulis* exposed to 20mg 10nm CeO₂NPs/l. Control organisms fed unexposed mussels (control n=4, exposed n=6)

Fig 4.12: Mean Cerium content in the respiratory and ionic gills of *C. maenas* having been allowed to feed for 24 hours on *M. edulis* exposed to 20 mg/l 10nm CeO₂NPs/l. Control organisms fed unexposed mussels (* = significant difference, $p < 0.05$, *t*-test, control n=4, exposed n=6)

Table 4.3: Actual average cerium concentrations found in the various organs of exposed and control crabs having been allowed 24 hours to feed on a mussel exposed to 20mg/l NM-211 (10nm) CeO₂NPs

Fig 4.13: Oxidative Stress and Lipid Peroxidation in the Stomach, Hepatopancreas, Respiratory and Ionic Gill of *C. maenas* allowed 24 hours to consume a mussel (*M. edulis*) previously exposed to 20mg/l 10nm CeO₂NPs (NM-211). * = significantly different to control ($p < 0.05$)

Chapter 5

Table 5.1: Mean Cerium concentrations in the gill, digestive gland and mantle of *M. edulis* following exposure to 100µg/l 2nm ¹⁴⁰CeO₂NPs. (X) = n-number. d/d = data deficient. (*) = significantly higher than control ($p < 0.05$).

Fig 5.1: Differences in TBARS, SOD, GST and CAT activity (mean \pm SE) between unexposed *M. edulis*, and those exposed to dextran or 2nm $^{140}\text{CeO}_2\text{NPs}$ for four hours (n = 8 per treatment). * = significant difference from control

Table 5.2: Mean Cerium concentrations in the stomach, hepatopancreas, gills and haemolymph of *C. maenas* following consumption of *M. edulis* containing c. 512.5ng Ce. (X) = n-number. d/d = data deficient. (*) = significantly higher than control ($p < 0.05$, *t*-test). AE = Assimilation Efficiency. TTF = Trophic Transfer Factor

Table 5.3: Actual cerium values (ng) found in *C. maenas* following consumption of *M. edulis* exposed to 100 $\mu\text{g/l}$ 4nm $^{140}\text{CeO}_2\text{NPs}$ for 4 hours. AE = Assimilation Efficiency (= ng Fed/ng Recovered). D = Data deficient. *data only available for 1/10 control crabs, and 8/10 exposed crabs.

Fig 5.2: Differences in TBARS, SOD, GST and CAT activity in the organs of *C. maenas* following trophic transfer of 2nm $^{140}\text{CeO}_2\text{NPs}$ from *M. edulis* to *C. maenas* (n = 10 per treatment). No significant differences recorded. Blue = Control, Red = Exposed.

Chapter 6

Table 6.1: Average Silver concentrations (ng Ag/l) for selected oceans, and (*) areas of known high anthropogenic inputs (Barriada *et al.* 2007)

Fig 6.1: Silver concentrations (ng/g dry weight) in the gill, digestive gland and mantle of *M. edulis* following exposure to AgNPs (NM-300K; 10 $\mu\text{g/l}$) over 48 hours (samples were pooled from n=6 to n=1, hence statistical analysis has not been performed)

Fig 6.2: Silver concentrations (ng/g dry weight) in the gill, digestive gland, and mantle of *M. edulis* following exposure to AgNRs (NM-302; 10 $\mu\text{g/l}$) over 48 hours (samples were pooled from n=6 to n=1, hence statistical analysis has not been performed)

Table 6.2: Dimensions of the AgNPs and AgNRs used in this experiment

Fig 6.3: Significant differences in induced biological effects in Gill, Digestive Gland and Mantle tissue after **4 hours** following exposure of *M. edulis* to AgNPs

and AgNRs (10µg/l). ■ = Control, ■ = AgNPs, ■ = AgNRs. * = significantly different from control. ◇ = Form-related significant difference ($p < 0.05$). n=8 per treatment

Fig 6.4: Significant differences in induced biological effects in Gill, Digestive Gland and Mantle tissue after **8 hours** following exposure of *M. edulis* to AgNPs and AgNRs (10µg/l). ■ = Control, ■ = AgNPs, ■ = AgNRs. * = significantly different from control. ◇ = Form-related significant difference ($p < 0.05$). n=8 per treatment

Fig 6.5: Mean Silver concentration (µg/g dry weight) in the gill, digestive gland and mantle of *M. edulis* following exposure to AgNO₃, the AgNP NM-300K, its dispersant NM-300D, the AgNR NM-302, and its dispersant NM-302D, at a concentration of 10 µg Ag/l for 24 hours. n = 4 per treatment (pooled from n=8). * = significantly higher than control ($p < 0.05$, one-way ANOVA)

Table 6.3: Average total silver content (µg) found in gill, digestive gland and mantle tissues of individual *M. edulis* (n=8, pooled to n=1) following 24hrs exposure to 3.33µg Ag (10µg/l) through AgNPs (300K), AgNRs (302K) or AgNO₃, or to the equivalent concentration of their nano-dispersants (300D, 302D) alone (silver-exposed totals in **bold**)

Fig 6.6: Differences in **Gill** TBARS, SOD, GST and CAT activity between control mussels and those subjected to AgNO₃, AgNPs (300K), AgNRs (302), and their respective dispersants (300D, 302D) following 24 hours exposure at 10µg/l Ag. n=8 per treatment. Symbols indicate significant difference ($p < 0.05$, one-way ANOVA with Tukey's HSD): * = from Control; † = from AgNO₃; ▢ = between dispersants; ● = between nanoform and its own dispersant

Fig 6.7: Differences in **Digestive Gland** TBARS, SOD, GST and CAT activity between control mussels and those subjected to AgNO₃, AgNPs (300K), AgNRs (302), and their respective dispersants (300D, 302D) following 24 hours exposure at 10µg Ag/l. n=8 per treatment. * = Significant difference from Control ($p < 0.05$, one-way ANOVA with Tukey's HSD)

Fig 6.8: Differences in **Mantle** TBARS, SOD, GST and CAT activity between control mussels and those subjected to AgNO₃, AgNPs (300K), AgNRs (302), and their respective dispersants (300D, 302D) following 24 hours exposure at

10µg Ag/l. n=8 per treatment. Symbols indicate significant difference ($p < 0.05$, one-way ANOVA with Tukey's HSD): * = from Control; † = from AgNO₃; • = between nanoform and its own dispersant; rd = from rod dispersant 302D; pd = from particle dispersant 300D

Author's Declaration

I, Antony Baker, made the following contributions to the **review paper** presented in this thesis in Appendix A, and modified for inclusion in Chapter 1. I researched and wrote the manuscript, which was edited before submission by the co-authors, Professors Charles R Tyler & Tamara S Galloway.

Chapter 1: General Introduction

Parts of this Chapter have been previously published in:

Baker TJ, Tyler CR & Galloway TS (2014) Impacts of metal and metal oxide nanoparticles on marine organisms, *Environmental Pollution* (186) 257-271

DOI: 10.1016/j.envpol.2013.11.014

A copy has been included in Appendix A

(ResearchGate: 122 Citations; 1,396 Reads as of 10/02/2018)

1.1 Introduction

Nanotechnology uses nanomaterials that are most commonly defined as having at least one dimension between 1 and 100 nm (OECD 2009), and manufactured nanomaterials may take the form of a single nanoparticle (NP), wire, or thin-walled tube. Over a thousand consumer products are currently listed to contain NPs, including sunscreens, paints, semiconductors and cosmetics (PEN 2012), with the global market value of nanomaterial-containing products estimated to reach €2 trillion in 2015 (REACH 2015). As the use and prevalence of these particles inevitably increases, so will their discharge into freshwater and marine environments.

Code / Material		Mean Particle Size (nm)	Primary Particle Size (nm)	Specific Surface Area (m ² /g)
NM-101	TiO ₂	38	6	320
NM-102	TiO ₂	132	20	90
NM-103	TiO ₂	186	20	60
NM-104	TiO ₂	67	20	60
NM-105	TiO ₂	95	22	61
NM-110	ZnO	150	42	13
NM-111	ZnO	140	34	16
NM-200	SiO ₂	47	20	230
NM-201	SiO ₂	62	8-15	160
NM-202	SiO ₂	108	8-15	200
NM-203	SiO ₂	137	8-20	226
NM-204	SiO ₂	75	8-20	144
NM-211	CeO ₂	-	10	66
NM-212	CeO ₂	28	33	28
NM-300K	Ag	15	15	-
NM-302 (Rod)	Ag	Nominally 100-200nm x 5-10µm		-

Table 1.1: Properties of reference metal and metal oxide nanomaterials (the NM-series) carried by the OECD/Joint Research Council (JRC 2011).

Nanoparticles may enter marine systems either directly (through aerial deposition, effluents, dumping and run-off) or indirectly e.g. via river systems. The OECD has highlighted four metal and metal oxide [Me(O)] NPs as of high interest due to their inherent properties, widespread use and commercial importance, namely cerium oxide (CeO₂), silver (Ag), zinc oxide (ZnO) and titanium dioxide (TiO₂) (a more comprehensive list of the properties of the reference NPs for each of these materials can be found in Table 1.1). Widely

used as a fuel additive in diesel engines (Envirox) to reduce particulate emissions (Park *et al.* 2008), CeO₂NPs are also used as glass polishers, as purifiers of Mischmetal, and in heat-resistant coatings (EPA 2009). Exploited for their antibacterial properties (Jeong *et al.* 2005, Lee *et al.* 2005, Shrivastava *et al.* 2007), AgNPs are found in over two hundred consumer products, including deodorants and socks (Luoma 2008), and are especially effective against *E. coli* (McQuillan *et al.* 2012). ZnONPs are found in paint, cosmetics, animal feeds and fertilisers and, much like TiO₂NPs, are commonly employed in sunscreens where the particles protect against cell damage by blocking UV light (JRC-IRMM 2011).

Toxin	US Fresh Water (µg/l)		US Salt Water (µg/l)		UK Salt Water (µg/l)	
	Acute	Chronic	Acute	Chronic	Acute	Chronic
Cadmium	2.0	0.25	40	8.8	-	2.5
Copper	2.33	1.45	4.8	3.1	-	5
Gold	-	-	-	-	-	-
Iron	-	1000	-	-	-	1000
Nickel	470	52	74	8.2	-	30
Silica	-	-	-	-	-	-
Silver	3.2	-	1.9	-	1	0.5
Titanium	-	-	-	-	-	-
Zinc	120	120	90	81	-	10

Table 1.2: US EPA Aquatic Life Criteria Water Quality Standards (EPA 2009), and UK Environmental Quality Standards (SEPA 2005) for certain metal ions in fresh and/or salt waters

Natural nanoparticles are found widely in nature and sources include ash, desert dusts, aerosols and metal oxide particles. Some plants synthesize NPs that are used to reduce metal uptake in contaminated soils, and anaerobic bacteria may use them in respiration (Bernhardt *et al.* 2010). Although evolved to deal with natural nanomaterials and their fluctuations over millennia, it is not known how organisms will cope with high discharges of anthropogenic nanomaterials into the environment. Currently there are no safe guidelines regarding the release of Me(O)NPs into fresh or salt water. The UK has released Environmental Quality Standards, whilst the US EPA has released Aquatic Life Criteria based on the biotic free ligand model, which concerns metal ions (Table 1.2). However one major difference between metal NPs and metal ions is charge. AgNPs, for example, have a slightly negative charge,

whilst ionic silver exists as the Ag^+ ion (Liu and Hurt 2010). Guidelines for titanium, gold, cerium and silicon have also not been examined, despite their increasing use as NPs in manufactured products.

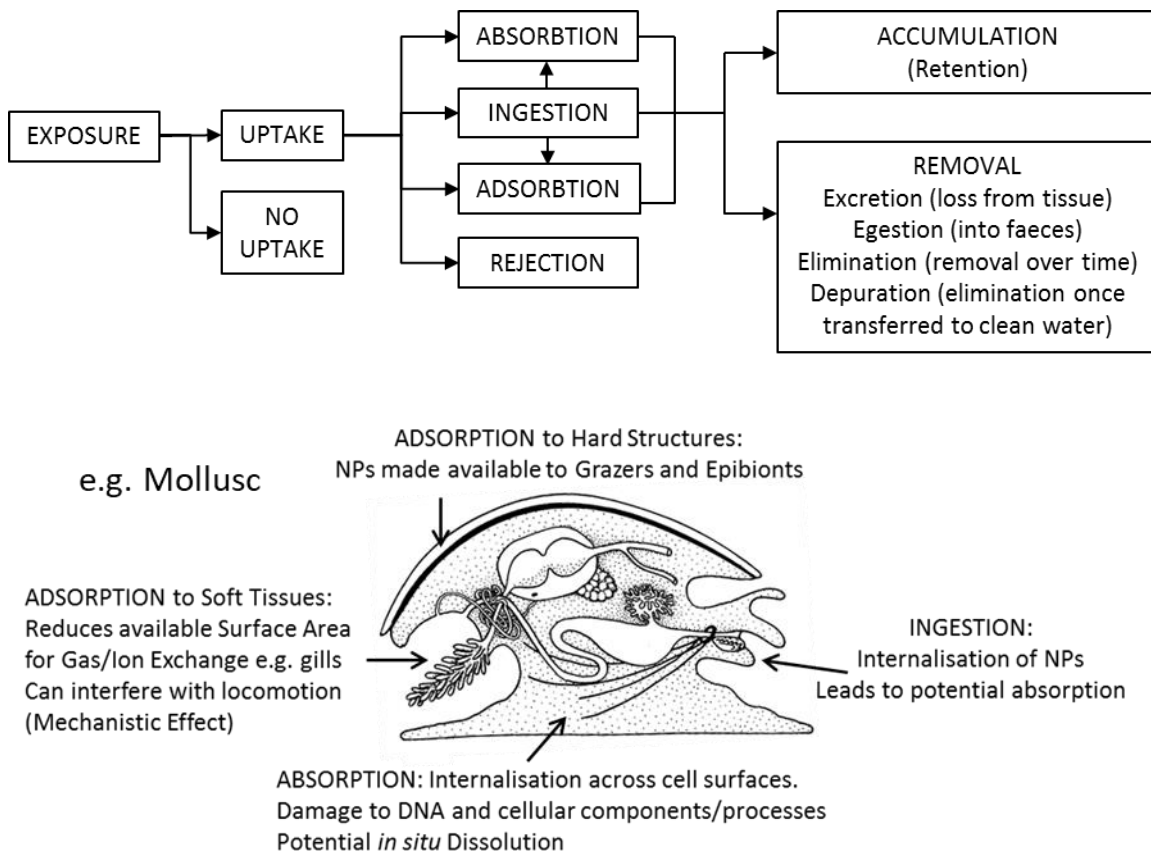


Fig 1.1: Stages of interactions of NPs with organisms with regards to uptake, accumulation and depuration [Mollusc Image from Biodidac (Livingstone 1995)]

NPs may be taken up by, and induce effects in, organisms in many different ways, however the exact method for this is particle specific (Bhatt and Tripathi 2011). Uptake of NPs refers to the physical removal of particles from the water column by the organism. Once taken up, the NP may adsorb to a cell (without being internalised) and smother essential pores and membrane functions (Fig 1.1). Alternatively, depending on size, it could enter the cell by endocytosis, via ion transport systems, or be absorbed via diffusion through pores (with the potential for pore stretching or damage) or across cell membranes. If proteins have bound to the NPs, they may also be taken up by receptor-mediated transport (Fig 1.2). Ingestion refers to NPs that have been taken into the stomach. Once in the stomach they may again be adsorbed or absorbed, or

simply egested further down the line and removed in the faeces. Loss of particles from inside the cell is referred to as excretion, and it may be that such particles are excreted back into the gut, again for removal into the faeces. Accumulation of NPs refers to particles retained by the organism that are neither excreted nor egested. Elimination refers to the loss of NPs over time (either through excretion or egestion), whilst depuration refers to the loss of NPs over time once the organism has been transferred to a clean water source.

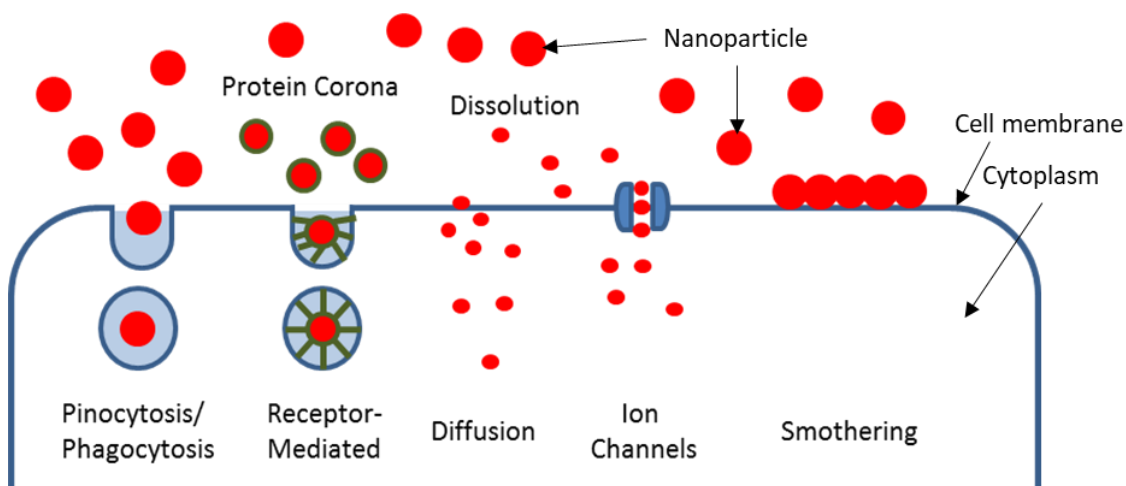


Fig 1.2: Interactions of nanoparticles with cell membranes.

In the case where NPs have entered a cell, they can potentially interfere with electron transport processes, or facilitate reactive oxygen species (ROS) production by hampering organelle functions. ROS production may lead to nucleic acid damage, protein oxidation or disruption of cell membranes.

To date, the vast majority of aquatic nanoparticle research has been performed on freshwater species, including *Daphnia magna* (waterflea), *Lymnaea stagnalis* (pond snail) and *Caenorhabditis elegans* (nematode). From these studies, results have highlighted a range of sub-lethal effects including reduced swimming (Asghari *et al.* 2012), reduced growth and reproduction (Zhao and Wang 2011), bioaccumulation (Rosenkranz *et al.* 2009), digestive stress and reduced feeding (Croteau *et al.* 2011, Croteau *et al.* 2011). Despite extensive research on freshwater species, little study has been directed towards marine organisms. In 2013, published data was available for just eight phyla and, of these, many reports were limited to a single class, order or species (Fig 1.3). It

is not yet clear how best to extrapolate freshwater data for marine organisms given that the properties of NPs will change according to exposure media, as will the biological, behavioural and respiration characteristics of marine organisms.

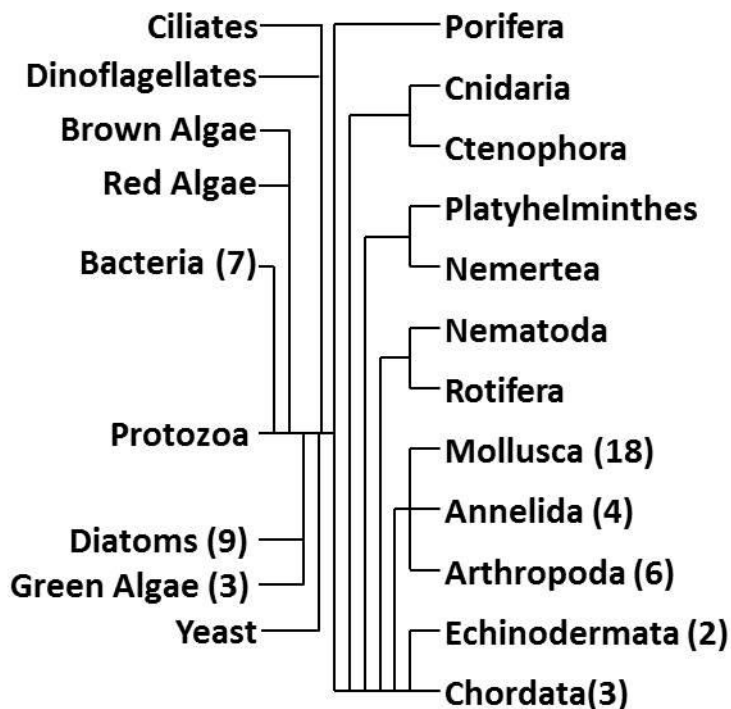


Fig 1.3: A Simple Phylogenetic Tree for Marine Organisms. (X) denotes number of studies (published prior to 2013) concerning marine phyla where some metal or metal oxide nanoparticle toxicity testing has occurred in marine media

The aims of this Literature Review are to highlight the behaviour of NPs in marine environments, to understand prior work in the field, and to determine where knowledge gaps exist regarding NP toxicity to marine organisms. From this the aims of this thesis can be discussed regarding how to best add to this body of knowledge.

1.2 Some Relevant Characteristics of Me(O)NPs

Whilst it might be assumed that the over-riding characteristic of a nanoparticle is its nano-size, it is a combination of characteristics, including size, shape, aggregation/agglomeration, dissolution, charge and surface reactivity that will

define its behaviour and effects (Bhatt and Tripathi 2011). Different exposure media will also affect the particle in different ways, causing changes in particle behaviour. The difficulties of NP characterisation in aqueous media have been covered in other comprehensive reviews (Domingos *et al.* 2009, Baalousha *et al.* 2012, Baalousha *et al.* 2012), however it is worth examining in detail some of the most important properties of Me(O)NPs and their behaviour in marine waters, since their physical and chemical characteristics will differ from those in freshwater, affecting both toxicity and bioavailability to marine organisms.

1.2.1 Size and Shape

The most defining aspect of any Me(O)NP is size i.e. one dimension between 1 and 100nm. However as well as different sizes, NPs can exist as different shapes. CeO₂NPs for example can exist as angular polyhedrons (Singh *et al.* 2014), AgNPs have been synthesised as rods, pyramids, wires and cubes (Khodashenas and Ghorbani 2015), whilst carbon NPs are often manufactured as single or multi-walled tubes (Zhang *et al.* 2011). In the case of rods and wires the diameter is normally on the nano-scale, whilst tubes tend to have walls only a few nanometres thick; this means that the rod, wire or tube may well be several microns in length, but still classed as a nanoparticle. A secondary toxicity may exist with sharp edges (of points, or triangles) causing mechanical damage e.g. piercing tissues and cell membranes (Baalousha *et al.* 2012). This sizing aspect will affect the potential uptake of such NPs across cell barriers, and may also cause clogging of membrane pores.

Both particle size and shape will therefore determine how NPs react with organisms and their surroundings, and will also dictate whether NPs can penetrate into organisms, tissues or cells, and this will relate to an organism's lifestyle, physiology and feeding habits.

The Echinodermata (sea stars, sea urchins, sea cucumbers), for example, is a vast phylum whose members display filter, deposit and suspension feeding as well as active hunting and scavenging (Barnes *et al.* 2001). A major distinguishing feature of the echinoderms is the water vascular system which

allows movement and stops the body from collapsing. Water is drawn into the organism via the madreporite, a small, sieve-like structure with pores of around 10 μm in diameter (Ferguson and Walker 1991), large enough for even the largest free-floating NPs to penetrate and be further circulated around all tissues.

Whilst the internalisation aspect of NP accumulation might usually be from feeding, drinking or physiological respiration, certain micro-organisms may have different methods for internalising particles. The peptidoglycan cell wall layer of bacteria, for example, has been estimated as permeable to objects around 2 nm in size (Demchick and Koch 1996) which may allow direct penetration of the smallest nanoparticles. Research has shown that Gram-positive bacteria (*Bacillus subtilis*) are more susceptible to AgNPs (4 nm) than Gram-negative bacteria (*Shewanella oneidensis*, *Escherichia coli*) because Gram-negative bacteria have an outer cell wall to protect their peptidoglycan layer, Gram-positive bacteria do not and thus the AgNPs were free to penetrate this layer (Suresh *et al.* 2010).

Once internalised, smaller NPs can be taken up by cells through pinocytosis, larger NPs by phagocytosis, whilst some NPs can create their own membrane channels (Wang *et al.* 2012). The extent of this internalisation will then further depend on NP size and shape. This has previously been demonstrated with rotifers - microscopic ciliated animals that ingest organic detritus from the water column, and provide a key role in nutrient recycling – whereby a 2 day exposure showed that whilst larger polystyrene NPs (≥ 83 nm) could only be found in the stomach and intestine, 37 nm NPs could be found in tissues, having breached the intestinal wall (Snell and Hicks 2011). This suggests that size is particularly important when determining potential uptake by tissues, and could lead to toxicity from intracellular dissolution when studying smaller, soluble particles (although the authors do acknowledge that the concentrations used in this study [$\geq 720\mu\text{g/l}$] were not environmentally relevant). Similarly, whilst studies have shown that NPs based on chitosan (Alishahi *et al.* 2011) and polylactic-co-glycolic acid (Tian and Yu 2011) are directed to the gastrointestinal tracts of the rainbow trout (*Oncorhynchus mykiss*) and the Japanese flounder (*Paralichthys olivaceus*) respectively following oral ingestion, in the case of the

flounder particles less than 100 nm entered non-phagocytotic cells whilst larger NPs were taken up by monocytes.

Accurately measuring NP size is however a problem since comparing sizing between X-ray diffraction (XRD), atomic force microscopy (AFM), and transmission / scanning electron microscopy (TEM / SEM) will produce slightly different results, with wide variation depending on the exposure medium (examples of this can be found in Table 1.3). In the case of characterisation by Dynamic Light Scattering (DLS), larger particles in the sample are able to mask smaller particles, thereby particle size distribution data is often inaccurate (Domingos *et al.* 2009).

	Nano ZnO			Nano CeO ₂	
	NM-110	NM-111	NM-112	NM-211	NM-212
CAS / EINECS No.	1314-13-2 / 215-222-5			1306-38-3 / 215-150-4	
XRD (nm)	41.5	33.8	24.1	10.1	33.3
SEM (nm)	150 ± 60	140 ± 70	43 ± 4	-	28 ± 10
CPS (DI, nm)	193 ± 3	-	277 ± 7	340 ± 50	135 ± 4
CPS (SW, nm)	309 ± 10	-	510 ± 40	520 ± 90	187.6 ± 1.7
BET SSA (m ² /g)	12.4 ± 0.6	15.1 ± 0.6	27.2 ± 1.2	66 ± 2	27.2 ± 0.9
ζ Potential (DI, mv)	24.3 ± 0.4	-	24.6 ± 0.4	28 ± 2	33 ± 2
Stability (DI, mins)	4038	-	2526	780	2676
Stability (SW, mins)	738	-	444	534	288
XPS Ratio (Ce ⁴⁺ :Ce ³⁺)	-	-	-	94.3: 5.7	93.1: 6.9

Table 1.3: Examples of well-characterised zinc oxide (JRC-IRMM 2011) and cerium oxide micro- and nanoparticles, highlighting size variation between characterisation methods, and behavioural differences in differing media (CAS = Chemical Abstracts Service, EINECS = European Inventory of Existing Commercial Chemical Substances, XRD = X-Ray Diffraction, SEM = Scanning Electron Microscopy, CPS = CPS Disc centrifuge, BET SSA = Braun Emmet Teller Specific Surface Area, XPS = X-ray Photoelectron Spectroscopy, DI = Deionised Water, SW = Sea Water).

1.2.2. Aggregation, Dissolution or Both?

1.2.2.1 Aggregation or Agglomeration?

The European Commission's Joint Research Centre (JRC) defines nanoparticle aggregates as strongly (e.g. covalently) bonded assemblages of primary particles, whilst agglomerates are groups of particles or aggregates held

together by weak forces e.g. Van der Waal's forces. Agglomerates may also contain other particle types, such as clays and organics, alongside primary NPs (JRC 2014, Petersen *et al.* 2014).

In pristine, organic-free aquatic media nanoparticles tend to agglomerate together, and the extent of this agglomeration is dependent on surface charge, particle shape and size, and pH of the medium. In saltwater the increasing salinity, and therefore ionic strength, reduces the negativity of electrophoretic mobility of the particles to encourage agglomeration (Batley *et al.* 2012). Agglomeration tends to increase with concentration, due to more particles being available for interaction (Miller *et al.* 2010, Fairbairn *et al.* 2011). Capping agents such as citrate, polyvinylpyrrolidone (PVP) and gum arabic (Yang *et al.* 2012), as well as oleate and dodecylamine (Li *et al.* 2011), are employed to change the charge state of the NP, and to prevent agglomeration and aid dispersion in media of differing ionic strength (Bhatt and Tripathi 2011) by providing a barrier to the agglomeration potential of van der Waals' forces (Studart *et al.* 2007).

The introduction of organic matter into aquatic media can change NP behaviour. River systems contain a large amount of natural organic matter (NOM) and this has been shown to affect Me(O)NPs. Reduced agglomeration (and therefore reduced sedimentation) of CeO₂NPs has been observed in freshwater, with NOM increasing zeta potential of the particle, thus increasing electrostatic repulsion (Quik *et al.* 2010). Molecular weight of the NOM appears to be important, with low weight fulvic acids appearing to increase colloidal mobility, and high weight humic acids increasing agglomeration (Bhatt and Tripathi 2011).

Examination of TiO₂ (27 nm), CeO₂ (rods 67x8 nm) and zinc oxide (ZnO) NPs (24 nm) in seawater has shown a positive correlation between NOM, sedimentation and ionic strength (Keller *et al.* 2010). Contrary to results seen with freshwater, in seawater higher concentrations of NPs (> 100 mg/l) show significantly faster sedimentation than seen for lower concentrations (10 mg/l). Agglomeration speed of NPs in seawater is therefore related to concentration and NOM, and NPs used in toxicity tests are likely to quickly form large

agglomerates. Evidence also suggests divalent cations found in natural seawaters e.g. Ca^{2+} may destabilise the electrical charges on NOM-coated NPs leading to further agglomeration and sedimentation (Zhang *et al.* 2009).

Although not in a nanoparticulate form, experiments with ionic lead (Pb) have demonstrated that humic acids increase both its uptake by gills of the common mussel *Mytilus edulis*, and the toxicity to embryonic larvae of the sea urchin *Paracentrotus lividus* (Sánchez-Marín *et al.* 2007).

Both aggregated/agglomerated and single NPs may also demonstrate dissolution, depending on the particle type. For those NPs that do dissolve, surface area, and reactivity of the particle, will determine dissolution speed. Aggregation and agglomeration reduces surface area, and therefore dissolution potential (especially at high concentration). Capping agents have the effect of reducing dissolution, hence capped and uncapped particles may behave very differently from each other, especially in high ionic strength marine waters.

1.2.2.2 Dissolution

Currently there is no single model to determine NP toxicity. Existing models such as the Free Ion Activity Model (FIAM) or the Biotic Ligand Model (BLM) are based upon ionic concentrations of elements, and remain to be validated for NPs (Choi *et al.* 2009). There is some value in using these models since some Me(O)NPs show dissolution of metal ions in aquatic media. CeO_2 NPs are virtually insoluble (Zhang *et al.* 2012), copper (Cu)-based NPs show dissolution to Cu^{2+} (Bielmyer *et al.* 2006) and surface silver on AgNPs dissolves to Ag^+ (Batley *et al.* 2012). The extent of this dissolution, even between different particles types featuring the same metal, is based on a number of factors including particle size, coating and medium. In seawater, for example, the solubility of ZnONPs can be more than twice that of micron-size ZnO (Wong *et al.* 2010), and evidence suggests ZnONPs will continue to dissolve until media concentration reaches between 3.2 & 4.8 mg soluble Zn/l (Miller *et al.* 2010, Wong *et al.* 2010, Fairbairn *et al.* 2011). Particle shape will also have an effect on dissolution rate, and is generally related to surface area. Rods are

reportedly more toxic than spheres due to fast dissolution from points (Baalousha *et al.* 2012).

Once NPs have dissolved, the type of media will again dictate the fate of the free ion. In freshwater, dissolution of AgNPs leads to Ag^+ mostly found in Fe/Mn oxyhydroxide/sulphidic phases, but with increasing salinity AgCl complexes become more prevalent. In estuaries in the Adriatic Sea, the levels of dissolved Ag were higher than those of the river (Tappin *et al.* 2010). This suggests addition of Ag^+ in estuarine waters caused by remobilisation of sediments in a highly dynamic environment, and therefore estuarine organisms are likely to be exposed to higher concentrations of Ag^+ . Levels of dissolved Ag drop rapidly when moving from estuarine to full marine salinity, instead forming AgCl complexes. At constant salinity below the euphotic zone, increased concentrations of dissolved Ag suggest adsorption of Ag^+ to phytoplankton followed by downward transport and remineralisation at depth. As such, benthic organisms will be greatly exposed to these AgCl complexes. The point at which an NP dissolves therefore highly influences whether marine organisms will be exposed to the ionic metal, or the particulate form.

Effects of ion dissolution have been demonstrated in 96 hour studies on embryo development of the white sea urchin *Lytechinus pictus* (Fairbairn *et al.* 2011). The similarity of effects (arrested development, skeletal abnormality) between ZnONPs, micron ZnO and ionic Zn^{2+} suggested ion dissolution was the main driver of toxicity. Whilst exposure to insoluble CeO_2 NPs (rods, 67x8 nm) or TiO_2 NPs (27±4 nm) demonstrated no abnormalities up to concentrations of 10 mg/l, ZnONPs (24±3 nm) produced an EC_{50} toxicity of 99.5 µg/l, close to the US regulatory release limit (81 µg/l, Table 1.2). Doping the ZnONPs with 10% iron reduced dissolution to 80% over 24 hours at the lower concentrations, and to 24% at 10 mg/l (equilibrium). The lack of difference in toxicity between doped and non-doped NPs suggests that in each treatment enough zinc had dissolved within the timeframe of the experiment to cause the effects seen.

As primary producers, the potential for uptake of Me(O)NPs by marine algae, and subsequent toxic effects, could have far-reaching consequences across all trophic levels (Matranga and Corsi 2012). Growth of algal blooms is

synonymous with nutrient availability, however dissolution of ions from Me(O)NPs may actually compete with nutrient uptake, thereby reducing growth. Zn^{2+} for example has been shown to interfere with silica uptake in diatoms. ZnONPs (≥ 10 mg/l) inhibited growth of the diatoms *Chaetoceros gracilis* and *Thalassiosira pseudonana* with accumulation in *T. pseudonana* resulting in mortality (Peng *et al.* 2011), although not at relevant concentrations. *Phaeodactylum tricornutum* displayed fewer effects with growth only slightly inhibited, suggesting a lower nutrient demand for silica than the other species. Rod shapes (242 x 13.5 nm; 862 x 29.5 nm) also proved more toxic to *P. tricornutum* than spheres (6.3 nm; 13.5 nm) in this study, likely due to the increased surface area for dissolution. A particular issue with diatoms is that the negative charge associated with their silica casing may actually attract dissolved cations such as Zn^{2+} .

Larger ZnONPs (20-30 nm spheroids) have been shown to inhibit growth of *T. pseudonana* at only 0.5 mg/l, but the diatom *Skeletonema marinoi*, the chlorophyte *Dunaliella tertiolecta* and the prymnesiophyte *Isochrysis galbana* at concentrations of 1 mg/l over 96 hours (Miller *et al.* 2010). Inhibition was likely due to Zn^{2+} competing with manganese uptake, or through detoxification pathways competing with growth for energy demand. Secondary size-related effects may have been masked by the dissolution of zinc ions, and require further investigation to resolve this uncertainty. That TiO_2 NPs (20-30 nm semi-spheres, 1 mg/l) showed no effects was hypothesised as relating to a lack of dissolution. Dissolution as a result of increased surface area should explain why ZnONPs (26.2 ± 5.1 nm) have been shown as significantly more toxic to *T. pseudonana* and *Skeletonema costatum* than micron-Zn (216.2 ± 73.2 nm) over 96 hours (Wong *et al.* 2010), generating an LC_{50} of 2.36 – 6.65 mg/l. Similar EC_{50} values for exposure of *D. tertiolecta* to ZnCl_2 , ZnONPs (100 nm) and micron ZnO and have been recorded as 0.65 mg/l, 1.94 mg/l and 3.57 mg/l respectively (Manzo *et al.* 2013). That significant reduction in growth was seen at 0.23 mg/l for ZnCl_2 , 1 mg/l for ZnONPs/l and 3 mg/l for micron ZnO highlights dissolution as the primary driver of toxicity. Yet these values are far above environmental relevance, meaning that only highly acute, point source discharges are likely to affect marine algae.

Dissolution of Ag^+ is also believed to be the driver of toxicity for AgNPs. 50% inhibition (IC_{50}) in the growth of *P. tricornutum* has been recorded at 400 ± 110 , 2380 ± 1880 and $3690 \pm 2380 \mu\text{g/l}$ for ionic Ag, citrate-capped (14 nm) and PVP-capped (15 nm) AgNPs respectively (Angel *et al.* 2013). Referencing the particles to their dissolution rate shows equivalent Ag^+ concentrations for each IC_{50} value. Similar conclusions were drawn comparing AgNPs (PVP-capped, 10nm) and Ag^+ on the photosystem quantum yield of the coastal diatom *Thalassiosira weissflogii* (Miao *et al.* 2009). Adding NOM in this study completely mitigated toxicity, and this highlights the relevance of replicating environmental conditions in toxicity testing. Dissolved Ag^+ was seen to form AgCl complexes that sorbed to the diatoms' surface, thereby making algae vectors for AgCl transport to higher trophic organisms. One area highlighted is the mitigation of toxic metal accumulation through the release of exopolymeric substances (EPS); a slime-like secretion rich in proteins, lipids and polysaccharides used by organisms to remove excess carbon and for attachment to substrate (Wotton 2004). Whilst a definite inverse relationship existed between EPS concentration and toxicity, it is unknown as to whether EPS is actively released in the presence of Ag, or whether Ag disrupts the cell membrane to cause EPS release.

Similarly a 48 hour exposure of the sea lettuce *Ulva lactuca* to PVP-capped AgNPs ($58 \pm 27 \text{ nm}$) only reduced the yield of photosystem II at concentrations above $55 \mu\text{g/l}$, however AgNO_3 exposures showed negative effects at only $2.5\mu\text{g/l}$, (Turner *et al.* 2012). This suggests the Ag^+ ion is the main driver of toxicity, and that PVP-capping of the AgNPs may well have reduced the dissolution potential. Evidence of bioaccumulation was strongly associated with surface adsorption rather than internalisation, yet this could still provide a toxic substrate for surface grazers.

In freshwaters, the rainbow trout *Oncorhynchus mykiss* exhibits a stress-induced drinking behaviour associated with exposure to NPs. On this basis, effects seen in freshwater studies could be extrapolated to understand how *O. mykiss* may fare when moving from fresh to salt waters i.e. by naturally increasing drinking activity. For example, studies show a linear relationship between AgNP (10 or 35 nm, polymer-coated) exposure concentration and accumulation

in the liver, likely through uptake via the gut epithelium (Scown *et al.* 2010). Exposure to CuONPs (87±27 nm, 100 µg/l) has demonstrated 10% mortality after ten days at 20 µg/l (Shaw *et al.* 2012), just four times the regulatory limit (4.8 µg/l). Mortality was much higher when exposed to ionic copper (CuSO₄ - 85% in four days, 100 µg/l), yet there appear to be different target organs based on form. CuONPs showed significantly greater accumulation in the intestines (likely through drinking), whilst ionic copper resulted in a greater hepatic and branchial burden.

It becomes clear that following release, NPs are unlikely to remain as single particles or aggregates. Instead both the particles and any dissolved metal ions may be highly complexed by NOM and remain in suspension as they move toward the ocean. Further incorporation into larger agglomerates leads to faster sedimentation, and this places benthic organisms most at risk to NOM-coated NPs.

1.2.3 Quantifying Anthropogenic Release

There has been little empirical data published concerning anthropogenic release of nanoparticles, in part due to the difficulty of characterising sampled particles as originating from NP release, and also due to scant availability of industrial release data. As such many estimates highlighted below are based on models that may have little significance to actual release volumes or circumstances, and few recognise the marine environment as an important sink.

AgNPs are widely used as anti-microbials in commercial products such as deodorants and sticky plasters (Davies and Etris 1997), hence they are often the most modelled. Washing clothing leads to the release of NPs into freshwater systems, which will ultimately discharge to the marine environment. Studies on sports socks containing AgNPs (100 nm) found no correlation between the socks' Ag load (2-1360 µg/g sock), number of washes and their leach rate (Benn and Westerhoff 2008). This suggests that differing manufacturing processes will affect how much and how often the socks will release Ag. Once leached, the Ag dissolved, formed colloids, or remained as NPs, although exact ratios could not be determined. That the concentration of

Ag released was higher than environmental guidelines is troubling, however the characteristics of the exposure media (ultrapure water, not standard tap water) may have helped produce such high concentrations as free ions in tap water are likely to complex free silver ions.

The release of NPs to domestic wastepipes inevitably leads to wastewater treatment plants which drain to the oceans, hence it is worth examining their efficiency in dealing with NPs. Studies suggest wastewater treatment could remove 60-70% of NPs, whilst water purification plants could remove up to 96%, depending on the method employed (O'Brien and Cummins 2010). The authors also believed that TiO₂NP concentrations in surface waters could be fifty times higher than Ag- or CeO₂NPs. These models were based on comparable pharmaceutical removal times in wastewaters and not on measured rates of Ag complexation, hence the figures should be treated as a rough guideline only.

Studies on the river Rhine in Germany suggest that industrial and sewage effluent containing AgNPs could increase Ag concentrations in the river from 4 to 320 ng/l, and from 0.04 to 14 µg/g in the sediment over a 700 km course to the estuary (Blaser *et al.* 2008). Modelling of European waters in 2008 suggests modal AgNP concentrations of 0.8 ng/l in surface waters and 43 ng/l in sewage treatment plant effluent with increased sediment loading of 0.95 ng/g/yr (Gottschalk *et al.* 2009), but much higher levels for both ZnONPs (10 ng/l; 400 ng/l; 3 ng/g/yr) and TiO₂NPs (15 ng/l; 3500 ng/l; 358 ng/g/yr). In the US, concentrations in sediments were predicted to rise three-fold by 2012 (AgNPs: from 0.7 to 2.2 ng/g). Whilst the authors highlight sewage treatment plant effluents as a major NP-hazard, and that levels of AgNPs in surface waters may also prove a risk, a safety factor of 1000 was built into these models. Real-world examples show complex formation and sedimentation as the likely fate of any Ag⁺ dissolved from AgNPs (Wen *et al.* 2002). In Colorado, downstream of industrial plants releasing over 34 µg Ag/l in their effluents, only 70 ng Ag/l was found passing through a 100 nm filter. Of this, most was found as colloids (in an Fe/Mn oxyhydroxide/sulphide phase) rather than free Ag, and at a concentration well below the chronic toxicity standard (190 ng/l) set by the state.

Not all marine discharges of Me(O)NPs are derived from freshwater effluents. Use of TiO₂ and ZnONPs in sunscreens (Wahie *et al.* 2007) means a major source of these materials in the marine environment is people as they enter the sea. On average 25% of sunscreen will be washed-off on immersion (Danovaro *et al.* 2008), and estimates indicate the potential for some 250 tonnes of sunscreen-originated NPs to enter the marine environment each year (Wong *et al.* 2010). Regarding cerium, average background levels of 55 ng Ce/l in European streams, and 66.6 µg Ce/g in European sediments have been measured (Salminen 2005). Modelling also suggests use of CeO₂NPs in diesel fuels would add an almost negligible 0.02 ng/l, although under certain conditions e.g. storms, this could increase to 300 ng/l (Johnson and Park 2012). Such high exposures may be sporadic and acute, but this has implications for any thoroughfares tracking the coastline.

In organisms, background levels of Ce have been measured up to 3.17 µg/g (dry weight) in the digestive glands of the scallop *Chlamys varia* at clean sites (Ré Island) in the Bay of Biscay, and up to 10.85 µg/g in areas of high anthropogenic input (La Rochelle Bay) (Bustamante and Miramand 2005). Digestive glands contained over twice as much as that in gonads and gills, and 5 to 10-fold more than in the kidneys, muscle and soft tissues. Similar results were shown with Ag, with digestive glands from contaminated sites containing twelve times (61.2 µg/g) the Ag of clean sites, although all organs and other soft tissues showed heavy accumulation. Background levels of Zn in contaminated sites (kidneys: 38.2 mg Zn/g) were over twice those of clean sites with most tissues containing several hundred µg/g. Given such high background levels of Zn, and its role as a micronutrient for some marine organisms, a major challenge is to determine the threshold whereby the increased burden from Me(O)NP dissolution becomes damaging to marine organisms, and to consider environmental relevance in exposure testing. Currently estimated environmental concentrations of some Me(O)NPs are still far below those that have proven lethal effects, however less is known of how sub-lethal effects may impact on population stability (Batley *et al.* 2012).

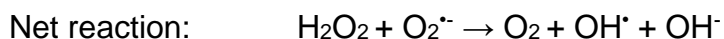
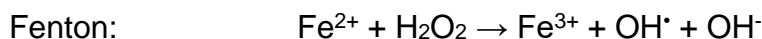
1.2.4 Propensity to Cause Biological Effects

The previous sections in this chapter have touched upon mortality as a result of Me(O)NP uptake through the generation of EC₅₀ values, however there is propensity for toxicants to cause sub-lethal effects when organisms are exposed to them. In particular there is a growing body of literature that mentions increased oxidative stress and lipid peroxidation as causes for concern when dealing with Me(O)NPs.

Regular cellular metabolism involving the reduction of oxygen leads to the formation of damaging reactive oxygen species (ROS) including the free radicals ($O_2^{\cdot-}$ [superoxide], OH^{\cdot} [hydroxyl] and HO_2^{\cdot}) as well as non-radicals such as hydrogen peroxide (H_2O_2), O_2 and O_3 , however the cell has evolved a number of mechanisms for dealing with them (Halliwell and Gutteridge 2007). Superoxide dismutase (SOD) is an enzyme comprising a number of metal (Cu/Zn, Mn, Fe, Fe/Mn) protein complexes involved in conjugating the superoxide ($O_2^{\cdot-}$) free radical. This reaction leads to the production of H_2O_2 , therefore the catalase (CAT) enzyme, produced in cell peroxisomes, is employed to catalyse the conversion of this H_2O_2 to water. Reduced glutathione (GSH), catalysed by glutathione peroxidase (GPx), also conjugates with H_2O_2 to form water, although CAT is the major enzyme involved in this process. It is when these systems of ROS and ROS-mediation are out of balance that oxidative stress occurs in an organism, either through increased quantities of oxygen free radicals, or reduced protection from them e.g. damage to anti-oxidant mechanisms (Kehrer 2000). The hydroxyl free radical (OH^{\cdot}) can also react with fatty acids found in membrane phospholipids to produce lipid hydroperoxides that can disrupt membrane functions (Halliwell 1991) and lead to lipid peroxidation. Lipid peroxides can also be neutralised through conjugation with GSH – in this instance catalysed by glutathione-s-transferase (GST) – to form stable lipids (Livingstone *et al.* 1992).

Over the last few years the question as to whether Me(O)NPs can directly or indirectly contribute to the formation of ROS has become important. Much of this chemistry is based on the Fenton and Haber-Weiss reactions (Fu *et al.*

2014), whereby free radicals can be both produced and quenched (i.e. conjugated by) by interactions with cellular iron (Fe):



In the case of other metals there is scope for Fenton-like reactions, whereby:



The difficulty lies in trying to distinguish whether it is the Me(O)NP itself or the ions that have dissolved from it that are most prominent when it comes to increasing oxidative stress in an organism (Lubick 2008). Over 48 hours, AgNPs (20-30 nm, citrate-capped, 0.2 µg/l) have been shown to cause greater oxidative damage in the hepatopancreas of the bivalve *Crassostrea virginica*, whilst AgNO₃ caused greater stress in the gills (McCarthy *et al.* 2013). This suggested capture of AgNPs and transport to the hepatopancreas, where they then caused damage *in situ*.

Evidence also exists of oxidative stress caused by insoluble Me(O)NPs. Exposing the ragworm *N. diversicolor* to insoluble CuONPs (197 nm) and ionic Cu (both at 10 µg/l) for example results in significant increases in CAT activity above the control, with CuONPs also causing significantly greater activity than ionic copper (Buffet *et al.* 2011). CuONPs also significantly increased GST activity above the controls, but not compared to ionic copper. In the same experiment CuONPs significantly increased SOD, GST and CAT activity in the bivalve *Scrobicularia plana* above both the control and the ionic form, with the ionic form causing little in the way of oxidative stress. This showed that insoluble CuONPs can generate ROS.

Other experiments with *Mytilus* ssp. exposed to insoluble NPs have shown similar results. AuNPs (13nm) have induced CAT activity in the digestive gland, and carbonylation in the gills (Tedesco *et al.* 2008), whilst nano-iron oxide (Fe₂O₃NPs, 50nm) increased lipid peroxidation (Kadar *et al.* 2010).

CeO₂ particles are unique in so much that the surface is composed of both Ce³⁺ and Ce⁴⁺ ions, which cycle their oxidation state. This cycling leads to an oxygen vacancy which can be filled, for example, by the superoxide free radical (O₂^{•-}), leading to a belief that CeO₂ can exhibit SOD-like activity and help ameliorate oxidative stress (Heckert *et al.* 2008). This mechanism was thought responsible for evidence of CeO₂ reducing oxidative damage in the livers of rats (Amin *et al.* 2011), in PC12 cell lines (Ghaznavi *et al.* 2015) and in nerve cells (Schubert *et al.* 2006), yet CeO₂ has also been shown to reduce the growth of the bacteria *B. subtilis* and *E. coli* but not *S. oneidensis*, despite both *E. coli* and *S. oneidensis* being Gram-negative (Thill *et al.* 2006).

In all it appears that the ability of Me(O)NPs to either induce or protect against oxidative stress is based on the organism to which they are exposed, and will also depend on the physico-chemical characteristics of the Me(O)NP being investigated (Gagnon and Fromm 2015). Further examples of such effects based on these properties will be detailed in the next section.

1.3 Specific Effects of Me(O)NPs on Marine Invertebrates and Bacteria

Marine organisms are divided into 32 phyla of the animal kingdom, in addition to having representatives in the Archaea, Bacteria, Chromista, Fungi, Plantae and Protozoan kingdoms (Appeltans *et al.* 2012). Despite their diversity and abundance, most studies have examined effects on a few representative species including *Pseudomonas* spp. (bacteria), *Thalassiosira* spp. (diatoms) and *Mytilus* spp. (bivalve mussels).

Organisms such as *Mytilus* are highly important in aquaculture as foodstuffs for humans. As such, uptake of Me(O)NPs that cause population instability or serve as a vector for trophic transfer can have wide-ranging implication on human health. What is surprising is that despite Crustacea forming part of the human diet, there has been little study concerning the effects of Me(O)NPs directed towards them. This section will highlight some of the work already carried out on marine invertebrates on Me(O)NP exposure, and a summary is given in Table 1.4.

1.3.1 Annelida

Annelids, such as the Polychaeta, are both sessile and motile habitat engineers, ingesting, processing and overturning a vast amount of sediment (Mermillod-Blondin and Rosenberg 2006). Polychaetes can be filter feeders, deposit feeders or errant scavengers and predators, and they are characterised by large, flowery external gills. Given the likely fate of NPs to agglomerate and/or fall out of the water column, organisms associated with the benthos may ingest these particles and become susceptible to their effects, or the particles may be clogged in their gills.

Following ingestion by the polychaete *Nereis diversicolor*, citrate-capped AgNPs (30 ± 5 nm; 250 ng/g sediment; 10 days) have shown agglomerations of particles in close association with the villi, and in the glycocalyx matrix of the worm's gut lumen (Garcia-Alonso *et al.* 2011). There were also single and agglomerated NPs close to the plasma membrane and in endocytotic pits. These pits were deemed responsible for the internalisation of the AgNPs, with evidence suggesting sequestration of the NPs in endosomes and lysosomes, which may lead to apoptosis after NP release to the cytosol following saturation of the lysosomes. Interestingly, endocytosis via clathrin mediation usually requires positively charged particles. These AgNPs were negatively charged, suggesting some change in the particle's charge following organism internalisation. Comparing the uptake of ionic silver against that of the AgNPs, this study also highlighted the association of Ag⁺ with metal-binding metallothionein proteins (MTLP), whilst AgNPs were associated with metal-rich granules and organelles. This may suggest either different uptake routes of aqueous and particulate silver, or that the study was not of a timescale to allow AgNP dissolution and sequestration within the MTLPs.

DNA damage in coelomocytes has also been demonstrated following a ten day exposure to AgNPs (PVP-capped, 20-200 nm), micron, and ionic Ag (1 – 50 µg Ag/g sediment), with genotoxic effects occurring at concentrations ≥ 25 µg/g in NP and micron exposures (Cong *et al.* 2011). In all cases the nano-form was deemed to be most toxic, hence positing a nano-scale effect not related to dissolution of Ag⁺. Although accumulation was similar for all forms of Ag,

bioaccumulation factors remained around 0.2, suggesting a non-accumulative equilibrium. Highlighted here also was the latent ability of *N. diversicolor* to partition and excrete heavy metals by way of granules, lysosomes, metallothioneins and coelomocytes, however the authors were unable to directly qualify by which method Ag could be detoxified.

1.3.2 Arthropoda

Although the arthropods comprise sea spiders and horseshoe crabs, it is the Crustacea e.g. crabs, prawns and lice, for which this phylum is most recognised in the marine environment. There are vast morphological differences between arthropods, resulting in a plethora of lifestyles and feeding methods, from benthic to sedentary, from scavenging to raptorial feeding (Barnes *et al.* 2001). Occupying all trophic levels, these organisms could be susceptible to trophic accumulation of NPs, uptake during ventilation, or through simple adsorption.

Most marine organisms have a microscopic, planktonic stage to their development, and it is at this stage that deleterious effects of NPs may have their greatest impact on future populations. 96 hour exposures have shown both ZnONPs (26.2 ± 5.1 nm,) and micron-ZnO (216.2 ± 73.2 nm, both at 4 & 40 mg/l) as more toxic to the nauplii of the copepod *Tigriopus japonicus* than to the amphipod *Elasmopus rapax* (Wong *et al.* 2010). The nauplii may have fed on bulk zinc agglomerates thereby enhancing their toxicity, whilst ZnONP colloids were also observed to limit movement by agglomerating on their shells. Comparisons between ZnONPs and ionic Zn (14 mg/l) were similar for both species suggesting that dissolved Zn was the main driver of toxicity, however since ZnONPs were more toxic to nauplii than ionic Zn, this suggests mechanical inhibition at the nanoscale. Reported LC₅₀ values of 0.37-1.19 mg/l are close to US regulatory standards of 0.08 mg/l (Table 1), and this has implications for acute release.

Agglomeration and sedimentation of NPs leaves benthic arthropods particularly at risk. The intertidal mud shrimp *Corophium volutator* showed significant reduction in growth, maturation and fecundity (Fabrega *et al.* 2012) following 100-day exposures to ZnONPs (35 ± 10 nm, 0.2 - 1mg/l). Zn was found in high

concentration in the hepatopancreas in insoluble sulphur-rich sphaerites – a common method of sequestration of heavy metals for detoxification in crustaceans. Full interpretation of the fate and behaviour of Zn in these experiments was complicated by the high and variable background concentration of Zn in natural waters and sediments. This issue was addressed by labelling the ZnONPs with ^{68}Zn (a non-radioactive stable isotope of Zn) allowing the ^{68}Zn ONPs and their contents to be quantified in different environmental compartments. Following a 7-day exposure in a model mesocosm, ^{68}Zn could be detected in all compartments (water, sediment, and body tissues) with significant uptake into sphaerites in the hepatopancreas. This showed that ^{68}Zn from ^{68}Zn ONPs was bio-available and was processed by the animals through normal physiological processes (Larner *et al.* 2012).

10 day exposures of the estuarine amphipod *Leptocheirus plumulosus* to ZnONPs (20-30 nm) and CuONPs (200-1000 nm) has produced LC_{50} values of 763 $\mu\text{g/g}$ (sediment) and 868 $\mu\text{g/g}$ respectively (Hanna *et al.* 2013). With only 20% mortality, no LC_{50} could be determined for nickel oxide NPs, despite 21% dissolution in 28 days. Whilst ZnONPs dissolved 65% in 3 days, copper dissolution was measured at only 1% in 90 days. This suggests dissolution as a driver of ZnONP toxicity, whilst CuONPs prove toxic regardless of dissolution. Comparing these LC_{50} values to Gottschalk *et al.*'s (2009) sediment loading model (Section 1.2.4) is comforting however, since loading estimations are only 3 ng Zn/g/yr.

Crustacea such as prawn and crab are organisms of high commercial importance, however mariculture is often blighted by bacterial infection. Exposing the tiger prawn *Penaeus monodon* to various gram-negative *Vibrio* bacteria twice daily for 2 days results in total mortality within 30 days (Kandasamy *et al.* 2012). However, exposure to *Vibrio* combined with bio-synthesised crystalline AgNPs ($11.3 \pm 2.1\text{nm}$; methoxy-compound-coated spheres; 300 $\mu\text{g/l}$) results in survival levels similar to those seen in unexposed prawns. Interestingly, those exposed to AgNP-only showed higher survival than control organisms. In all cases, exposure to AgNPs maintained or increased haemolymph phenol oxidase activity, as well as haemocyte counts. This suggests that AgNPs were taken up by the prawns, and may have been

responsible for reduced ATP production in the pathogens, as well as cell membrane damage through interacting with membrane-bound proteins. Haemolymph phenol oxidase activity suggest that some internal resistance occurred, but it was not determined if *Vibrio* were killed by AgNPs prior to ingestion i.e. within the feed mixture. Results indicate the antibacterial potential for bio-synthesised AgNPs in fish farms, although there is no knowledge of their long-term effects on the prawns, including the potential for bioaccumulation.

Dissolution of metal ions from Me(O)NPs (especially ZnONPs) appears to be a major driver of toxicity in arthropods, whilst sedimentation makes them more available to benthic organisms. Currently there is not enough data to assess the potential for trophic transfer in scavenging organisms such as crabs, however the suite of effects that NPs had on larvae, and at concentrations that may be present during acute exposure, suggests potential to wipe out populations at a very early life stage. Since the majority of marine organisms have a planktonic life stage, this could lead to far-reaching consequences across a host of creatures. Considering the commercial and ecological importance of arthropods, there is a distinct gap in our knowledge of how nanoparticles will affect these organisms, and their trophic transfer potential to higher species.

1.3.3 Bacteria

Bacteria are microscopic, single-celled organisms that play a highly important role in nutrient recycling, as well as being foodstuffs for many grazers. Any toxic effects from nanoparticles could impact local nutrient availability, whilst accumulation of these particles will make them available to higher trophic organisms.

AgNPs capped with biogenic proteins have proved to be more toxic than colloidal Ag to both Gram-positive (*Bacillus subtilis*) and Gram-negative (*Shewanella oneidensis*, *Escherichia coli*) bacteria, whilst oleate-capped AgNPs showed no toxic effects (Suresh *et al.* 2010). The reduced negative zeta potential of the biogenic-capped AgNPs may have aided their interaction with

negatively-charged bacteria, although the composition of the capping agent may also have played a role in toxicity.

Bacteria can be found as single organisms, or as single- or multi-species communities in biofilms. Biofilms act as safe havens for bacteria and provide signalling pathways to allow communities to better respond to their environment. Uncapped AgNPs (58.6 ± 18.6 nm; 1000 $\mu\text{g/l}$) had no effect on marine sediment biofilm assemblages over twenty days (Bradford *et al.* 2009), whilst citrate-capped AgNPs (65 ± 30 nm; 200 $\mu\text{g/l}$) significantly decreased the volume, biomass, and potential succession of bacteria in biofilms, but had little effect on the phylogenetic composition (Fabrega *et al.* 2011). The same citrate-capped AgNPs (2000 $\mu\text{g/l}$) caused significant growth reduction of the bacteria *Pseudomonas fluorescens*, and in this case toxicity was completely mitigated by the presence of humic acids (Fabrega *et al.* 2009), although such concentrations are not environmentally relevant. Further experiments on *Pseudomonas putida* biofilms at pH 7.5 suggested that fulvic acids increase the uptake of the AgNPs, but prevented bacterial cells from sloughing off the biofilm, and therefore decreased loss of biomass (Fabrega *et al.* 2009). AgNP agglomerates were observed at invaginations of the biofilm cell membrane, yet non-agglomerated AgNPs were observed inside the cell, suggesting there is a mechanism by which they can penetrate cell walls. Whilst these exposure concentrations have little environmental relevance, there is evidence of bacterial communities showing reduced growth when exposed to AgNPs (20 nm, polymer-coated) and ionic silver (Ag^+) at only 5 $\mu\text{g/l}$ (Doiron *et al.* 2012). However after 48 hours, growth recovered, likely due to the silver tolerance of certain species of bacteria which was highlighted by reduced species richness in the biofilm.

Studies on the effects of NPs on marine bacteria have so far all focussed on silver, given its prominence as an anti-microbial agent. Whilst most have used concentrations not relevant to the environment, there is evidence suggesting that AgNPs can inhibit growth of biofilms by targeting intolerant species, and at concentrations close to the regulatory limit (0.5 $\mu\text{g/l}$). The accumulation of NPs in biofilms will also make them available to grazers such as gastropods.

1.3.4 Echinodermata

A five day study exposing the sea urchin *Paracentrotus lividus* to tin oxide (SnO_2 ; 61 nm), CeO_2 (50-105 nm) and iron oxide (Fe_3O_4 ; 20-30nm) NPs at 10mg/l resulted in total mortality after only two days (Falugi *et al.* 2012). The animals could however be maintained for five days at 0.1 mg/l. All types of NP tended to agglomerate and were present in the digestive, immune and reproductive systems. Those in coelomocytes caused damage to the endoplasmic reticulum and Golgi apparatus. Fe_3O_4 NPs and CeO_2 NPs also caused the down-regulation of the immune system, and inhibition of cholinesterase (a biomarker of neurotoxic stress), although exposure concentrations were not environmentally relevant.

Despite not specifically using nanomaterials, the potential for Ce toxicity to urchins has been demonstrated (Oral *et al.* 2010). 100% mortality of *P. lividus* embryos was observed at 1720 $\mu\text{g/l}$ after 72 hours, whilst concentrations between 17.2 and 516 $\mu\text{g/l}$ resulted in abnormal mitosis, and developmental defects in offspring were concentration-dependent, whilst after only an hour sperm showed a decrease in fertilisation rate at 1720 $\mu\text{g/l}$. Similarly, exposures of *P. lividus* embryos exposed to 100 $\mu\text{g/l}$ of ionic Cu or 250 $\mu\text{g/l}$ of ionic Zn resulted in 100% mortality (Radenac *et al.* 2001). Certainly CeO_2 NPs are considered insoluble, however the dissolution potential of Cu^{2+} and Zn^{2+} from their NP form causes concern regarding exposure of sea urchin embryos. Some of the recorded effects on echinoderms are at concentrations within the regulatory limit. That these effects are on embryos has implications for population growth and stability, especially in coastal waters where inputs will be less diffuse.

1.3.5 Mollusca

Molluscs are one of the largest and most diverse marine phyla (incorporating squid, nudibranchs, limpets, snails and bivalves), and feeding habits include grazing, particle sorting, scavenging and hunting (Barnes *et al.* 2001). They can be either errant or sedentary, and they occupy all niches from exposed

rocky shores to deep oceans. This leaves them highly susceptible to coastal release, and sedimentation of, agglomerated Me(O)NPs.

1.3.5.1 *Bivalvia*

Bivalve water pumping rates can vary from 90 cm³/ hr (*Macoma nasuta*, 3.5 cm) to over 9.7 l/hr (*Mytilus californianus*, 9.2 cm) (Meyhöfer 1985) when filter feeding, leaving them highly vulnerable to ingestion of NPs from the water column. Bivalves normally feed on microplankton, raising the question of their uptake efficiency and selection of nano-size particles (Ward and Shumway 2004). Agglomeration enabled greater uptake of 0.5 - 1.0 µm particles by bivalves; clams (*Mercenaria mercenaria*) and mussels (*Mytilus edulis*) ingested more agglomerated particles than oysters (*Crassostrea virginica*) and scallops (*Argopecten irradians*), potentially due to post-capture particle selection methods (Kach and Ward 2008).

When embedded in agglomerates (> 100 µm - < 3 mm), *M. edulis* also uptakes NPs faster than *C. virginica* (Ward and Kach 2009). 100 nm beads have a longer gut retention time than 10 µm beads and are slowly egested over 72 hours, compared to 6 hours for the larger beads. This suggests particle sorting by the molluscs, with possible endocytotic uptake of the NPs by digestive cells. Many studies have synthesised marine snow in exposures, incorporating bacterial mucopolysaccharides to aid binding of small particles (Shanks and Edmondson 1989). Use of natural agglomerators for uptake may be unnecessary since *M. edulis* is capable of producing EPS as anionic, transparent exopolymer particles, and may therefore facilitate its own uptake of picoplankton as agglomerates (Li *et al.* 2008). Another theory infers that particle shape and charge may be more deterministic in uptake than particle size (Wegner *et al.* 2012). Availability to bivalves of NPs in agglomerates will likely be affected by NOM, agglomerate sinking rates, and frequency of re-suspension events i.e. storms.

Bivalve uptake of particles is primarily via the gills, following which they are sorted and sent to the digestive gland (Canesi *et al.* 2012). It could be expected that gills are a primary site for NP accumulation, however experiments with *M.*

edulis and AuNPs ($5.3 \pm 1\text{nm}$, $750\text{ }\mu\text{g/l}$) show accumulation primarily in the digestive gland (95%), with some in the gills (3.9%) and mantle (1.5%) (Tedesco *et al.* 2010). Similarly, in $\text{Fe}_3\text{O}_4\text{NP}$ (50 nm, polyethylene glycol capped, $370\text{ }\mu\text{g/l}$) exposures, *M. galloprovincialis* accumulated over 90% of the dose in its digestive gland within 8 hours, with over 75% still remaining following 72 hours depuration (Hull *et al.* 2013). NPs also penetrated the haemolymph, with 50% loss following depuration. In exposures with radio-labelled AgNPs ($< 40\text{nm}$, $0.7\text{ }\mu\text{g/l}$), 60% of the uptake accumulated in the soft tissues with maximum concentration in the digestive organs, whilst some 7% was found in the mussel's extrapallial fluid (Zuykov *et al.* 2011). When a mussel closes, it retains some water within the shell to keep the organism moist, and this extrapallial fluid can contain a number of different compounds, including amino acids, carbohydrates, peptides and other (in)organics (Zuykov *et al.* 2011). Over 90% of the Ag recovered in the fluid in this study was retained by a 3 kDa filter, suggesting Ag may be complexed by the high molecular weight organics found in the fluid.

Comparisons between Me(O)NPs and their ionic counterparts shows that form affects different organs. The bivalve *Ruditapes philippinarum* accumulates AuNPs ($21.5 \pm 2.9\text{ nm}$, citrate-capped; $6\text{--}30\text{ }\mu\text{g/l}$) more readily in digestive gland heterolysosomes (plateauing after 12 hours), whilst ionic Au was more associated with the gills (Garcia-Negrete *et al.* 2013). Use of glass NPs to study uptake in *M. edulis* effectively removes dissolution potential, thereby purely focusing on particle size. Glass NPs have been found in gill epithelial cells and digestive tubules, with cilia and microvilli aiding NP transfer to the hepatopancreas (Koehler *et al.* 2008). Evidence of NPs in the mitochondria, nucleus, and in endosomes suggests diffusion (of NPs $< 5\text{nm}$) and endocytosis ($5\text{--}25\text{nm}$) as methods of intracellularisation. NP-filled lysosomes also demonstrated agglomeration and apoptosis following a decrease in lysosomal stability, whilst increased lipofuscin levels and oxidative stress were noted in epithelial cells.

Oxidative stress is associated with dissolution of metal ions, yet such stress has also been demonstrated with insoluble NPs. After 24 hours exposure, gold (Au) NPs ($5.3 \pm 1\text{nm}$, $750\text{ }\mu\text{g/l}$) decreased thiol group availability of digestive gland

proteins in *M. edulis*, either through binding affinity, or through production of ROS (Tedesco *et al.* 2010). Currently there are no specific regulatory guidelines for Au release. It may be classed as 'other benign substances', and subject to a limit of 3 mg/l (O'Brien and Cummins 2010). At concentrations a quarter of this, these AuNPs also compromised lysosomal membrane stability, whilst increases in malondialdehyde, a by-product of lipid peroxidation, were observed. AuNPs (13nm) have also induced CAT activity in the digestive gland of *M. edulis*, and carbonylation in the gills (Tedesco *et al.* 2008). Similarly, CuONPs (197 nm, 10 µg/l) show accumulation in the bivalve *Scrobicularia plana* as well as increasing GST, CAT and superoxide dismutase (SOD) activity (Buffet *et al.* 2011). Although often soluble, these particular CuONPs demonstrated no dissolution, hence oxidative stress was a by-product of the nano-size. These NPs also had a significant effect on burrowing by *S. plana*, and impaired feeding rate.

In vitro studies on excised *M. edulis* gills (Kadar *et al.* 2010) have shown little difference in effect between nano-iron oxide (Fe₂O₃NPs, 50nm, 1000 µg/l) and iron chloride (Fe₂Cl₃, 100 µg/l). Over 90% of both were removed from the water column, both increased lipid peroxidation (if not significantly), and both increased size and number of blood cells. The nano-form also deposited on blood cell membranes, caused shrinkage of epithelial cells, and accumulated in small packages within granulocytes throughout the cytoplasm, whilst soluble Fe instead accumulated in electron-dense deposits mostly in lysosomes. The major difference highlighted here is route of uptake, as soluble Fe ions may enter the cell through clathrin-coated receptors and are then directed to dense, membrane bound granules. Fe₂O₃NPs however were taken up through pinocytosis, hence their random distribution in the cytoplasm. This in itself was believed to have severe effects on cell integrity over the long term.

In vivo work exposing *M. galloprovincialis* to TiO₂NPs (15-60nm, 96 h) has demonstrated that whilst oxidative stresses in the digestive gland occurred at 1 µg/l concentrations, these stresses could generally be dealt with by the mussel (Barmo *et al.* 2013). There was also an effect on gene transcription in the digestive gland. Of note is that these effects occurred at environmentally-relevant concentrations. Other studies with TiO₂NPs (22 nm) and *M.*

galloprovincialis highlight increases in neutral lipid content, significant reduction in lysosomal stability (in hematocytes) at concentrations $\geq 1\text{mg/l}$, and in the digestive gland at $\geq 0.2\text{ mg/l}$ (Canesi *et al.* 2010). Increases in lipofuscin were seen with both TiO_2 and silica dioxide (SiO_2 , 12 nm) NPs at $\geq 1\text{mg/l}$. SiO_2NPs showed significant CAT activity $\geq 0.2\text{ mg/l}$, an effect mirrored with 1mg/l TiO_2NPs , although TiO_2NPs stimulated GST activity $\geq 0.2\text{ mg/l}$. The primary target here was the digestive gland, with fewer effects seen in the gills. Interestingly, there are no regulatory limits for silicon, despite effects seen at low concentrations.

Comparing CuONPs ($31 \pm 10\text{ nm}$) and ionic Cu at $10\text{ }\mu\text{g/l}$, *M. galloprovincialis* exposures also highlight the effect of form on type of oxidative stress caused (Gomes *et al.* 2012). CuONPs were responsible for lower SOD activity than ionic Cu, whilst significant increases in both glutathione peroxidase (GPX) and CAT activity only occurred after seven days with both forms, but with contrasting results after fifteen days. Both caused lipid peroxidation, but whilst MT presence increased linearly with CuONPs, it was only noted after day fifteen with ionic exposure. Twice the concentration of CuONPs was seen in the gut compared to the gills, suggesting some selective particle sorting. NP agglomeration was highlighted as the main cause of toxicity. At $10\text{ }\mu\text{g/l}$ this dose is also very close to the UK regulatory limit ($5\text{ }\mu\text{g/l}$, Table 1.2).

In contrast, dissolution was the cause of oxidative stress in 48 hour exposures of *C. virginica* to AgNPs ($15 \pm 6\text{ nm}$, citrate-capped). Impaired embryonic development at $1.6\text{ }\mu\text{g/l}$ was demonstrated, with a significant dose-dependent lysosomal destabilisation of adult hepatopancreas cells at concentrations above 160 ng/l (Ringwood *et al.* 2010). At the same concentration, MT expression was found to be over twice as high in exposed adults, and a significant eighty times greater in exposed embryos. Whilst actual embryo development may not be affected until $1.6\text{ }\mu\text{g/l}$, oxidative stress can be induced at concentrations within the regulatory limit (500 ng/l).

Also at a relevant concentration ($10\text{ }\mu\text{g/l}$), CuONPs ($<50\text{ nm}$) and AgNPs ($<100\text{ nm}$) show accumulation and haemocyte damage in *M. galloprovincialis* following chronic exposure (water changed and re-dosed every 12 hours for 15

days), and this is principally related to length of exposure (Gomes *et al.* 2013a). Ionic copper showed the greatest effect, likely through ROS production, whilst the similarities between AgNPs and AgNO₃ exposures suggest dissolution as a driver of toxicity. However AgNPs also caused damage to different proteins than AgNO₃ highlighting a nano-effect not explained by simple dissolution (Gomes *et al.* 2013b). Exposures (1-400 µg/l) of AgNPs (26 nm) and TiO₂NPs (70 nm) have shown significantly reduced phagocytosis in the haemolymph of *C. virginica* compared to the control, with little difference between nano and ionic Ag (Abbott Chalew *et al.* 2012). Phagocytosis is an important part of removal of foreign objects for health of the organism, although it can also result in pathogen uptake.

Evidence exists of NPs causing oxidative stress yet bivalves, as do many marine organisms, use Zn as a micronutrient and may make use of metal ions dissolved from the NPs (Montes *et al.* 2012). Despite no effect on feeding rate, experiments with *M. galloprovincialis* suggested uptake of CeO₂NP rods ($67 \pm 8 \times 8 \pm 31$ nm) was greater than that of ZnONP spheroids (24 ± 3 nm) at all concentrations (1 - 10 mg/l). Even with lower uptake, Zn was retained far more readily than Ce. Only 1.5 - 4.1 µg Ce/g (dry weight) were accumulated at concentrations of 1 - 5 mg/l (with a significantly different 61.6 µg/g at 10 mg/l), whilst Zn accumulation was between 250 - 880 µg/g, significant with increasing concentration. The need for Zn as a micronutrient will have influenced its higher retention.

In Bivalves pseudofaeces production occurs as the last step in sorting edible particles, and then as a method of preventing the gills from over-clogging when in waters of high particle density (Wegner *et al.* 2012). Exposures to the CeO₂NPs resulted in hard pseudofaeces studded with NP-agglomerates, whilst ZnONP exposures produced soft gels with evenly distributed NPs (Montes *et al.* 2012). For both NP types the concentrations in pseudofaeces were much higher than those accumulated in soft tissue, increasing with increasing exposure concentration, however a sharp increase of Zn was seen in the pseudofaeces after the 72 and 96 hr exposure. This again suggests the mussels make some use of the dissolved Zn and egest superfluous material following saturation, and as such their accumulation rate appears to decrease

over time. Either way, the mussel transforms free particles into highly concentrated pseudofaeces that become more bioavailable to benthic organisms, and may complex with other organics.

The fate of NPs in bivalves appears related to both particle capture efficiency and to dissolution propensity (Table 1.4 details a more comprehensive list of effects of Me(O)NPs on bivalves). Work on metal uptake has suggested ionic Zn and Cd are taken up effectively due to facilitated transport, whilst anionic metals (selenium, chromium) compete for uptake with anions in seawater such as Cl^- and SO_4^{2-} (Wang 2001). There also may be a species-specific coupling, with the black mussel (*Septifer virgatus*) shown to accumulate Zn and Cd simultaneously to the same extent, supposedly via the same calcium channels. In the case of tissue distribution of NPs, it has already been shown that micron-scale plastic spheres can be transferred to the haemolymph of *M. edulis*, and that smaller particles are transferred more effectively (Browne *et al.* 2008). As such there is potential for NPs to enter the haemolymph and be distributed internally. There may also be intracellular ingestion of NPs via phagocytosis, leading to lysosome perturbation, membrane destabilisation, and oxidative stress in the form of lipid peroxidation and the reduction of thiol proteins. However, many organisms e.g. scallops, are already known to have detoxification processes for metal contaminants through metal-rich granule formation (George *et al.* 1980), hence further studies into detoxification are required.

Exposure of mussel larvae to Fe_2O_3 NPs and Fe_2Cl_3 has demonstrated a protective effect against toxicity with increasing acidity (Kadar *et al.* 2010). Whilst no effect was detected at pH 8.1 (natural seawater), at pH 7 the Fe_2O_3 NPs (40.1 ± 1.3 nm, 8 - 800 $\mu\text{g Fe / l}$) significantly increased shell development, an effect mirrored at pH 6 for soluble iron. The authors hypothesise that agglomerations of both forms of iron scavenge compounds that cause toxicity at lower pH, or may buffer pH changes around the cell. Such protection has implications considering long term ocean acidification, or acute acidic run-off.

1.3.5.2 Gastropoda

Gastropods are a highly diverse Class of molluscs that include limpets, whelks, periwinkles, abalones, venomous cone shells, and the shell-less “sea slugs” e.g. nudibranchs and sea hares. Feeding regimes vary from filter feeding, to grazing, to active predation of large (in)vertebrates. Slipper snails (*Crepidula fornicata*) have been shown to take up 0.5µm beads with great efficiency, however comparative studies that fed them similar-sized *E. coli* (300 – 800 nm) highlights difficulty in capturing particles <500 nm (Kach and Ward 2008). This suggests NPs are unlikely to be accumulated, albeit this is based on extrapolation of results from a single study concerning a suspension-feeding gastropod, and using insoluble particles.

Studies with the common rocky shore herbivore *Littorina littorea* (periwinkle) suggest AgNPs (58±27 nm, 20µg/l) do not accumulate in the organism following aqueous exposure, but some may adhere externally to the head and gills (Li *et al.* 2012). High Ag concentrations in the faeces do suggest uptake (likely through feeding on micronutrients or debris), yet none of the metal is retained. When feeding on *U. lactuca* contaminated with AgNPs there was no significant bioaccumulation from trophic transfer. Comparative studies with AgNO₃ suggested that the Ag⁺ ion determines Ag accumulation by *L. littorea*, and that more Ag is taken up via aqueous exposure than is accumulated through trophic transfer.

Exposure of the abalone *Haliotis diversicolor supertexta* to uncapped TiO₂NPs (≤ 10 nm; 96 h) has demonstrated increased lipid peroxidation with increasing concentration, with GSH activity significantly lower at concentrations ≥ 1 mg/l (Zhu *et al.* 2011). Most interestingly there was an increase in nitric oxide production at ≥ 1 mg/l, which has been linked to oxidative stress. Unfortunately, no comparison with soluble or micron TiO₂ means toxicity may not be directly related to a nano-form.

ZnO, Cu and AuNPs have caused oxidative stress in bivalves at concentrations close to the regulatory limit. NPs can also adhere to the soft tissues of gastropods with potential for localised dissolution, yet oxidative stresses

following this are so far unstudied. Given the variety of form and feeding in Molluscs, studies are desperately needed in other Classes. Cephalopods for example have a natural affinity for rare earth elements such as Ce (Oral *et al.* 2010).

Organism	Uptake Method and Effects
Bacteria	Gram-positive bacteria more susceptible than Gram-negative. NPs may affect the composition, but not function, of biofilms, but accumulation may make them available to predatory grazers
Algae	NPs may adsorb to cell surfaces. Ions dissolved from NPs can interfere with nutrient uptake and therefore limit growth. Negative charge on diatom casings may attract dissolved cations.
Arthropods	NP adsorption to nauplii limits movement; Nauplii may feed on NPs. Zn^{2+} dissolution a driver of sub-lethal toxicity.
Annelids	Ingestion of sedimented NPs by deposit feeders, and of floating NPs by filter feeders. Sub-lethal effects seen even with insoluble NPs.
Bivalves	NPs trapped by EPS; some stay trapped in gills, some transferred to the digestive system, most rejected into pseudofaeces. May use some dissolved Zn^{2+} as a micro-nutrient. Oxidative stress noted even with insoluble NPs.
Gastropods	Adsorption to body may cause oxidative stress <i>in situ</i> . Not significant accumulators in mesocosm studies
Echinoderms	Down-regulation of immune system in adults; ion dissolution may cause larval mortality in chronic exposures.
Stenohaline Fish	May lodge in gill mucus and dissolve. NPs accumulate in the gut following drinking; carbonate production may biotransform and release dissolved ions.
Euryhaline & Diadromous Fish	Ion dissolution interferes with change in gill function moving from full marine to fresh water. Encourages stress-related drinking, leading to uptake of NPs in the gut.
Mesocosms	Bivalves and biofilms suggested as major NP accumulators in simple mesocosm studies, based upon mass:accumulation ratios.

Table 1.4: A summary of potential uptake methods and effects of nanoparticles on various marine organisms

1.4 Trophic Transfer

Trophic transfer relates to the accumulation of chemicals/toxicants etc. by an organism following consumption of another organism previously exposed to those factors. The complexity of marine food webs means that most organisms are both predators and prey, hence trophic accumulation could involve a variety of sources. Micro-organisms such as algae form the base of most food webs, hence NP accumulation by these organisms could lead to widespread transfer. The copepod *Acartia tonsa*, for example, demonstrates reduced reproduction and increased mortality following consumption of diatoms laced with ionic Ag (0.64 µg/l), Cu (1.2 µg/l), Zn (0.3 µg/l) and nickel (2.4 µg/l), and at concentrations relevant to environmental guidelines (Bielmyer *et al.* 2006). Trophic transfer of quantum dots from ciliate protozoans to rotifers, and subsequent presence in rotiferan endosomes has also been demonstrated (Holbrook *et al.* 2008). Transfer from bacteria (*E. coli*) to ciliates could not be shown, since the surface coating of the quantum dots may have been unsuitable for uptake by the bacterium's usual membrane transport systems. Regarding bivalves, *S. plana* accumulates more AgNPs (40 nm, 10 µg/l, 15 days) in the cytosol when exposed via water, than it does when exposed via microalgal feed (Buffet *et al.* 2013). No significant effect on feeding rate was recorded compared to the control, however CAT activity was significantly higher in both exposures, whilst GST and SOD activity increased in dietary exposures. Given dissolution of the AgNPs, similarities in effect with ionic silver highlight Ag⁺ as the driver of toxicity.

Bacterial biofilms have been mentioned as uptake sites for NPs, and were the greatest accumulators (> 60%) of AuNPs (rods, 65 x 15 nm, dose concentration not recorded) in mesocosm studies (Ferry *et al.* 2009). Low uptake by the Eastern mud snail *Ilyanassa obsoleta* (0.05%) was surprising given its grazing habits on biofilms. Uptake by the minnow *Cyprinodon variegatus* was low and confined to the digestive system (likely through drinking), with little concentration in either the grass shrimp *Palaemonetes pugio* or the cordgrass *Spartina alterniflora*. Juvenile clams (*M. mercenaria*) managed to accumulate over 5% of the AuNPs despite only accounting for 0.01% of the total biomass of the system (including water and sediment), again underlining filter feeders as

organisms linked to potential high uptake of NPs and subsequent biotransformation.

Given the number of consumer products (CPs) containing NPs, it is worth examining the effect of discarded CPs on marine organisms. A recent study assessed AgNPs and ionic Ag in an estuarine mesocosm, as compared to socks, teddy bears and sticky plasters containing AgNPs (Cleveland *et al.* 2012). Whilst AgNPs (20, 80nm) and Ag⁺ were rapidly removed from the water column, the CPs continuously leached silver for over thirty days. Ionic Ag had very little effect on the shrimp *P. pugio*, with highest body concentrations from CPs and 20nm AgNPs. Cordgrass (*S. alterniflora*) stalks showed only minor accumulation after sixty days exposure to 20nm AgNPs, and a slight significant accumulation in the leaves following exposure to the toy bear after sixty days, and to the sticky plaster after both forty eight hours and sixty days.

Importantly this study again highlighted both biofilms and bivalves as major accumulators of NPs. Biofilms contained elevated Ag levels for a day after CP exposure and for a week after NP exposure, although Ag⁺ had no effect on burden. Whilst CP-exposed snails maintained high body burdens of Ag (presumably from trophic transfer following consumption of biofilms), those exposed to AgNPs and ionic Ag took up, then depurated, excess silver over time. Filter-feeding juvenile hard clams (*M. mercenaria*) in NP and CP treatments maintained high tissue concentrations of Ag, however clams exposed to ionic Ag showed no body concentration, yet after only thirteen days 90% of these had surfaced and died. Adsorption of silver from the sand, rather than direct uptake, was believed to be responsible for the mortality. The sand itself contained no significantly higher burden of silver compared to the controls; the highest burdens recorded were associated with CPs, most likely through constant leaching (82 - 99% over sixty days). This study highlights the variation of effects on different species not only by different delivery methods of silver (ionic, NP, CP), but also that size of the NP, dissolution, and the manufacturing process of CPs will make a difference to the availability and effects of NPs in marine systems.

The issue of trophic transfer and NPs is particularly complex. One organism may consume many different food sources for instance, and there is some evidence of freshwater snails avoiding NP-contaminated foodstuffs (Croteau *et al.* 2011). Whether this is an active avoidance, or a side-effect of digestive damage is unknown, as is their propensity to switch to another food source. There is also still a need to first understand single organism uptake and simplified food chains before investigating and quantifying bioaccumulation in mesocosms and food webs.

1.5 Conclusion

Nanoparticle toxicology in aquatic systems is complex. In the first instance particle size, shape, chemistry and capping agents will all play a role regarding the stability, and thus bioavailability, of the NP within any media. Release kinetics then become a factor as NPs are complexed into hetero-agglomerates along the course of a river, with mobility and agglomeration determined by the molecular weight of natural organic matter in the water. As ionic strength increases in the pathway to estuaries and oceans, so zeta potential decreases, causing agglomeration and promoting rapid sedimentation.

Essentially nanoparticles are unlikely to remain nano-sized in exposures to marine organisms. They agglomerate with increasing salinity, thereby reducing surface area for dissolution. Dissolved metal cations e.g. Ag^+ are also likely to be complexed by e.g. free chlorine anions in salt waters, limiting impact to situations where particles are adsorbed or internalised, then dissolve *in situ*.

As such the likely fate for many agglomerated NPs is the benthos, with implications principally for in-fauna and associated biota. In particularly dynamic environments e.g. estuaries, NPs could be re-suspended thereby making agglomerated NPs available to many other organisms in the water column. Filter, suspension and deposit feeders have been shown to uptake both nano and micron-size particles during feeding, other invertebrates may suffer from clogged gills during ventilation (Fig 1.4).

The four major ways in which nanoparticles may interact with an organism are: 1) adsorption to the surface (cell, organ or body), 2) cellular internalisation (absorption), 3) dissolution of ions from the NP and 4) mechanistic nano-effects (Fig 1.4). At the cell surface NPs may be taken up across cell membranes by pinocytosis or phagocytosis. If proteins in the water column adsorb to them, they may be taken across by receptor-mediated transport. Dissolution of the NP could lead to direct diffusion, or they might be taken across by ion channels, actively competing with other ions the cell requires. Otherwise, NPs may simply adsorb to the surface (smothering), thereby reduce membrane function (Fig 1.5)

Whilst mortality has only been recorded at concentrations exceeding environmental relevance, oxidative stress has been observed at levels well within regulatory limits. This suggests a nano-effect not explained by the dissolution of metal ions, and hence negates the use of the BLM alone to evaluate toxicity.

Whilst there are clear and major gaps in our knowledge of the effects of Me(O)NPs on marine organisms, information is being gathered slowly. Limited studies on bacteria suggest Gram-positive are more susceptible than Gram-negative, whilst effects on algae are dependent on particle type, dissolution, and the propensity to compete with other ionic nutrients for uptake. By far the majority of invertebrate testing has involved bivalves (in particular *Mytilus* spp.), whilst effects on vertebrates have been confined to a few estuarine fishes e.g. *C. variegatus*, *O. melastigma*. In trophic transfer mesocosm studies it is bivalves and biofilms, not gastropods and fish, which appear to be the major accumulators of Me(O)NPs, despite gastropod grazing habits on biofilms. This however leaves many species, many phyla, and even other kingdoms untested with regards to the effects of Me(O)NP (especially the Cnidaria, which incorporates corals, anemones and jellyfish). Other combination factors such as nutrient availability, pressure, temperature and pH have not been investigated at all. Perhaps the greatest threats recorded have been to embryos, likely due to their small size, and at concentrations realistic for acute exposure. Embryos of many marine species settle in shallow coastal waters, putting them most at risk from point source NP discharges.

The oceans are a vast resource containing innumerate food webs. Current data indicates that NPs can have highly adverse effects on key organisms such as primary producers, damage to which would have far-reaching impacts not only on nutrient production and food availability in marine trophic webs, but also on carbon and silicon cycling. The agglomeration properties of NPs make them directly available to larger organisms, whilst their uptake and adsorption properties also allows micro-organisms to become vectors for delivery to higher organisms through trophic transfer.

Current anthropogenic discharge of Me(O)NPs is not of a volume that chronic exposure would be expected to be harmful to marine organisms. Acute exposures may have an extremely localised impact, but the diffuse nature of the oceans means effects will not be widespread. It is potentially only on beaches where continuous use of sunscreen may expose a large number of organisms to raw Me(O)NPs following immersion, yet such scenarios are understudied. This is not to say that Me(O)NPs could not become problematic, given that manufacture, and release, of NPs is set to dramatically increase in the coming years. A fuller understanding of the long term consequences of these particles in the marine environment is warranted and, importantly, also a need to relate the effects and release of these NPs to biomarkers in ecologically relevant species that can be used to inform on potential impacts on marine systems.

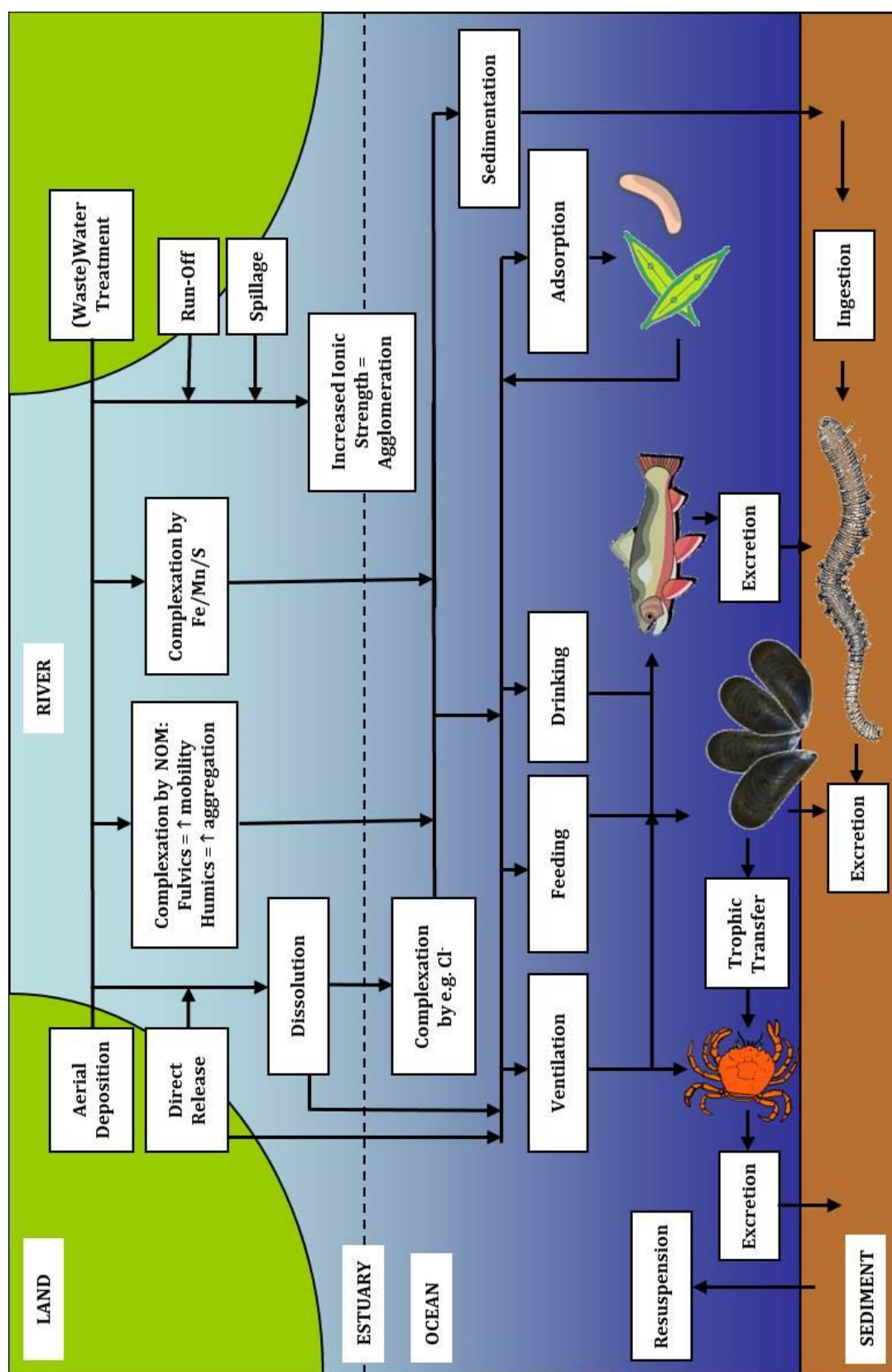


Fig 1.4: Sources of Nanoparticle release, their behaviour, and potential uptake routes for organisms in the marine environment

1.6 Aims and Objectives

The Literature Review highlights some important issues with regards to NP toxicity in the marine environment, including biotransformation of particles, the vulnerability of bivalves to nanoparticle discharges, and the potential for trophic transfer through marine food webs.

The aim of this thesis is to evaluate the bioaccumulation and biological effects of Me(O)NPs in a simple marine food chain. This aim will be addressed through the use of a marine bivalve, the common blue mussel *Mytilus edulis*, and its predator the shore crab *Carcinus maenas* (further rationale behind choice of these organisms is given in Chapter 2).

These organisms will be used to fulfill the following objectives:

1. To assess the accumulation potential of CeO₂NPs and AgNPs by the mussel *M. edulis*. It is hypothesized that maximum uptake will be in the digestive gland after 4 hours.
2. To assess the biological effects of Me(O)NPs on the mussel *M. edulis*. It is hypothesized that CeO₂NPs have an anti-oxidant effect, whilst AgNPs will induce oxidative stress. Both this and the previous objective are discussed in Chapters 3 and 6.
3. To assess the potential for trophic transfer of CeO₂NPs between *M. edulis* and *C. maenas*. It is hypothesized that the digestive organs of the crab will be a site of major accumulation of CeO₂NPs following trophic transfer.
4. To assess the biological effects of CeO₂NPs on *C. maenas* following trophic transfer. It is hypothesized that there will be limited biological effects due to low retention following trophic transfer. Both this and the previous objective are discussed in Chapters 4 and 5.

The ability for *M. edulis* to accumulate Me(O)NPs in its major organs will be assessed through a series of controlled feeding studies. Subsequently the biological effects of these particles will be appraised around the point of maximum accumulation. The feasibility of the consumption of *M. edulis* by *C. maenas* will be investigated, and methodology for further experimental work

drawn from this data. Understanding trophic transfer will be through examining where Me(O)NPs accumulate in *C. maenas*, how they reach these tissues, and what consequential biological stresses they place on them.

Initially these objectives will be examined using insoluble CeO₂NPs since insoluble particles reflect the effect of nano-size without interference from ion dissolution. This makes them useful in tracing particle movement through an organism. Due to the high background concentrations of Ce, exposing organisms to these particles at concentrations towards environmental realism is challenging. As such methodology has been developed to analyze uptake and tissue partitioning using isotopically-labelled (non-radioactive) CeO₂NPs which allows tracking of the NPs within our experimental setup with precision. This allows for the detection of accumulation even when high background concentrations of the metal ion exist.

Exposure studies will also be performed using soluble AgNPs of varying morphology. This will allow for understanding of the way in which size, shape and solubility may affect the uptake by, and subsequent biological effects induced in, *M. edulis*. Given the lower background concentrations of silver generally found in bivalves, there is feasibility here to expose at concentrations close to both environmental realism and regulatory guidelines for silver release.

Chapter 2 outlines the rationale behind both the organisms of choice (the mussel *M. edulis* and the crab *C. maenas*) and the Me(O)NPs (CeO₂NPs, AgNPs, and their characterization data) used throughout the experiments in this thesis. It also introduces the methodology used to expose these organisms to the various Me(O)NPs, and the assays and statistical tests used to investigate oxidative stress and lipid peroxidation.

Chapter 3 details a series of experiments to assess the uptake of CeO₂NPs by adult *M. edulis* over time, as a factor of size and concentration, and examines the subsequent reduction or increases in biological effects (oxidative stress and lipid peroxidation) caused by these NPs. The results from these experiments are used to govern exposure conditions necessary to investigate the potential for trophic transfer in later chapters.

Chapter 4 describes a series of experiments whereby adult *M. edulis* are first exposed to CeO₂NPs, then subsequently fed to their predator, the crab *C. maenas*. These experiments provide information on how CeO₂NPs can be trophically transferred from a mussel to a crab, and highlights both the organs and tissues of the crab of greatest uptake, as well as the subsequent biological effects (oxidative stress and lipid peroxidation) induced in the crab as a result of consuming the NP-laden mussels. Also included is a study on the accumulation of CeO₂NPs by *C. maenas* through aqueous exposure, and subsequent biological effects.

Chapter 5 uses a novel method of stable isotope-labelled CeO₂NPs to determine uptake of CeO₂NPs by *M. edulis* and subsequent trophic transfer to *C. maenas* at concentrations towards environmental realism, as well as subsequent biological effects. This method is imperative when dealing with exposure of organisms to concentrations of toxicants that are closer to or lower than the natural background concentrations found in the organism.

Whilst Chapters 2-5 have employed insoluble CeO₂NPs, Chapter 6 examines the uptake of soluble AgNPs by *M. edulis* in order to ascertain whether subsequent biological effects (oxidative stress and lipid peroxidation) are caused simply by dissolution of the particle into an ionic form, or whether a separate nano-effect exists due to the size of the particles used. Also examined are the differences caused by AgNP morphology, whereby uptake and effects induced by spherical particles are contrasted against those caused by nanorods.

Chapter 7 concludes the thesis, highlighting the place of this novel research in an emerging field, explores the limitations of the research, and makes recommendations for future study.

Chapter 2: Materials and Methods

2.1 Choice of Me(O)NPs and Me(O)NP Properties

This section details the characterisation of the CeO₂NPs used in Chapters 3 & 4 that were provided by the Nanomaterials Repository of Reference Materials Catalogue of the Joint Research Council (JRC), Belgium, the isotopically-labelled ¹⁴⁰CeO₂NPs specifically manufactured for use in Chapter 5, and the Ag-nanoforms used in Chapter 6 that were also supplied by the JRC. With regards to imaging of all the particles, Transmission Electron Microscopy (TEM) images were taken using a JOEL JEM-1400 TEM with a Gatan ES 100W CCD camera at the University of Exeter Bio-imaging suite. Particle sizing was accomplished by analysing the images using Image-J software (Rasband 1997-2015).

2.1.1 JRC Cerium Oxide NPs

Cerium oxide (CeO₂) NPs are used in diesel fuels to reduce particulate emissions (Park *et al.* 2008), and are also used as glass polishers, as metal purifiers, and in heat-resistant coatings (EPA 2009). Measurements of European streams have shown median Ce background levels of 55 ng/l (FOREGS 2005). The use of CeO₂NPs in diesel fuels has been estimated to add an almost negligible 0.02ng Ce/l to waterways, although certain conditions involving high rainfall washing across roads could increase this to 300 ng/l (Johnson and Park 2012) and have implications for any bodies of water close to roadways. Currently there are no guidelines regarding the release of CeO₂, however a regulatory limit of 3 mg/l is suggested based upon Surface Water Directive limits for other benign materials (O'Brien and Cummins 2010).

CeO₂NPs are considered virtually insoluble in fresh and salt waters (Zhang *et al.* 2012) hence any effects caused by them will not be a result of ion dissolution. This allows their use as an effective biomarker since loss through dissolution is negligible at neutral pH, however biological effects on organisms may still be caused due to their highly reactive surface. As detailed in Chapter

1.2.4, the surface of the particle is subject to spontaneous redox cycling between Ce^{3+} and Ce^{4+} . This gives it both pro- and anti-oxidative properties with the potential for causing or preventing oxidative stress (OS) in an organism (Korsvik *et al.* 2007).

CeO_2NPs used during method development and in Chapters 3 & 4 were supplied by the JRC and comprised of (nominally) 10nm (NM-211), 28nm (NM-212) and 600nm (NM-213, micron-size comparison) particles. These particles have previously been well-characterised by the JRC (Singh *et al.* 2014); Table 2.1 highlights some of the major differences between their properties.

	NM-211 Nano- CeO_2	NM-212 Nano- CeO_2	NM-213 Micron- CeO_2
CAS / EINECS	1306-38-3 / 215-150-4		
XRD Crystallite Size (nm)	10.1	33.3	33.3
Mean Feret's \varnothing from SEM (nm)	-	28 ± 10	600 ± 400
CPS Size (DI, nm)	340 ± 50	135 ± 4	570 ± 80
CPS Size (SW, nm)	520 ± 90	187.6 ± 1.7	650 ± 80
BET Specific Surface Area (m^2/g)	66 ± 2	27.2 ± 0.9	4.3 ± 0.1
Zeta Potential (DI, mv)	28 ± 2	33 ± 2	-7 ± 6
Half-life Stability (DI, mins)	780	2676	432
Half-life Stability (SW, mins)	534	288	294
XPS Ratio ($\text{Ce}^{4+}:\text{Ce}^{3+}$)	94.3 : 5.7	93.1 : 6.9	92.0 : 8.0
Ce^{3+} Specific Surface Area (m^2/g)	3.76	1.88	0.34

Table 2.1: Properties of the JRC NM-Series of CeO_2NPs (CAS = Chemical Abstracts Service; EINECS = European Inventory of Existing Commercial Chemical Substances; XRD = x-ray diffraction; SEM = scanning electron microscope; CPS = disc centrifuge; BET = Brunauer-Emmett-Teller; mv = millivolts; DI = deionised water; SW = saltwater; XPS = X-ray Photoelectron Spectroscopy (Singh *et al.* 2014)

NM-211, NM-212 and NM-213 were supplied as dry powders. Prior to use in any experiment or imaging, all CeO_2 particles were dispersed according to a method adapted from the PROPSPECT Protocol for Nanoparticle Dispersion (PROSPEcT 2010). Briefly, a few drops of DI water were added to 150mg CeO_2 and mixed into a thick paste with a glass rod. A further 100ml of DI was then added and mixed thoroughly. This was then sonicated (Cole Parmer CPX130 Ultrasonic Processor, 20khz, 90% amplitude) on ice for twenty minutes immediately prior to use to make a stock solution.

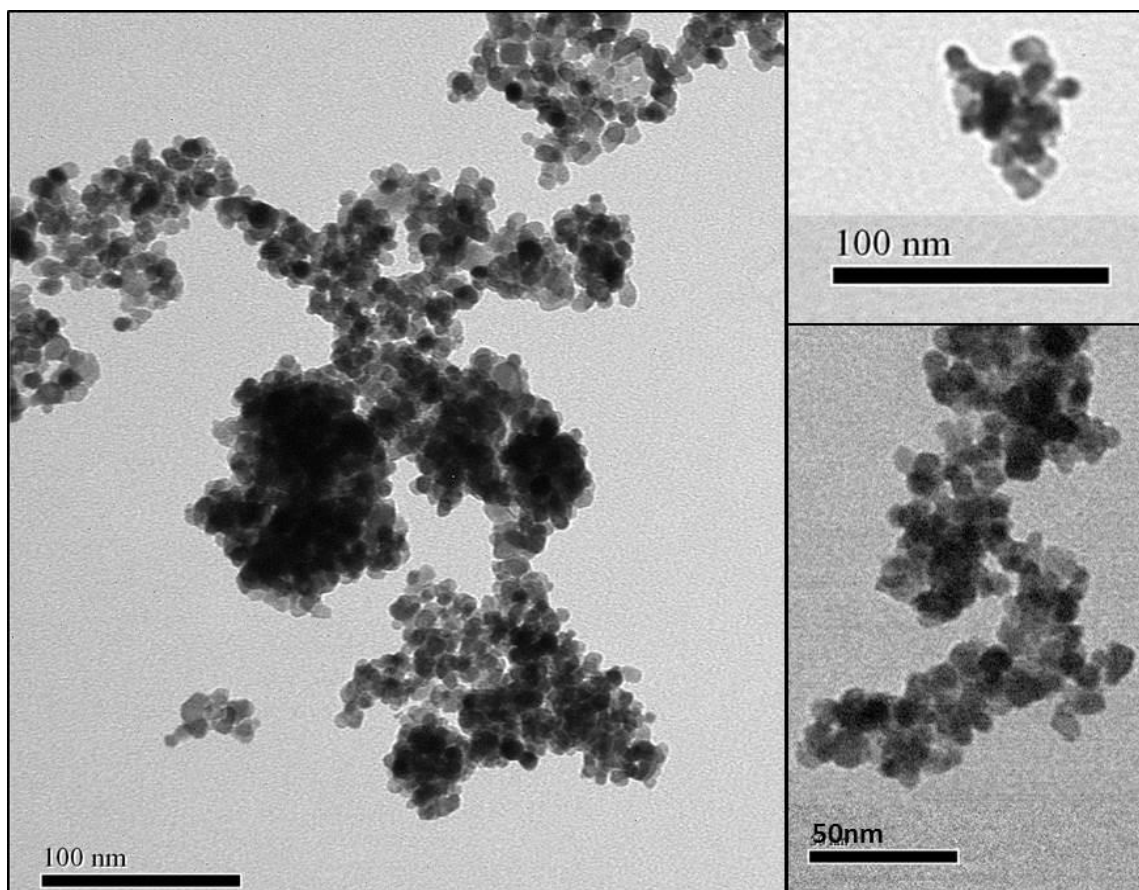


Fig 2.1: TEM images (x400,000) of NM-211 (10nm) CeO₂NPs

In fair agreement with the XRD characterisation provided in Table 2.1 (10.1nm), NM-211 comprised angular polyhedron crystals with an average length of the longest face being 11.12nm (± 2.54 std dev, $n = 256$). Under regular drying conditions during grid preparation for TEM, the particles were seen as clumps of several hundred nanometres, yet single particles could still be measured (Fig 2.1). It is unknown whether these were aggregates as remnants from the dispersion process, or newly formed agglomerates as a result of the drying process.

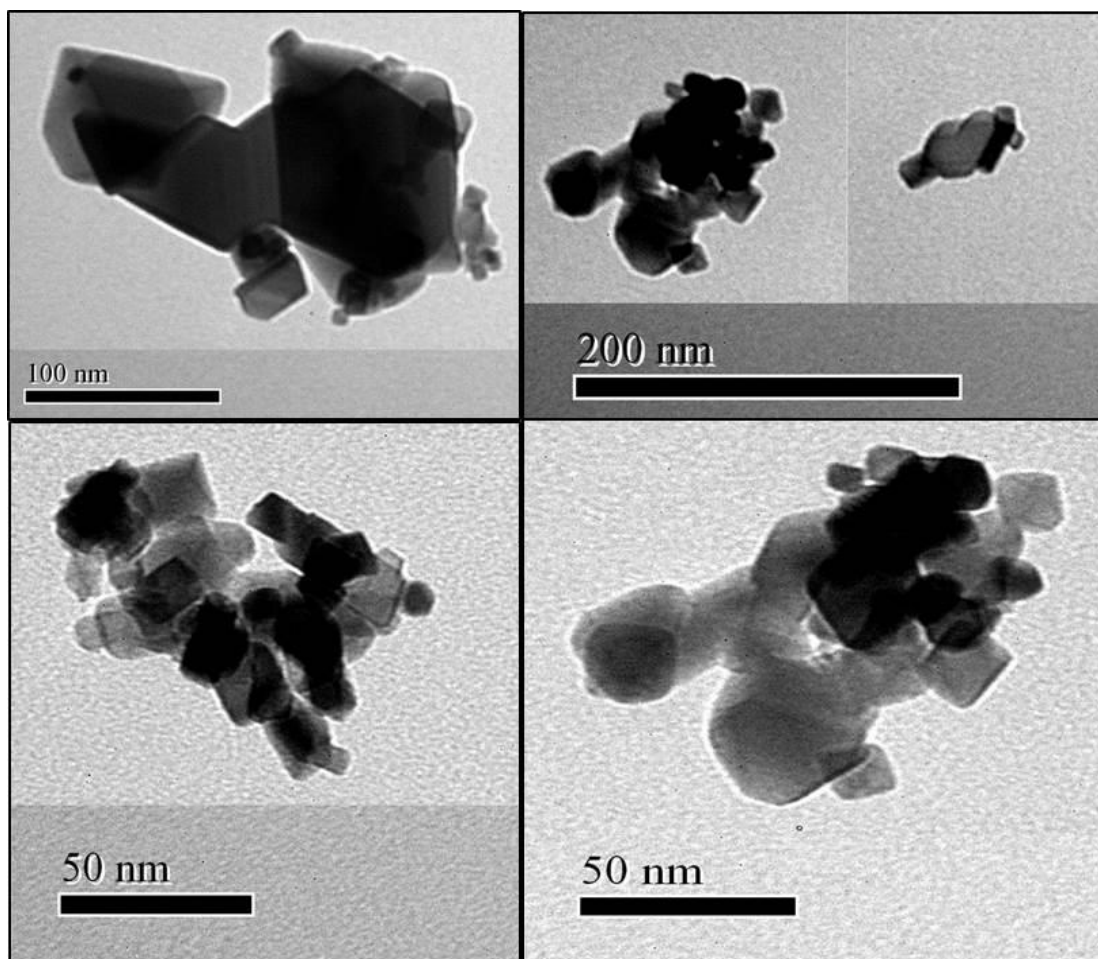


Fig 2.2: TEM images (x400,000) of NM-212 (28nm) CeO₂NPs

NM-212 (Fig 2.2) comprised angular polyhedron crystals with an average length of the longest face being 33nm (± 26.52 std dev, $n = 72$). Whilst the average size of the particles broadly agreed with the 28nm nominal size given in Table 2.1, the distribution of sizes ranged from 9-129nm. Under regular drying conditions during grid preparation for TEM, again the particles were visualised as clumps, but it was not determined if these were aggregates or agglomerates.

2.1.2 Isotopically-Enriched ^{140}Ce Cerium Oxide NPs

Given that background levels of Ce in the scallop *Chlamys varia* have been measured between 3.17 and 10.85 $\mu\text{g/g}$ off the coast of north-west France, (Bustamante and Miramand 2005), conducting exposure studies of bivalves at environmentally-relevant concentrations becomes difficult as any further uptake can be masked by the background concentrations. Use of non-radioactive, isotopically-labelled CeO_2NPs circumnavigates this problem by showing uptake as a specific increase in the ratio of one stable isotope as compared to another stable isotope. In this case ^{140}Ce is known to comprise the majority of the mole fraction of Ce isotopes, being 88.45%, whilst ^{142}Ce comprises 11.11% (de Laeter *et al.* 2003). This gives a known ratio of $^{140}\text{Ce}/^{142}\text{Ce}$ in organism tissues. Using NPs crafted exclusively from ^{140}Ce in uptake and trophic transfer experiments intentionally skews this ratio by artificially increasing the amount of ^{140}Ce present in the organism. By analysing this ratio it allows for accurate determination of increased concentrations of ^{140}Ce despite high background levels (Larner and Rehkamper 2012). A similar method has previously been used to track the uptake of isotopic zinc by the mud shrimp *Corophium volutator* (Larner *et al.* 2012).

Much as they did in the Larner (2012) studies mentioned above, Prof Mark Rehkamper and Dr Adam Laycock at Imperial College, London, supplied CeO_2NPs crafted exclusively from ^{140}Ce for use in this thesis. Particles were supplied in 6K molecular weight dextran at a concentration of 4mg/ml. Due to the small size of the $^{140}\text{CeO}_2\text{NPs}$ and the interference of dextran in the solution, clear TEM images of the particles could not be taken and it was therefore challenging to accurately identifying large numbers of particles for measurement. Fig 2.3 highlights the particles in question as dense black dots. Particles ($n = 29$) measured between 1.26 – 2.94nm, with an average of 1.86nm (std dev $\pm 0.43\text{nm}$).

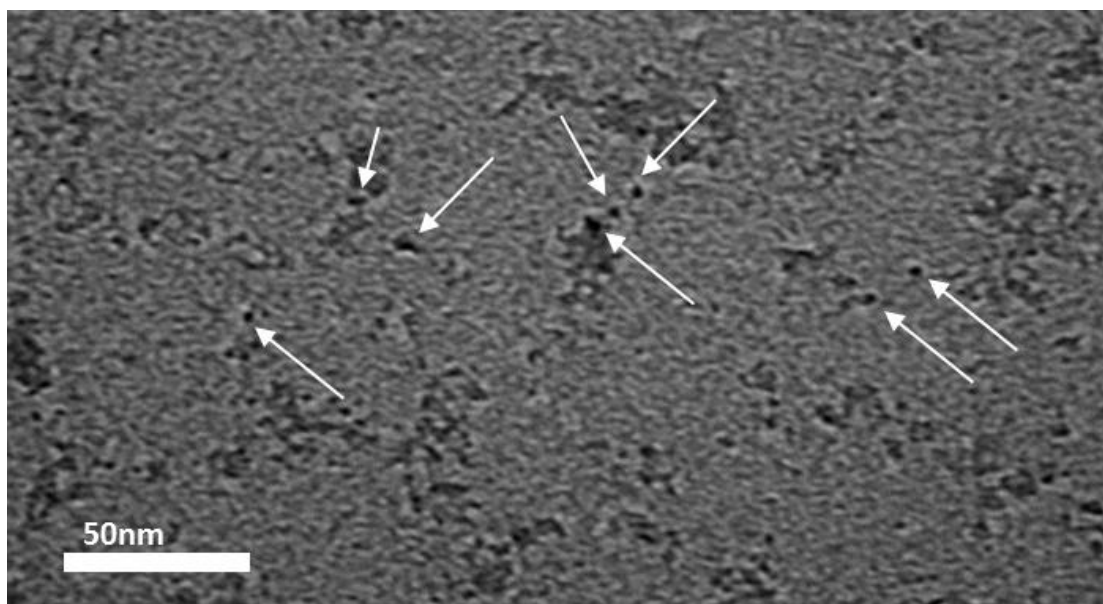


Fig 2.3: TEM image (x400,000) of $^{140}\text{CeO}_2\text{NPs}$. Arrows highlight some of the particles, here shown as extremely dense black dots.

2.1.3 JRC Silver NPs

Silver (Ag) NPs are found in over two hundred consumer products such as deodorants and socks (Luoma 2008) due to their antibacterial properties (Jeong *et al.* 2005, Lee *et al.* 2005, Shrivastava *et al.* 2007). Washing clothes leads to release of AgNPs into freshwater systems which will ultimately discharge to the marine environment (Benn and Westerhoff 2008). Historically it is the ionic form of silver that has proven the most damaging to living things, and therefore dissolution potential of Ag^+ from the AgNP becomes important when assessing toxicity as it may lead to oxidative stress and lipid peroxidation in organisms (Lubick 2008).

Given this potential for dissolution it is worth examining various morphologies of AgNPs in exposures as shape will contribute towards dissolution speed based upon exposure of differing surface areas. Two particle types were therefore chosen: silver spheres and silver rods. Rods are believed to dissolve quicker due to fast dissolution from points (Baalousha *et al.* 2012), thereby increasing availability of the ion in a shorter timescale. These silver nanoforms, and their associated dispersants, were supplied by the Nanotechnology Industry Association (NIA) via Mercator GmbH and form part of the JRC Repository of NM-Series of Representative Manufactured Nanomaterials as part of the OECD WPMN Sponsorship Programme on the Safety Testing of Manufactured Nanomaterials.

NM-300K comprised 2000mg of silver nanoparticle dispersion containing (nominally) 10% w/w% silver nanospheres (AgNPs) with a diameter <20nm. These were acquired pre-dispersed in a solution including 4% w/w% each of Polyoxyethylene (20) Sorbitan mono-Laurat (Tween 20) and Polyoxyethylene Glycerol Trioleate (Comero *et al.* 2011). NM-300DIS is a sample of the dispersant used in NM-300K, comprising the same chemicals at the same concentrations, however without the silver nanoparticles. This solution could be used as a control when examining biological effects to ascertain whether effects were caused by the nanoform, or their dispersants.

NM-302 comprised 2000mg of silver nanoparticle dispersion with a nominal 8.6% w/w% silver nanorods (AgNRs), and dimensions given as 100-200nm width and 5-10µm length. These were acquired pre-dispersed in a solution including <2% w/w% of acrylic/acrylate copolymer and polycarboxylate ether, and <1% w/w% polyvinylpyrrolidone (Robinson *et al.* 2014). NM-302DIS is a sample of the dispersant used in NM-302, comprising the same chemicals at the same concentrations, however without the silver nanorods. As before, this solution could be used as a control.

Prior to use in any experiment or imaging, both NM-300K and NM-302 and their respective dispersants were dispersed according to a method adapted from the JRC (Comero *et al.* 2011). Briefly, the vial of NPs (or their dispersants) was lightly agitated by shaking for 2 minutes. 20mg of the solution was weighed in a volumetric flask and made up to 100ml with Milli-Q water to form a stock solution. This solution was then immediately used in exposures.

2.1.3.1 Characterisation of Silver Nanoparticles NM-300K

As shown by TEM (Fig 2.4), AgNPs (NM-300K) were generally spherical with no evidence of aggregation or agglomeration on the grid. They measured between 7-51nm in diameter (n= 320) with an average diameter of 16.8nm (±4.3nm SD). 87.5% of these particles measured between 10 and 20nm (Table 2.2). This is in broad agreement with the nominal sizing, however over 11% of the particles measured were greater than 20nm, despite being labelled as <20nm.

Diameter (nm)	< 10	10 - < 15	15 – < 20	20 - < 30	≥ 30
Percentage %	0.63	29.69	57.81	10.31	1.56

Table 2.2 Percentage of AgNPs (NM-300K) falling within a defined size range, following measurement using TEM images (x400,000) analysed with Image-J software (n = 320)

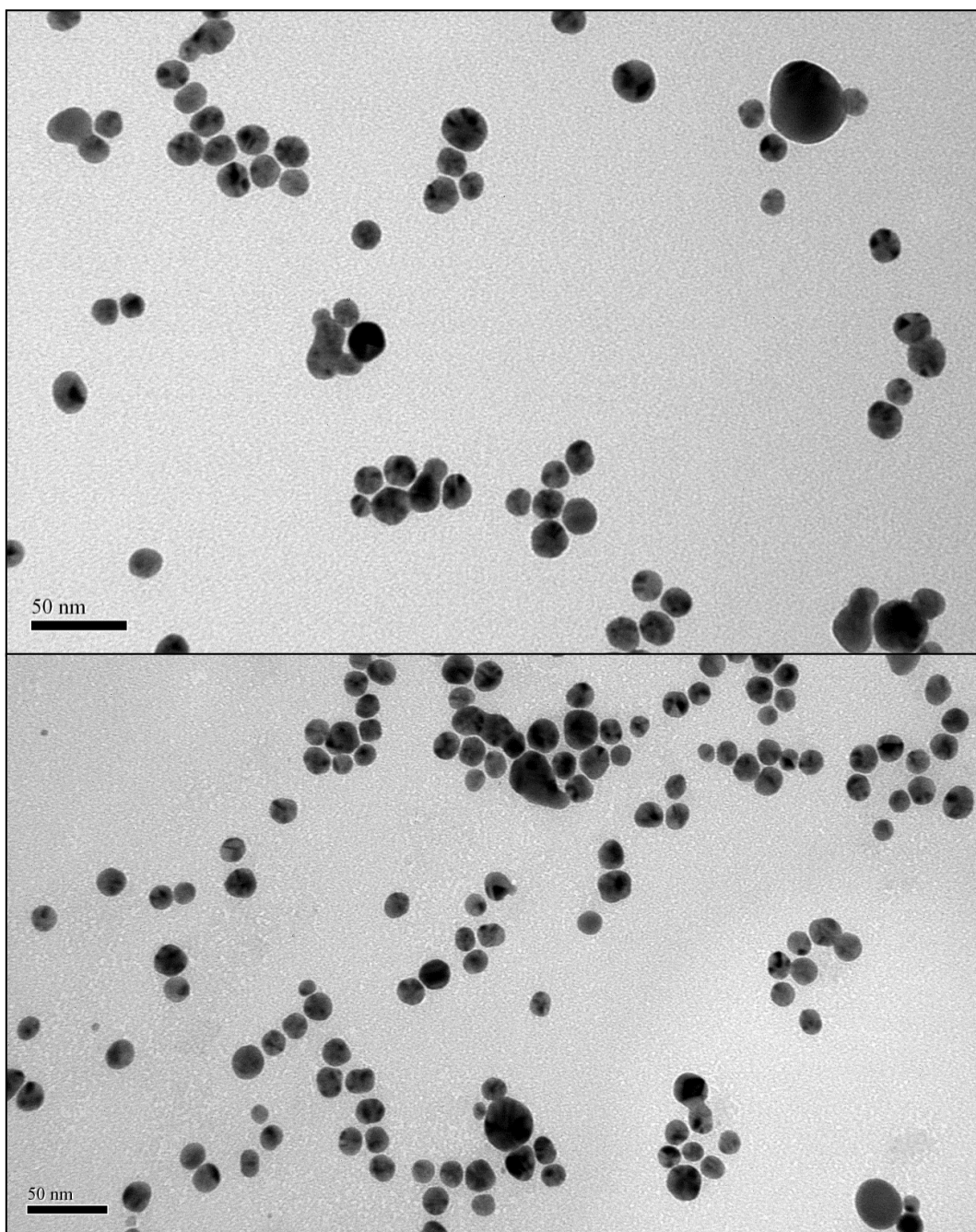


Fig 2.4: TEM images (x400,000) of silver nanoparticles (NM-300K)

2.1.3.2 Characterisation of Silver NanoRods NM-302

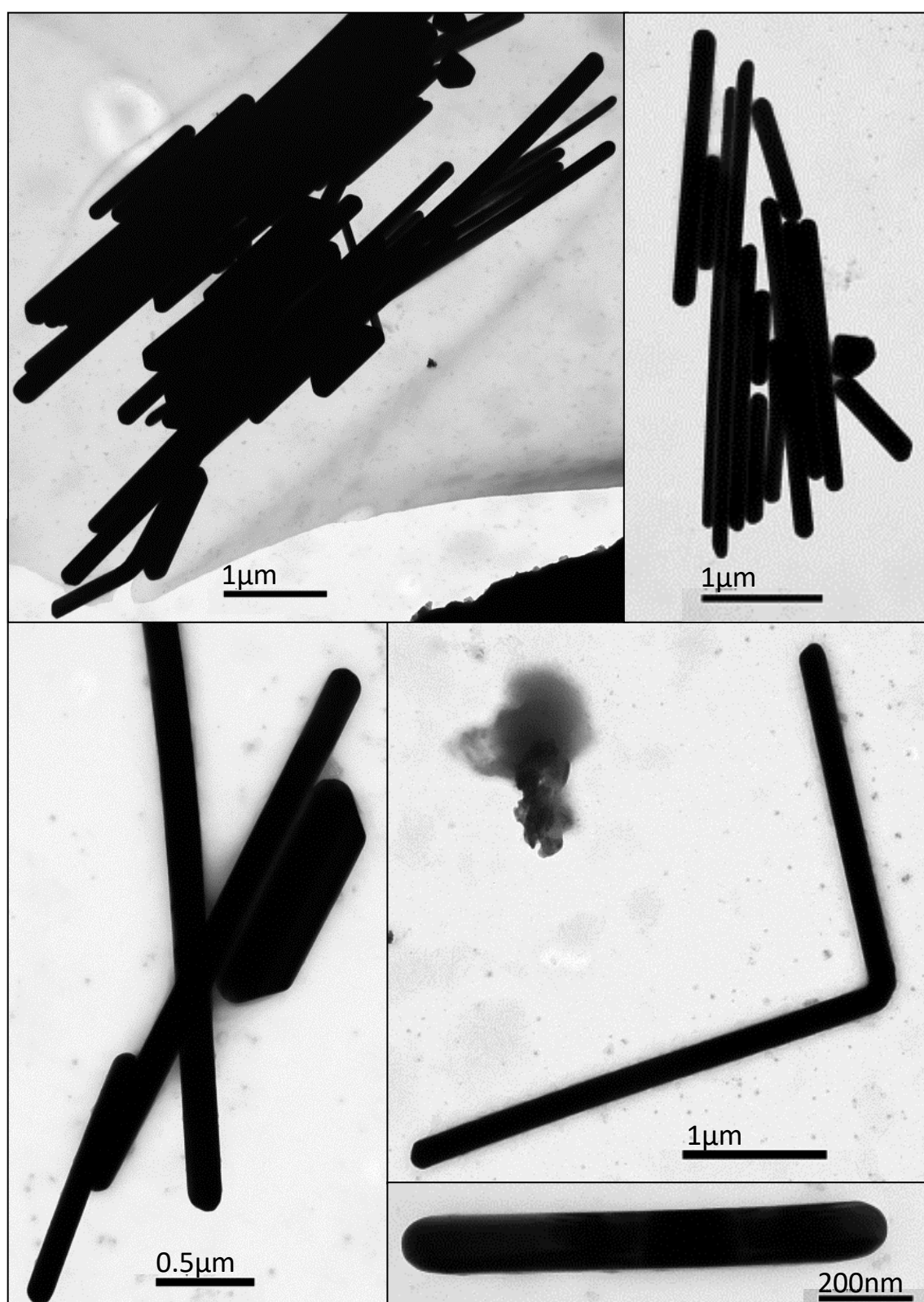


Fig 2.5: TEM images (x400,000) of silver nanorods (NM-302)

As shown by TEM in Fig 2.5 the AgNRs (NM-302) were found in different morphological forms including wires, bent rods, and sphere-like objects, and were prone to clumping together on the grid. They had an average length of 2676nm (± 2176 nm SD) with an average width of 213nm (± 121 nm SD) ($n=52$). One measured rod had a width less than 100nm (3617 x 87nm). Whilst 67.3% of the rods fell within the nominal width sizing of 100-200nm, only 13.5% also reached the nominal length of 5-10 μ m. 84.6% were < 5 μ m long, which may be due to breakages. Several smaller forms were barely rod-shaped at all, measuring 415x365nm. Such 'circular' particles may also be broken ends of larger rods. Fig 2.6 shows a scatterplot of width and length of measured rods. A Pearson product-moment correlation showed no clear relationship between width and length [$r(50) = -0.157$, $p=0.269$].

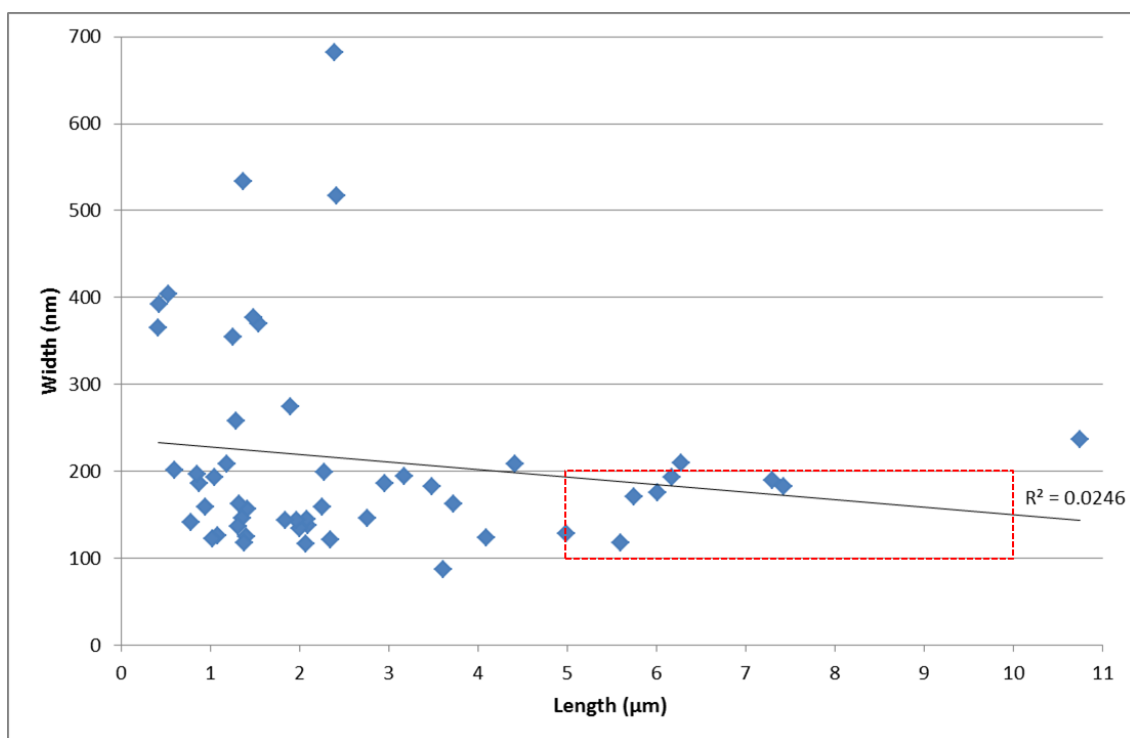


Fig 2.6: Scatterplot showing length and width of silver nanorods (NM-302) following measurement using TEM images (x400,000) and analysed using Image-J software ($n = 52$). Red box = nominal size range

2.1.4 Silver Dissolution

AgNP dissolution was measured by spiking 330ml water samples in 400ml beakers with either AgNPs (NM-300K) or AgNRs (NM-302) at nominal concentrations of 10 μ g Ag/l (n = 2 per timepoint). 15ml samples were removed at 4, 24, and 48 hours and ultra-filtrated in Amicon Ultra-15 centrifuged filter devices with a 3KDa cut-off for 2 hours at x4000g. Filtrate was collected and acidified with 70% nitric acid (HNO₃) to a concentration of 10%. Unfiltered particles were re-suspended in 70% HNO₃ within the tubes for 24 hours then re-filtered, and diluted to a concentration of 10% for analysis via ICP-MS. Samples were pooled to n=1 per timepoint. Prior to ultra-filtration, tubes were preconditioned with 0.1M copper nitrate for 2 hours in order to minimise clogging of binding sites within the filter (Cornelis *et al.* 2010), which was then further centrifuged for 2 hours at x4000g. The tubes and filter were kept moist by rinsing them thoroughly with DI, and then centrifuging a further 15ml of DI through the filter (x4000g) for 2 hours immediately prior to use.

Stock samples of both NM-300K and NM-302 were sent to Plymouth University for analysis by Inductively Coupled Plasma Mass Spectrometry (ICP-MS, see 2.2.1) to assess actual concentrations of silver. Despite following protocols for dispersion, there were differences between nominal and actual concentrations used in this experiment. It was found that the stock solution of NM-300K contained only 9.23 μ g Ag/l, and NM-302 contained only 3.75 μ g Ag/l. This difference in concentration makes it difficult to accurately compare between results for the two particle morphologies.

Fig 2.7 shows dissolution of NM-300K and NM-302 at 4, 24 and 48 hours. After 4 hours over 50% of the NM-300K has passed through a 3kDa filter, and this rises to over 90% after 24 hours, before stabilising. In the case of NM-302, after 4 hours over 20% of the silver has passed through 3kDa filter, rising to over 70% after 24 hours. This then remains relatively constant for the next 24 hours.

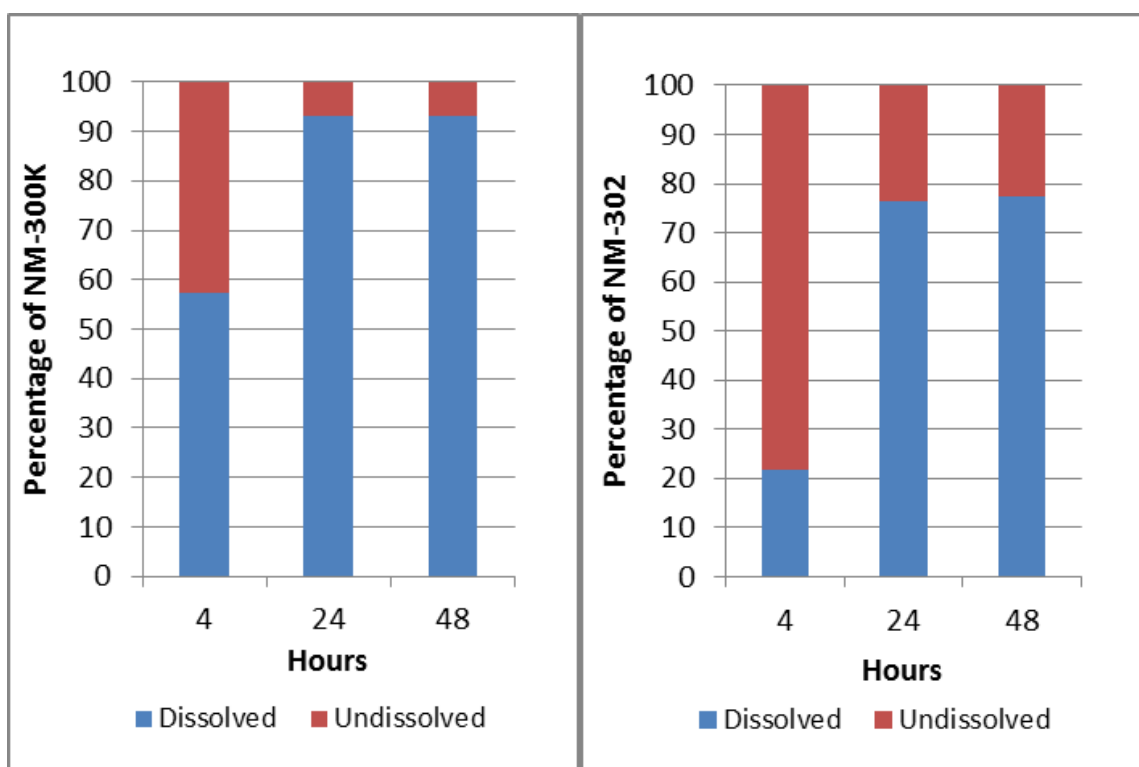


Fig 2.7: Percentage dissolution of silver from NM-300K (9.23 μ g/l) and NM-302 nanorods (3.75 μ g/l) following 4, 24 and 48 hours in 330ml artificial seawater (n=1 per timepoint per treatment, pooled from n=2)

Free silver ions can complex with free chloride ions to form AgCl, which precipitates out of solution at concentrations above 500 μ g Ag/l (Krauskopf 1956). There was no visual evidence of this, and this is likely due to the low concentrations of Ag that would have dissolved from the particles. Since concentrations used during this experiment were less than 10 μ g/l, then any formation of AgCl will remain dissolved, and this will be reflected in the high percentage of “dissolved” silver shown in Fig 2.7.

2.2 Sample Processing for Metal Analysis and Assessing Biological Effects

2.2.1 Dissection of *M. edulis* and *C. maenas*

Immediately following exposure, specimens of *M. edulis* were slightly prised open, and all fluid drained to prevent cross-contamination. Where applicable, 1.5ml of haemolymph was then drawn from the posterior adductor muscle using a 21g syringe. After this, the adductor muscle was cut with a scalpel, allowing the mussel to open fully. At this point the foot was removed and discarded, and the digestive gland separated out for analysis. The gills were then removed, including the palps. Finally, the mantle was removed. The rest of the mussel was discarded.

For *C. maenas*, immediately following exposure, and where applicable, 1ml (minimum) haemolymph samples were drawn by piercing the crab at the base of the third walking leg with a 21g needle and syringe. Crabs were then placed in the -80°C freezer for four hours i.e. until death. After this the legs were removed and discarded. The carapace was then cut open and the top removed, revealing the internal organs. The gills could then be dissected out, the stomach removed, and finally the hepatopancreas was removed. The rest of the crab was discarded.

Following dissection, tissue samples were fully homogenized 1:1 [frozen weight (g):volume (ml)] with phosphate buffered saline (PBS; tablets – Sigma P4417; 0.01M phosphate buffer, 0.0027M potassium chloride, 0.137M sodium chloride, pH 7.4) on ice for 1 minute. A 1 ml sub-sample was taken (if necessary) for assays concerning biological effects (see 2.3.2). The rest of the sample was freeze dried for 48 hours for acid digestion (2.2.1).

2.2.2 Acid Digestion for Metal Analysis

Metal concentration analysis of the samples can be obtained using Inductively Coupled Plasma Mass Spectrometry (ICP-MS) or ICP Optical Emission

Spectrometry (ICP-OES), which requires ionised forms of the metal. To provide this the tissue samples, and any metals inside them, can be digested in acid to solubilise the metals into metal ions. Control samples are also digested to provide an average of background levels of metals in the organisms. Freeze-dried samples were acid digested in a Milestone Ethos EZ Microwave Digestion System. A freeze-dried sample weight of less than 0.5g was placed in a pressure vessel with 7ml HNO₃ and 1ml H₂O₂. Up to 10 of these samples could be digested at any one time. The protocol followed was one advised by the manufacturer as suitable for digestion of marine bivalve tissue ["Oyster Tissue" (MilestoneSRL 2013)], whereby the temperature of the vessel was gradually brought up to 200°C for 15 minutes, maintained at this temperature for a further 15 minutes, then allowed to cool until the sample temperature was below 60°C. This digested the sample to completion, and the solution was further diluted to 50ml with DI before being sent to the Analytical Research Facility at Plymouth University. Metal content in the liquid samples was measured using both a Thermo Scientific, X Series 2 ICP-MS instrument and a Varian 725-ES ICP-OES instrument.

2.2.3 Assays for Biological Effects (Lipid Peroxidation and Oxidative Stress)

Sub-samples (1ml) taken for biological effects assays were further diluted in 9 ml PBS to achieve a final dilution of 1 in 20. This was vortexed for 30 seconds, and 1 ml of this dilution sampled, then centrifuged at 13,000 rpm for 9 mins. The resulting supernatant was used for oxidative stress and lipid peroxidation assays. Absorbance values for biological assays were read in triplicate in 96-well plates on a Tecan NanoQuant Infinite M200 Pro spectrophotometer. All chemicals were purchased from Sigma-Aldrich.

2.2.3.1 The Bradford Protein Assay

Differences in size of different organs in each mussel lead to different quantities of protein, and therefore differences in normal cellular activity including anti-oxidant defences. To account for this, the protein content of the sample is

assessed and the ratio of enzyme activity to protein content determined. All results from the assays listed below were normalised against the protein content before statistical analysis was performed.

Protein content of the samples was analysed by a method adapted from Bradford assay (Bradford 1976). Bradford reagent (Sigma B6916; 0.01% w/v Coomassie Brilliant Blue G-250, 4.7% w/v ethanol, 8.5% w/v phosphoric acid) was diluted 1:5 with de-ionised water (DI), and 200µl of this added to 5µl of diluted sample supernatant, per sample, in triplicate in a 96-well plate. This was incubated for 20 minutes at room temperature, then the absorbance read at 595nm. Calibration standards were created from Bovine Serum Albumin (BSA) diluted to a concentration of 2mg/ml DI, with further serial dilutions to 1, 0.5, 0.25, 0.125, 0.0625, 0.03125 and 0mg/ml (blank).

2.2.3.2 Lipid Peroxidation – The Thiobarbituric Acid Reactive Substances (TBARS) Assay

Lipid peroxidation was measured by the TBARS assay. This assay measures levels of malondialdehyde (MDA), a by-product formed during lipid degradation of polyunsaturated fatty acids by ROS. Thiobarbituric acid (TBA) reacts with MDA to produce a pink colour suitable for spectrophotometric analysis (Marnett 1999).

The TBARS assay required a buffer solution of Phosphate Buffered Saline (PBS, Sigma P4417, 0.01M phosphate buffer, 0.0027M potassium chloride and 0.137M sodium chloride, pH 7.4) and 0.1M disodium ethylenediaminetetraacetate dihydrate (EDTA). Also required were 50% (w/v) trichloroacetic acid (TCA), 1.3% (w/v) thiobarbituric acid (TBA) in 75mM sodium hydroxide (NaOH), and 1mM butylated hydroxytoluene (BHT) in 95% ethanol. Calibration standards were made from 0.01M 1,1,3,3-tetraethoxypropane in 95% ethanol, and further diluted with EDTA+PBS buffer to 20, 10, 5, 2.5, 1.25, 0.625, 0.3125 and 0 µM.

100µl of supernatant (per sample) was incubated in a 1.5ml sample tube along with 300µl PBS+EDTA, 150µl TBA, 100µl TCA and 20µl BHT at 60°C for one hour, then put on ice for 15 minutes to stop the reaction. Samples were centrifuged at 13,000 rpm for 7 minutes. The resulting supernatant was diluted

to 50% with PBS+EDTA and absorbance read at 530nm at 25C. Standards were treated as above, however standards were used in the plate-reader without being further diluted by PBS+EDTA. Results are reported as $\mu\text{mol MDA/mg protein}$.

2.2.3.3 *The GST (Glutathione-S-Transferase) Assay*

Glutathione-S-Transferase catalyses the conjugation of reduced glutathione (GSH) to substrate molecules, (which can include toxicants), hence reducing oxidative stress in an organism. In this assay GST activity can be measured by absorbance increase following the conjugation of GSH with 1-chloro,2,4-dinitrobenzene (CNDB). 200mM sodium phosphate buffer was made by mixing 200mM monosodium phosphate and 200mM disodium phosphate until pH6.5. 42mM GSH was prepared by dissolving GSH in assay buffer. 42mM CNDB was made by dissolving CNDB in 100% ethanol. 0.5ml of this was added to 20ml of assay buffer to produce a daily working mix.

25 μl of diluted sample supernatant was added in triplicate to 96-well plate. 0.5ml of 42mM GSH were added to the working mix, then 200 μl immediately added to each well. Absorbance was read every 30 seconds at 340nm for 3 minutes. Blank samples replaced supernatant with 25 μl assay buffer.

GST activity was calculated as $\mu\text{mol / min / ml / mg protein}$ using the following equation:

$$\frac{(\text{Absorbance/min}) \times (\text{Reaction Volume}) \times \text{dilution factor}}{[(\text{CNDB extinction co-efficient} = 9.6\text{mM}^{-1}) \times (\text{path length}) \times (\text{Sample Vol})]}$$

2.2.3.4 *Oxidative Stress – The Superoxide Dismutase (SOD) Assay*

The SOD assay measures the activity of SOD enzymes in the samples when quenching free radicals. The addition of xanthine oxidase to a substrate solution containing nitroblue tetrazolium chloride (NBT) causes a colour change reaction over time which can be measured spectrophotometrically. The presence of SOD in a sample will inhibit the extent of this colour change, and thus SOD activity of the sample can be assessed.

SOD buffer solution was made by mixing 0.043M sodium carbonate (Na_2CO_3) and 0.043M sodium bicarbonate (NaHCO_3) until pH 10.2. Substrate solution was made by mixing 0.1mM (7.6mg) xanthine, 0.1mM (18.6mg) EDTA, 0.025mM (12mg) NBT and 25mg BSA in 500ml of buffer. This solution was light reactive and therefore kept foil-wrapped until use. Enzyme solution was made by diluting xanthine oxidase (25 unit stock, Sigma X4500) in a 1:80 ratio with buffer, and vortexing immediately prior to use. For sample analysis, 10 μl of enzyme solution was added to 5 μl of sample supernatant, 30 μl of buffer and 195 μl of substrate solution in a 96-well plate in triplicate, shaken for 5 seconds, and absorbance was immediately read at 25°C every 45 seconds for 25 cycles at 573nm. Blank wells received no supernatant, but 35 μl of buffer instead. Standard solutions were made by diluting SOD (from bovine erythrocytes, Sigma S7571) with PBS down to 3, 1, 0.7, 0.5, 0.4, 0.2, 0.1 and 0.05 U SOD/ml. Standards were analysed in the same way as the samples. Results are reported as U SOD Activity / ml / mg protein.

2.2.3.5 *The CAT (Catalase) Assay*

The CAT assay measures the conversion of H_2O_2 to water catalysed by catalase. This can be quantified by measuring the decrease in absorbance at 240nm which relates to the loss of H_2O_2 from test wells following the introduction of catalase (Beers Jnr and Sizer 1952).

50mM potassium phosphate buffer (KH_2PO_4) was made with DI, and adjusted to pH7.0 using 1M potassium hydroxide (KOH). Catalase for standards was diluted from bovine liver catalase using the buffer to concentrations of 0.5, 1, 2, 3, 4, 6, 8 and 10U catalase/ml. 10mM H_2O_2 solution was made up using K_2PO_4 buffer. Standards for catalase activity were made by running 100 μl of each standard against 100 μl of H_2O_2 solution in a UV-transparent, flat-bottom 96-well plate, read every 10 seconds for 5 minutes at 240nm in a plate reader. Catalase activity in samples was obtained by replacing the standard with 100 μl of diluted sample supernatant. Results are reported as U CAT Activity / min / mg protein.

2.2.4 Data Analysis

Data on biological effects was analysed using SPSS v.20. Data was tested for normality using the Shapiro-Wilk Test in order to determine which statistical test was most appropriate. Normal data was analysed by *t*-test or one-way ANOVA followed by Tukey's HSD post-hoc test. A one-way ANOVA was chosen above multiple *t*-tests in order to reduce the likelihood of Type I errors i.e. false positives. A Tukey's HSD post-hoc test was chosen over a Bonferroni correction since Bonferroni is sometimes thought to over-correct for Type I errors (Perneger 1998), leading to an increase in Type II errors i.e. false negatives. Non-normal data was first log transformed and then, if normalised, analysed by as above. If data remained non-normal, it was then analysed by a Mann-Whitney (MW) U-test. This test was chosen due to the low sample sizes ($n \leq 10$). Significance was assumed at $p < 0.05$.

2.3 The Blue Mussel *Mytilus edulis*

2.3.1. Pertinent Physiology



Fig 2.8 The mussel *M. edulis* covered in barnacles (left) and cleaned of epibionts (right)

The Bivalve mussel *M. edulis* is an abundant and steadfast organism found in shallow coastal waters ranging all over the north-east and north-west Atlantic shores. Populations can be both sub- and inter-tidal due to its ability to lock in water by closing its shell.

Mussels can attach to a variety of substrates by means of laying down byssus threads. This leads to large, dense beds of mussels as many will use the same anchor points together, and even overlay each other by securing themselves to others' shells. This pattern of colonisation in turn increases interstitial space and habitat complexity for other flora and fauna (Tyler-Walters 2008). Mussels themselves are often found covered in barnacles (Fig 2.8). In 2012, UK aquaculture production was estimated at over 26,000 tonnes, with an estimated value of over £27 million (Ellis *et al.* 2015). This makes *M. edulis* commercially, as well as ecologically, important.

As filter feeders *M. edulis* draw in, and filter, up to several litres of water per hour (Vahl 1973). Whilst primarily used as a method of food capture, this characteristic also makes them highly competent at clearing silty waters, and simultaneously puts them at high risk from discharges of toxicants in near-shore environments. This property makes mussels known vectors to humans for contaminants and toxic algal blooms, resulting in illnesses such as paralytic shellfish poisoning (Burrell *et al.* 2013).

Mussels take in water via the inhalant siphon (Fig 2.9). This passes over the large fleshy mass of the mantle, before being sieved through the gills, and removed via the exhalant siphon. Uptake of any particles (food or otherwise) by the mussel is initially likely to be via entrapment in a matrix of latero-frontal cirri on the gills (Riisgård *et al.* 1996).

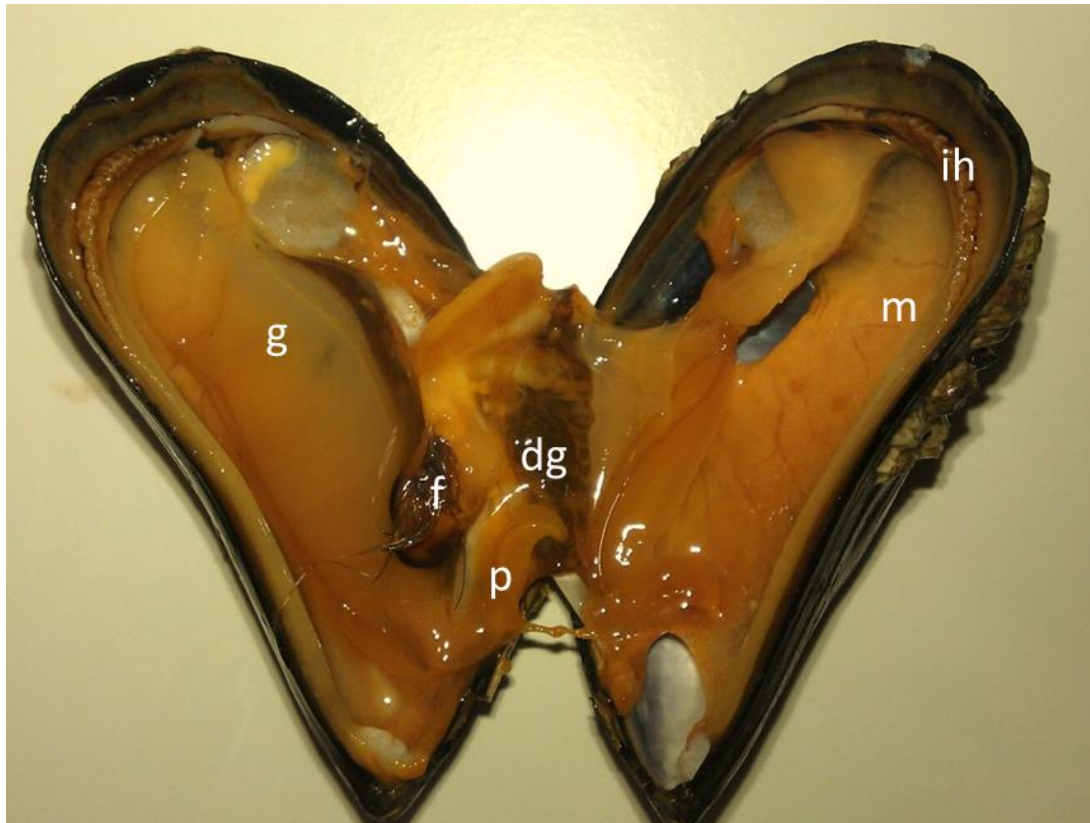


Fig 2.9: Internal anatomy of *M. edulis*. dg = digestive gland, f = foot, g = gills, ih = inhalant siphon, m = mantle, p = palps

These cirri are formed of a network of interlocking cilia, about 20-30 μ m long (Silvester and Sleight 1984), forming a mesh with a hole size estimated at around 1x1.5 μ m (Riisgård *et al.* 2011). Smaller particles should pass through the net, larger particles should become trapped. Trapped particles are then moved via cilia to the palps which are responsible for sorting particles for either ingestion, or rejected into pseudofaeces and sent along a rejection tract on the mantle. Unsuitable particles can be rejected by the gills themselves and sent straight to the mantle rejection tract. Despite extensive study, the exact mechanism by which the palps determine edibility is still unknown (Riisgård *et al.* 2011), although particle charge and wettability have been rejected (Rosa *et*

al. 2013). In all, the transfer process takes around 1/25 of a second (Riisgård *et al.* 1996).

Given an inter-ciliary mesh of about 1x1.5µm in a living mussel, it would be expected that particles around this size would have a greater propensity for being trapped. An early study (Jørgensen 1974) found that 1µm latex spheres cleared with around 20% efficiency, 2µm with 60%, and 5-18µm with 100%, yet it is argued that mesh size will not be the only defining factor of particle retention. Beat action of the cilia, for example, could create micro-currents that force smaller particles onto the capturing filaments (Silvester and Sleight 1984). More recently Kach and Ward (2008) noted difficulties in uptake of particles less than 1µm, with uptake increasing when particles were embedded in agglomerates (Kach and Ward 2008, Ward and Kach 2009). This leaves the question of whether *M. edulis* will be able to accumulate any nanoparticles at all given their size compared to that of the capture mesh.

Despite this, and as highlighted in the previous chapter, many authors have used *M. edulis* in their experiments involving nanoparticles (Koehler *et al.* 2008, Tedesco *et al.* 2008, Tedesco *et al.* 2010, Tedesco *et al.* 2010, Zuykov *et al.* 2011, Hu *et al.* 2014) enabling useful comparisons between previous works and the experiments presented in this thesis.

Given their dynamic and exposed habitat *M. edulis* are naturally hardy to mechanical stress and dehydration, allowing them to be easily maintained in a laboratory. They are fed upon by a range of organisms including gulls, sea stars, dog whelks and crabs (Tyler-Walters 2008), making them ideal candidates for trophic transfer experiments.

2.3.2 Method Development: Exposure of *M. edulis* to Me(O)NPs

2.3.2.1 Collection of *M. edulis*

Mussels (c.6cm, c.30g) were collected from Starcross, Exeter, in the SW of England, UK (50.625917, 3.4441330), cleaned of epibionts, and acclimated in the aquarium for seven days (artificial seawater [ASW], 34 ppt, pH 8.14, 14°C, 12L:12D) prior to each experiment. They were fed once daily on 0.5ml of Iso1800 *Isochrysis* algal culture (Reed Mariculture) diluted in 15ml ASW and shaken before introduction to the holding tank.

2.3.2.2 The Effect of Marine Snow on CeO₂NP Uptake by *M. edulis*

Bivalves normally feed on microplankton, hence this raises the question of their uptake efficiency and selection of nano-size particles (Ward and Shumway 2004). Agglomeration enables greater uptake of 0.5-1.0µm particles by bivalves, and *M. edulis* takes up NPs embedded in agglomerates (>100µm - <3mm) faster than the oyster *Crassostrea virginica* (Ward and Kach 2009). Beads of 100nm have a longer gut retention time (72 hours) than 10µm beads (6 hours). This suggests particle sorting by the molluscs, with possible endocytotic uptake of the NPs by digestive cells. This experiment used agglomeration as a variable in order to understand efficacy of Me(O)NP uptake by *M. edulis* and to develop methods for future exposures.

The aim of this scoping study was to determine whether marine snow (flocculation) is a necessary component of NP accumulation by *M. edulis*. Marine snow is present in natural seawater systems, and is comprised of microscopic organisms and particles. Bacterial mucopolysaccharides in the snow aid binding of small particles (Shanks and Edmondson 1989), hence it is used in many studies to synthesise natural particle agglomeration. The hypothesis is that mussels will accumulate more Ce when the CeO₂NPs are embedded in marine snow.

Method

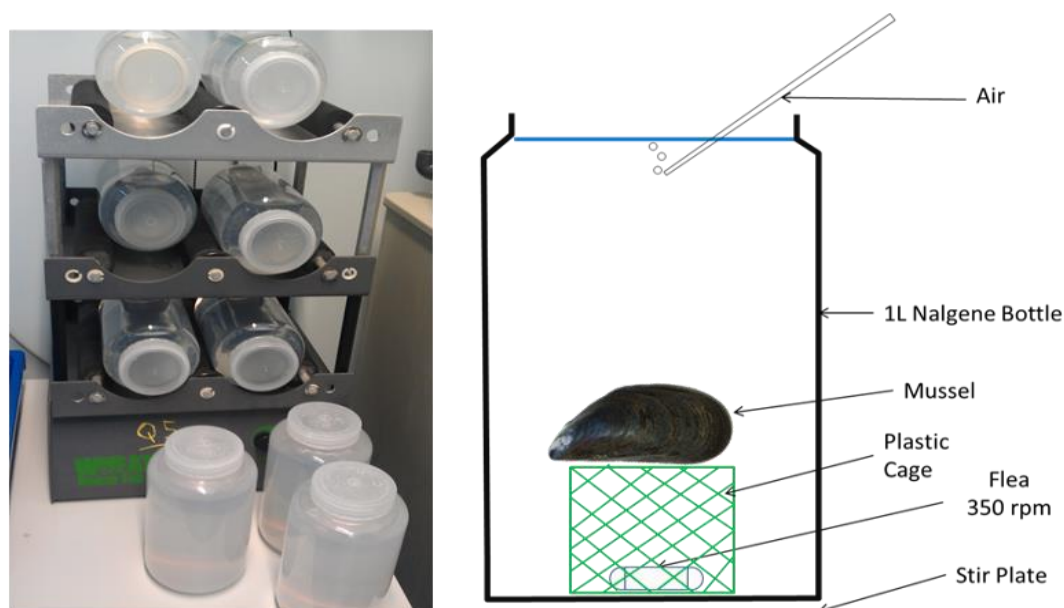


Fig 2.10: Marine snow manufacture (left) and *M. edulis* exposure technique (right)

Prior to the experiment, *M. edulis* (average 27 ± 3.4 g wet weight, length 5.8 ± 2.2 cm) were collected and stored as detailed in 2.5.2.1. Marine snow was produced by rolling 1L natural seawater (collected from Starcross, Devon) and NM-212 CeO₂NPs (28nm, 10 mg/l) for 72 hours in 1L nalgene bottles (Fig 2.10) on a Wheaton 120 Vac Benchtop Roller (3 rpm). Mussels were then placed individually on plastic cages either in a bottle containing marine snow (n=6), a bottle containing 1L natural seawater spiked with NM-212 (10mg/l, n=4), or a bottle with seawater only (control, n=4). Bottles were stirred by magnetic flea on stir plates (350rpm, ThermoScientific VarioMag 15) and aerated via glass pipette. After 72 hours mussels were removed, and gill, mantle and digestive gland dissected out, snap-frozen, freeze dried and acid digested for metal content analysis as per Chapter 2.2.1. Data was pooled, hence no statistical analyses were performed.

Results & Discussion

Results show that exposed organisms accumulated Ce greatly above control levels, and that increases in accumulation by *M. edulis* when comparing flocculated and unflocculated CeO₂NPs are tissue specific (Fig 2.11). Bivalve

uptake of particles is usually primarily via the gills, following which they are sorted and sent to the digestive gland (Canesi *et al.* 2012). As the first barrier to particle capture, gills are potentially a primary site for NP accumulation. The results show that whilst Ce accumulation in the mantle and gill were similar for flocced and unflocced exposures, in the digestive gland unflocced exposures resulted in twice the Ce accumulation as flocced exposures.

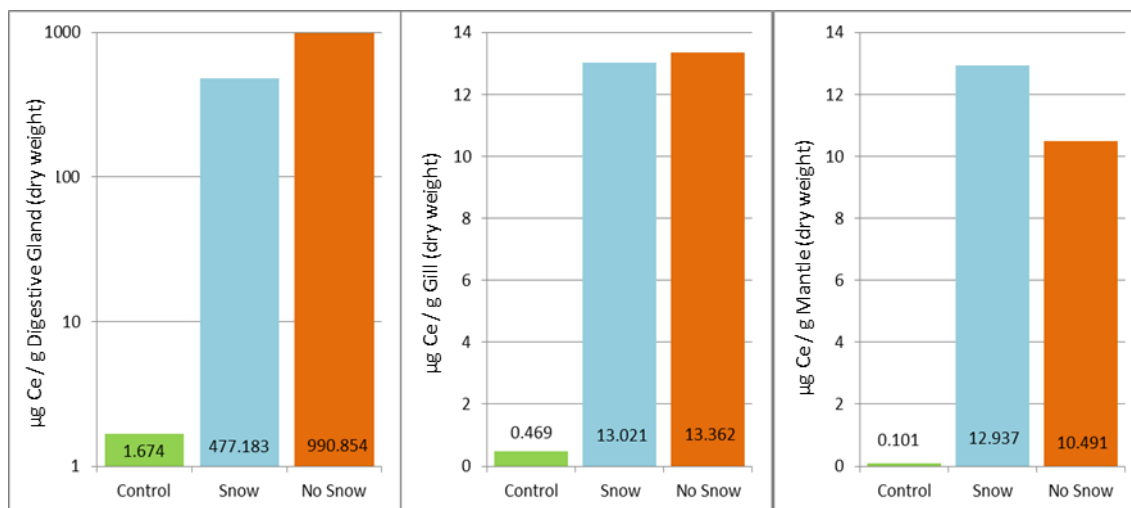


Fig 2.11: Cerium accumulation ($\mu\text{g/g}$ dry weight) following uptake of 28nm CeO_2NPs [10 mg/l, with and without marine snow] for 72 hours by *M. edulis* into the Digestive Gland, Gill and Mantle. Note that y-axis for stomach content is a log scale. Samples pooled to $n=1$ per treatment.

Table 2.3 shows the percentage of total accumulated Ce found in each tissue. For both flocced and unflocced CeO_2NPs the digestive gland is the primary target, followed by the mantle and gills. These results tally with an earlier study whereby insoluble AuNPs ($5.3 \pm 1\text{nm}$, 750 $\mu\text{g/l}$) accumulated primarily in the digestive gland (95%), with some in the gills (3.9%) and mantle (1.5%) of *M. edulis* (Tedesco *et al.* 2010).

	Digestive Gland %	Gill %	Mantle %
Flocculated	94.97	1.23	3.80
Unflocculated	97.42	0.46	2.11

Table 2.3: Percentage of total cerium uptake found in each tissue ($n=1$)

These preliminary results suggest that particles do not need to be within marine snow for uptake. In exposure media particles tend to agglomerate and the

extent of this agglomeration occurs due to surface charge, particle shape and size, and pH of the solution. In saltwater the increasing salinity, and therefore ionic strength, reduces mobility of the particles, encouraging agglomeration (Batley *et al.* 2012), and this notion will be further explored with regards to DLVO theory in Chapter 3. Agglomeration is also affected by NP concentration; higher concentrations agglomerate faster, presumably due to more particles being available for interaction (Miller *et al.* 2010, Fairbairn *et al.* 2011). NM-212 has a half-life dispersion stability time of only 288 minutes in seawater (Table 2.1), so these NPs will not remain nano-sized for long, and will agglomerate into larger particles that are more easily taken up. *M. edulis* is also capable of producing exopolymeric substances (EPS) as anionic, transparent exopolymer particles, and may therefore facilitate its own uptake of picoplankton as agglomerates (Li *et al.* 2008). Particle shape and charge have also been suggested as more deterministic in uptake than particle size (Wegner *et al.* 2012).

Marine snow manufacture requires natural seawater, the content and quality of which can vary dramatically between experiments. Since marine snow has been shown as unnecessary in maximising CeO₂NP uptake by *M. edulis*, this will now be discarded as a method of exposure in further studies. Use of filtered (0.2µm) artificial seawater (FASW) instead will allow for consistency in both content and chemistry.

This study also highlighted problems when using a cage as a method of supporting *M. edulis*. By laying down byssal threads, mussels were able to move around in the beaker and interfere with the stir fleas. In future experiments mussels will be secured to a suspended ice lolly/craft stick to reduce movement as per Kach & Ward (2008).

2.3.2.3 Efficacy of CeO₂NP Uptake by M. edulis when exposed Individually, and as a Group

In the previous study mussels were exposed as individuals. There is a space and time constraint placed when doing this, and it may be more efficient to expose groups of mussels in larger beakers. The aim of this experiment was to

investigate whether uptake of CeO₂NPs by *M. edulis* in a group would differ significantly as compared to single organism uptake. The hypothesis is that group exposure would reduce uptake efficiency as compared to exposing single *M. edulis*.

Method

Given previous issues with the plastic cage, a different exposure method for mussels was used. Twenty-four hours prior to exposure, mussels were removed from their holding tanks, dried, weighed, and a piece of Velcro (1 x 1.5cm) super-glued (Loctite 454) to the upper left shell. The corresponding piece was glued to a craft/lolly stick (Kach and Ward 2008). These were both allowed 4 hours to dry, then the mussels and craft sticks were well rinsed in ASW and left overnight in separate static tanks in 24 litres ASW before exposure to leach out any toxins. Sticks and mussels were rinsed thoroughly again directly prior to exposure.

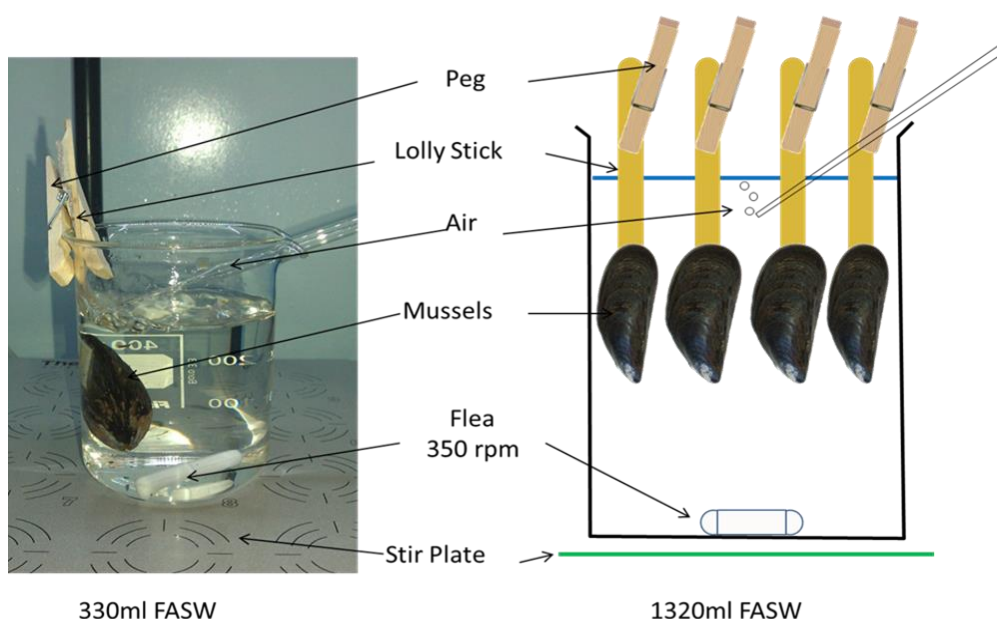


Fig 2.12: Methodology for exposure of *M. edulis* to CeO₂NPs singularly (left) and in a group (right)

Mussels were attached to the lolly sticks, and clipped by clothes peg in either single 400ml beakers (330ml FASW, n=7), or four per 2L beaker (1320ml FASW, n=8). Beakers were stirred via flea (350rpm) and aerated with a Pasteur pipette at a rate of 1 bubble per second (Fig 2.12). Mussels were allowed to acclimate

in the beakers for 20 minutes before exposure, and a visual inspection ensured that all mussels were open and pumping water. Any mussels not open were replaced and allowed to acclimate, until all mussels were open and visibly pumping. Iso1800 algal feed (Reed Mariculture) was added at 5,000 cells/ml, along with CeO₂NPs (NM-212, 3mg/l). Given the fast pumping rate of *M. edulis* (c. 1l/hour) and the low stability time of the particles used, the exposure time was reduced from 72 hours to 4 hours. Over 4 hours the mussels would still re-circulate the beaker water about 12 times, thereby assuring uptake. This also has the potential to reduce stress on the organisms caused by fluctuating pH and ammonia levels resultant of spending 72 hours in a confined area (to be examined in 2.3.2.4). Whole body tissues were dissected for metal content analysis.

Results & Discussion

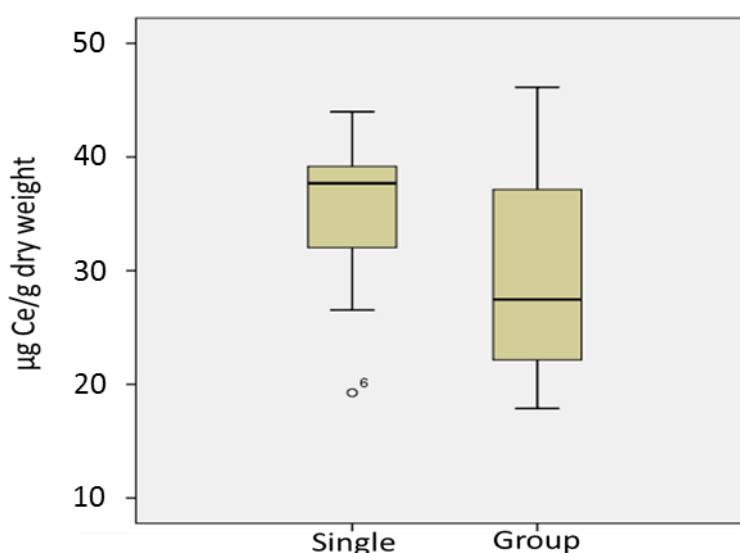


Fig 2.13: Mean Cerium concentrations (µg/g d.w.) in *M. edulis* when exposed to 3 mg/l CeO₂NPs either singularly (n=7) or in groups of 4 (n=8). (6) = Outlier

Despite a greater mean Ce whole body burden for single exposure (34.8 ± 3.3 SE µg/g d.w.) compared to group exposure (29.7 ± 3.4 SE µg/g d.w.), this was not significantly different [*t*-test, $t(13) = 1.07$, $p = 0.305$]. However, an outlier had been identified by SPSS (Fig 2.13, “6”), due to its unusually low uptake compared to other mussels under that treatment. Removal of this outlier from the statistical analysis did not create a significant difference [*t*-test, $t(12) = 1.72$, p

= 0.111). Differences in uptake may be due to different pumping rates of *M. edulis*, and increased number of surfaces and surface area in group exposure could lead to increased surface adsorption of NPs (Oral *et al.* 2010, Li *et al.* 2012), and therefore less available in the water column for uptake. Mussels may also have blocked each other's uptake by diverting water flow. Whilst no significant difference could be determined, single exposure led to higher average Ce content. As such *M. edulis* should be exposed individually in order to maximise accumulation of Ce by the mussels without increasing the inherent variability that occurs when groups of mussels are exposed. Due to limitations in apparatus, single exposure also allows for a greater number of replicates in future experiments. Evidence of an outlier suggests that this experiment should be repeated with a higher n-number, unfortunately the financial cost of analysis did not make this viable.

2.3.2.4 Measuring Oxygen, pH and Ammonia

Oxidative stress can be triggered in an organism in many ways, including reduced oxygen (Vig and Nemcsok 1989), increasing ammonia (Lima *et al.* 2007) and fluctuating pH (Gazeau *et al.* 2013). Before embarking on any oxidative stress-related experiments, exposure conditions were tested to ensure that there was no controllable factor that might affect subsequent results. The aim of this series of experiments is to determine if the current exposure method for *M. edulis* is resistant to fluctuations in oxygen, ammonia and pH levels. The hypothesis is that the current system is suitable for exposing *M. edulis* to Me(O)NPs without risk of generating unintended oxidative stress.

Oxygen Percentage

i) Water Oxygen content under Low and High Bubble regimes

In previous experiments air had been bubbled into the exposure beakers from the top. Combined with stir-fleas agitating the surface of the water, this was assumed to be suitable for oxygenating the water thoroughly, yet had not been actually tested. Here mussels were set-up individually in 330ml FASW as per

Chapter 2.3.2.3. Mussels received air bubbled at either 1 bubble per second from a top-fed aeration system (n=5), or 5 bubbles per second from a bottom-fed aeration system (n=6, Fig 2.14). Water oxygen concentration levels were measured using a Mettler Toledo SG9 dissolved oxygen meter.

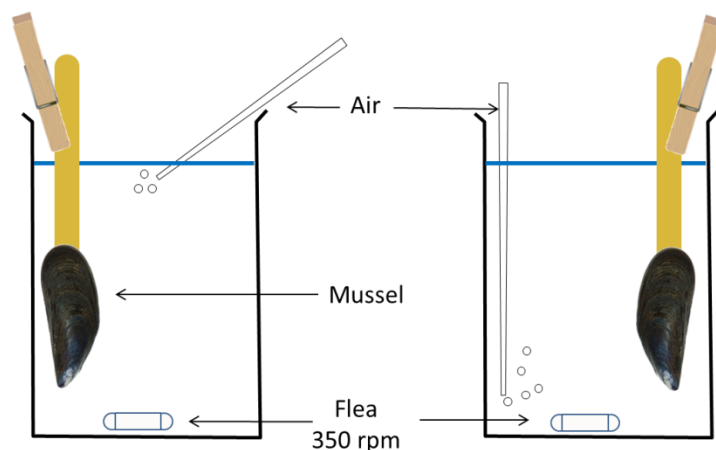


Fig 2.14: Exposure technique to compare oxygen consumption by *M. edulis* under low bubble (left) and high bubble (right) conditions

Results

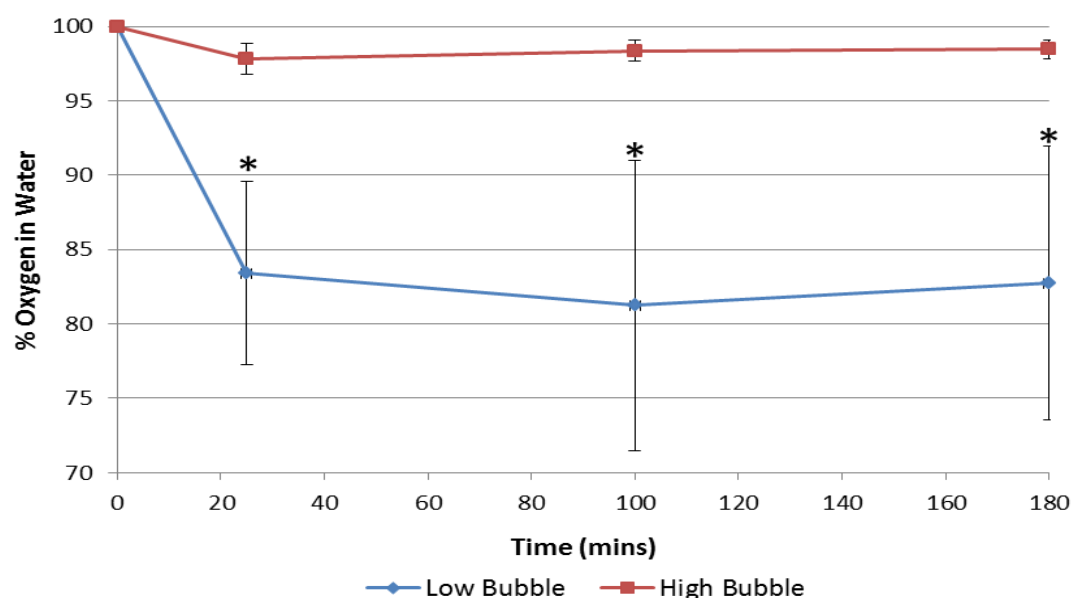


Fig 2.15: Mean Percentage oxygen in water following mussels exposed to CeO_2NPs (1mg/l) for 3 hours under low bubble (n=5) and high bubble (n=6) conditions (with std. dev.). (*) denotes significant difference ($p < 0.005$, t -test)

Fig 2.15 shows the effect of bubbler strength and position of oxygen content of the exposure water. Under previous experimental low bubble conditions, oxygen percentage dropped to around 83% in 25 mins, then stabilized for 155 mins. Under high bubble conditions the oxygen percentage only drops to around 98% after 25 mins before stabilizing.

A *t*-test showed no significant difference in oxygen percentage at 0 mins between treatments [$t(9)=0.06$, $p=0.954$]. However *t*-tests showed differences in oxygen percentage between low and high bubble regimes was significant at 25 mins [$t(9)=-5.69$, $p=0$], 100 mins [$t(9)=-4.33$, $p=0.002$], and 180 mins [$t(9)=-4.23$, $p=0.002$]. In aquaculture literature it is suggested that oxygen concentration should be kept above 50% for *M. edulis* (Barrento *et al.* 2013) and, whilst both aeration regimes achieve this, the variability in results under low bubble conditions points towards using high bubble conditions to effectively maintain oxygen stability. In the future the high bubble method will be employed when exposing *M. edulis*.

ii) Effect of CeO₂NP Concentration on O₂ Consumption

In the previous experiment bubble strength affected water oxygenation whilst an unfed mussel is in a beaker. There is a possibility that the act of feeding could increase O₂ consumption, and that a toxicant in the water may further affect this process. In this experiment O₂ concentration in exposure waters will be measured under conditions of mussels feeding on algae (5,000 cells/ml), and in combination with three concentrations of NM-212 (28nm) CeO₂NPs: 1, 3 and 5mg/l. This experiment will be carried out under the 'high bubble' exposure method validated in the previous experiment.

Results

Fig 2.16 shows the oxygen concentration over 300 mins of exposure waters of mussels fed only algae, and fed algae along with 1, 3 or 5 mg/l CeO₂NPs. All treatments show a drop in oxygen concentration of between 2 and 4% in the first 60 mins, however after this time levels stay fairly consistent, with perhaps a

slight increase. There was no significant difference in oxygen concentration between treatments at any time point [One-way ANOVA, $df = (3,20)$; 60mins: $F=2.74$, $p=0.07$; 120mins: $F=0.927$, $p=0.45$; 180mins: $F=2.12$, $p=0.89$; 240mins: $F=5.24$, $p=0.67$; 300mins: $F=0.458$, $p=0.72$]. These results show that CeO₂NPs do not affect oxygen consumption by *M. edulis* within this system.

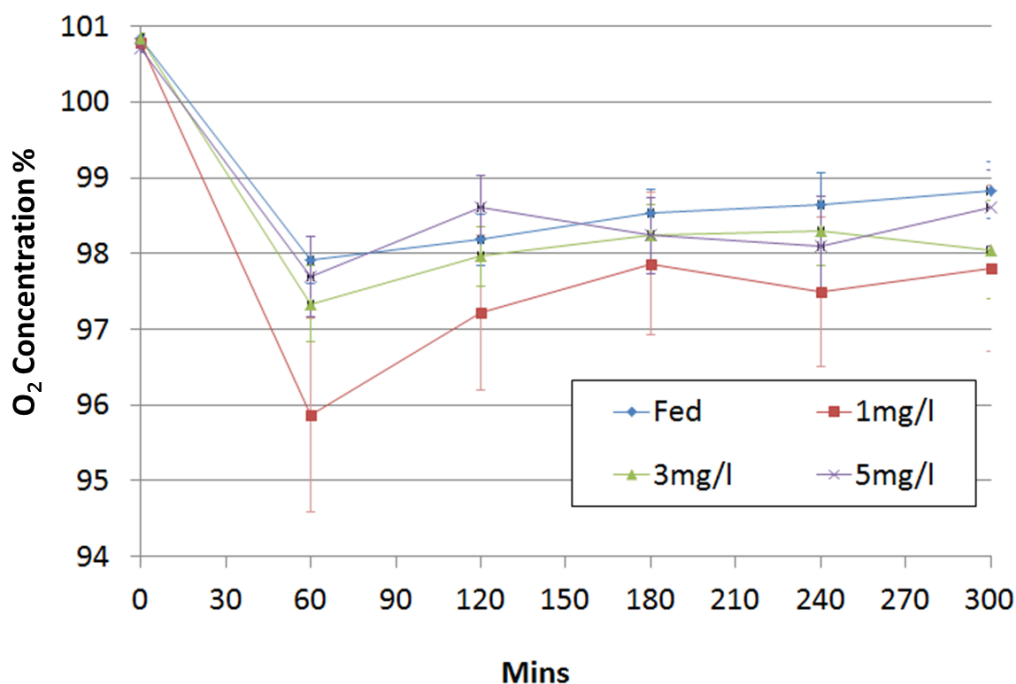


Fig 2.16: Mean Seawater oxygen concentration following exposure of *M. edulis* to algae, and to algal feed in combination with 1, 3 and 5 mg/l CeO₂NPs (n=6 per treatment).

Ammonia Levels

Rising ammonia levels are known to cause oxidative stress (Lima *et al.* 2007) and these stresses can mask any biological effects caused by exposure to Me(O)NPs. The current exposure method for *M. edulis* involves an acute toxicant in a static water system that could cause a build-up of ammonia in longer term exposures.

Mussels (n=6) were individually exposed (as per 2.3.2.3, under high aeration conditions) to NM-212 (28nm) CeO₂NPs at 3mg/l for up to 56 hours, with water samples taken after 8, 24, 48 and 56 hours. Total ammonia concentration was measured on a Hach DR3900 spectrophotometer using the manufacturer's approved method (Hach 2009). Briefly, samples were pooled, and ammonia

salicylate reagent was dissolved in a water sample and left for 3 mins. Ammonia cyanurate reagent was then added and left for 15 mins. This produced a green colour which could be compared against a DI blank. Total ammonia values were converted to free NH_3 content based upon the characteristics of the water sample.

Results

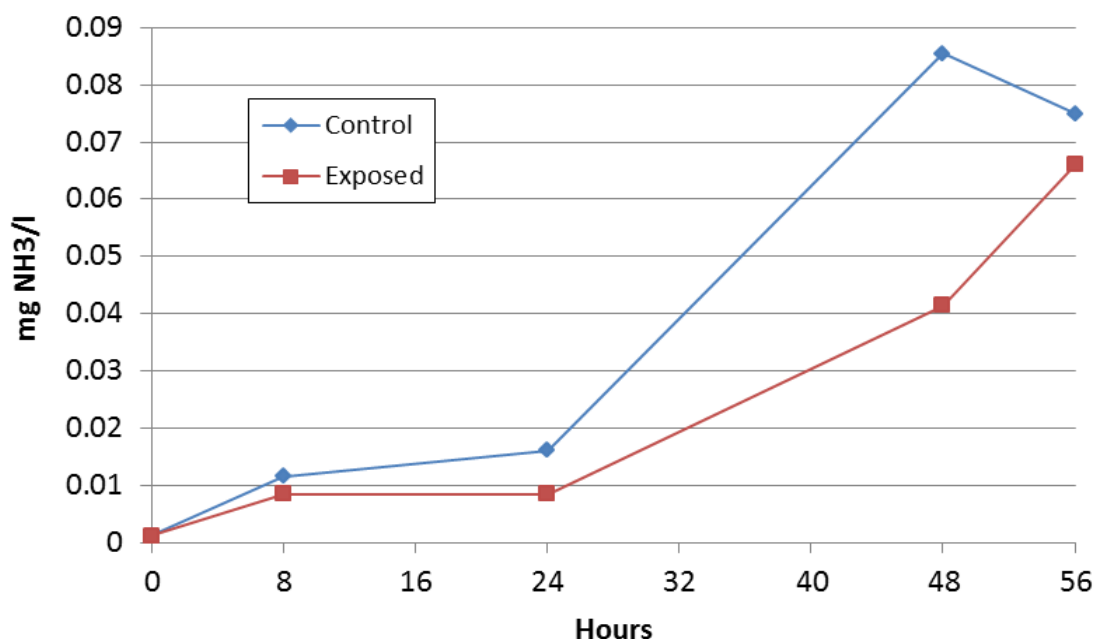


Fig 2.17: Seawater sample (34ppt) NH_3 content following exposure of *M. edulis* to 28nm CeO_2NPs (3mg/l) over 56 hours at 14°C. Control mussels were unexposed. Results pooled to $n=1$, hence no statistical analysis performed.

Fig 2.17 shows NH_3 levels in both control and exposed treatments rose to around 0.01mg/l after 24 hours, but then rose sharply to around 0.07mg/l after 56 hours. There has been no safe ammonia limit derived for *M. edulis*. Previous authors have shown the 96 hour LC_{50} value for the green mussel *Perna viridis* (2.4cm) to be 7.6mg NH_3 /l, with first mortality being 20% after 48 hrs at 5.5mg/l (Reddy and Menon 1979). Another study stated that *M. edulis* is ammonia tolerant up to 1.7mg/l (Sadok *et al.* 1995), whilst Barrento, Lutpash *et al.* (2013) suggested maintaining the organisms at less than 0.2mg NH_3 /l to ensure no ill effects. Given that the highest value achieved here over the 56 hours was less than 0.09mg/l, this exposure method is suitable to prevent ammonia build-up in the case of acute exposures.

pH Levels

Concerns over ocean acidification have led researchers to investigate the antioxidant responses of mussels under fluctuating pH. In particular, significant increases in SOD and CAT activity have been shown in *Mytilus coruscus* when pH drops from 8.1 to 7.3; however this was not significant when pH dropped to 7.7 (Hu *et al.* 2015). This experiment has been designed to measure pH levels in the exposure system in order to understand whether any pH fluctuations exist that might have an impact on oxidative stress in *M. edulis*, thereby masking biological effects caused by Me(O)NPs.

Mussels (n=6) were exposed (as per 2.3.2.3, under high aeration conditions) to either nothing, to algal feed only (at 5,000 cells/ml) or to algal feed plus 1mg/l NM-212 (28nm) CeO₂NPs for 23 hours. pH was measured on a Mettler Toledo SG23 pH/conductivity meter after 1, 2, 3, 4, 5 and 23 hours.

Results

Fig 2.18 shows that despite treatment type, the pH profile of all three treatments is similar over 23 hours. There is an initial drop off over the first 4 hours, and this then stabilises for the rest of the experiment. No significant difference was recorded between any treatments [One-way ANOVA, df=(2,15); 60mins: $F=0.195$, $p=0.83$; 120 mins: $F=0.11$, $p=0.9$; 180 mins: $F=0.182$, $p=0.84$; 240 mins: $F=0.301$, $p=0.74$; 300 mins: $F=0.349$, $p=0.71$; 1380 mins: $F=0.581$, $p=0.57$]. Experiments with *M. galloprovincialis* have shown that reducing pH from 8.03 to 7.48 makes no significant impact on mussel respiration, clearance and ingestion rates (Fernández-Reiriz *et al.* 2012). As (potentially) inter-tidal rocky shore organisms, mussels are generally subjected to high daily fluctuations of pH. The results here, whereby pH drops around 0.1 units over the timeframe of the experiment, shows that the system used for mussel exposure is not subject to any great pH fluctuations that might induce uncontrolled biological effects.

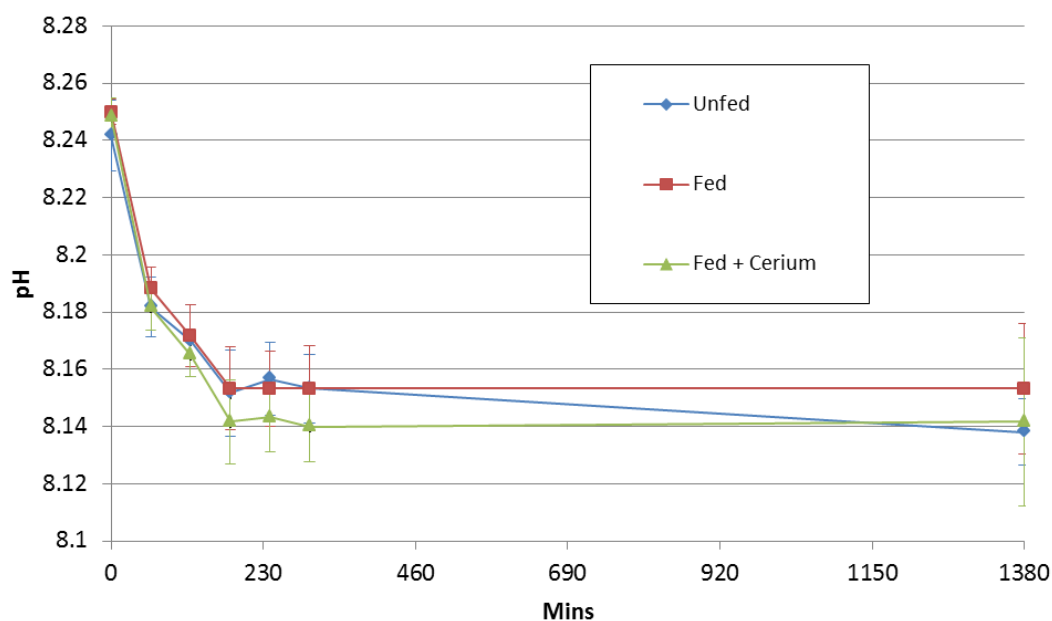


Fig 2.18: Mean pH (with error bars) over 23 hours (1380) mins of exposure water for *M. edulis* (n=6) left unfed, fed algae at 5,000 cells/ml, and fed algae with 1mg/l CeO₂NPs (NM-212, 28nm)

Conclusions

The current exposure methodology set-up is suitable for resisting changes in ammonia and pH that could mask biological effects in *M. edulis* exposed to Me(O)NPs. Oxygen concentration however was found to drop too rapidly under previous aeration methods. This method is to change by oxygenating the beaker lower in the water column and at a higher bubble rate, thereby allowing more time for oxygen to dissolve in the water.

2.3.3 Final Apparatus for Exposure of Me(O)NPs to *M. edulis*

Prior to exposure eight 400ml beakers are filled with 330ml 0.2µm filtered ASW and arranged on a Variomag 15 stir-plate at 230rpm. These are covered with an acrylic plate drilled with holes for the introduction of mussels, and for aeration. Prior to introduction the mussels are further rinsed in FASW, then attached to the rinsed craft sticks, which are then held in place in the beakers by a clothes peg, hovering the mussel 2cm below the water line. Pasteur pipettes are introduced as an air supply and bubbled from 2cm above the

bottom of the beaker (Fig 2.19). This now forms a stable, repeatable method for exposing mussels that is suitable for both Me(O)NP uptake and biological effects assays.

There are pros and cons of using such a system. For example, some mussel populations are inter-tidal. This means they would not be continuously subject to waterborne toxicants, but instead might hold water within them to prevent desiccation at low-tide; water which may contain toxicants and then subject them to constant internal exposure. Other populations however – including those used in aquaculture – are entirely sub-tidal, and this system is a better exemplar for those populations. This system also reflects populations that might be found submerged in rock pools, whereby mussels are constantly subject to a finite volume of toxicant-bearing water.

In the natural environment Me(O)NPs are likely to agglomerate and sink; allowing the particles to sink in these exposures without having a stirring mechanism would leave them more susceptible to adsorption to the surfaces of the beakers rather than interact with the organism. As such, in order to reduce such adsorption, this system employs a stir flea to keep particles in suspension. It could be suggested that, since the sea is not static, wave action and currents would also keep particles suspended therefore use of a stir flea adds a degree of environmental realism.

The notion of exposing mussels either individually or in groups was discussed in Chapter 2.3.2.3. The pilot experiments presented here were designed to maximise uptake into the mussel for future trophic transfer experiments. In reality, mussel beds are dense, highly complex environments with multiple overlaps and surface areas than could act as adsorptive sinks for nanoparticles. Large mussel groups would also result in micro-currents, variety of pumping rates and competition for food sources. As such the system does not necessarily prove a good exemplar for this, however mussel communities are also found in open ocean and these laboratory-based studies are confined to finite volumes of water. As mentioned above, this system is a better exemplar of areas where isolated mussel communities might be found, such as in rock pools.

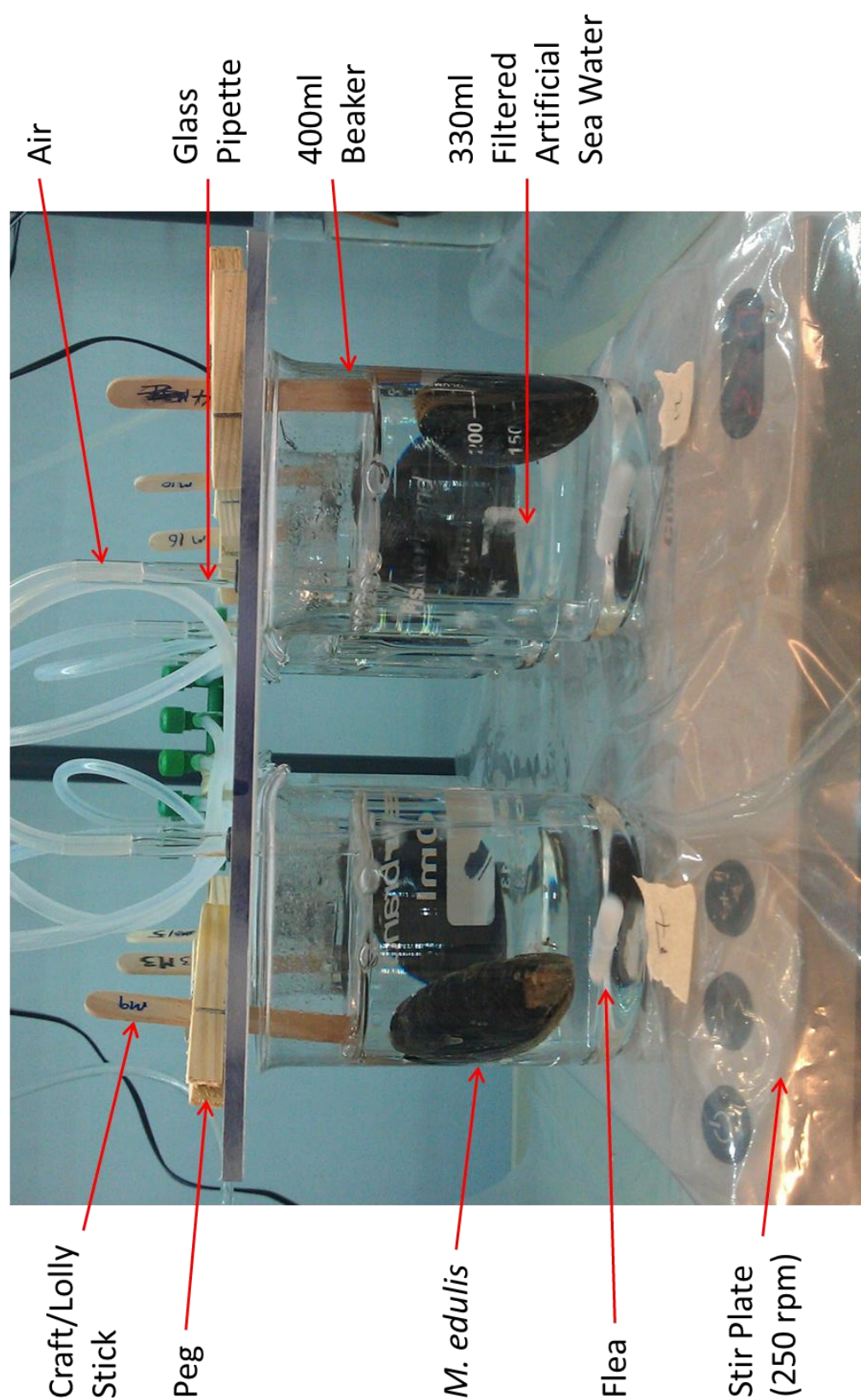


Fig 2.19: Standardised equipment set-up for the exposure of *M. edulis* to Me(O)NPs

2.4 The Shore Crab *Carcinus maenas*

2.4.1 Pertinent Physiology



Fig 2.20: The Shore Crab *Carcinus maenas*

The Crustacean shore crab *Carcinus maenas* (Fig 2.20) is a euryhaline rocky shore predator and voracious scavenger. Although found down to a depth of 60m, it is usually most abundant in the shallows. It can also survive out of water for periods longer than 7 days (Perkins 1967). Since *C. maenas* is a natural predator of *M. edulis*, this makes it a useful organism through which to study trophic transfer following consumption of mussels exposed to Me(O)NPs.

The crab has four pairs of walking legs (the 2nd to 5th legs), and two claws, or chelae. These are responsible for tearing food and feeding the organism (Crothers 1967). As food is taken into the mouth it is crunched and chopped by the maxillae and mandibles then passes down the oesophagus into the anterior chamber of the stomach (Fig 2.21). This is mixed with digestive juices from the posterior chamber and ground down by the ossicles in a gastric mill. This section filters large particles out into the posterior chamber, then through the mid gut towards the hind gut and anus, whilst smaller particles and fluids may pass down the ventral groove and through the filter press (gland filter).

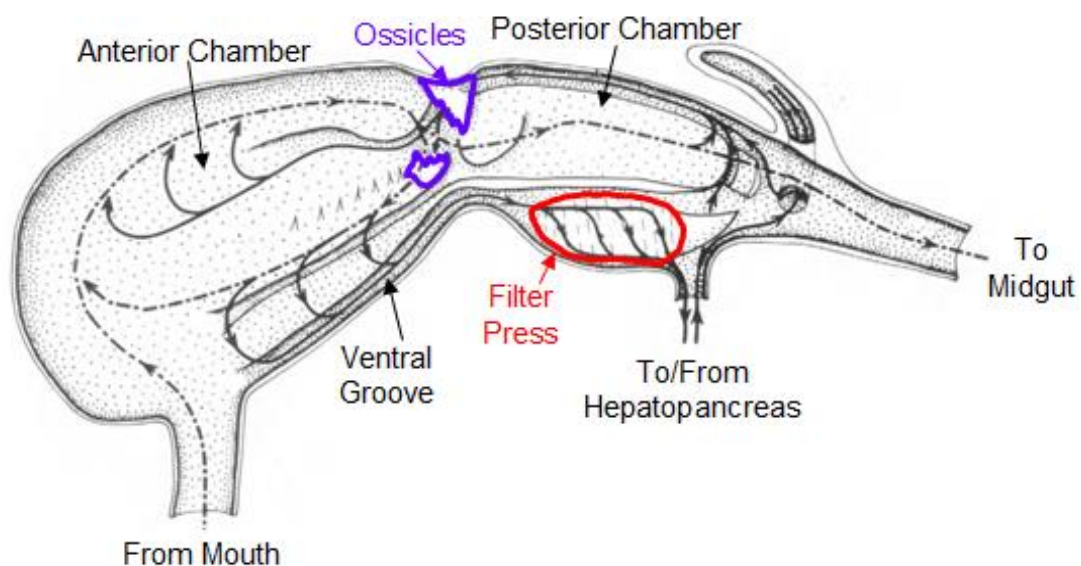
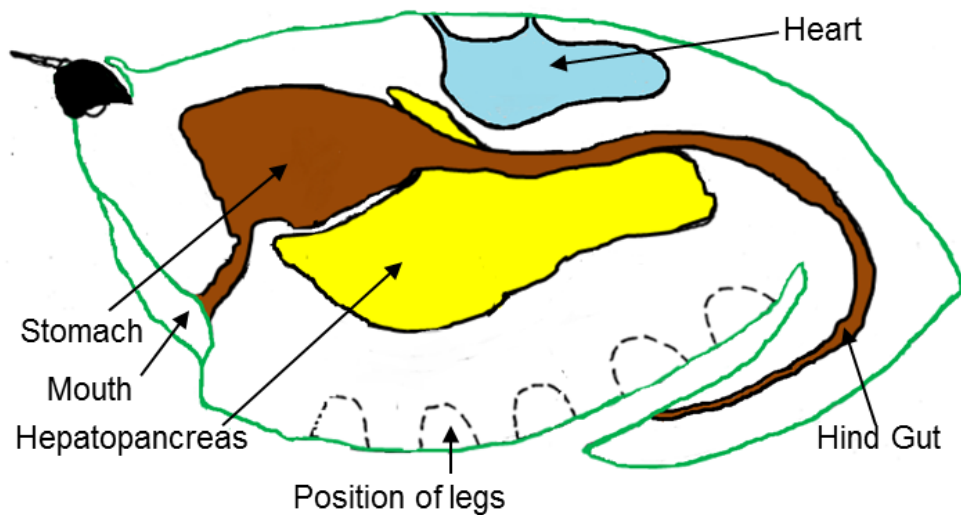


Fig 2.21 Top: Simplified internal anatomy of the main digestive features of *C. maenas* [adapted from (McLaughlin 1980)], and Bottom: potential routes taken by ingested materials through the stomach (dotted lines = solid food, solid lines = fluid). [adapted from: (Dall and Moriarty 1983)]

The filter press is a series of setae designed to stop particles greater than $1\mu\text{m}$ from entering the hepatopancreas. This means that free Me(O)NPs - and even large agglomerates - should be able to penetrate the filter press, but that the uptake of any that are found embedded in consumed products is based upon the efficiency of the food's breakdown by the anterior chamber of the stomach.

C. maenas has nine pairs of gills; the front six are used mainly for gas exchange and the rear three are also involved in osmoregulation (Hebel *et al.* 1999). When immersed the crabs draw water in through a hole in the base of each leg, but mainly through a hole beneath the chela. This is circulated through the branchial chamber mostly over the gas exchange gills and out through the mouth. This is achieved by means of a scaphognathite, a modified beating gill that drives the water flow and keeps the other gills clean (Crothers 1967). The flow is reversed occasionally to help oxygenate the posterior gills, and this method is also used when the organism is buried in substrate, or when the aerating holes are blocked. In the case of the crab being out of water (emmersed) or in dirty water, clean water is held in the branchial chamber and also aerated by means of the mouth. This allows the animal to stay out of water for long periods simply by oxygenating the water around its gills.

2.4.2 Method Development for Feeding Exposed *M. edulis* to *C. Maenas*

2.4.2.1 Collection of *C. maenas*

C. maenas were purchased from a fisherman at Exmouth docks, Devon, UK, where they had been collected in crab traps scattered off the coast of Exmouth (50.604595, -3.4121332). Female crabs with all legs intact (c. 70g, carapace length c. 7cm) were selected and stocked at a density of 20 crabs per 24L flow-through tank, and fed once every three days on commercially-bought frozen mussels (Gamma Slice). Prior to exposure the crabs were starved for a week to help prompt them to eat the presented mussels in trophic transfer experiments.

2.4.2.2 Consumption of *M. edulis* by *C. maenas* when Immersed

It was unknown how successfully a crab would eat any mussel under our experimental conditions, let alone one exposed to Me(O)NPs. A major objective of this study was to investigate how crabs reacted to being fed in the apparatus that was available.

When feeding, food passes from the mouth of the crab to the stomach, then through into either the hepatopancreas for absorption or the hindgut for egestion. Crabs are known to feed by tearing up their prey, and there is also potential for loose particles to enter the water column and be taken up during ventilation into the branchial chamber and associate with the gills.

It is hypothesized that the stomach of the crab will be a major site of accumulation of Ce due to feeding on CeO₂NP-laced mussels. Gills will also show some Ce accumulation due to free-floating CeO₂NPs entering the water column (Hebel *et al.* 1999).

Method

Crabs were collected and stored as per chapter 2.4.2.1. *M. edulis* were exposed individually as per chapter 2.3.3 to 20mg/l of NM-212 (28nm) CeO₂NPs for 72 hours prior to crab feeding. An hour before feeding, crabs (n=4 [control], n=6 [exposed]) were placed individually into 3l of FASW in 9l glass tanks to acclimate. Aeration was provided by airstone (>10 bubbles per second).



Fig 2.22: Tank set-up for feeding exposed *M. edulis* to immersed *C. maenas*

Following exposure, mussels were removed and rinsed three times, dried, then the adductor muscle cut and the organism opened, drained of extrapallial fluid, the foot removed, and the gill, digestive gland and mantle scraped clear of the shell for easier feeding. Two mussels (i.e. one set of these tissues; 6 exposed, 4 unexposed) was then placed (back in shell) in each crab tank (Fig 2.22) and

the crabs allowed to feed for 24 hours in darkened conditions. This was then repeated a second time for a total of two mussels fed over 48 hours.

The gill, digestive gland and mantle of 11 mussels (7 exposed, 4 control) were also immediately snap frozen, freeze-dried, and used for whole-body Ce content analysis as per Chapter 2.2.1. Following feeding crabs were removed, and the gills, stomach and hepatopancreas dissected out and snap-frozen, then freeze-dried and acid digested for Ce content analysis.

Results and Discussion

Exposed mussel data was not normal (Shapiro-Wilk, $p=0.01$), and was thus log transformed to normality before analysis by t -test. At $63.7\mu\text{g Ce/g d.w.}$ (± 30.3 std error [SE]), exposed mussels therefore contained significantly [$t(9)=3.737$, $p=0.005$] more Ce than control mussels ($3.1 \pm 2.01\mu\text{g Ce}$).

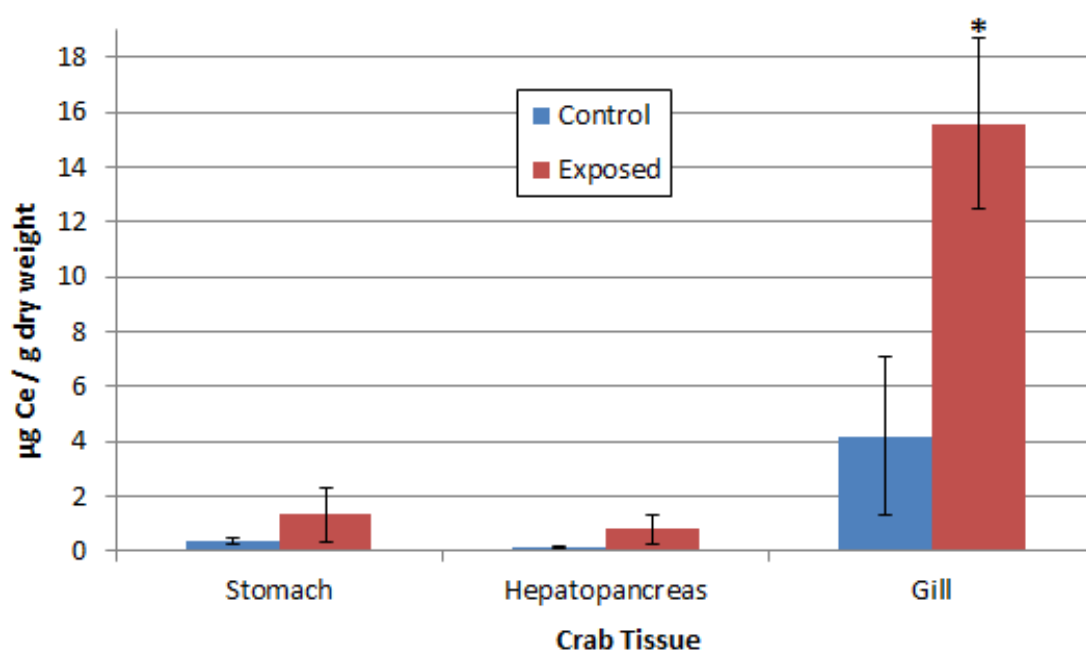


Fig 2.23: Mean Cerium content ($\mu\text{g/g d.w.}$) of the stomach, hepatopancreas and gills of crabs fed unexposed (control) *M. edulis* and those fed *M. edulis* exposed to $20\text{mg/l CeO}_2\text{NPs}$. (*) = significant difference ($p<0.05$, t -test). Control $n = 4$, Exposed $n = 6$.

Regarding crab tissues, control data for both the stomach and hepatopancreas was found to be non-normal (Shapiro-Wilk, $p=0$) and was therefore log transformed for normality and analysis by t -test. This then showed no significant

difference between the Ce load of the stomach [$t(8)=0.256$, $p=0.804$] or hepatopancreas [$t(8)=1.292$, $p=0.232$] in crabs fed exposed mussels compared to unexposed mussels. Part of the reason for this may be in the variability of the data (Fig 2.23). In particular there were high error bars noted for the stomach of the exposed-fed crabs.

It was hypothesised that the stomach would be a major organ of accumulation yet crabs fed exposed mussels had no significant difference in Ce content to the control. Given that crabs were allowed 24 hours to feed per mussel, it may be that the crabs fed early and any stomach Ce content was already processed and either in the hepatopancreas, the hind gut, or egested as faeces. The hepatopancreas Ce content was not significantly different to the control. The fact that the average Ce content in both the stomach and hepatopancreas is higher (although not significantly) and has a greater spread of data means that some Ce is likely to have been trophically transferred from the mussel to the crab, but this cannot be said conclusively.

The gills of crabs fed exposed mussels have a significantly greater Ce burden than those of control crabs (t -test, $t(8)=-2.51$, $p=0.036$). This increased presence of Ce could be a result of absorption by the hepatopancreas, with Ce then sent to the gills for detoxification, possibly via the haemolymph. However since no haemolymph samples were taken, and since the gills were not dissected into osmoregulatory and respiratory forms, then understanding this route of transit and potential differences in gill function cannot be achieved here.

Another reason for high levels of Ce in the gills is that they may have accumulated Ce from the surrounding waters as a facet of the crab tearing up the Ce-laden mussels to feed. Samples of post-exposure crab water were analysed for Ce content. Exposed data was not normal (Shapiro-Wilk, $p=0.011$), therefore data was log transformed for normality and analysis by t -test (Levene's Test for Equality of Variance showed heterogeneity of variance, $p=0.014$). Results then showed that water in which crabs were fed exposed mussels contained 2.91 ± 2.1 (SE) $\mu\text{g Ce/l}$, significantly higher [$t(4.564)$, $t=-2.914$, $p=0.037$] than the water containing unexposed mussels ($0.062 \pm 0.01\mu\text{g/l}$). It is plausible that during ventilation, the gills adsorbed some of the free-floating Ce

that was released either as the crabs tore up their prey, or from break-up of free-floating faeces.

Unfortunately the methodology of this experiment was not robust enough to significantly decipher between accumulation by the crabs of Ce through a trophic transfer route, and that accumulated from water-borne exposure routes. Some of the crabs in the experiment were unable to fully consume two mussels over the 48-hour period, and the data may have been skewed by this. Future experiments will feed the crab out of water (i.e. emersed) to negate the water-borne exposure route, and make it possible to recover faeces for Ce content analysis to help understand the fate of trophically transferred CeO₂NPs. Crabs will also only be fed one mussel over 24 hours, and only crabs that have fed significantly on their prey will be considered for analysis. Where possible any unconsumed remains will also be analysed for Ce content to allow for more accurate mass balance modelling.

Chapter 3: Bioaccumulation and biological effects of CeO₂NPs in *M. edulis*

3.1 Abstract

The use of manufactured NPs is increasing, with their ultimate fate being marine ecosystems. CeO₂NPs are widely used to increase fuel efficiency in diesel engines, and as metal polishers. Current studies on CeO₂NPs highlight conflicting results over whether they possess pro- or anti-oxidant properties, and thus could negatively affect biological processes in organisms.

Here uptake of 10nm, 28nm and 600nm CeO₂ by *M. edulis* is examined as a function of time, particle size, and concentration, as is their potential to affect biological processes. Briefly, individual mussels were placed in 330ml artificial seawater and dosed with three sizes of CeO₂ (10, 28, 600nm) at concentrations between 1 and 5 mg/l, along with algal feed to encourage feeding. Gill, digestive gland and mantle tissues were then dissected for Ce concentration and biological effects.

Results show that maximum 10nm CeO₂NP uptake is after four hours in mantle and digestive gland tissues, but 8 hours for the gill. Whole body uptake is limited to roughly 5% of the offered dose within 4 hours, and this is quickly removed. The digestive gland is the tissue of greatest uptake (95% of body burden). Lower concentrations accumulate in *M. edulis* more efficiently than higher concentrations. Micron-size (600nm) CeO₂ demonstrated anti-oxidant properties, however 10nm CeO₂NPs had no significant effects on oxidative stress or lipid peroxidation.

3.2 General Introduction

The global production of CeO₂NPs in 2010 was estimated at a maximum of 10,000 metric tons per year (t/yr) comprising use in optics, fuel catalysts, medical applications and coatings, with around 300t/yr reaching waterways (Keller *et al.* 2013). The median background concentration of Ce in European streams has been measured at 55 ng/l (FOREGS 2005). In the San Francisco Bay area Ce concentration in wastewater treatment plant effluent has been estimated as 10-1000ng/l (Keller and Lazareva 2014). Another study has estimated worldwide effluent concentrations averaging only 0.01ng/l, with anthropogenic surface water inputs estimated at 10-100ng/l (Gottschalk *et al.* 2013), although the authors indicated these were likely over-estimated and based on scant data. Particulate emissions of CeO₂NPs from diesel combustions is expected to add only 0.02ng Ce/l, although in stormy conditions road run-off could increase this to 300 ng/l (Johnson and Park 2012).

Bivalves are particularly susceptible to accumulation of Ce from background concentrations in the water. Whole body concentrations of Ce in the bivalve *Chlamys varia* off the coast of western France have been measured between 0.36-0.92 µg Ce/g d.w. in non-industrial areas, and between 3.59-4.5 µg/g d.w. in sites close to a processing plant of rare earth elements (Bustamante and Miramand 2005). There are currently no regulations surrounding safe concentrations of Ce in water however a limit of 3 mg/l has been suggested based upon Surface Water Directive limits for other benign materials (O'Brien and Cummins 2010).

The bivalve blue mussel *Mytilus edulis* is an abundant UK coastal organism and OECD sentinel species, with a water pumping rate than can turn over several litres per hour (Vahl 1973). This makes them efficient filters of seawater, and leaves them especially vulnerable to water-borne toxicants such as near-shore discharges of NPs. This was shown in a mesocosm study (Ferry *et al.* 2009) in which juvenile clams (*M. mercenaria*), despite only accounting for 0.5% of the biomass, managed to accumulate over 5% of the insoluble AuNPs (rods, 65 x 15 nm) offered, more than the 4% accumulated by grass, grass shrimps, sheephead minnows and snails combined (the majority - 61% - was

accumulated by biofilms [39% of biomass] whilst some 35% stayed in the water).

CeO₂NPs are considered insoluble in natural fresh and marine waters (Zhang *et al.* 2012), and any effects on organisms are unlikely to result from significant ion dissolution, as is often shown with ZnO and AgNPs (Baker *et al.* 2013). The spontaneous redox cycling between Ce³⁺ and Ce⁴⁺ ions on its surface leads to an oxygen vacancy that can be filled by the superoxide free radical. This leads authors to believe that CeO₂ may display SOD-like activity that helps prevent oxidative stress in organisms. This has been shown in mice for example in protecting nerve cell (HT22) lines (Schubert *et al.* 2006) and reducing cardiac endoplasmic reticulum stress (Niu *et al.* 2007), however CeO₂NPs have also been linked with increased cytotoxicity to *Escherichia coli* (Thill *et al.* 2006) and damage to the algae *Pseudokirchneriella subcapitata* (Hoecke *et al.* 2009) due to adsorption to cell membranes. Exposure to insoluble AuNPs has been shown to induce increased digestive gland ROS production (Tedesco *et al.* 2010) and gill CAT activity (Tedesco *et al.* 2008) in *M. edulis*, showing that oxidative stress can be instigated in bivalves without particle dissolution.

There are two key aims of this Chapter. The first is to use *M. edulis* in a series of experiments to study the bioaccumulation and biological effects (changes in oxidative stress and lipid peroxidation) of CeO₂NPs to investigate whether the suggested regulatory limit of 3mg/l is sufficient to protect the organism from sub-lethal effects. The second aim is to use this bioaccumulation data to guide planning of future studies into trophic transfer between *M. edulis* and the crab *C. maenas*.

Two sizes of JRC CeO₂NP (as per Chapter 2.2.1) will be used, 10nm (NM-211) and 28nm (NM-212), as well as a 600nm 'micron-size' comparison particle (NM-213). This larger particle is closer in size to the optimum food size (1-5µm) for *M. edulis* (Møhlenberg and Riisgård 1978), and also serves to help ascertain if biological effects are induced purely through the presence of Ce, or if there is a nano-specific effect.

The first experiment explores accumulation and elimination of 10nm CeO₂NPs by *M. edulis* over 56 hours firstly in order to determine at which timepoint the mussels become most loaded with Ce, and secondly to understand subsequent elimination of Ce from the gill, digestive gland and mantle. The second experiment explores the uptake of the three sizes of CeO₂ into the gill, digestive gland and mantle of *M. edulis* as a factor of size and concentration. The third experiment compares the potential of 10nm CeO₂NPs and 600nm micron-size CeO₂ to induce biological effects in *M. edulis* and explores subsequent recovery from these effects.

3.3 Time Series Uptake of 10nm CeO₂NPs by *M. edulis*

3.3.1 Introduction

A major hypothesis of this thesis is that CeO₂NPs can trophically transfer from *M. edulis* to *C. maenas*. To maximise the concentration of Ce in *M. edulis* for these future experiments it is necessary to understand how the organism accumulates CeO₂NPs over time.

M. edulis has a pumping rate of several litres per hour (Jones *et al.* 1992) hence it would be expected that exposure to toxicants is likely to result in rapid uptake. Maximum uptake of tributyltin tin (TBT) for example has been measured at around 90 minutes with depuration over 24 hours (Laughlin *et al.* 1986). The uptake kinetics between ionic and insoluble metals will differ since ionic forms accumulate across cell membranes via diffusion and ion-mediated channels (Rainbow 2009), hence it is not relevant to extrapolate accumulation kinetics of insoluble CeO₂NPs from ionic metal data. Similarly, extrapolating from algal cell clearance rate is unreliable considering that initial mussel gill capture efficiency of particles less than 1µm has been shown as less than 20%, compared to 100% for particles of algal cell size (5-18µm) (Jørgensen 1974), and that pumping rate can vary based upon algal concentration in the water (Riisgård *et al.* 2011).

When it comes to comparable information for acute uptake of insoluble non-organic or metallic particles then there is scant time series data available. Microplastics (1-80µm) have been observed in the digestive gland of *M. edulis* after three hours exposure, with maximum uptake after 12 hours (von Moos *et al.* 2012), but again these were of a size more closely related to their prey. Another study (Ward and Kach 2009) showed that both *M. edulis* and *C. gigas* ingested large agglomerates of 100nm polystyrene spheres in only 45 minutes, yet did not take up any disagglomerated NPs. This suggests that agglomeration speed of NPs may then become a factor in their uptake.

M. edulis has been shown to accumulate 5nm (Tedesco *et al.* 2010) and 15nm (Tedesco *et al.* 2010) AuNPs and 68x8nm CeO₂NP rods (Montes *et al.* 2012) within 24 hours exposure, and glass nanofibres (20-200nm Ø) within 12 hours

(Koehler *et al.* 2008). Studies have highlighted the digestive gland as the major tissue of NP accumulation in *M. edulis* (Canesi *et al.* 2010, Tedesco *et al.* 2010, Tedesco *et al.* 2010, Garcia-Negrete *et al.* 2013, Hull *et al.* 2013, Gomes *et al.* 2013b), yet it has also been noted that pseudofaeces are the fate for the majority of Me(O)NPs, showing that if NPs are being captured, they are mostly rejected before ingestion (Montes *et al.* 2012).

The aim of the following experiment is to perform a 56-hour scoping study to determine after how long, and into which tissues, *M. edulis* will accumulate its maximum Ce load following exposure to 10nm CeO₂NPs, and whether this Ce is retained or eliminated.

The hypotheses are that *M. edulis* will show maximum Ce concentrations in its tissues within 8 hours of exposure to CeO₂NPs, that the digestive gland will be the major site of accumulation, and that Ce accumulated in the digestive gland will show the slowest elimination, although all tissues will have eliminated Ce within 56 hours.

3.3.2 Method

To determine an uptake profile for nano-CeO₂ over time, mussels (c. 30g) were exposed individually in 330ml FASW and received a 1mg/l dose of 10nm (NM-211) CeO₂NPs along with algal feed (as per Chapter 2.3.3). They were removed following 4, 8, 24, 32, 48 and 56 hours exposure (n=7 per timepoint), and gill, digestive gland and mantle were dissected out, freeze-dried and acid digested. Digested samples were pooled from n=7 into a single sample per timepoint to be analysed by ICP-MS for Ce content (as per Chapter 2.2.). 0 hours was used as a control for background concentrations i.e. no Ce added.

3.3.3 Results & Discussion

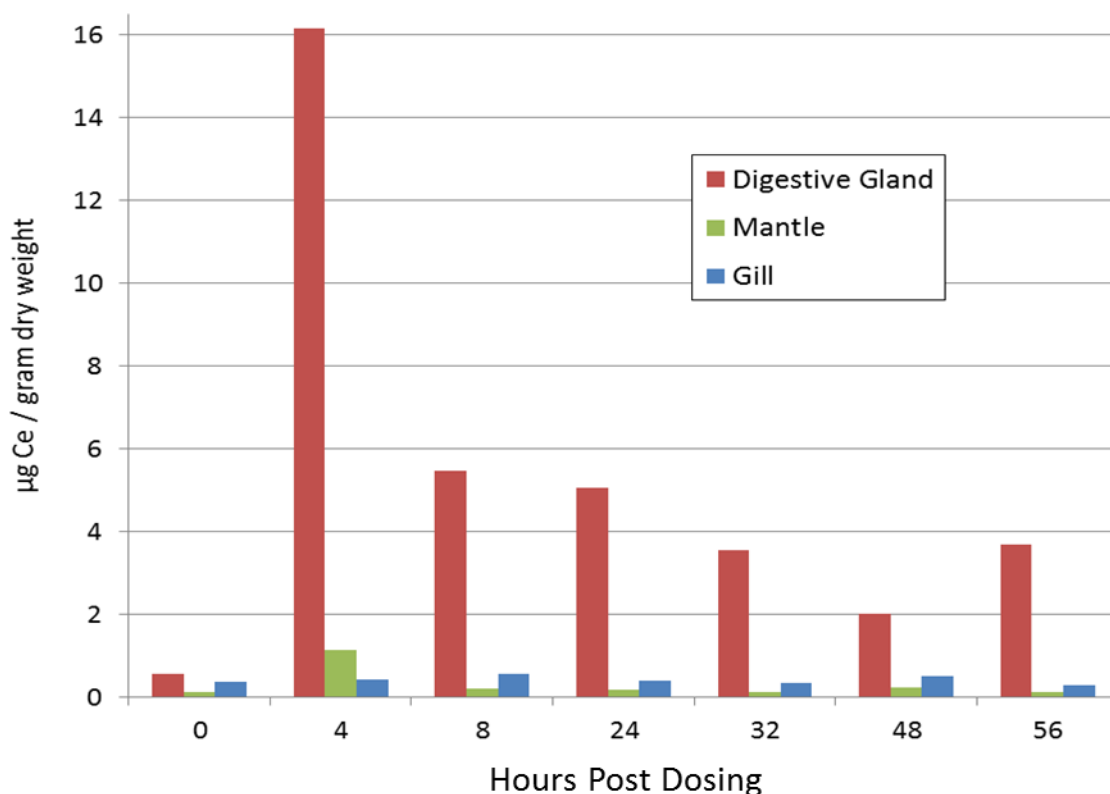


Fig 3.1: Cerium concentrations found in the digestive gland, mantle and gill (µg Ce/g dry weight) of *M. edulis* following exposure to 10nm (NM-211) CeO₂NPs at 1mg/l for 56 hours (samples pooled to n=1 from n=7 per timepoint)

Fig 3.1 shows the accumulation of Ce in various organs of *M. edulis* over 56 hours following exposure to 10nm CeO₂NPs at 1mg/l. It was hypothesised that maximum uptake would be in the digestive gland after 8 hours; here maximum uptake was in the digestive gland followed by the mantle, but both after 4 hours, and both over 10 times higher than the control. In the gills maximum concentration occurred after 8 hours, and was barely double that of the control. It was also hypothesised that all tissues would have eliminated their accumulated Ce burden by 56 hours. Instead the digestive gland shows elimination towards 56 hours but is not fully clear, whilst the gill and mantle appear to have eliminated accumulated cerium by this point.

Mussels are able to filter several litres of water per hour (Meyhöfer 1985) whilst introducing algal feed with the NP dose encourages the mussels to increase their filtration rate (Riisgård *et al.* 2011). The rapid uptake of these particles could then be explained by the mussels rapidly turning over the 330ml of spiked

seawater in the beakers. Previous experiments using *M. galloprovincialis* and 50nm Fe₃O₄NPs for example have highlighted a half-life loss of NPs from the system of just 1.2 hours (Hull *et al.* 2013).

There are two potential main uptake routes of the CeO₂NPs: as individuals/aggregates/agglomerates, or adsorbed to algae. Particles captured by the gills are generally sent to the palps to be sorted for edibility. Inedible particles are rolled in mucus into pseudofaeces and sent to the mantle rejection tract to be removed. Edible particles are ingested and broken down by the style. Particles still too coarse are deemed inedible and sent to the midgut and intestine for egestion, whilst fine particles are sent to the digestive diverticula and digestive tubules for intra-cellular digestion and absorption. Any particles then still considered indigestible can be removed from the tubules in vacuoles and sent to the intestine (Riisgård *et al.* 2011).

The digestive gland shows a rapid drop in concentration between 4 and 8 hours. Ward and Kach (2009) showed that nano-sized particles had a longer residence time than 10µm polystyrene spheres in the digestive gland of *M. edulis* due to penetration of digestive tubules and possible endocytosis. It is possible to speculate then that much of the Ce accumulated in the digestive gland in the first 4 hours is deemed inedible and rapidly egested from the digestive gland, not reaching the digestive tubules. There is slower elimination after this point, and the similarity between 32 and 56 hour levels suggests some retention by the organism. The pH of the mussel's digestive gland and style is only slightly acidic, at around pH 6.5 (Langton 1977). CeO₂ requires a much stronger acidic environment to dissolve effectively (Um *et al.* 2011, Joshi *et al.* 2012), hence it is highly unlikely that the CeO₂NPS are being dissolved and Ce accumulated via ionic uptake.

In terms of the mantle, this organ secretes acid mucopolysaccharides (AMPs) that help keep rejected pseudofaeces stuck to the mantle surface before they are removed through the exhalent siphon (Beninger *et al.* 1999), and these might prove particularly adhesive for NPs (Marigomez *et al.* 2002). Accumulation of Ce by the mantle is very rapid (4 hours), however there is almost total elimination by 8 hours and full elimination by 56 hours. The mantle

surface is covered in cilia designed to move particles (Beninger *et al.* 1999) which may explain why the mantle is able to eliminate Ce itself.

In terms of the gill, Ce concentrations show maximum increase after 8 hours, but return to control levels within 56 hours. Ce accumulation potential for this organ is likely to be particle adsorption to the gill filaments or trapping in the inter-ciliary space. Again, the functional nature of the organ i.e. to transport particles, is probably responsible for its ability to eliminate itself of Ce.

Concurrent with adsorption to the gill and mantle, there is potential for internalisation of NPs into these organs. Colloidal iron hydroxide has been found in pinocytotic vessels in gill epithelial cells, with evidence of these vesicles fusing with other lysosomes and emptying into the haemolymph, where they were engulfed by haemocytes (George *et al.* 1976). There is also evidence of mantle uptake of iron particles, possibly through endocytosis, yet mantle epithelial cells are also known to secrete metals. Haemocytes known as brown cells are able to engulf internalised metals from other organs and transport them, via them haemolymph, for excretion either via the stomach, or to mantle epithelial cells (Marigomez *et al.* 2002). It is possible to hypothesise then that the slow elimination rate of the digestive gland might in part be due to it being a detoxification terminus for metals accumulated by other organs. It would be worth examining the haemolymph in future exposures in order to better understand this process.

There are a number of potential adsorptive sinks for CeO₂NPs in this system that might lock them away from potential uptake through the course of the experiment. These include air lines, the beakers, the supportive measures for the mussel (Velcro & lolly sticks), the mussel shell, and any organs or tissues not examined e.g. the foot and skirt. Exposure to colloidal iron for example has highlighted transfer of the iron to, and sequestration in, the byssal threads (George *et al.* 1976). Hull *et al.* (2013) found that their empty system (including mussel shell) could adsorb iron oxide NPs at a rate of 50% every 20 hours. It is possible that changing the exposure system could result in greater concentrations of CeO₂NPs being taken up, and in real-world scenarios the complexity of the mussel's habitat will have a bearing on accumulation potential.

Table 3.1 shows extra Ce accumulation in the three tissues over time as a percentage of the dose offered (269µg Ce in 330µg CeO₂) to the mussel. Total accumulation by the gill, stomach and mantle is a maximum of 5.82% and this is similar to the values measured by Montes *et al.* (2012) where 95% of a Ce nanorod dose fed to *M. galloprovincialis* was converted to pseudofaeces, and of Ferry *et al.* (2009) which showed *M. mercenaria* accumulating 5% of the AuNPs offered in a mesocosm study.

% Uptake in:	4 hrs	8 hrs	24 hrs	32 hrs	48 hrs	56 hrs
Gill	0.037	0.063	0.034	0.003	0.037	0
Digestive Gland	4.786	1.462	0.984	0.638	0.218	0.572
Mantle	1.001	0.115	0.132	0.024	0.098	0
Total	5.824	1.640	1.151	0.665	0.035	0.557

Table 3.1: Percentage accumulation of cerium by the gill, digestive gland, or mantle, and whole body of *M. edulis* following exposure to 330µg (1mg/l) of 10nm CeO₂NPs at for 4, 8 24 or 32 hours (= timepoint with highest percentage uptake). Figures are calculated by subtracting cerium background (control, = 0 hr) concentration from tissue concentration at each timepoint, and then dividing by the dose of cerium received (NB: CeO₂ contains 81.4% cerium).

This experiment supports the work of other studies (Canesi *et al.* 2010, Tedesco *et al.* 2010, Tedesco *et al.* 2010, Garcia-Negrete *et al.* 2013, Hull *et al.* 2013, Gomes *et al.* 2013b) that show the digestive gland as the bivalve's organ of maximum NP uptake. However some differences between these studies and this experiment are notable, particularly in accumulation speed and elimination rates. In this experiment *M. edulis* rapidly accumulated CeO₂NPs within 4 hours before concentration dropped towards 56 hours. In the Hull *et al.* (2013) study, exposure of *Mytilus galloprovincialis* to 50nm iron oxide NPs showed levels of iron concentration in the digestive gland were still high after 72 hours depuration following exposure, although exposure to 12nm cadmium (Cd) NPs showed levels quartering after 72 hours depuration. The authors suggest that the usefulness of iron as a micronutrient might influence its retention, whereas non-essential metals (such as Cd) are removed quickly through, for example, metal granule formation. Cerium is not an essential metal for bivalves, therefore the speed at which it has been removed suggests that it is being

effectively partitioned and eliminated by *M. edulis*, as shown with CeO₂NPs by both Conway *et al.* (2014) and Montes *et al.* (2012).

This experiment acted as a scoping study to examine the accumulation and elimination of a single size of nanoparticle at a single concentration. It showed that maximum uptake of CeO₂NPs by *M. edulis* was roughly 5% of the dose, and occurred after 4 hours. This timepoint can be used as a guide for mussel-loading during trophic transfer experiments. Further studies are needed to understand the behaviour of different sizes of CeO₂, especially comparisons to a non-nano-sized equivalent to confirm if nano-size changes the accumulation and effects of CeO₂.

3.4 CeO₂NP Uptake as a Factor of Size and Concentration

3.4.1 Introduction

The dynamics of NPs in liquid media becomes complex as, due to their small size, they start to behave more like colloids and less like particles. In order to understand how NPs behave authors have applied Derjaguin-Landau-Verwey-Overbeek (DLVO) theory which concerns the attraction and repulsion of colloids (Hotze *et al.* 2010).

DLVO theory is based on the sum total force of attractive van der Waals (VdW) forces and the effects of repulsion by the Electrostatic Double Layer (EDL). VdW forces concern the attraction of surfaces in close proximity. The EDL comprises the particle's surface charge, and the electric field generated by it (Handy *et al.* 2008). Ionic content of the liquid media is important in understanding particle agglomeration as ions such as Na⁺ and Cl⁻ act to compress the EDL. Particles therefore become closer and this allows attractive VdW forces to take hold. In high ionic strength media such as seawater VdW forces become prominent and NP agglomeration is more likely.

It is possible to roughly quantify DLVO forces – and therefore agglomeration potential of NPs in liquid media - by measuring the electrokinetic, or zeta (ζ), potential. The ζ -potential measures the difference in charge between the liquid attached to the particle's surface and the liquid medium itself. The closer the value is to 0, the less stable the particles will be and more likely to agglomerate (Hotze *et al.* 2010).

Table 3.2 details the size, ζ -potential and half-life stability (time taken for 50% of the particles to agglomerate) of the JRC CeO₂ particles used in this thesis. In DI water the ζ -potential of 600nm NM-213 is the closest of the three particles to 0, making it more likely to agglomerate, and this is reflected in it having the shortest half-life stability. With increasing ζ -potential both 10nm (NM-211) and 28nm (NM-212) particles are shown to have increasing half-life stability in DI. The situation is different however in seawater. Although ζ -potential measurements in seawater were not taken, half-life stability shows that the smallest (10nm) CeO₂NPs have the highest stability (534 mins) whilst 28nm

and 600nm both agglomerate nearly twice as fast (288 and 294 mins respectively). The optimal food size for *M. edulis* uptake is believed to be at least 1µm (Riisgård *et al.* 2014). Agglomeration speed and therefore increasing particle size over time may then determine how the CeO₂NPs interact with the mussel.

	NM-211 Nano-CeO ₂	NM-212 Nano-CeO ₂	NM-213 Micron-CeO ₂
XRD Crystallite Size (nm)	10.1	33.3	33.3
Mean Feret's Ø from SEM (nm)	-	28 ± 10	600 ± 400
Zeta Potential (DI, mv)	28 ± 2	33 ± 2	-7 ± 6
Half-life Stability (DI, mins)	780	2676	432
Half-life Stability (SW, mins)	534	288	294

Table 3.2: Properties of the JRC NM-Series of CeO₂NPs (XRD = x-ray diffraction; SEM = scanning electron microscope; DI = deionised water; mv = millivolts; SW = saltwater (Singh *et al.* 2014)

Collision theory determines that reaction rate increases with concentration as more particles are available for interaction. In cases of aggregated or agglomerated particles, increasing concentration has been shown to increase agglomeration speed (Keller *et al.* 2010). In the first instance it could be hypothesized that as increasing concentration increases agglomeration, the particles reach an optimal uptake size and this should increase accumulation. However whilst the clearance rate of mussels has been shown to increase with increasing particle (seston) concentration, this is only to a threshold above which the mussel is not physically capable of handling more particles (Riisgård *et al.* 2011). As such with increasing concentration, and therefore increasing visibility of particles, there is still a limit on the mussel's physical ability to accumulate particles.

The aim of this section is to detail a scoping study to understand the differences in accumulation by *M. edulis* following exposure to differing sizes and concentrations of CeO₂NPs. The hypotheses for this study are that larger primary particle sizes of CeO₂NP will be accumulated more than those of smaller primary particle size, that higher concentrations of CeO₂NPs will accumulate in relatively higher concentrations in *M. edulis* than lower

concentrations of CeO₂NPs, and that the digestive gland will be a major site of accumulation.

3.4.2 Method

To determine how size and concentration affects uptake of CeO₂NPs, mussels (c. 30g, n = 7 per treatment) received one of three JRC CeO₂NPs (10nm, 28nm, 600nm: see Chapter 2.2.1) at either a 1 or 5 mg/l dose, and were exposed for 24 hours, via the method outlined in Chapter 2.3.3.

Immediately upon removal the mussel was slightly prised open and 1.5ml haemolymph drawn from the posterior adductor muscle using a 21g syringe. This was immediately acidified to 10% with nitric acid for Ce concentration analysis. After this the gills, digestive gland and mantle were dissected out, freeze dried and acid digested. All acidified samples were pooled from n = 7 to n = 1, and analysed for Ce content by ICP-MS as per 2.2.1.

3.4.3 Results & Discussion

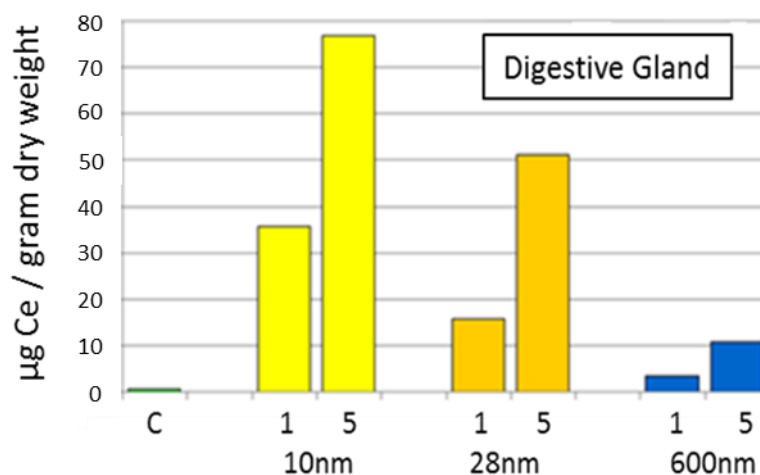


Fig 3.2: Cerium concentrations found in the digestive gland (µg Ce/g dry weight) of *M. edulis* following 24 hours exposure to 10nm (NM-211), 28nm (NM-212) and 600nm (NM-213) CeO₂ at 1 and 5 mg/l (samples pooled from n=7 to n=1). C= Control

Fig 3.2 shows Ce accumulation in the digestive gland. Increasing the CeO₂ concentration 5-fold results only in Ce accumulation increases between 2- and

4-fold. Particle accumulation also decreases with increasing particle size. The previous experiment in this chapter showed maximum accumulation of 10nm CeO₂NPs after 4 hours with elimination towards 56 hours. This experiment was performed over 24 hours therefore the mussel is most likely in a state of elimination (at least of 10nm CeO₂NPs) following the initial exposure.

Regarding the particles used, it is known that agglomeration increases with both increasing size and concentration. Larger, coarser particles are also known to be quickly egested by the mussel. Nanoparticles have previously been shown to both penetrate digestive tubules (Koehler *et al.* 2008) and have a longer residence time in the digestive gland than micron-size particles (Ward and Kach 2009). The results shown in this experiment therefore suggest that if they are being accumulated, larger CeO₂ particles are not retained as effectively in the digestive gland as smaller particles.

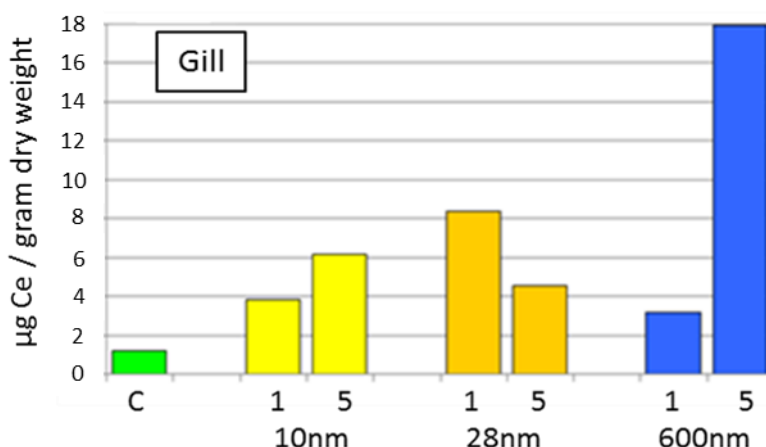


Fig 3.3: Cerium concentrations found in the gill (µg Ce/g dry weight) of *M. edulis* following 24 hours exposure to 10nm (NM-211), 28nm (NM-212) and 600nm (NM-213) CeO₂ at 1 and 5 mg/l (samples pooled from n=7 to n=1). C= Control

Fig 3.3 shows Ce concentrations in the gill. Increasing concentration 5-fold increases accumulation 1.5-fold with 10nm CeO₂NPs, but 5-fold with the 600nm particles. In the case of 28nm particles there appears to be a 50% decrease in accumulation with increased concentration. There is no clear pattern emerging with gill accumulation. Further investigation would be needed to understand whether different size particles have different methods of being accumulated by the gill be it for example surface adsorption, gill mesh entrapment, or

internalisation. If uptake by gills were to be primarily through pinocytosis (George *et al.* 1976), it might be expected that smaller particles would be accumulated to a greater extent.

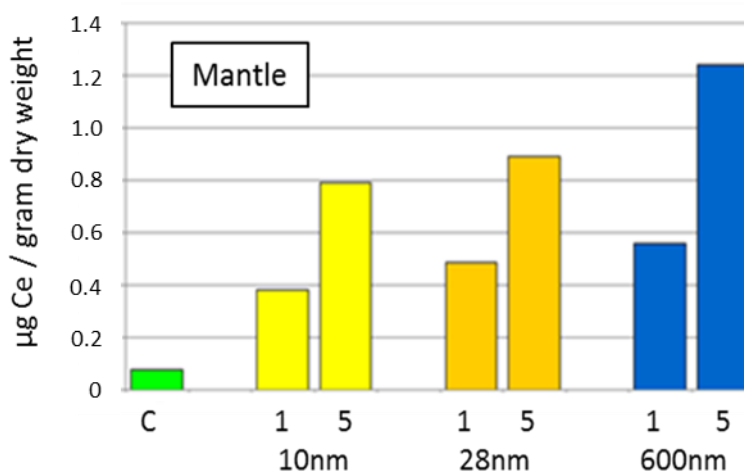


Fig 3.4: Cerium concentrations found in the mantle ($\mu\text{g Ce/g dry weight}$) of *M. edulis* following 24 hours exposure to 10nm (NM-211), 28nm (NM-212) and 600nm (NM-213) CeO₂ at 1 and 5 mg/l (samples pooled from $n=7$ to $n=1$). C= Control

Figure 3.4 shows Ce concentrations in the mantle. Increasing concentration from 1 to 5mg/l barely doubles Ce accumulation. It could be suggested that increasing particle size increases accumulation, but there is only a 50% difference in accumulation between 10nm and 600nm particles, and without statistical evidence it cannot be conclusively said that particle size has affected mantle Ce accumulation. Cerium accumulation in the mantle is the lowest of all tissues (per g d.w.) and again its ciliated surface and general function as a pseudofaeces rejection tract may aid in preventing accumulation (Beninger *et al.* 1999).

Fig 3.5 shows Ce concentration in the haemolymph. Exposure to 10nm CeO₂NPs results in a concentration-related increase in Ce in the haemolymph, whilst exposure to both 28nm and 600nm particles does not. In terms of haemolymph penetration, 18 hour exposures of *M. galloprovincialis* to 50nm iron oxide have shown NPs penetrating haemolymph, with depuration taking over 122 hours (Hull *et al.* 2013). Exposure to cadmium quantum dots (12 x 6nm) also showed haemolymph penetration, but at levels 100x lower than that

of the iron oxide, and almost total depuration by 72 hours (again, reduced retention of cadmium was assumed due to its lack of function as a nutrient).

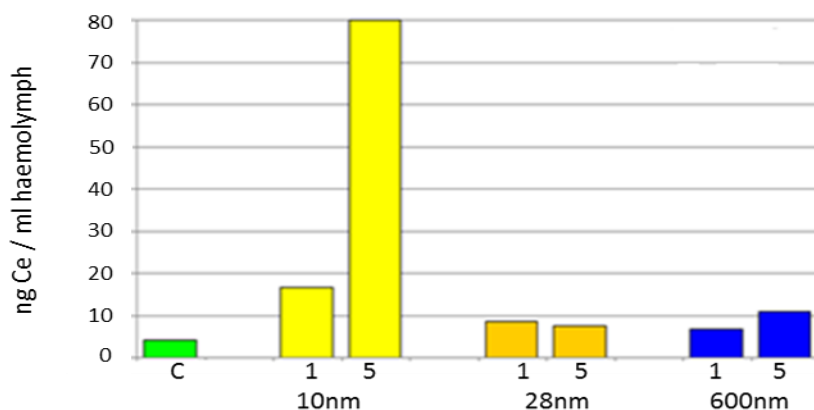


Fig 3.5: Cerium concentrations found in the haemolymph ($\mu\text{g Ce/ml}$) of *M. edulis* following 24 hours exposure to 10nm (NM-211), 28nm (NM-212) and 600nm (NM-213) CeO_2NPs at 1 and 5 mg/l (pooled samples). C= Control

Phagocytic cells can engulf metals (oxides) and transport them via the haemolymph (Marigomez *et al.* 2002), so the presence of Ce in the haemolymph should not be surprising. This would similarly be the case if the gills were accumulating CeO_2NPs during pinocytosis. The results here show Ce concentrations in the haemolymph are between 60 and 100-fold lower than those of the surrounding exposure media. Such concentrations could have resulted with minimal contamination from the surrounding media when drawing the haemolymph and, without statistical power, it would be difficult to conclusively say that CeO_2NPs have penetrated the haemolymph.

In general, increasing concentration increases accumulation of Ce with all particles and all tissues, except with 28nm CeO_2NPs in the gills. A 5-fold increase in concentration has, however, generally resulted in little more than doubling of accumulation. A similar pattern was shown by Montes *et al.* (2012), where only a tripling of uptake by *M. galloprovincialis* occurred when comparing 1 and 5mg/l CeO_2 -nanorod exposures. It is possible to speculate that mussel particle handling ability might be responsible for this. There is a limit to mussel particle processing rate after which all particles are immediately locked away into pseudofaeces and lost as a route of uptake (Montes *et al.* 2012). Increasing concentration will increase CeO_2NP agglomeration, which would

lead to an increased density of particles potentially visibility to the mussel. If this concentration becomes too high then particles are automatically rejected, regardless of the particle type. Increasing NP concentration therefore could have effectively saturated the mussel's particle handling ability and limited potential particle accumulation.

Total accumulation (digestive gland + mantle + gill) of Ce by *M. edulis* suggests that 10nm CeO₂NPs are retained most readily by the organism (Table 3.3). By examining individual tissues it can be concluded that the digestive gland accumulates 10nm (NM-211) particles most readily (3.19% of dose), however the gills (0.34%) and mantle (0.1%) accumulate 28nm (NM-212) particles most readily. Contrary to the hypothesis, lower concentrations of particles also accumulated more readily than higher concentrations of particles, and this may be a facet of mussel pumping rate reduction with increased particle concentration. The results are similar to Montes *et al.* (2012), Ferry *et al.* (2009) and the previous experiment, whereby mussels accumulated roughly 5% of the offered dose.

CeO ₂ Particle Size and Concentration	% Dose Accumulated by:			
	Digestive Gland	Gill	Mantle	Total
10nm (1mg/l)	3.19	0.15	0.06	3.40
10nm (5mg/l)	1.57	0.05	0.03	1.65
28nm (1mg/l)	1.47	0.34	0.10	1.91
28nm (5mg/l)	1.02	0.03	0.04	1.10
600nm (1mg/l)	0.26	0.11	0.09	0.46
600nm (5mg/l)	0.17	0.11	0.04	0.32

Table 3.3: Percentage uptake of cerium in the tissues of *M. edulis* following exposure to various sizes and concentrations of CeO₂ for 24 hours (**bold** = maximum uptake)

Table 3.4 shows the proportionate partitioning of accumulated Ce in the digestive gland, gill and mantle of *M. edulis*. The results here for 10nm CeO₂NPs echo both the first experiment in this chapter, and a study using gold nanoparticles (<20nm) where the digestive gland accumulated 95%, the gill 3.9% and the mantle 1.9% of the dose (Tedesco *et al.* 2010). The differences in tissue partitioning between 10nm and 600nm CeO₂NPs highlight that choosing an appropriate timepoint for exposure of *M. edulis* can affect

interpretation of the results. In this instance the slow elimination of 10nm CeO₂NPs over 24 hours highlights the digestive gland as the organ of maximum uptake, whilst the gill and mantle are more prominent for 600nm particle retention. Without the clarification of the results seen in Table 3.3 and the uptake kinetics described in the previous study, the accumulation of 600nm CeO₂ in the gills and mantle could be given more prominence than is deserved. Instead it must be concluded that nano-CeO₂ is retained by the organism much more readily than micron-sized CeO₂. The next step then is to understand how this retention affects biological processes in the organism.

CeO₂ Particle Size and Concentration	% Accumulated Dose found in:		
	Digestive Gland	Gill	Mantle
10nm (1mg/l)	93.95	4.40	1.63
10nm (5mg/l)	95.51	2.83	1.97
28nm (1mg/l)	77.18	17.68	5.12
28nm (5mg/l)	92.84	3.15	4.01
600nm (1mg/l)	57.07	23.04	19.85
600nm (5mg/l)	54.60	34.18	11.20

Table 3.4: Percentage of an accumulated dose of CeO₂NPs [10, 28 or 600nm, at concentrations of (1) or (5) mg/l) found in different tissues of *M. edulis* following 24 hours exposure

3.5 Examining Biological Effects – Oxidative Stress and Lipid Peroxidation

3.5.1 Introduction

Free radicals are produced naturally in cells as part of cell systems for dealing with, for example oxygen. These systems may become out of balance however through either increases in free radicals and reactive oxygen species (ROS), or through a depleted ability to deal with regular levels of damaging components. When this happens there may be damage to cellular components and/or increased energy expenditure in attempts up-regulate anti-oxidant defences. This is known as oxidative stress.

The free radical superoxide ($O_2^{\cdot -}$) for example is used by phagocytes in the immune system to kill foreign entities such as bacteria. However without a system of removal, superoxide can lead to further formation of damaging chemicals and free radicals. One of these is the hydroxyl radical HO^{\cdot} . Interactions of the hydroxyl radical with lipid membranes can causes damage to ion transport systems and alter receptor functionality, leading to difficulties in the cell maintaining ion gradients (Acworth and Bailey 1995). The method of hydroxyl formation based on interactions of superoxide and hydrogen peroxide (H_2O_2) is known as the Haber-Weiss reaction:



The second method, known as the Fenton reaction, is based on the interaction of hydrogen peroxide with a transition metal e.g. iron, copper:



Of note is that hydrogen peroxide is involved in both these reactions; interestingly superoxide in itself can also convert to hydrogen peroxide:



It is currently unknown as to whether H_2O_2 is itself damaging, or due to its propensity to convert into the hydroxyl free radical.

In order to remove superoxide, cells initially use superoxide dismutase (SOD) to convert the superoxide into hydrogen peroxide (Fig 3.6). In *M. edulis* two forms of SOD have been identified; a cytosolic or extracellular copper-zinc (Cu/Zn-SOD) form and a mitochondrial-based manganese (Mn-SOD) form (Pipe *et al.* 1993). Cu/Zn-SOD is thought to respond to cellular demand since it has been found in numerous cellular compartments, whilst Mn-SOD is mostly responsible for mediating superoxide produced as a result of respiratory electron transfer (Miller 2012).

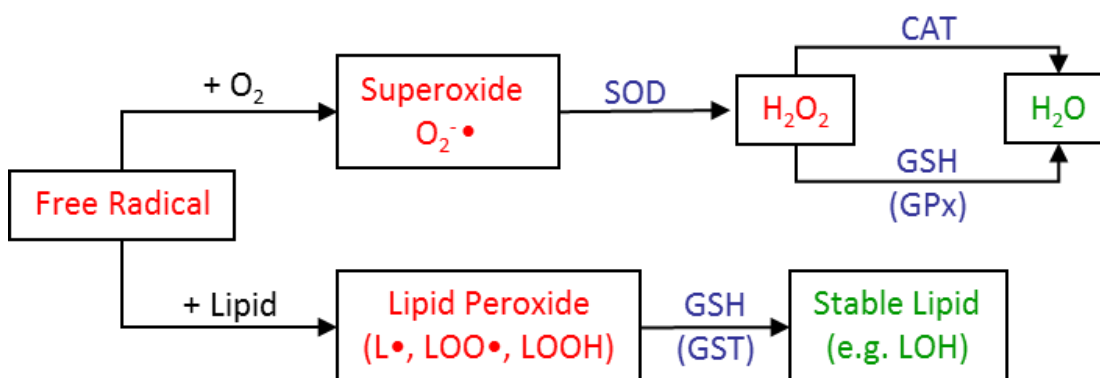


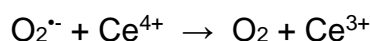
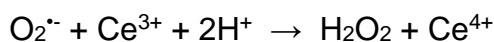
Fig 3.6: Simplified pathway for methods of cellular free radical detoxification.

Red = Damaging Component, Blue = Conjugating Enzyme, Green = Stable End Product

Since hydrogen peroxide is also damaging, the cell also produces the catalase (CAT) enzyme in the peroxisomes to convert this H_2O_2 into water. Reduced glutathione (GSH) is similarly able to convert H_2O_2 to water through conjugation with glutathione peroxidase (GPx), although CAT is regarded as the dominant enzyme for this (Livingstone *et al.* 1992).

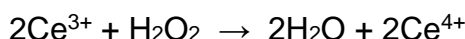
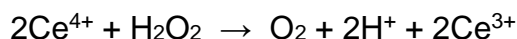
Interactions of free radicals with lipids forms lipid peroxides including lipid radicals, lipid peroxyradicals and lipid hydroperoxides. Again GSH is able to bind to lipid peroxides (by acting as an e^- or H^+ donor) through conjugation with Glutathione-S-Transferase (GST), to form oxidised glutathione (GSSG). Failure to do so can cause other toxic by-products such as aldehydes (Halliwell and Gutteridge 2007). GST has also been shown to independently bind with other damaging compounds such as pesticides and DDT, and ROS such as the hydroxyl radical $\bullet OH$ (Howie *et al.* 1990, Sherratt and Hayes 2001).

Spontaneous redox cycling between Ce^{3+} and Ce^{4+} ions on the surface of CeO_2 leads to an oxygen vacancy that can be filled by superoxide, which is thought to have a SOD-like effect (Heckert *et al.* 2008) and therefore may be important in helping ameliorate oxidative stress. There are two proposed reaction pathways by which this might occur (Korsvik *et al.* 2007):



These pathways are similar to the Haber-Weiss reaction (Chapter 1.2.4), and involve the quenching of the superoxide free radical by Ce, suggesting an antioxidant activity (Nimse and Pal 2015). However the reaction involving Ce^{3+} still produces H_2O_2 as a by-product therefore despite their SOD-like activity, CeO_2NPs might still induce cellular processes that catalyse H_2O_2 into H_2O , such as catalase and glutathione activity.

Other authors have suggested that CeO_2 can also have a CAT-like effect via the following reaction pathways (Nicolini *et al.* 2015):



Experimental evidence has shown that CeO_2 particles with a greater proportion of surface Ce^{4+} may demonstrate CAT-like activity (Pirmohamed *et al.* 2010), whilst those with a greater proportion of Ce^{3+} demonstrate more SOD-like activity (Heckert *et al.* 2008).

All the JRC CeO_2NPs used to date in this Chapter have a surface Ce^{4+} content of greater than 90% (Table 3.5), which indicates they should exhibit CAT-like activity. The surface ratio of Ce^{3+} increases with increasing size, however since (by weight) the surface area of smaller particles is much greater, then the smaller particles will have greatest surface area of Ce^{3+} ions during exposures. Table 3.5 shows that 10nm NM-211 has 5.7% of its surface comprising Ce^{3+} , whilst 600nm NM-213 has 8% surface Ce^{3+} . Despite this, NM-211's greater surface area per gram means that organisms will be exposed to $3.76\text{m}^2 \text{ Ce}^{3+}/\text{g}$,

compared to only 0.34m² Ce³⁺/g in exposures to NM-213. Given that the stability of the smaller particles is also greater, this surface will be available for longer. It could be expected then that 10nm JRC CeO₂NPs will have a different effect on SOD activity compared to larger JRC CeO₂NPs.

	NM-211 Nano-CeO ₂	NM-212 Nano-CeO ₂	NM-213 Micron-CeO ₂
XRD Crystallite Size (nm)	10.1	33.3	33.3
Mean Feret's Ø from SEM (nm)	-	28 ± 10	600 ± 400
% Ce ⁴⁺ :Ce ³⁺ (XPS Ratio)	94.3 : 5.7	93.1 : 6.9	92.0 : 8.0
BET Specific Surface Area (m ² /g)	66 ± 2	27.2 ± 0.9	4.3 ± 0.1
Ce ³⁺ Specific Surface Area (m ² /g)	3.76	1.88	0.34
Half-life Stability (SW, mins)	534	288	294

Table 3.5: Properties of Properties of the JRC NM-Series of CeO₂NPs. XRD = x-ray diffraction; SEM = scanning electron microscope; XPS = X-ray Photoelectron Spectroscopy; BET = Brunauer-Emmett-Teller; SW = Seawater (Singh *et al.* 2014)

The response of an organism to oxidative stress and lipid peroxidation can be quantified by measuring either the activity levels of these enzymes (SOD, CAT), their conjugators (GST), or their by-products (e.g. MDA), as discussed in Chapter 2.2.2. In particular the SOD and CAT assay are imperative when trying to understand either the SOD or CAT-like activity of CeO₂, and its propensity to act as an anti-oxidant. CeO₂ is also known to conjugate the hydroxyl radical •OH (Xue *et al.* 2011) which initiates lipid peroxidation. As such use of TBARS and GST assay following exposures will provide suitable endpoints to measure changes in lipid peroxidation.

The experiments in this chapter so far have highlighted that maximum accumulation of CeO₂NPs by *M. edulis* is within 4 hours, and that the organ of greatest uptake is the digestive gland. Smaller particles have also been shown to have a longer residence time than larger particles, and the mussel is generally able to eliminate itself of accumulated Ce within 56 hours.

The aim of this study is to understand how CeO₂NPs affect biological processes in *M. edulis*, such as oxidative stress and lipid peroxidation (LPx), and whether these effects are nano-specific. The hypotheses for this experiment are that exposure of *M. edulis* to 10nm and 600nm CeO₂ will reduce oxidative stress in

the gills, digestive gland and mantle, that 10nm CeO₂ will have a greater effect at reducing oxidative stress than 600nm CeO₂, and that changes in biological activity caused by these particles will return to control levels within 24 hours of exposure.

3.5.2 Method

To compare the biological effects of exposure to nano-CeO₂ or micro-CeO₂, mussels (n=8 per treatment) received a 3mg/l dose of either 10nm (NM-211) or 600nm (NM-213) CeO₂ particles along with algal feed, as per Chapter 2.3.3. Exposure times were 8 hours and 24 hours. Control mussels received algal feed only. Assays for TBARS, SOD, GST and CAT (oxidative stress) activity were performed as per the method detailed in Chapter 2.2.2. Data was analysed for normality using Shapiro-Wilk. Normal data was analysed by one-way ANOVA, or *t*-test in the case of two comparators. Non-normal data was first log-transformed, then analysed via ANOVA if made normal. Log-transformed data which was still non-normal was analysed by Mann-Whitney U-Test data (see Chapter 2.2.3).

3.5.3 Results & Discussion

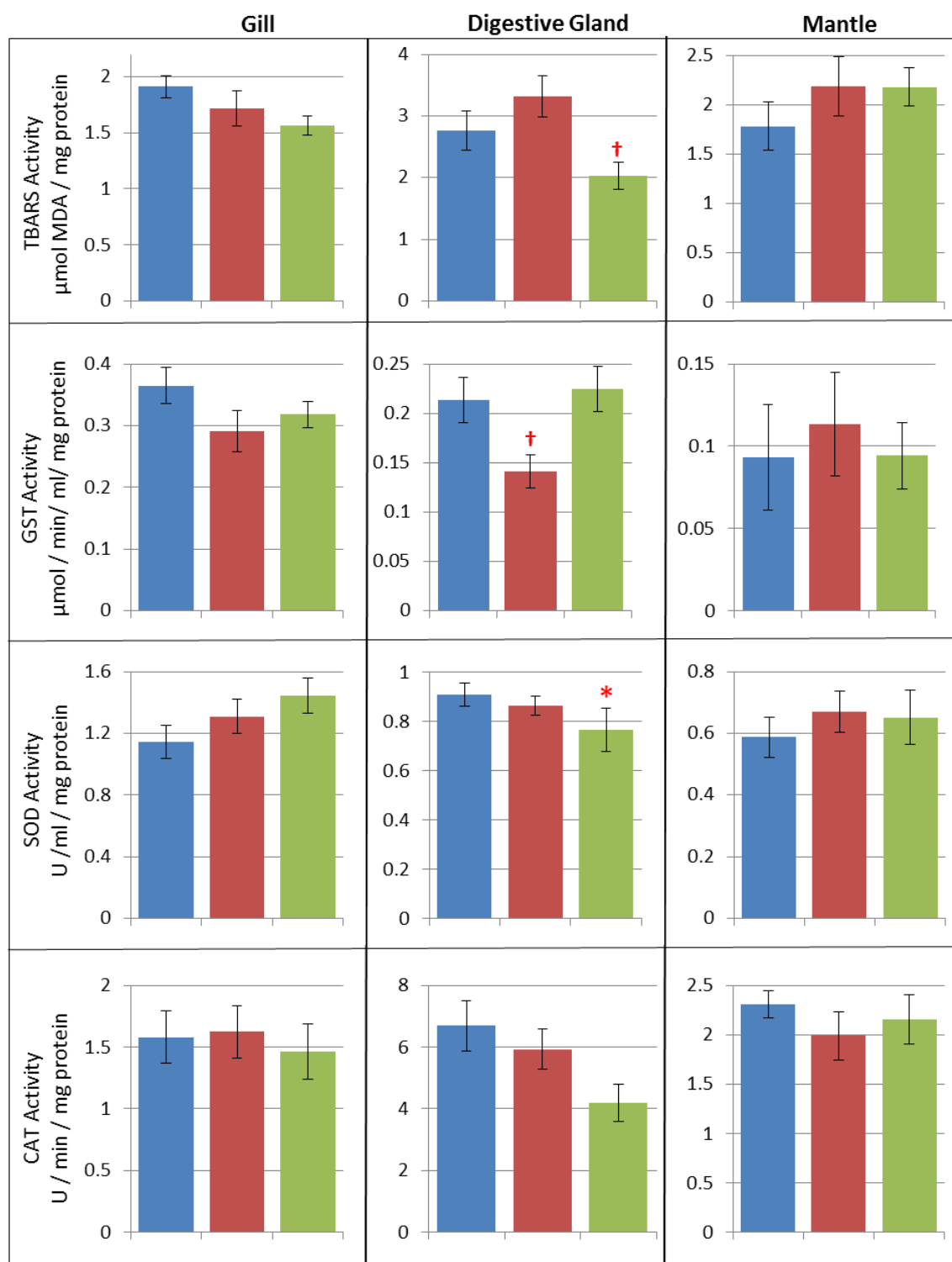


Fig 3.7a: Significantly different effects from biological assays (TBARS, GST, SOD, CAT) performed on the gill, digestive gland and mantle of *M. edulis* following exposure to Nano (10nm) or Micro (600nm) CeO₂NPs at 3 mg/l for **8 hours**. ■ = Control, ■ = Nano, ■ = Micro. n = 8. * = significantly lower than control, † = significantly lower size-related effect ($p < 0.05$).

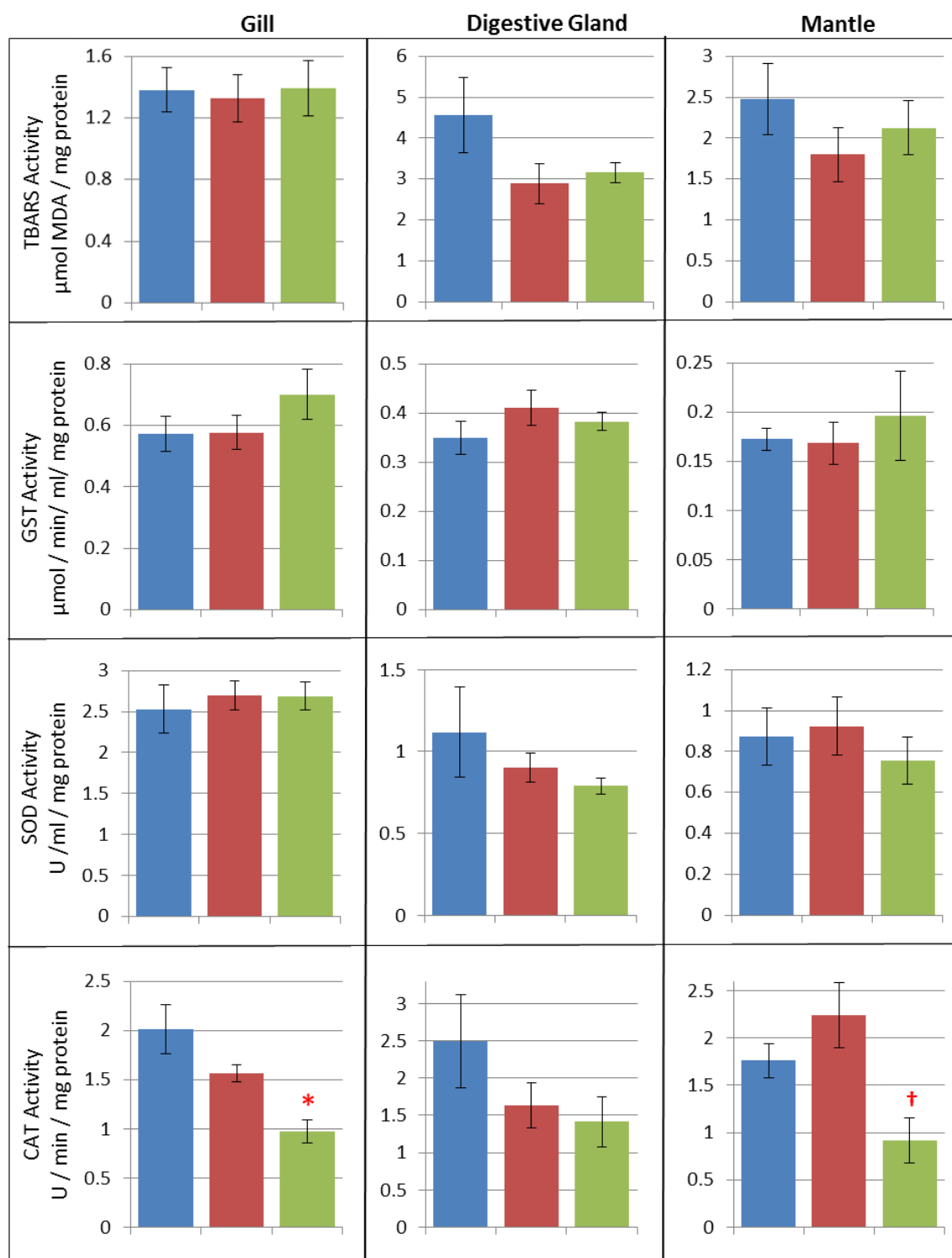


Fig 3.7b: Significantly different effects from biological assays (TBARS, GST, SOD, CAT) performed on the gill, digestive gland and mantle of *M. edulis* following exposure to Nano (10nm) or Micro (600nm) CeO₂NPs at 3 mg/l for **24 hours**. ■ = Control, ■ = Nano, ■ = Micro. n = 8. * = significantly lower than control, † = significantly lower size-related effect ($p < 0.05$).

Figs 3.7a and 3.7b show the results of various biological effects assays on the different tissues of *M. edulis* following exposure to 3mg/l of 10nm or 600nm CeO₂ for either 8 or 24 hours. Contrary to the hypothesis, biological processes are affected to a greater extent following exposure to 600nm micro-CeO₂ than to 10nm nano-CeO₂.

After 8 hours, SOD activity is significantly lower (Mann-Whitney U-Test, $U=9$, $p=0.015$) in the digestive gland following micro-CeO₂ exposure as compared to the control [Shapiro-Wilk indicated micro-CeO₂ data was not normal ($df = 8$, $p=0.01$), and this was not changed following log transformation, hence a non-parametric test was used]. Also in the digestive gland, one-way ANOVAs revealed significant differences between 10nm and 600nm treatments in TBARS [$F(2,21)=4.903$, $p=0.018$; Tukey's post-hoc, $p=0.014$] and GST activity [$F(2,21)=4.596$, $p=0.022$; Tukey's post-hoc, $p=0.028$], but not between either particle and the Control.

After 24 hours, there was a significant reduction [one-way ANOVA, $F(2,21)=9.583$, $p=0.001$] in CAT activity in the gill following 600nm exposure as compared to the control (Tukey's post-hoc, $p=0.001$). CAT activity in the mantle also significantly [one-way ANOVA, $F(2,20)=6.942$, $p=0.005$] differed between 10nm and 600nm treatments (Tukey's post-hoc, $p=0.004$).

TBARS activity is indicative of lipid peroxidation and GST is involved in conversion of lipid peroxides to stable lipid forms (Halliwell and Gutteridge 2007). As such it would be expected that any changes in TBARS activity would be reflected in and GST activity yet this appears not to be the case. In the digestive gland 8 hour's post-dosing, TBARS activity is significantly lower following micro-CeO₂ as compared to nano-CeO₂, and vice-versa for GST activity.

CeO₂ is known to conjugate, apart from superoxide, other free radicals such as the hydroxyl radical $\cdot\text{OH}$ (Xue *et al.* 2011), which is important in initiating lipid peroxidation (Ayala *et al.* 2014), therefore some reductions in TBARS and GST activity are not surprising. Reduced GST activity has been linked to a protective effect against increased oxidative stress in human red blood cells (Evelo *et al.*

1993) and brain fluids (Lovell *et al.* 1998), therefore reduced GST activity in the digestive gland might indicate nano-CeO₂ having a greater protective effect than micro-CeO₂. If this was the case however then reduced lipid peroxides should also result in reduced TBARS activity, something not seen here with nano-CeO₂. This could therefore mean that GST is in fact being depleted at a rate faster than it could be produced (Carlson *et al.* 2008, Piao *et al.* 2011). Similarly, it would be expected that reduced TBARS activity following micro-CeO₂ exposure would therefore lead to reduced GST activity yet this is not the case. GST is also known to conjugate a range of xenobiotics (Meister and Anderson 1983), hence along with its role in conjugating GSH and lipid peroxides, it may also be conjugating directly with the micro-CeO₂. Investigating GSH levels in future experiments might help understand this process.

In terms of other studies investigating Me(O)NPs and lipid peroxidation, CuONPs have been shown to increase lipid peroxidation in exposures of *M. edulis* (Gomes *et al.* 2012), and others have reported increased lipid peroxidation during periods of nanoparticle-related oxidative stress (Buffet *et al.* 2012, Pan *et al.* 2012). However another study suggested that decreases in TBARS activity in the gills of *C. gigas* following metal exposure was resultant of the organism quickly up-regulating its metallothionein (proteins involved in metal chelating and detoxification) response, thereby attempting to block lipid peroxidation before it might occur (Géret 2002). It would be worth measuring metallothionein in future experiments in order to determine if the decreased TBARS activity following micro-CeO₂ exposure is actually a side-effect of increased metallothionein production.

These reductions in TBARS and GST are neither significantly different from the control, nor have these effects from either particle lasted until 24 hour's post-dosing. This suggests that these effects are both limited and transitory, despite the previous studies in this chapter indicating that 10nm nano-CeO₂ had a longer residence time in the digestive gland.

The only effect on SOD activity is a significant reduction in the digestive gland after 8 hours following micro-CeO₂ exposure as compared to the control. Under weak or acute oxidative stress, organisms often display increased enzyme

activity as they up-regulate their response to a toxicant. Reduced SOD activity can indeed point to an amelioration of oxidative stress, yet under high or chronic stress, there may also be decreased activity as the toxicant itself can damage, for example, the SOD enzyme, or the mitochondria where they are produced (Halliwell and Gutteridge 2007). The question then, is whether the reduced SOD activity caused by micro-CeO₂ is evidence of pro-oxidant or anti-oxidant activity. Interestingly there is a similar magnitude of drop in digestive gland CAT activity at this timepoint, however this could not be determined as significantly different from the control.

The only significant reduction in CAT activity as compared to the control is 24 hours' post-dosing in the gill, again with micro-CeO₂, and this might be a side-effect of the SOD-like activity of CeO₂. The surface of the micro-CeO₂ used in this experiment has previously been characterised as comprising over 90% Ce⁴⁺ (as per Table 3.4). It has been suggested (Korsvik *et al.* 2007) that Ce⁴⁺ conjugates the superoxide free radical ($O_2^{\cdot-} + Ce^{4+} \rightarrow O_2 + Ce^{3+}$) in a reaction which, unlike that with Ce³⁺ ($O_2^{\cdot-} + Ce^{3+} + 2H^+ \rightarrow H_2O_2 + Ce^{4+}$), does not produce H₂O₂ as a by-product. Less H₂O₂ production should therefore lead to reduced CAT enzyme production and therefore less activity. Given that these effects are not instigated until 24 hours' post-dosing, it is unknown how long such an effect might last.

It was hypothesised, and would be expected, that nano-CeO₂ might have a greater set of effects than micro-CeO₂ since the previous experiment in this chapter (3.4) showed nano-CeO₂ was accumulated in greater quantities than micro-CeO₂. This has not proven to be the case and one reason for this discrepancy might be due to the available reactive surface of the particles. Table 3.5 showed that despite nano-CeO₂ having a higher surface proportion of Ce⁴⁺ than micro-CeO₂, due to its small size it had a reactive surface area of Ce³⁺ over 10-fold greater. This being the case, then in any SOD-like reaction involving Ce³⁺ ($O_2^{\cdot-} + Ce^{3+} + 2H^+ \rightarrow H_2O_2 + Ce^{4+}$), H₂O₂ would be produced in greater quantities by nano-CeO₂, thus CAT activity would be not as reduced. This might explain why CAT activity in the mantle is significantly lower 24 hours' post-dosing with micro-CeO₂ than it is with nano-CeO₂. However it is also fully possible that nano-CeO₂ is just simply having little impact.

One of the hardest issues to determine with regards to biological effects is whether their reduction is due to a protective effect, or an over-whelmed OS defence. In terms of other studies, few authors working on bivalve interaction with insoluble Me(O)NPs have reported reductions in activity of one anti-oxidant enzyme without the increase of another. Exposures of *M. galloprovincialis* to TiO₂NPs (1 & 10µg/l) have resulted in significantly reduced GST activity, but dose-related increased CAT activity (Barmo *et al.* 2013). Similar exposures to nano-carbon black (NCB, 5mg/l) and SiO₂NPs (1mg/l) resulted in decreased CAT gill activity, with carbon fullerenes (C60, 5mg/l) decreasing gill GST activity. Simultaneously, NCB and SiO₂NPs (200µg - 5mg/l) and C60 (1mg/l) increased digestive gland CAT, with all particles (5mg/l) increasing digestive gland lipid peroxidation (Canesi *et al.* 2010). From this it was concluded that increased digestive gland enzyme activity highlighted the organ as a target for oxidative stress, but the gills were not. Similarly Tedesco *et al.* (2010) noted gold nanoparticles affecting lipid peroxidation (LPx) in the digestive gland of *M. edulis*, but little in the other organs.

Comparable to the experiments in this chapter, the Canesi *et al.* (2010) study was run at a similar timeframe (24h) with similar concentrations (up to 5mg/l) of angular particles. Both pointed to particle agglomeration leading to uptake, and both noted decreased gill CAT activity at high concentrations. The major difference between them however is that here the 600nm micro-CeO₂ consistently significantly reduced a suite of biological activities across all tissues. Similar results were shown in a study whereby CeO₂NPs reduced SOD, GSH, GPx and CAT activity whilst protecting rat liver from oxidative stress (Amin *et al.* 2011). Another study examining the algae *P. subcapitata* exposed to CeO₂NPs with various characteristics concluded that surface levels of Ce³⁺ of 40% and over is what drove growth inhibition and toxicity, as opposed to size, shape or ζ-potential (Pulido-Reyes *et al.* 2015). All the JRC particles used in this study had a Ce³⁺ surface of less than 10% (Table 3.4). All this information together suggests that exposure to micro-CeO₂ has an anti-oxidative effect in *M. edulis*.

The use of 3mg/l concentrations of CeO₂ in this experiment was to determine if the suggested regulatory limit would be sufficient to protect *M. edulis* from harmful biological effects following exposure. Concurrent with the hypothesis,

the results show that there is no significant evidence of any harmful effects caused by 10nm nano-CeO₂, whilst some evidence exists of 600nm micro-CeO₂ ameliorating oxidative stress in the digestive gland in the short-term. Overall the mussels are able to recover well from acute exposure, even at concentrations many-fold higher than current anthropogenic outputs.

3.6 Conclusion

This chapter examines the differences in accumulation of various sizes and concentrations of CeO₂NPs over time in *M. edulis*, and subsequent inducement of biological effects. Results show that, under conditions involving an algal feed, maximum uptake of 10nm CeO₂ by *M. edulis* is around 5% of an offered dose, after about 4 hours. The digestive gland is the major organ of accumulation (95%), with elimination of Ce still occurring over 56 hours. Gill and mantle accumulation combined is roughly 5% of total accumulation, with total elimination by 56 hours.

The results also show that all sizes of CeO₂NP can be accumulated; the smallest particles (10nm) have the longest residence time in the digestive gland whilst 28nm particles are most readily accumulated by the gill. Particle concentration can be a limiting factor in uptake, since increasing particle concentration 5-fold from 1 to 5mg/l only resulted in a 2-fold increase in accumulation. This may be due to the physical handling capability of the mussel, or the particles quickly agglomerating at high concentration to a point they are immediately rejected.

There was no evidence of any notable significantly increased biological effects caused by any CeO₂ particle at 3mg/l. Micro-CeO₂ particles did show some significant reductions in oxidative stress (SOD, CAT activity) yet these effects were isolated and transient. There were no effects caused by nano-CeO₂ that were significantly different to the control.

There were some variations in Ce concentration between the tissues of mussels in different exposures; for example average digestive gland stomach content

after 24 hours in Chapter 3.3 was around 5µg/g compared to around 20µg/g in Chapter 3.4. One reason for this might be due to differences in mussel size leading to differences in pumping rate. Another reason might be due to the differences in the effectiveness of sonication of the particles. In particular, and as highlighted in Chapter 2.1.1, despite intense sonication the particles still appeared heterogeneous in size and shape under TEM. As such, when dosing the mussels during these exposures any larger aggregates that remained would skew the final concentration data. Since results were pooled it could also be due to one mussel with extremely high uptake skewing the group average.

In the marine environment nanoparticles are unlikely to remain nano-sized for long, instead rapidly agglomerating to micron size, especially with increasing concentration and salinity. That CeO₂NPs do not dissolve under normal conditions means that these particles are likely to both homo- and hetero-agglomerate to much larger sizes, unlike soluble Me(O)NPs which will dissolve and expose marine organisms to free ions. As highlighted in this chapter, CeO₂NPs appear to have a critical timescale by which they can be accumulated by different structures.

Mussels have specifically evolved to filter valuable food sources out of highly particulate and turbulent marine environments hence the lack of adverse biological effects caused by these insoluble particles is not surprising. Environmental release concentrations of CeO₂NPs are currently low (10-100 ng/l), and even under extreme circumstances (1µg/l) are predicted as several hundred-fold lower than the assumed – and tested - regulatory limit of 3mg/l. This study shows that *M. edulis* can recover from a worst-case, acute spill scenario. However, given that a single dose exposure allows time for recovery of the organism in terms of both Ce elimination and biological effects, for interest it would be worth examining accumulation and oxidative stress over more chronic time periods to assess long-term impacts on organism health, and the effects of re-dosing when no such recovery period is available.

Chapter 4: Uptake of CeO₂NPs by *C. maenas* through Immersed Exposure and Emerged Trophic Transfer, and their Biological Effects

4.1 Abstract

The shore crab *C. maenas* is a euryhaline inter-tidal scavenger, and a predator of *M. edulis*. Given the ability for *M. edulis* to process particulate matter, there is potential for trophic transfer - and possible biomagnification - of toxicants up the food chain. Here the uptake of CeO₂NPs and subsequent biological effects in *C. maenas* is examined through immersed exposure, and through trophic transfer via the consumption of *M. edulis* previously exposed to CeO₂NPs.

Immersed exposures to suspended particles for 4 and 8 hours highlighted the gills of *C. maenas* as the major site of CeO₂NP accumulation, even following 12 hours' depuration. 10nm CeO₂NPs significantly increased SOD activity in the stomach and gills after 12 hours' depuration, whilst micro-CeO₂ was linked to significant SOD reduction after 4 hours in the stomach and hepatopancreas.

In emerged trophic transfer experiments, despite Ce concentrations subsequently being much higher in the gills, stomach and mantle of *C. maenas*, trophic transfer of 28nm CeO₂NPs could not be statistically significantly proven. A trophic transfer factor of 0.66 (± 1.1) indicated that these NPs are unlikely to biomagnify in food chains.

Trophically transferred 10nm CeO₂NPs were found in significant levels in the stomach & hepatopancreas, and the respiratory & ionic gills of *C. maenas* with no indication of biomagnification. This was associated with a significant increase in SOD and TBARS activity in the stomach, and SOD and CAT activity in the hepatopancreas, but no significant effect in the gills. It was noted that variable digestion and excretion rates had affected accumulation, indicating that long term studies into depuration are required to fully understand the extent and effects of Ce retention.

4.2 General Introduction

One characteristic of persistent pollutants is their potential to bioaccumulate in organisms over time, which may then allow for trophic transfer to animals higher up the food chain (Murai *et al.* 2008, Fortibuoni *et al.* 2013). It was shown in Chapter 3 that nano-CeO₂ was accumulated to a greater extent by *M. edulis* than micro-CeO₂. It might be reasonable to assume then that nanoparticles can be trophically transferred from *M. edulis* more readily than larger particles due to this greater initial accumulation.

A recent study (Hawthorne *et al.* 2014) tracked the trophic transfer of micro- and nano-CeO₂NPs through a terrestrial food chain, by initially growing zucchini in soil containing 1200µg/g of each particle type. After 28 days the micro-CeO₂ exposed plants contained an average 12.9µg Ce, whilst the NP-exposed plants contained 64.9µg Ce, significant at 23-times the control. Following this, a leaf from the plant was fed to the cricket *Acheta domesticus* for 14 days. Control crickets and those fed micro-CeO₂-exposed leaves contained a similar 0.015µg Ce/g, whilst nano-fed crickets contained a significant 0.034µg/g, with faeces contents respectively of 0.248, 0.393 and a significant 1.01µg Ce/g. These crickets were then fed to wolf spiders (family Lycosidae). Cerium concentrations in control and micro-CeO₂-fed spiders were not detectable, those in NP-fed spiders contained 0.005 µg Ce/g, however replication issues prevented this being significant. This experiment showed that CeO₂NPS could be trophically transferred across two trophic levels to a detectable level, whilst micro-CeO₂ could not. The major reason the authors stated for this was likely the initial uptake, however they were unable to compare their studies with any other trophic transfer studies due to lack of comparison between micro- and nanoparticles.

In terms of NPs in the freshwater environment, TiO₂NPs in *Daphnia magna* have been shown to be trophically transferred to the zebrafish *Danio rerio* (Zhu *et al.* 2010). Initial exposures of *Daphnia* to 0.1 or 1mg/l TiO₂NPs resulted in concentrations of 4.5 and 61.1mg/g. Feeding these to zebrafish resulted in steady-state concentrations of 0.107 and 0.522 mg/g respectively. Those fed a higher concentration of TiO₂NPs contained more TiO₂, however a 15-fold

increase only resulted in a 5-fold increase in burden showing that, much like the uptake patterns in Chapter 3, lower concentrations accumulate more effectively. It was concluded that trophic uptake was not of a level whereby biomagnification might occur further through the food chain, likely due to fast egestion of the TiO₂NPs by the zebrafish.

Quantum dots in zooplankton (CdSe/ZnS) have also been shown to be trophically transferred to *D. rerio* having been incubated in zooplankton, however there was little retention by the fish, and little evidence of transfer to other organs bar the stomach (Lewinski *et al.* 2011). Quantum dots were also shown to trophically transfer from the protozoan *Tetrahymena pyriformis* to the rotifer *Brachionus calyciflorus*, however again the authors suggested further trophic transfer would be unlikely due to fast depuration rates (Holbrook *et al.* 2008). This highlights that replicating natural feeding rhythms is key to understanding the magnitude of effect of trophic transfer.

In terms of the marine environment, CeO₂NPs have been shown to trophically transfer from the from algae *Isochrysis galbana* to *M. galloprovincialis* (Conway *et al.* 2014), and from the algae *Cricosphaera elongate* to the sea urchin larvae *Paracentrotus lividus* (Gambardella *et al.* 2014), but it has also been shown that waterborne exposures of AgNPs to the bivalve *S. plana* resulted in greater silver burden than those fed AgNPs through an algal diet (Buffet *et al.* 2013).

The scoping study experiments into trophic transfer presented in Chapter 2.4.2 showed that despite consumption of *M. edulis* laden with CeO₂NPs whilst immersed, *C. maenas* showed no significant accumulation of Ce in the digestive gland or hepatopancreas, yet the gills were a significant site of accumulation. It was thought that allowing 24 hours for the crab to feed might have resulted in speedy uptake and depuration from the digestive organs. Due to the crab's feeding habits, particles of Ce-laden mussel floated through the water column, and it was thought that the high levels of Ce found in the gills might have resulted from uptake of CeO₂NPs during ventilation.

Another recent study (Farrell and Nelson 2013) showed that having consumed *M. edulis* laden with microplastics, particles were subsequently found in the

stomach of *C. maenas* for the first four hours, yet had fully depurated by 24 hours, similar to results highlighted above. The same study also highlighted accumulation in the gills but again the method employed (feeding crabs mussel flesh in a bucket) might have resulted in uptake into the gills of free microplastics during ventilation, since the authors themselves note that microplastics “were in high enough concentrations to be visible to the naked eye when [the mussels] were cut open”. Similar to the scoping studies presented in Chapter 2.4, it has previously been demonstrated that *C. maenas* accumulates microplastics in the gills during ventilation (Watts *et al.* 2014) therefore the results derived from trophic transfer experiments involving sloppy feeders in an aqueous environment are likely to be tainted by other avenues of internalisation. Whilst this would partially mimic what happens in nature, variables such as current speed, substrate availability and the presence of other (feeding) organisms would affect how exposed the crab is to NPs released during feeding. Since *C. maenas* can also feed out of water establishing accumulation and effects purely from trophic transfer becomes necessary.

A major hypothesis of this thesis is that Me(O)NPs will be trophically transferred between marine organisms by ingestion. The experiments in this chapter aim to negate potential uptake from ventilation by feeding the crabs out of water. Removing ventilation as a route of gill accumulation allows better understanding of where Me(O)NPs actually accumulate within the organism during trophic transfer, and possibly which routes of depuration might be involved in ridding the organism of toxicants.

The first study in this chapter examines the uptake of 28nm CeO₂NPs by *C. maenas* following consumption of *M. edulis* whilst emersed. The second study compares the immersed uptake of suspended 10nm CeO₂NPs and 600nm micro-CeO₂ to ascertain if differences in uptake are related to particle size. Biological effects (oxidative stress and lipid peroxidation) are also examined, as is the ability for the organism to depurate these particles once accumulated. The third study examines the emersed-fed trophic transfer of 10nm CeO₂NPs between *M. edulis* and *C. maenas*, with particular emphasis on understanding how gill function might affect the partitioning of these particles in the crab, and whether they induce biological effects.

4.3 Trophic Transfer of 28nm CeO₂NPs from *M. edulis* to *C. maenas* through Emerged Feeding

4.3.1 Introduction

To determine whether *C. maenas* can accumulate CeO₂NPs through ingestion of *M. edulis*, the experiment from Chapter 2.4.2 will be repeated but the crabs will be fed in air. When immersed, crabs ventilate their gills by drawing in water mainly through a hole beneath the claw. Water circulates over the gills and out through holes near the mouth. Any contaminants in the water column are washed over the gills. When moving from water to land (emerged), water is held in the gill chamber and oxygenated by drawing air in through the holes near the mouth (Taylor and Butler 1973), accompanied by the beating of the scaphognathite. Performing exposures out of water should therefore eliminate ventilation as a method of inspiring particles.

Crabs ingest food through the mouth after which it passes into the stomach and is further ground down in the gastric mill. From here particles are either sent to the mid-gut, hind gut and anus for defecation, or to the hepatopancreas for further digestion. The hepatopancreas is guarded by a filter press that only allows access to particles smaller than 1µm, with larger particles diverted to the intestine (Crothers 1967). It is the ability of nanoparticles to breach this filter press that becomes most pertinent, and thus the hepatopancreas might prove a hotspot for both particle residence and subsequent biological effects (see also Chapter 2.6.1).

In the blind-ended digestive tubules of the hepatopancreas are found a number of differentiated digestive cells. Fibrillar (F) cells are involved in secretion of digestive enzymes and pinocytosis, which appear to form blister (B) cells when a sufficient number of vacuoles join together (Dall and Moriarty 1983). Resorptive (R) cells appear to be responsible for lipid storage, and for taking up metals and binding them into calcium phosphate granules in membrane-bound vesicles. These granules have previously been found to contain trace metals including silver, cadmium, barium and Ce, their concentrations fluctuating according to background seawater concentrations (Simmons *et al.* 1996).

Granule-rich R-cells can be eliminated from the organism as part of the regular cell cycle, whereby older cells are separated out into the gut lumen and removed in the faeces. However these granules can also be stored, leading to bioaccumulation as is often seen with calcium which is retained by some crabs until shell moult then used to form the new shell (Hopkin and Nott 2009).

Since this experiment will feed CeO₂NP-exposed *M. edulis* to *C. maenas* out of water (emersed) there will be no circulating medium and therefore there should be no contact between the gills and food. As such the gills are not expected to be a site of accumulation of Ce though trophic transfer. The stomach should well be a site of Ce accumulation, and because of this there may be potential for CeO₂NPs to enter the hepatopancreas.

The hypothesis for this experiment is that CeO₂NPs will be trophically transferred following consumption of CeO₂NP-laden *M. edulis* by *C. maenas*. It is also hypothesised that Ce will accumulate in the stomach and hepatopancreas, but not the gills.

4.3.2 Method

M. edulis (c. 30g, n = 8) were exposed for 4 hours to 28nm CeO₂NPs (JRC NM-212) at 20mg/l as per Chapter 2.3.3. Control mussels were exposed to algae only. Four mussels from each treatment were retained for ICP-MS analysis of Ce accumulation, the rest were opened carefully, the flesh loosened from the shell, and presented to the crabs open and in the shell.

As per Chapter 2.4.2, a single crab (c. 70g, carapace width c. 6.7cm) was placed in a 9L glass tank, but without water. A piece of blue roll was moistened and placed in the corner of the tank to provide humidity, and a section of drainpipe served as both refuge and enrichment (Fig 4.1). The tanks were darkened, and the crab allowed 24 hours to feed on a single, exposed mussel (opened). 24 hours was eventually chosen as a timepoint since crabs had shown reluctance to feed whilst emersed during the first 8 hours of the experiment. Control crabs were fed unexposed mussels.



Fig 4.1: Set-up for feeding *M. edulis* to *C. maenas* out of water

After 24 hours the gill, stomach and hepatopancreas of crabs which had fed were dissected out, snap-frozen, freeze-dried and acid digested for ICP-MS analysis as per Chapter 2.2. Visible faeces were also removed from the bottom of the tank and analysed for Ce content by digestion in 1ml 70% HNO_3 on a hotplate, followed by dilution to 5% acid with DI for ICP-MS analysis.

4.3.3 Results and Discussion

In terms of accumulation by *M. edulis*, exposed mussels contained significantly more (t-test, $t(6)=-16.07$, $p=0$) Ce (181.01 ± 50.59 [SE] $\mu\text{g Ce/g d.w.}$), than control organisms (0.23 ± 0.05 $\mu\text{g/g}$, $n=4$). This yielded an average Ce content of 192 ± 38.4 μg per exposed mussel fed to the crab. A dose of 20mg/l CeO_2NPs is equivalent to a total dose of 5.43mg Ce . At $192\mu\text{g}$, the mussel therefore accumulated $3.54 \pm 0.71\%$ of the total Ce offered over 4 hours, similar to the values seen in Chapter 3.

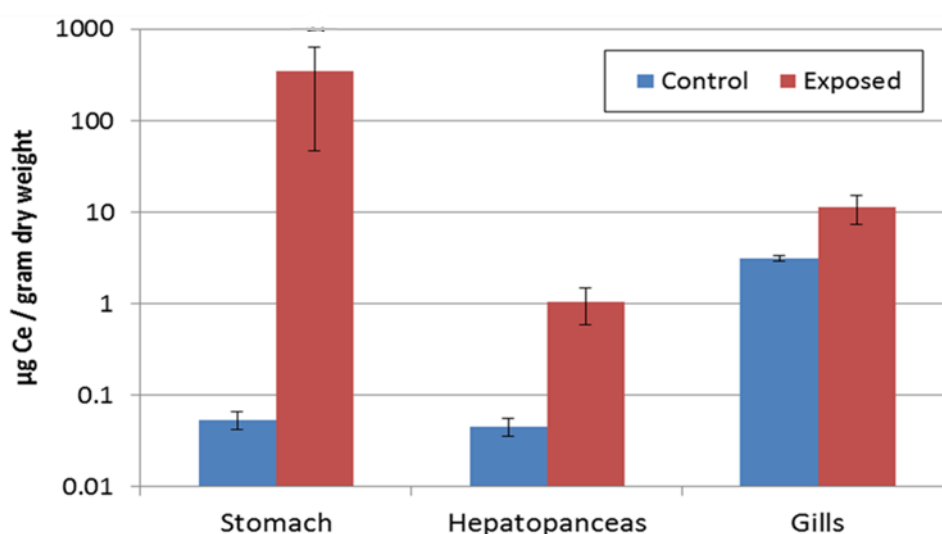


Fig 4.2: Average cerium concentrations ($\mu\text{g Ce/g d.w.}$) found in *C. maenas* tissues following consumption in air of exposed *M. edulis*. Please note the log scale axis used on the y-axis. $n=4$ per treatment. No significance recorded.

Fig 4.2 details the accumulation of Ce in *C. maenas* having been allowed 24 hours to consume - whilst emersed - a mussel laden with CeO_2NPs . The stomach was the organ of greatest uptake (346 ± 299 $\mu\text{g/g d.w.}$), yet despite almost negligible control data (0.05 ± 0.01 $\mu\text{g/g}$), variance in the exposed data prevented this from being significantly different [Welch's t -test, $t(3.085)=-5.54$, $p=0.082$ (exposed data was not normal [Shapiro-Wilk $p=0.016$] and was log transformed for normality. Levene's Test for Equality of Variance showed variances were not equal i.e. $p=0.001$)].

Average Ce levels in the exposed hepatopancreas (1.03 ± 0.5 $\mu\text{g/g}$) were higher than the control (0.04 ± 0.01 $\mu\text{g/g}$) yet, contrary to the hypothesis, a t -test

showed this not to be significant [$t(6)=-2.176$, $p=0.072$]. Similarly, average levels in exposed gills ($11.2 \pm 3.9 \mu\text{g/g}$) were over three times higher than those of the control ($3.1 \pm 0.2 \mu\text{g/g}$), but again not considered significant [$t(3.019)$, $p=0.128$. Variances unequal (Levene, $p=0.02$)]. It could not be demonstrated either that there was any significant difference in uptake between organs [one-way ANOVA, $F(2,9)=1.378$, $p=0.301$]. As such it is impossible to confirm the hypothesis that trophic transfer of CeO_2NPs from *M. edulis* to *C. maenas* is feasible.

Low n-number ($n = 4$) likely explains why Ce concentrations in the gills, digestive gland and hepatopancreas of crabs exposed to CeO_2NP -laden *M. edulis* were not significantly greater than the control, but another reason might be due to variation in feeding rate between crabs. The standard error bars in Fig 4.2 show that whilst very little variation exists in background Ce concentrations within control crabs, there is a great deal of variation in Ce concentrations found in exposed crabs.

Table 4.1 clarifies this by showing the total Ce content found in each tissue of the crabs that had consumed exposed mussels. The amount of Ce in the exposed crabs is higher than the range for control crabs. It also clarifies that there is wide variation in the accumulation of Ce by different tissues in each crab, in some cases up to four orders of magnitude, and this likely reflects why it was not possible to ascertain significant differences between control and exposed crabs.

The crabs were allowed 24 hours to feed, but were not monitored for the last 16 hours of the experiment. Previous observations (Hopkin and Nott 2009) on the feeding of *M. edulis* to *C. maenas* have shown that the mussel is broken down in the gastric mill in the first 12 hours, with smaller particles passing to the hepatopancreas. Within 12-48 hours larger particles are removed in the faeces, whilst waste products are being removed from the hepatopancreas. Beyond 48 hours the faecal products from the hepatopancreas have been removed. Crabs feeding at different times and rates would therefore have been in different stages of digestion when the experiment ended, thus explaining the wide variation in uptake in different tissues.

CRAB	Control (n=4) (Min – Max)	Exposed			
		1	2	3	4
<i>Mussel Burden</i> ($\mu\text{g Ce}$)	-	192 \pm 38			
<i>Total Not Eaten</i> ¹ ($\mu\text{g Ce}$)	-	0	102.9	68.6	63.2
<i>Total Ingested</i> ² ($\mu\text{g Ce}$)	-	192	89.1	123.4	128.8
Stomach ($\mu\text{g Ce}$)	0.05 - 0.1	198	34	0.6	0.3
Hepatopancreas (Ce μg)	0.01 - 0.03	0.2	1	0.6	0.3
Gill (Ce μg)	0.71 - 0.79	0.6	2.1	4.9	1.2
Total in Tissue ($\mu\text{g Ce}$)	0.79 - 0.90	198.9	37.1	6.1	1.9
% Retention	n/a	104	42	5	1.5
Faeces ($\mu\text{g Ce}$)	0.01 - 0.07	0.01	0.8	17.9	23.5
Total Processed ($\mu\text{g Ce}$)	0.82 - 0.97	199	37.9	23.7	25.4
Trophic Transfer Factor	-	2.29	0.3	0.04	0.008

Table 4.1: Actual total cerium content (μg) of the stomach, hepatopancreas, gills and faeces of the crabs used in this experiment (n=4 per treatment). NB: ¹Total Not Eaten values based upon weight of mussel not eaten. ²Total Ingested value = Average Mussel Burden – Total Not Eaten

It is possible to calculate Trophic Transfer Factors (TTF) from the results to understand the likelihood of Ce biomagnifying through the food chain. A TTF > 1 is a sign of potential biomagnification (Mathews and Fisher 2008). Trophic transfer factors in this experiment have been calculated as:

$$\frac{\text{Average Extra Cerium content in the crab / g dry weight}}{\text{Average Cerium content in mussel / g dry weight}}$$

This yields an average TTF of 0.66 (± 1.1 at 95% Confidence Interval). Trophic transfer factors of less than 1 are not considered likely for biomagnification, therefore a TTF of 0.66 should not be considered overtly hazardous. This factor also appears artificially high given the range of values seen in the stomach, and the likely impact of point of digestion upon accumulation in the stomach. In fact, the TTFs for exposed crabs 1-4 were 2.29, 0.3, 0.04 and 0.008 respectively, highlighting this point. By comparison an experiment involving trophic transfer of methylmercury (MeHg - a chemical well known to bioaccumulate in food chains), polonium (Po) and cadmium (Cd) from *Daphnia pulex* to the killifish

Fundulus heteroclitus returned TFFs > 1 for MeHg and Po, but 0.1 for Cd (Mathews and Fisher 2008). This led the authors to conclude that MeHg and Po will biomagnify up the food chain. Another review on TFFs for MeHg fed to trout and minnows returned values consistently greater than 1, yet peaking at 7 with an inverse correlation to concentration (DeForest *et al.* 2007). A similar inverse correlation relationship was shown for other metals, despite TFFs barely breaching 1. This highlights that metal assimilation is less efficient at higher concentrations, but still indicates that, with a TTF of 0.66 ± 1.1 , Ce is not likely to be a source of bioaccumulation up the food web even at lower concentrations. Whole body accumulation was not measured so it is possible that other tissues may hide a Ce burden not discovered in this experiment.

It is noticeable in these results (Table 4.1) that as the Ce concentration in the stomach decreases, so the concentration in the faeces increases confirming that much of the CeO₂NPs are egested into the faeces. The crustacean *Corophium volutator* has previously shown to bioaccumulate CeO₂NPs, yet to also egest them in the faeces (Dogra *et al.* 2016), whilst trophic transfer of CeO₂NPs between zucchini and crickets has yielded high Ce concentrations in the faeces (Hawthorne *et al.* 2014).

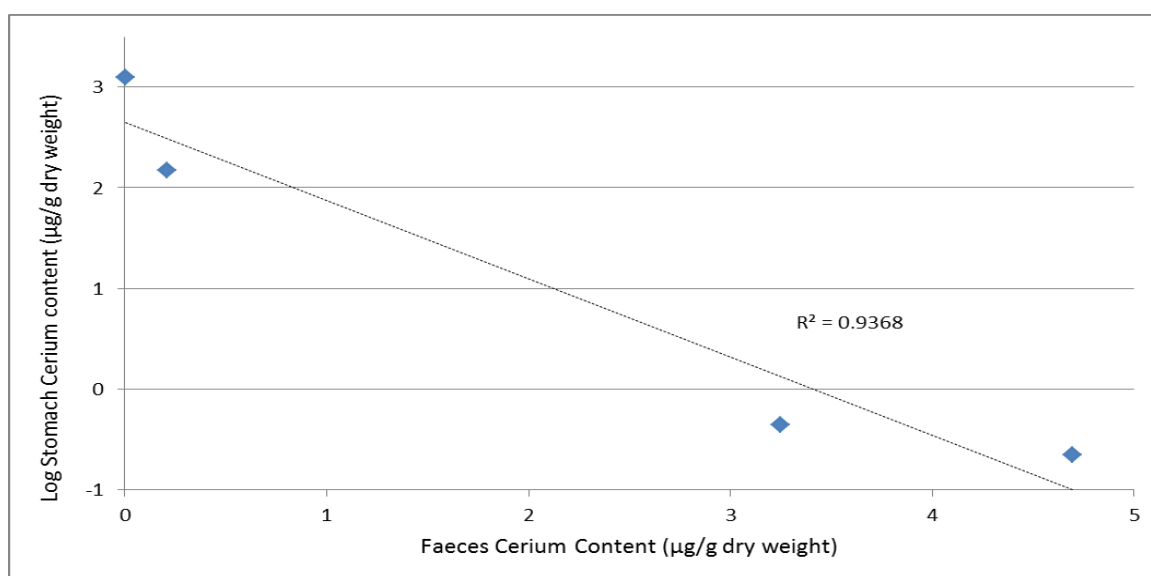


Fig 4.3: Correlation between accumulation of cerium in the stomach and faeces of *C. maenas* following consumption of *M. edulis* exposed to CeO₂NPs. Relationship is significant ($p = 0.032$, Linear Regression)

Fig 4.3 shows a regression analysis between concentrations found in the stomach, and those found in the faeces. A significant inverse relationship is seen here ($p = 0.032$), suggesting that much of the Ce efficiently transits through the organism, and is contrary to the hypothesis concerning accumulation in the stomach.

With regards to crabs 1-3, concentrations in the gills and hepatopancreas also increase as concentrations in the stomach decrease. This suggests that particles are able to breach the filter press and reach the hepatopancreas, even if it cannot be statistically proven in this experiment. Regarding crab 4, concentrations are low in all tissues yet the concentration recovered in its faeces is the highest of all the crabs. Taking these results together it appears that the stomach and hepatopancreas are able to eliminate Ce to some extent through removal of CeO₂NPs in the faeces.

What is not clear is how CeO₂NPs might be able to reach the gills, and in higher concentrations than those seen in the hepatopancreas. One possibility is contamination from the maxillipeds and scaphognathite around the mouthparts, which have parts that probe the branchial chamber through the exhalent aperture. During feeding it is possible that some contaminated food has been swept into the branchial chamber, however to yield such concentrations as seen in crab 3 would require over 0.5g of fresh mussel tissue to enter the branchial chamber.

CeO₂NPs may possibly be carried in the haemolymph, which has direct circulation to the gill chamber. In *C. maenas* the anterior gills are responsible for respiration, whilst the posterior gills are involved in ion regulation (Crothers 1967), therefore the crab may even actively direct Ce to the gills as a method of detoxification, a process previously discovered for zinc (Bryan 2009). It will be necessary in future studies to differentiate between these gills in the analysis in order to ascertain whether Ce is being passively accumulated in the gills, or actively removed.

Combined retention values for the three organs drop across the four crabs from 100% down to 1.5%, showing over 98% elimination in some cases. In terms of

the initial dose of 5.43mg Ce fed to the mussel, in the case of crab 4 this equates to only 0.035% of the original dose being accumulated.

The assumption of Ce being eliminated can only be made for the tissues shown, as translocation could agglomerate particles in other tissues such as the legs, and it would be worth examining whole organism concentrations in future to understand translocation. Indeed, apart from crab 1, it has not been possible to mass balance the soft tissue and faeces burden back to the amount fed to each crab. The first reason for this is due to the variability in mussel uptake ($192 \pm 38\mu\text{g}$) which would determine exactly how much Ce was initially fed to the crab. The second reason regards the assumptions concerning how much was both fed to, and eaten by the crab. In particular, Ce distribution in the mussel is likely to be heavily digestive gland-biased, therefore a crab eating 0.2g of mussel digestive gland would receive a much greater dose of Ce than one consuming 0.5g of mussel mantle, for example. Uneaten mussel tissue was not analysed for Ce content, and again this adds variability to the calculations.

Despite Ce concentrations in every tissue being higher than the control, they were not found to be significant and thus this study cannot conclusively support the work of Farrell and Nelson (2013) by showing that the trophic transfer of particles less than 500nm is possible between *M. edulis* and *C. maenas*. In particular, despite this study removing the element of contamination through ventilation, there was still evidence of gill accumulation of Ce. It will be necessary to examine different gill types in future experiments to help understand why this is so. This study also highlighted Ce uptake into the stomach and, more crucially, the hepatopancreas, but concentrations found in the crab's faeces suggested that most Ce is eliminated from these two organs. An average Trophic Transfer Factor of 0.66 ± 1.1 suggests that trophic transfer of Ce is not likely to lead to biomagnification through the food chain, especially since the TFF calculated is likely an over-estimate based on variable digestive rhythms.

4.4 Immersed Uptake and Depuration of 10nm and 600nm JRC CeO₂NPs by *C. maenas*

4.4.1 Introduction

In Chapter 2.4.2 the gills of *C. maenas* were shown to accumulate 28nm CeO₂NPs during aqueous trophic transfer experiments, however at least part of this burden was thought due to contamination from the ventilation of particles released during sloppy feeding. In the previous study an increased concentration of Ce was noted in the gill despite removing ventilation as a route of uptake, however it was not known if the organism was passively accumulating Ce in the gills, or actively accumulating it with the intention of depuration, as might be seen with zinc (Bryan 2009).

Crabs draw water into the branchial chamber mostly through a hole beneath the claw, which circulates over the gills and out through holes near the mouth. Due to the way the water circulates, different gills have different functionality. The anterior sets are mostly involved in respiration as they receive the most aeration, whilst the posterior sets are more involved in osmoregulation and ion exchange. Occasionally the direction of water flow is reversed in the chamber to help flush the posterior gills and remove impurities (Crothers 1967). Due to both differences in function and water circulation, it is possible that the gill sets might accumulate NPs in different fashions, for example increased accumulation through either increased water contact of anterior gills or use of posterior gills as a method of metal depuration.

The gills of *C. maenas* are covered in a chitinous cuticle layer, restricting access to gill epithelial cells (Henry *et al.* 2012). This layer is diffusive and should therefore restrict access to ions only, not particles. A number of pores do run through the chitin however they are only a few nanometres wide, so are likely to be impenetrable to all but the smallest NPs (Smith 1942). As such it is possible that insoluble CeO₂NPs will not be able to breach this layer, and may therefore have no biological effect on the gills.

Accumulation of NPs by *C. maenas* gills has not yet been studied, however since CeO₂NPs tend to agglomerate in high salinity media (Batley *et al.* 2012), it

is possible their accumulation would be similar to the smallest of microplastics. Both 500nm and 8-10µm nanoparticles have been associated with the gills of *C. maenas* during aqueous exposures in contaminated water (Farrell and Nelson 2013, Watts *et al.* 2014).

This experiment aims to understand how differences in size of CeO₂NP affect accumulation and depuration in the stomach, hepatopancreas and gills of *C. maenas* following aqueous exposure, but more importantly to help understand if differences exist in accumulation and depuration between the respiratory and ionic gills. The experiment will also examine the ability for CeO₂NPs to affect biological processes (oxidative stress and lipid peroxidation) at the suggested regulatory limit of 3mg/l, as has been explored in Chapter 3.

Similar to earlier experiments with *M. edulis*, this experiment will expose the crab *C. maenas* to 10nm CeO₂NPs or 600nm micro-CeO₂ as waterborne contaminants in order to understand in which tissues the accumulation of Ce might occur. This will allow better understanding of how sloppy feeding might influence particle accumulation in certain organs.

Initial uptake periods of 4 and 8 hours were chosen since crabs have been shown to ventilate at a similar rate to mussels (Taylor 1976), and in the previous chapter it was shown that mussel accumulation of CeO₂NPs was at a maximum at around 4 hours. Some crabs will then be transferred to clean water for 12 hours to investigate depuration.

The hypotheses for this study are that the ionic gills will accumulate more Ce than respiratory gills, and that the gills will be a site of major oxidative stress and lipid peroxidation.

4.4.2 Method

C. maenas were collected as per Chapter 2.4 and exposed to a single dose of either 10nm CeO₂NPs (JRC NM-211) or 600nm micro-CeO₂ (JRC NM-213) at the assumed regulatory limit of 3mg/l in a plastic tank containing 3l FASW (34 psu, pH 8.1, Fig 4.4). This resulted in a dose of 9mg CeO₂NPs, equivalent to 7.33mg Ce. Control crabs were placed in the same conditions, but not exposed to anything. Groups of crabs (n = 6 per treatment) were removed for analysis after 4 and 8 hours. A further group was transferred after 8 hours into clean FASW and allowed 12 hours to depurate before being removed for analysis. The stomach, hepatopancreas, respiratory gills and ionic gills were dissected out of each organism.

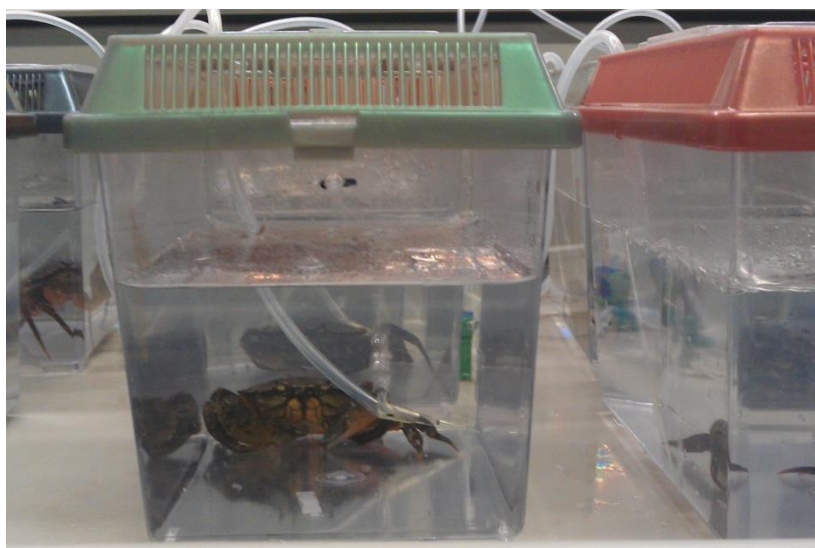


Fig 4.4: Set-up for aqueous exposure of *C. maenas* to CeO₂

Following freeze-dry and acid digestion, Ce concentration of individual tissues was determined via ICP-MS following the method outlined in Chapter 2.2. Cerium concentration samples were pooled hence no statistical analysis was performed on these results. Assays for TBARS, SOD, GST and CAT activity were performed as per the method detailed in Chapter 2.2.3. Oxidative stress data was analysed as per Chapter 2.2.4 (n = 6 per treatment), with *p* assumed significant at < 0.05.

4.4.3 Results

4.4.3.1 Bioaccumulation

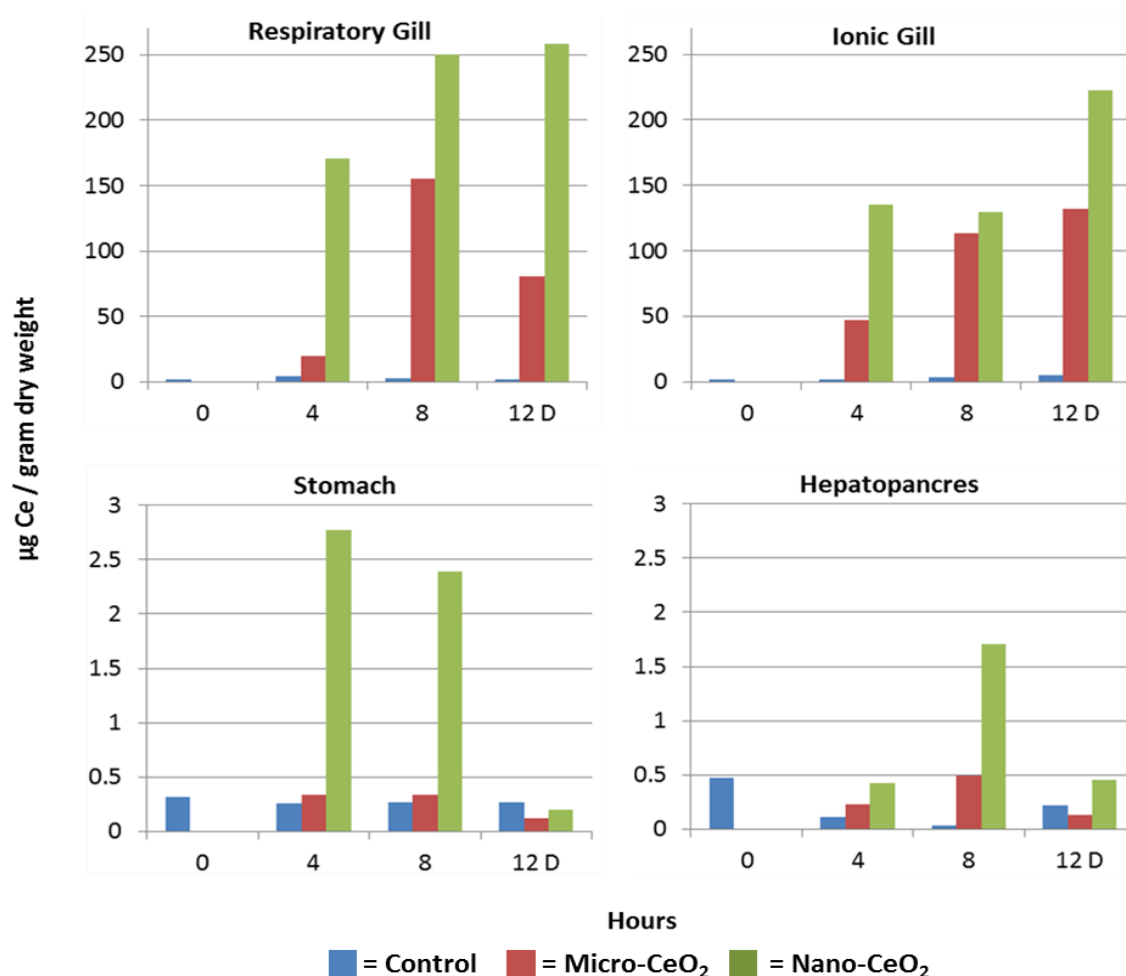


Fig 4.5: Cerium concentrations (µg/g dry weight) found in the ionic gill, non-ionic gill, hepatopancreas and stomach of *C. maenas* following exposure to 10nm (NM-211) and 600nm (NM-213) CeO₂NPs at 3 mg/l (C = Control/unexposed, M = 'Micro-CeO₂' [600nm], N = Nano-CeO₂ [10nm]) for 4 hours, 8 hours, or following 12 hours' depuration (NB: samples were pooled from n=6 to n=1, hence no statistical analysis could be performed).

Following aqueous exposure, *C. maenas* accumulation of both micro- and nano-CeO₂ was most prominent in the gills, with stomach and hepatopancreas concentrations up to two orders of magnitude lower (Fig 4.5). This is true at all time points, and even following depuration. Under optimal conditions crabs can filter over 2.5l water per hour over their gills (Taylor 1976), hence the gills as tissues of major accumulation is not surprising. Crabs are also known to filter

feed to some extent (Jennings and Rainbow 1979), hence the uptake of Ce in the stomach and hepatopaneas is also not surprising. In all cases nano-CeO₂NPs have been accumulated to a greater extent than micro-CeO₂.

	Control (Unexposed)			Micro-CeO ₂			Nano-CeO ₂		
				600nm, NM-213			10nm, NM-211		
Time (Hours)	4	8	12D	4	8	12D	4	8	12D
Respiratory Gills	2.12	1.36	1.21	10.05	65.70	49.60	108.25	97.15	149.15
Ionic Gills	1.11	2.16	3.98	22.30	60.15	94.75	97.85	128.80	185.80
Stomach	0.23	0.21	0.18	0.32	0.18	0.09	3.08	1.64	0.13
Hepatopaneas	0.44	0.18	0.91	1.00	1.72	0.73	1.89	7.50	2.02
Total µg Cerium	3.90	3.92	6.27	33.67	127.74	145.16	211.07	235.09	337.10
% Accumulated	-	-	-	0.46	1.74	1.98	2.88	3.21	4.60

Table 4.2: Total µg Cerium found in the various organs of *C. maenas* following exposure to 27mg of 600nm Micro-CeO₂ or 10nm CeO₂NPs (3 mg/l) for 4 hours, 8 hours, and following 12 hours' depuration. % Accumulation derived from (Total Extra µg Cerium/Ce dose of 7.33mg)

The total percentage accumulation figure for nano-CeO₂ is lower than 5% - similar to the figures shown for *M. edulis* in the previous chapter, with figures for micro-CeO₂ plateauing at 2% (Table 4.2). This suggests that bioaccumulation is limited, however further time-points for depuration might contradict this. A recent study on the ventilation of microspheres by *C. maenas* (Watts *et al.* 2014) showed that the gills accumulated between 0.39 and 7.7% of the initial concentration over 16 hours, again similar to the results shown here since gills accounted for over 95% of the accumulated Ce.

In the respiratory gills Ce concentrations from both nano- and micro-CeO₂ exposures increased over the 8 hours, and this is not surprising since the organ would be continuously bathed in CeO₂NP-rich water during ventilation. The ionic gills show continuous accumulation of micro-CeO₂ over 8 hours, whilst nano-CeO₂ is mostly accumulated over 4 hours and levels maintained over 8 hours. In both instances the rate of uptake of micro-CeO₂ after 4 hours is much less than that of nano-CeO₂. Particles in the ionic gills accumulated to a lesser extent than those in respiratory gills, likely due to current flow around the branchial chamber meaning that they are bathed in less water than their respiratory counterparts.

The gill lamellae of *C. maenas* are around 60µm wide, and spaced around 40µm apart. Neither particle type is likely to agglomerate to a size to become trapped in this space. The epithelial surface of the gill is composed of a cuticle made of chitin, and microscopic study reveals bacteria often living on the gill surface in huge numbers (Goodman and Cavey 1990). This cuticle is known to bind trace metals (Henry *et al.* 2012) therefore it is possible that particles and agglomerates would be able to adhere to either this, or the bacterial assemblages, thus explaining how Ce might be accumulated on gill tissue during the course of the experiment. Bacterial assemblages have previously been shown to be great accumulators of insoluble AuNPs (Ferry *et al.* 2009). Exposures of the fiddler crab *Uca rapax* to microplastics have shown microplastics adhering to the gill surface, and the authors questioned why such anthropogenic particles were particularly adhesive when other natural detritus (e.g. sand) was not (Brennecke *et al.* 2015).

What is unknown is if Ce is able to breach this chitin cuticle and reach the gill epithelium and haemolymph. This cuticle is known to be ion-selective and diffusive (Bryan 1971), but given the insolubility of the CeO₂ used (Dogra *et al.* 2016) then uptake as ions is likely negligible. A number of pores of several nanometres width run through the cuticle and extend into the epithelial cells (Smith 1942). The average size of the nano-CeO₂ was 11 ± 2.5 nm, therefore it is highly unlikely that they were able to penetrate these pores. In a similar experiment microplastics (8-10µm) were found adhered to the gill cuticle of *C. maenas*, but none were found internalised (Watts *et al.* 2014).

After 12 hours' depuration the concentration of nano-CeO₂ remains high in the respiratory gills, whilst the concentration of micro-CeO₂ drops. In the ionic gills depuration appears not to affect Ce levels accumulated from micro-CeO₂, however there is an increase in Ce from nano-CeO₂ exposure. It could be speculated that the size of these particles affects how well they can be depurated. The cleansing action of the flabellum is more prominent on the anterior, respiratory gills. This action might be able to dislodge larger particles from the gill cuticle due to their elevated profile, yet may struggle to remove strongly adhered particles or those which show a lower profile and therefore be more resistant to this sweeping action (in much the same way that bacteria are

not removed). Particles which have been dislodged could then either be removed during normal ventilation, however they may also be beaten into the path of the posterior, ionic gills and adhere to them instead.

One other possible reason for increases in gill Ce during depuration might be due to translocation of Ce from the stomach or hepatopancreas. The gills are a known site of depuration for metals such as zinc (Bryan 1971) although this generally applies to ionic forms, and not insoluble particle. The sheer magnitude of difference however between Ce concentration of the stomach/hepatopancreas and that of the gills (Fig 4.5, Table 4.2) means that this cannot be the major reason for increase during depuration, however haemolymph concentration is worth examining in future studies.

The final possible reason is that particles loosely adhered to the carapace were dislodged on transfer to clean water. This could then recirculate CeO₂ through the tank making it possible to be recaptured on the gills. Examination of Ce content of the clean water over the time of depuration might shed more light on this. Pre-washing the crabs before introduction into clean water could help reduce such contamination in the future.

Cerium concentrations in the stomach after 4 and 8 hours following exposure to nano-CeO₂ are much higher than those from micro-CeO₂ exposure, which are almost negligible. After 12 hours depuration however all Ce concentrations in the stomach are back to control levels. In the hepatopancreas nano-CeO₂ caused increased Ce levels after 8 hours, which are again mostly removed after 12 hours' depuration. Variable control levels prevent drawing the conclusion as to whether or not any micro-CeO₂ was accumulated in the hepatopancreas over the 8 hours, however the trend is still towards loss after 12 hours' depuration. Either way, the concentrations of nano-CeO₂ are still much greater than micro-CeO₂. The apparent transition of these particles through the organs and towards depuration is similar to the digestive rhythms explored by previous authors, whereby egestion of indigestible particles can occur as early as 12 hours (Hopkin and Nott 2009).

The data presented in Fig 4.5 is slightly misleading, as it suggests the stomach accumulated more Ce than the hepatopancreas. In fact, the average dry weight of the stomach was only 0.76g, compared to 4.25g for the hepatopancreas, and therefore the actual average concentrations of Ce in hepatopancreas were generally higher than the stomach, even with control organisms (Table 4.2). The only exception to this is with 10nm particles, whereby stomach concentration increases after 4 hours then steadily drops, with the hepatopancreas then showing its maximum at 8 hours. This again highlights the likely movement of CeO₂NPs through the stomach to the hepatopancreas.

The increased uptake of 10nm CeO₂NPs compared to 600nm particles might be due to size and agglomeration rate, with the nano-CeO₂ thought to agglomerate at half the speed of the micro-CeO₂ (Singh *et al.* 2014). Increased agglomeration would lead to increased settling, with increased adsorption removing agglomerates from the system. Filter feeding by the crab would also limit the number of larger particles entering the stomach. With the filter press designed to restrict access only to smaller particles, perhaps as small as 100nm (Hopkin and Nott 2009), even if larger agglomerates have entered the stomach, they are unlikely to enter the hepatopancreas. It is possible to speculate then that the smaller the particle remains, the more likely it appears to be accumulated by the various organs of the crab.

Cerium concentrations in the faeces and haemolymph were not measured in this experiment, therefore it cannot be said for certain if Ce was fully eliminated from the crab i.e. via faeces, or if the Ce was translocated to another part of the organism e.g. via the haemolymph. Evidence of Ce has previously been found in calcium phosphate granules stored in the hepatopancreas of *C. maenas* (Simmons *et al.* 1996) therefore total depuration may not actually occur.

4.4.3.2 Biological Effects

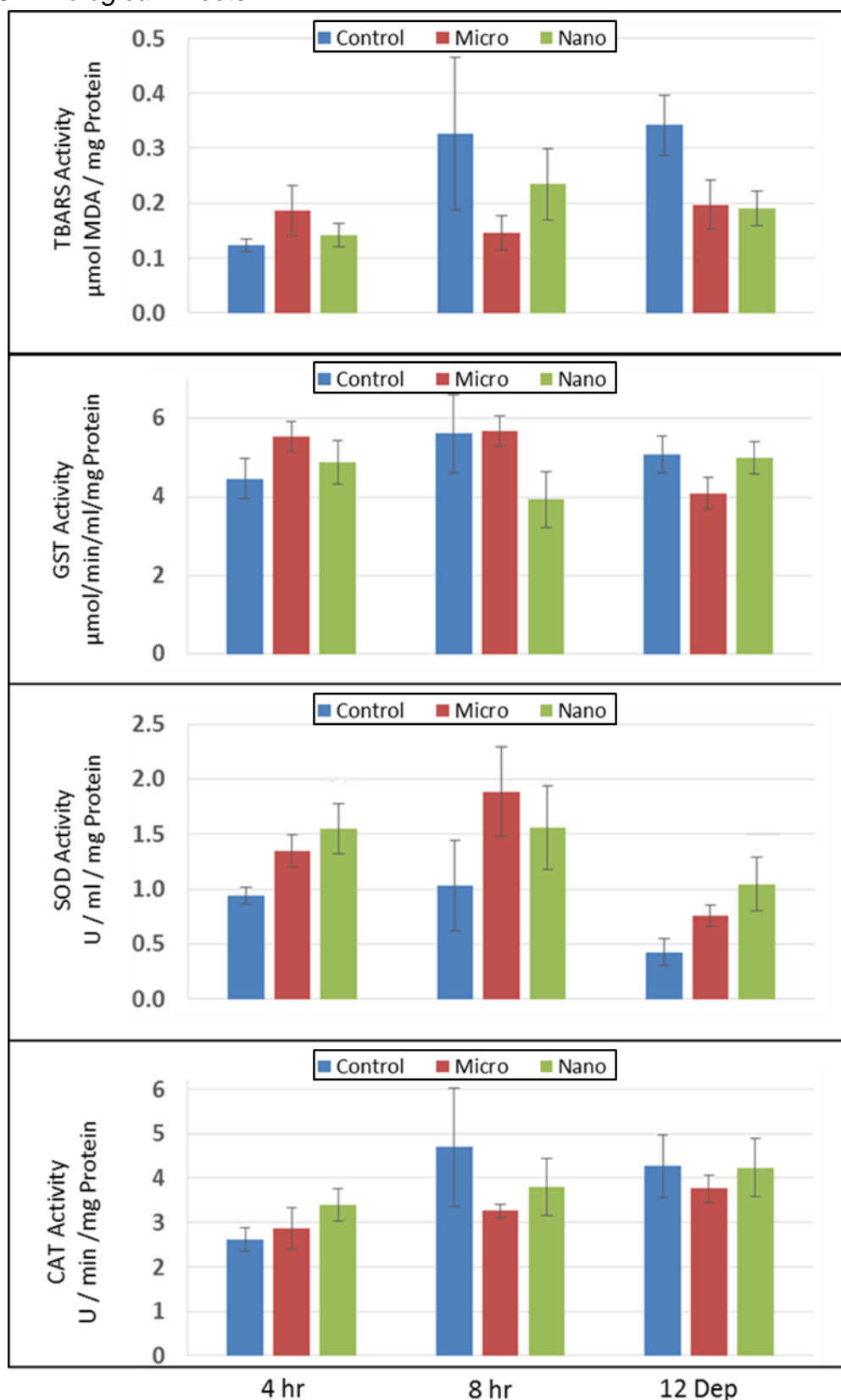


Fig 4.6: Oxidative stress and lipid peroxidation in the **Respiratory Gill** of *C. maenas* following aqueous exposure to 3mg/l 600nm Micro-CeO₂ (NM-213) and 10nm CeO₂NPs (NM-211). n=6. No significant difference recorded.

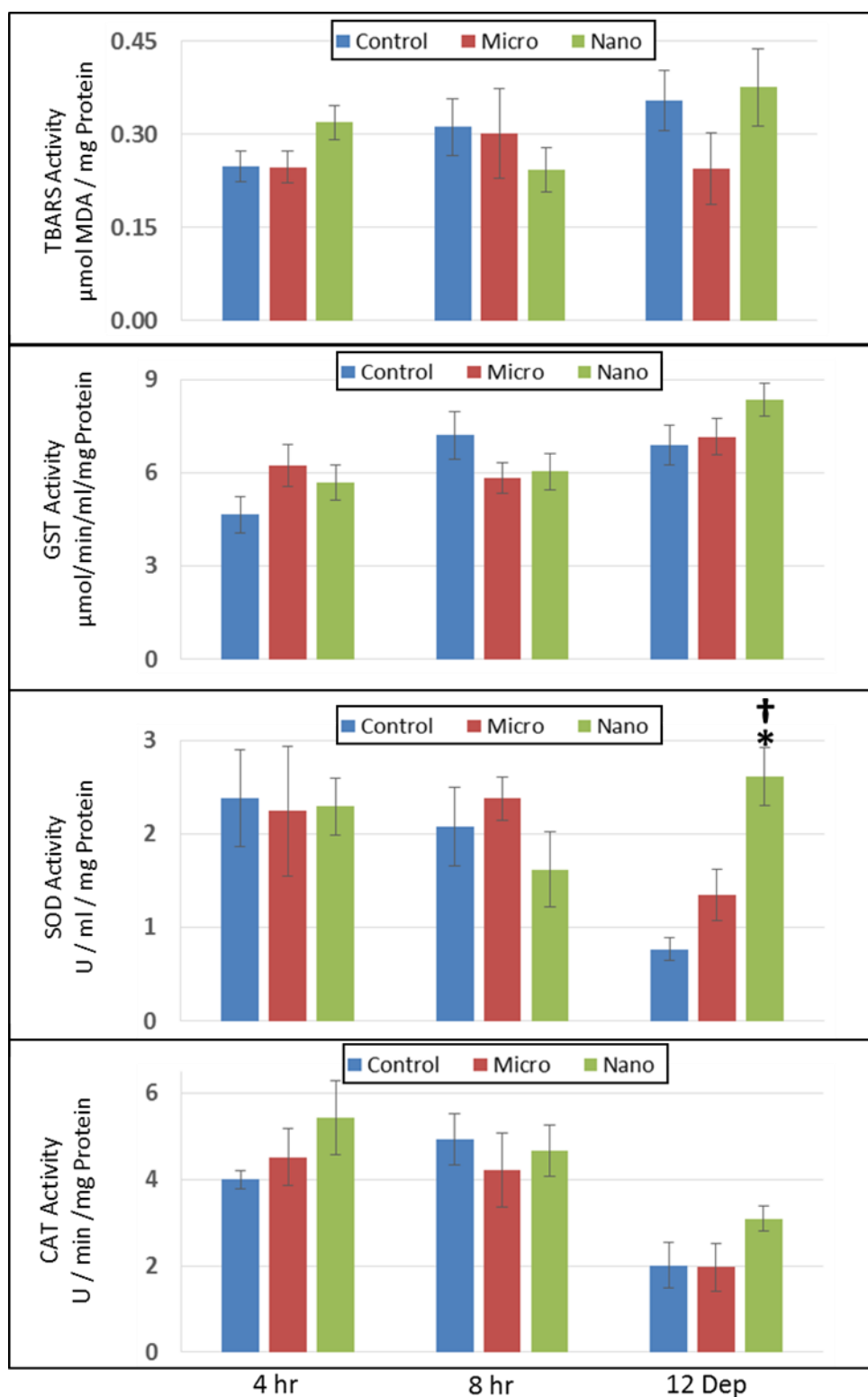


Fig 4.7: Oxidative stress and lipid peroxidation in the **Ionic Gill** of *C. maenas* following aqueous exposure to 3mg/l 600nm Micro-CeO₂ (NM-213) and 10nm CeO₂NPs (NM-211). Significant difference ($p < 0.01$, one-way ANOVA with Tukey post-hoc) from unexposed control (*) or between particle types (†). n=6

In terms of the respiratory gills, despite a trend towards decreased TBARS activity and increased SOD activity following exposure to both particle sizes, one-way ANOVAs found no significant differences in any biological effects between any groups ($p>0.05$).

In the ionic gills (Fig 4.7), after 12 hours' depuration SOD activity significantly increased [one-way ANOVA: $F(2,15)=14.337$, $p=0$] in nano-CeO₂ exposed crabs, compared to both the control (Tukey's post-hoc: $p=0$) and micro-CeO₂ (Tukey: $p=0.007$). In terms of bioaccumulation, Ce levels in nano-CeO₂ exposure had actually increased at this timepoint and it may be that this has driven the increased SOD activity.

Neither particle shows any effect on TBARS or GST activity, and despite SOD effects in the ionic gill 12 hours' post-exposure, there is also no effect on CAT activity. That very few effects are seen despite such high concentrations suggests that these particles are not penetrating the gill cuticle, and therefore do not affect gill cell processes. Given the number of bacterial epibionts on the gill cuticle it might even be that the biological effects were due to CeO₂ interacting with these bacteria, and not from the gills themselves. CeO₂NPs (10nm) have demonstrated an anti-bacterial effect at concentrations as low as 34µg/l in 16-hour incubation exposures against *E. coli*, *Bacillus subtilis*, *Salmonella enteritidis* and *Staphylococcus aureus* (Babu et al. 2014). The authors suggested that surface redox cycling following adhesion to the bacterial surface would lead to oxidative stress and cell death, and this was also suggested in another experiment exposing *E. coli* to 7nm CeO₂NPs (Thill et al. 2006).

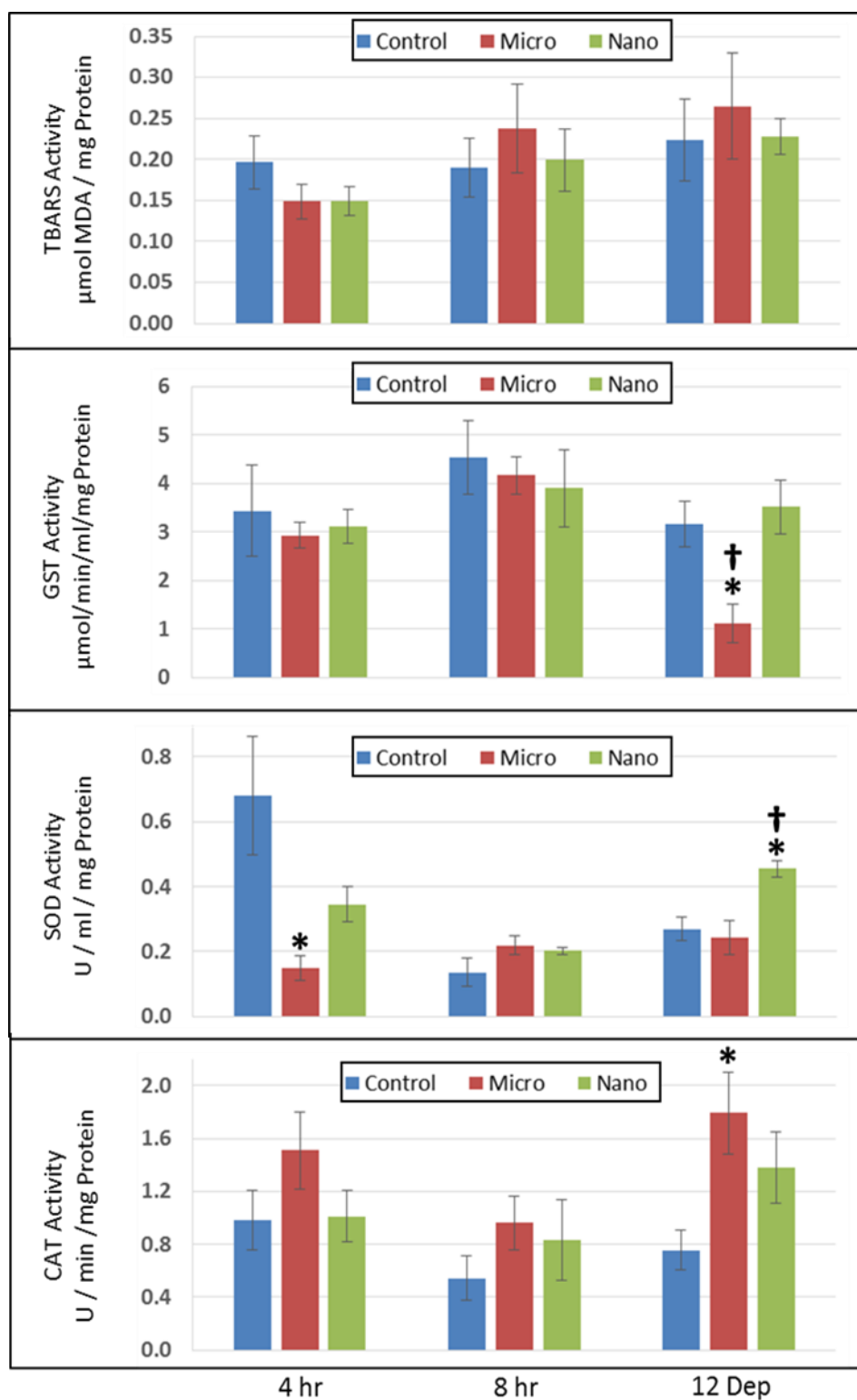


Fig 4.8: Oxidative stress and lipid peroxidation in the **Stomach** of *C. maenas* following aqueous exposure to 3mg/l 600nm Micro-CeO₂ (NM-213) and 10nm CeO₂NPs (NM-211). Significant difference ($p < 0.05$) from unexposed control (*) or between particle types (†). n=6

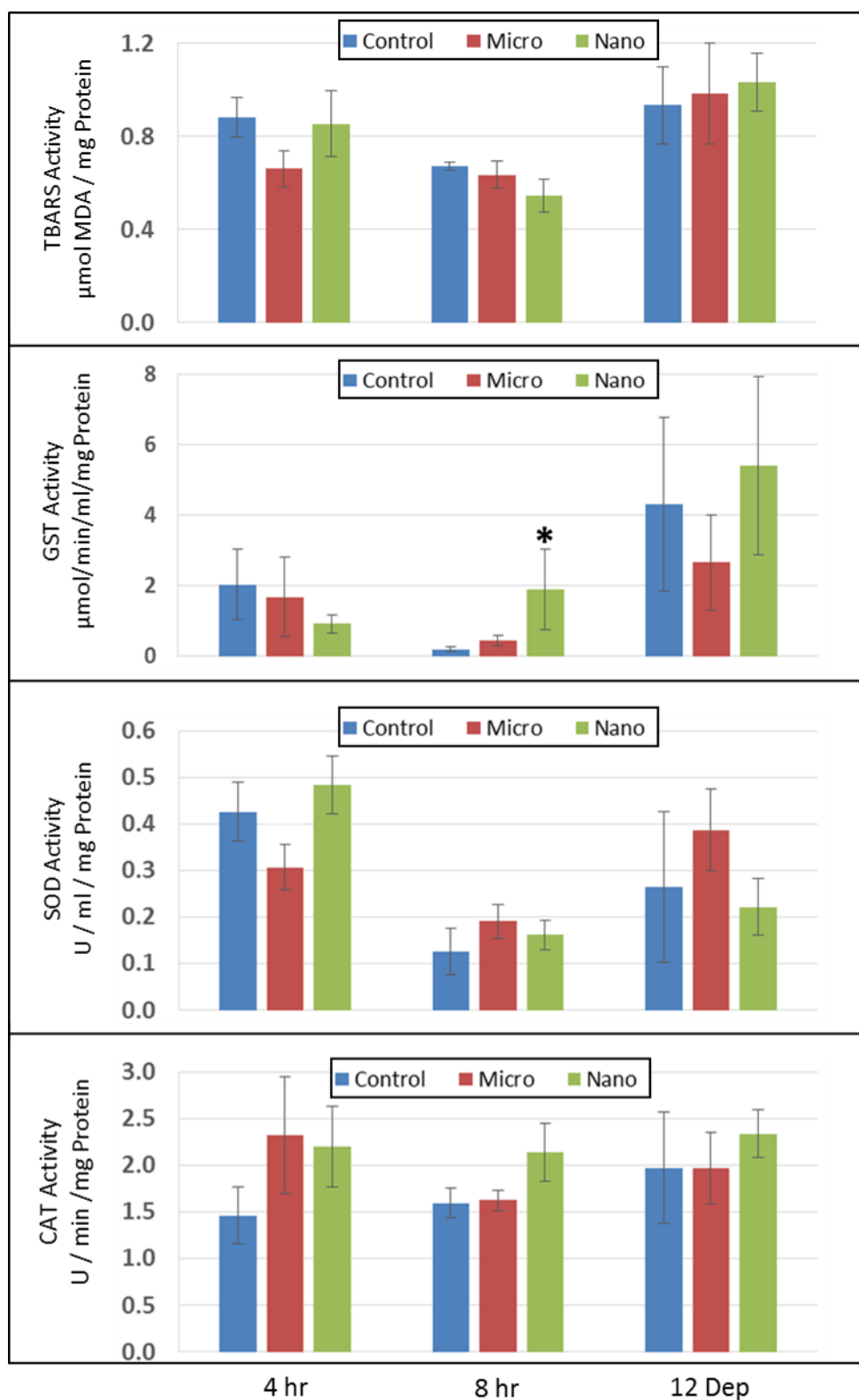


Fig 4.9: Oxidative stress and lipid peroxidation in the **Hepatopancreas** of *C. maenas* following aqueous exposure to 3mg/l 600nm Micro-CeO₂ (NM-213) and 10nm CeO₂NPs (NM-211). Significant difference ($p < 0.05$, Mann-Whitney U-test) from unexposed control (*). n=6

In the stomach (Fig 4.8) there was a significant reduction in GST activity after 12 hours' depuration following micro-CeO₂ exposure as compared to the control [*t*-test: $t(10)=3.649$, $p=0.004$], Micro-CeO₂ also significantly reduced GST activity as compared to nano-CeO₂ [Mann-Whitney: $U=2$, $p=0.009$ (nano-data found to be not normal [Shapiro-Wilk: $p=0.005$] and log transformation did not alter this, hence use of a non-parametric test)].

In terms of SOD activity, and despite less accumulation than nano-CeO₂, a one-way ANOVA [$F(2,15)=5.741$, $p=0.014$] showed that after 4 hours micro-CeO₂ significantly reduced SOD activity as compared to the control (Tukey: $p=0.012$) in the stomach. This suggests a protective effect.

Following nano-CeO₂ exposure SOD activity increased significantly [one-way ANOVA: $F(2,15)=8.56$, $p=0.003$] after 12 hours' depuration compared to both micro-CeO₂ (Tukey: $p=0.005$) and the control (Tukey: $p=0.012$), but had no other effects (Fig 4.8). This suggests a slight pro-oxidant response, although there was no related significant increase in CAT activity. There was however a significant increase [one-way ANOVA: $F(2,15)=4.197$, $p=0.036$] in CAT activity at this timepoint as compared to the control (Tukey: $p=0.029$) following micro-CeO₂ exposure.

GST is known to bind to damaging ROS such as •OH, as well as aid binding of GSH with lipid peroxides (Howie *et al.* 1990). Reduced demand for GST therefore suggests fewer free radicals following micro-CeO₂ exposure and a protective effect of the particles. Alternately it might be that GSH is being depleted as it attempts to conjugate either lipid peroxides or hydrogen peroxide under extreme oxidative stress (Carlson *et al.* 2008), therefore GST activity reduces simply because it cannot conjugate GSH if there is less GSH. Depleted GSH as a result of conjugating lipid peroxides might explain why no change in TBARS (MDA) activity is recorded, since GSH is conjugating lipid peroxides into stable lipid alcohols before they can form aldehydes. At this time point there is also a significant increase in CAT activity which suggests that H₂O₂ production has increased. Since it is known that GSH can also conjugate H₂O₂ then this might give weight to the theory of depleted GSH (Vidal-Linan *et al.* 2010). Such an extreme pro-oxidative stress is unlikely, especially given the

low concentrations involved and since in the previous chapter micro-CeO₂ exhibited anti-oxidative properties in *M. edulis*, however it would be worth examining GSH and GPx levels in future to clarify this.

In the hepatopancreas (Fig 4.9) effects are more limited than the stomach, and this is not surprising since accumulation per gram was lower. Compared to the control, GST activity significantly increases following 8 hours' nano-CeO₂ exposure [Mann-Whitney: $U=0$, $p=0.004$ (Shapiro-Wilk normality test showed data to be non-normal [$p=0$] even following log-transformation, hence use of a non-parametric test)], suggesting up-regulation to protect from the particles. This effect appears transitory and isolated since it does not re-occur at a later time point, although this might be due to the variability in the control data. There is no evidence of changes in SOD or CAT activity at any time point in the hepatopancreas, and no evidence of any biological effects following 12 hours' depuration in the hepatopancreas, indicating recovery.

The results have shown that in general, both micro- and nano-CeO₂ are accumulated by the gills, stomach and hepatopancreas of *C. maenas* following 8 hours' aqueous exposure, with smaller particles accumulating to an equal or greater extent than larger particles. There is some evidence of micro-CeO₂ having a short-term anti-oxidant effect on the stomach. Nano-CeO₂ tends to have a mild pro-oxidant effect in the stomach, but the effects of both particle types are transitory and isolated. These results are similar to those seen in Chapter 3.5 whereby micro-CeO₂ was associated with an anti-oxidant effect.

Following 12 hours' depuration, in all treatments levels of Ce in the stomach and hepatopancreas are depurated to control levels. Respiratory gills show depuration of micro-CeO₂, but not of nano-CeO₂. Ionic gills show no depuration of micro-CeO₂, whilst concentrations of nano-CeO₂ show increase. Action of the flabellum and water currents may influence the movement of particles between gill types. It was also shown that nano-CeO₂ was able to induce increased SOD activity in the ionic gill during depuration. This effect appears to depend on the amount accumulated by the gill, but may also be a residual effect of interactions with bacteria on the gill surface.

The crabs selected for experiments in this chapter were of a red colour morph. Green crabs are synonymous with recent moulting and intertidal activity, whilst red crabs are indicative of intermoult, are heavier with a thicker carapace, and spend longer in the sub-tidal (Styrishave et al. 1999). This suggests that green crabs might have a higher tolerance to variable conditions, and may have a stronger stress response to deal with this. Subsequently they may be less affected by stressors from accumulated NPs than would red crabs. Future studies should therefore focus on comparison between the two colour morphs or various moult stages, especially since intertidal organisms are more likely to be exposed to anthropogenic input.

In terms of the environment, this experiment shows that some oxidative stresses can still be initiated following acute exposure at the recommended environmental release limit of 3mg/l. In reality current anthropogenic inputs (10-1000 ng/l) are many thousand-fold lower than this limit so it is unlikely even with a 10-fold increase in production that there would be much stress placed on *C. maenas* following acute exposure. However, bar spillage, the nature of anthropogenic input is often chronic and of lower concentration therefore further studies are required to understand the response of *C. maenas* under these conditions i.e. whether the crab is able to eliminate Ce at a rate faster than it accumulates it.

4.5 Trophic Transfer of 10nm JRC CeO₂NPs from *M. edulis* to *C. maenas* whilst Emerged

4.5.1 Introduction

Experiments in this chapter have yet been unable to determine if the gills or hepatopancreas of *C. maenas* have significantly accumulated CeO₂NPs following trophic transfer. In Chapter 4.4 immersed exposures to suspended CeO₂NPs demonstrated increases in Ce concentration in the ionic gills following depuration. As such the question as to whether the gills are a site of detoxification of accumulated Ce is still uncertain, as is the mechanism by which gills could accumulate Ce during trophic transfer.

A previous study has shown greater uptake of 3µm microplastics than 9.6µm microplastics into the haemolymph of *M. edulis* (Browne *et al.* 2008) however this could not be replicated by Watts *et al* (2014) using 10µm spheres, and it was considered whether size was factor as to whether particles could enter the haemolymph. Indeed, 500nm microplastics have also been found in the haemolymph of *C. maenas* following trophic transfer from *M. edulis* (Farrell and Nelson 2013). Nanoparticles are therefore of a size considered possible to enter the haemolymph and this could provide a route of transit around the organism – to the gills for example - and therefore also a method through which to depurate Me(O)NPs.

This study will examine trophic transfer of 10nm CeO₂NPs from *M. edulis* to *C. maenas* in a dry environment (emerged). Cerium burdens of the stomach and hepatopancreas will be examined, as will those of the haemolymph, respiratory gills and ionic gills in order to ascertain whether ionic gills are actively used in Ce depuration. Again the impact of Ce accumulation on oxidative stress and lipid peroxidation will be examined.

The hypotheses are that the Ce will be found in the haemolymph of crabs eating exposed mussels, that the crab's ionic gills will have a greater burden of Ce than the respiratory gills, that Ce will be accumulated in the hepatopancreas, and that Ce will have no impact on biological effects.

4.5.2 Method

Mussels were exposed (as per Chapter 2.3.3) to 20mg/l 10nm CeO₂NPs (NM-211), then fed to *C. maenas*. Crabs were allowed 24 hours to feed in dry, darkened conditions as per Chapter 4.3 (Control n=4, Exposed n=6). Following this 1ml (minimum) haemolymph samples were drawn by piercing the crab at the base of the third walking leg with a 21g needle and syringe. Crabs were then dissected into gill, respiratory gill, stomach and hepatopancreas samples. Tissue samples were freeze-dried, acid-digested and analysed for Ce content as per Chapter 2.2. Haemolymph samples were digested in 1ml 70% HNO₃ on a 60°C hotplate for 24 hours, then diluted to 5% acid content for ICP-MS analysis. TBARS, SOD, GST and CAT activity were assessed as per Chapter 2.2.3, and statistical analysis performed as per Chapter 2.4.

4.5.3 Results and Discussion

M. edulis exposed to 20mg/l 10nm CeO₂NPs (NM-211) for four hours contained an average of 1269 ± 879 (SE) $\mu\text{g Ce/g dry weight}$, equivalent to a total average of 818 ± 466 (SE) μg per mussel. The uptake by these mussels was variable, and governed by variability of stomach content, which ranged from 135 to 2180 $\mu\text{g Ce}$.

Ce content (Fig 4.10) in the stomach of *C. maenas* fed exposed mussels (1426 ± 505 $\mu\text{g/g dry weight}$) was significantly higher [*t*-test, $t(5)=-2.816$, $p=0.037$ (based on unequal variance, Levene's $p=0.046$)], than the control (1.59 ± 0.78 $\mu\text{g/g}$). The same was true of the hepatopancreas [2.71 ± 0.83 v 0.59 ± 0.37 $\mu\text{g/g}$; $t(8)=-2.823$, $p=0.022$ (data log transformed as control data not normal: Shapiro-Wilk $p=0.008$)].

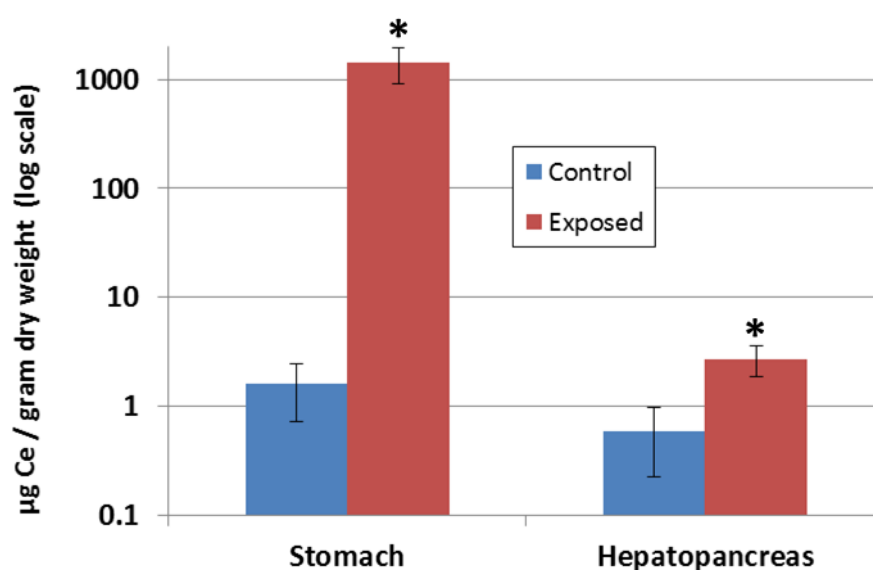


Fig 4.10: Mean Cerium content in the stomach and hepatopancreas of *C. maenas* having been allowed to feed for 24 hours on *M. edulis* exposed to 20mg 10nm CeO₂NPs/l. Control organisms fed unexposed mussels (* = significantly different to control, $p<0.05$, *t*-test, control $n=4$, exposed $n=6$) NB: Y-axis on a log-scale for clarity.

Each crab eating an exposed mussel produced faeces containing an average of 21.23 ± 13 $\mu\text{g Ce}$, compared to 0.017 ± 0.013 $\mu\text{g Ce}$ for the control (faeces were not weighed, hence no statistical analysis can be performed). There was no significant difference in Ce content in the haemolymph (Fig 4.11), with the

control in fact showing greater variability and concentration than exposed crabs [t-test: $t(8)=1.54$, $p=0.162$ (all data log transformed as not normal: Shapiro Wilk $p<0.031$)].

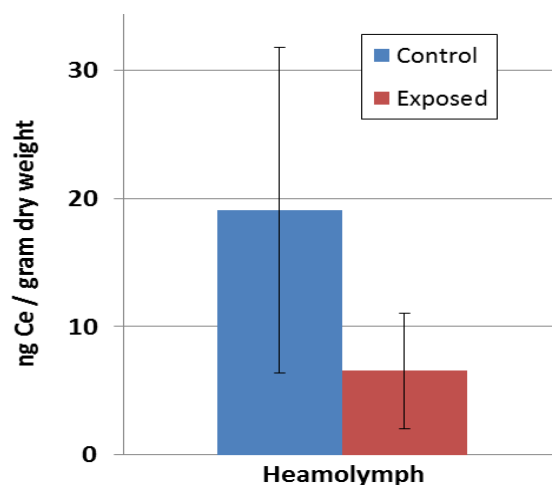


Fig 4.11: Mean Cerium content in the haemolymph of *C. maenas* having been allowed to feed for 24 hours on *M. edulis* exposed to 20mg 10nm CeO₂NPs/l. Control organisms fed unexposed mussels (control n=4, exposed n=6)

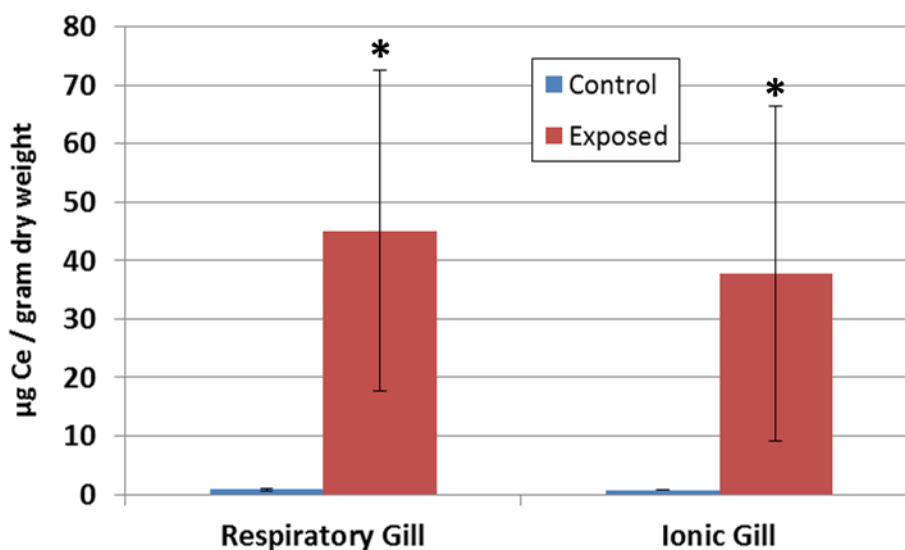


Fig 4.12: Mean Cerium content in the respiratory and ionic gills of *C. maenas* having been allowed to feed for 24 hours on *M. edulis* exposed to 20 mg/l 10nm CeO₂NPs/l. Control organisms fed unexposed mussels (* = significant difference, $p < 0.05$, t -test, control n=4, exposed n=6)

Cerium content in the respiratory gills (45.1 ± 27.5 µg/g) was significantly (t -test: $t(8)=-5.0393$, $p=0.001$) higher than the control (0.83 ± 0.20 µg/g). Cerium

content of the ionic gills ($37.8 \pm 28.7 \mu\text{g/g}$) was also significantly [$t(8)=-4.051$, $p=0.004$] higher than the control ($0.78 \pm 0.11 \mu\text{g/g}$ respectively) [all exposed gill data log transformed for normality (Shapiro-Wilk $p<0.05$)]. Contrary to thoughts that the ionic gills might contain a greater Ce burden than respiratory gills, there was no significant difference between them [$t(10)=0.637$, $p=0.539$] (Fig 4.12).

It is not surprising that the stomach is the likely target organ of crabs fed mussels laden with Ce. It is entirely possible that the Ce measurements are simply from yet-to-be-digested mussel that the crab has eaten. It would be worth attempting to examine digestion across more timepoints to gain a better understanding of transit of NPs through the digestive system. Of more interest is that the hepatopancreas also contained significantly elevated Ce, proving that these CeO_2 NPs are able to breach the filter press. Feeding of *C. maenas* on *M. edulis* laced with colloidal gold has shown particles less than 100nm entering the hepatopancreas (Hopkin and Nott 2009). However the authors found no evidence of these particles entering epithelial cells, and in fact these particles were eventually removed from the hepatopancreas within 48 hours and later found in the faeces. It is noteworthy that particles <100nm were egested up to 5 days after initial consumption (when they were fed again). This suggests that their residence in the digestive organs is dictated by how often the crab feeds, and subsequently removes, waste.

In comparison, experiments feeding plastic microspheres (8-10 μm) to *C. maenas* has shown their presence in the foregut and faecal pellets up to two weeks after consumption, and up to 6 times longer than normal food particles (Watts *et al.* 2014). It was suggested that these microspheres may have become trapped in the setae guarding the filter press, hence increasing their residence time. It is possible that agglomerated NPs could also become trapped in this region, and demands further investigation. In terms of digestive rhythms, the hepatopancreatic, granule-containing R-cells are known to have a lifespan of up to 5 days. Taken together this shows that investigating gut and hepatopancreas concentrations over longer timescales are necessary to fully understand elimination.

Accumulation in the gills is surprising. If the crab was actively depurating Ce then there should be a greater burden in the ionic gills than the respiratory gills, yet there was no significant difference in burden. It was hypothesised that haemolymph may have transferred Ce from the hepatopancreas to the gills yet no additional Ce in the haemolymph was detected. It has previously been demonstrated that 500nm microplastics penetrated the haemolymph of *C. maenas* following trophic transfer experiments, and that their concentration was highest following 24 hours' digestion, but remained for days (Farrell and Nelson 2013) so evidence of Ce in the haemolymph should exist.

Following injection into the hepatopancreas, 100nm CdNPs have been shown to cause morphological effects, such as lesions, in the digestive tubules of the mud crab *Scylla olivacea* (Kavitha et al. 2013). This physical damage allowed haemocytes to invade the tubules, thus providing a mechanism by which NPs might enter the haemolymph – either directly or following haemocytic phagocytosis. The method of injection and the concentrations used (20mg Cd/kg crab) are somewhat excessive, but highlight that physical damage in the tubules could allow NPs to enter the haemolymph.

Based on this then the lack of detectable Ce in the haemolymph is surprising, but an unlikely source might provide evidence that particle size might dictate residence location: viruses. Injection of bacteriophages, proteins or the polio virus into the haemolymph of the crab *Callinectes sapidus* showed size-dependant accumulation, with bacteriophages becoming concentrated in the hepatopancreas, and proteins and the polio virus (about 30nm) concentrating in the gills (McCumber and Clem 1977). As haemolymph travels through the gills it passes branchial podocytes – fixed nephrocytes known to be involved in pinocytosis of haemolymph-based proteins, which might also drink in any nanoparticles in the fluid (Johnson 1987). If nanoparticles have breached the haemolymph it is possible that this explains why they might translocate to the gills. These podocytes are also found in the antennal gland, from where urine is excreted, and is also a depuration site for lead (Vogt and Quinitio 1994). Measurements of Ce in this gland or the urine were not taken, and this might be primary route of Ce depuration to examine in the future.

Regardless of podocytes, any Ce penetrating the haemolymph might be captured by phagocytic haemocytes, responsible for engulfment and removal of foreign objects. These phagocytes, once engorged, are known to clump in hemal spaces of low flow rate, or where there are tight corners, such as the gills, and this effect is known to occur as early as 6 hours (Smith and Ratcliffe 1980, Johnson 1987). The combined effects of branchial podocytes and clumping haemocytes might then explain why the gills are a hotspot for Ce accumulation. Haemolymph was sampled from the joint of the third walking leg, therefore if any haemolymph-based Ce is clumping in the gills, it might not be present in the sample. Attempts to extract gill haemolymph in future would shed better light on this subject.

One final reason why the gills might be a sight of accumulation is due to ecdysis, whereby the crab sheds the chitin layer on the gills during moult. The crab *Cancer irroratus* has been shown to actively accumulate iron at the base of its gills prior to the moult phase, which is then removed during ecdysis (Martin 1973). In order to understand whether such actions are applicable to the removal of Ce however would require long-term investigation whereby the moult phases of the test organisms are recorded. All crabs used in the experiment were red in colour and therefore late intermoult i.e. due to moult (Reid *et al.* 1997), so it is entirely feasible that removal via ecdysis might explain increased gill concentration.

Mussels fed 20mg of CeO₂NPs accumulated a total average of 818 ± 466 (SE) µg per mussel, or 15.1%. Crabs fed one of these mussels accumulated an average of 181µg, equivalent to 23% of the dose, or a Trophic Transfer Factor of 0.142 (±0.1 at 95% confidence interval) (Table 4.3). However much of this was in the stomach of *C. maenas* and subject to egestion, therefore the combined percentage accumulation of the hepatopancreas and gills was only 1.14%. Total percentage accumulation across the two trophic levels was only 0.17%. Initial concentrations were over 5-fold higher than the suggested regulatory limit, therefore at the regulatory limit this is likely to further reduce uptake. Again, these exposure levels are many-fold higher than anthropogenic inputs highlighting that in the natural world trophic transfer of CeO₂ is possible but exceptionally limited, and probably below detection limits.

Crab	Control Average	1	2	3	4	5	6	Exposed Average	S.E.
Stomach µg	0.19	330	250	356	70.6	63.4	34.4	184.1	59.2
Hepatopancreas µg	0.33	0.98	3.68	3.36	0.96	0.79	2.62	2.064	0.54
Respiratory Gills µg	0.06	0.48	12.8	5.51	0.98	0.82	2.87	3.912	1.94
Ionic Gills µg	0.05	0.47	16.5	3.46	0.98	0.39	1.13	3.815	2.57
Total µg	0.63	332	283	368	73.5	65.4	41.0	194	61.1
Total µg ex. Stomach	0.44	1.92	32.9	12.3	2.91	2.00	6.62	9.79	4.91
Average µg Ce Fed		818 ± 466 Std Error							
% Accumulation		41	32	44	9	8	5	23	7
(% excl. Stomach)		0.18	3.98	1.46	0.30	0.19	0.76	1.14	0.6
Dry Weight (g)	0.74	0.83	0.93	1.48	1.53	1.40	1.17	1.22	0.12
µg/g dry weight	0.84	401	305	250	48.2	46.6	35.2	181	64.7
µg Ce/g d.w. Fed		1269 ± 879 Std Error							
TTF (Crab/Mussel)		0.315	0.240	0.196	0.037	0.036	0.027	0.142	0.05
TTIF excl. Stomach		0.004	0.001	0.007	0.001	0.001	0.03	0.007	0.005
Faeces µg Ce		81.5	6.25	33.1	1.46	4.65	0.477	21.23	13.03
Mussel Remains		6.25	1029	103	68.1	102	94.9		

Table 4.3: Actual average cerium concentrations found in the various organs of exposed and control crabs having been allowed 24 hours to feed on a mussel exposed to 20mg/l NM-211 (10nm) CeO₂NPs

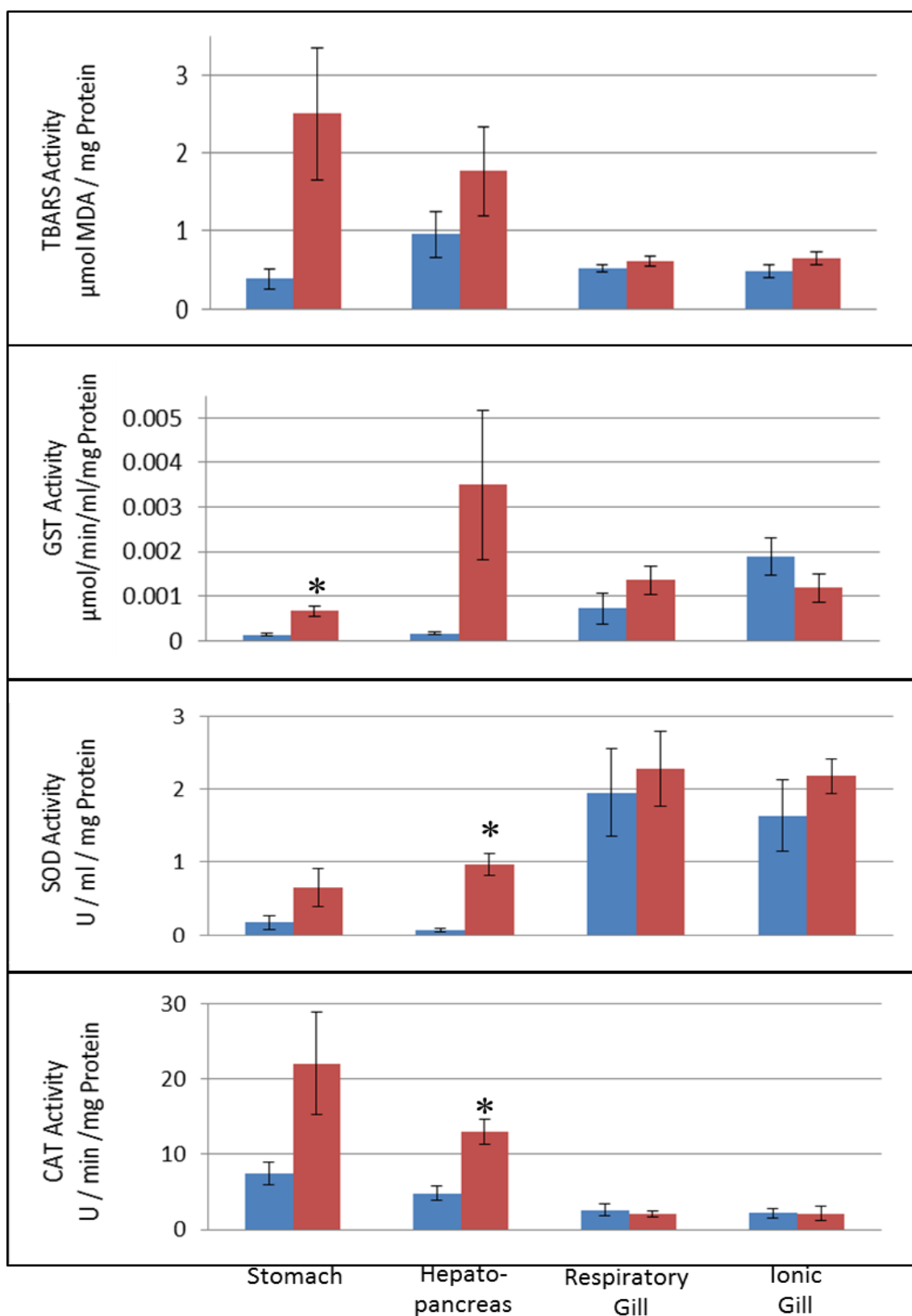


Fig 4.13: Oxidative Stress and Lipid Peroxidation in the Stomach, Hepatopancreas, Respiratory and Ionic Gill of *C. maenas* allowed 24 hours to consume a mussel (*M. edulis*) previously exposed to 20mg/l 10nm CeO_2NPs (NM-211). * = significantly different to control ($p < 0.05$) (control n=4, exposed n=6)

In terms of biological effects on lipid peroxidation, GST activity in the stomach of crabs consuming exposed mussels was significantly higher than the control [t -test, $t(8)=-3.782$, $p=0.005$]. TBARS activity in the stomach was higher than the control, but not significantly [t -test, $t(8)=-1.995$, $p=0.081$]. This suggests minor pro-oxidative stress and is surprising since the stomach wall is composed of a layer of semi-permeable chitin with little lipid content, whilst the epidermis below that contacts the haemolymph is rich in lipids (Morris and Tentori 1985). It has already been suggested that insoluble CeO₂ cannot cross the chitinous borders and therefore the lipid peroxidation is unlikely to be from interaction with the stomach epithelium. It is possible however that effect is actually an artefact of the interference of CeO₂NPs with the consumed mussel tissue. Experiments in Chapter 3 showed few biological effects of CeO₂NPs on mussels at 3mg/l, however this experiment was performed at 20mg/l, and therefore potential exists for such high concentrations to cause oxidative stress or lipid peroxidation in *M. edulis*.

Despite lower Ce concentrations than in the stomach, in the hepatopancreas SOD activity was significantly higher in crabs consuming exposed mussels [t -test, $t(8)=-4.765$, $p=0.001$], as was CAT activity [t -test, $t(7)=-4.0$, $p=0.005$]. This again suggests minor pro-oxidative stress, and a measured response from the crab. Again, increases in CAT activity often accompany increases in SOD activity due to the production of H₂O₂ as a by-product of superoxide conjugation (Halliwell and Gutteridge 2007). There was a similar magnitude of increase in GST activity, although variability in the data precluded this from significance.

Since Ce concentrations in both the stomach and hepatopancreas were significant then it is not surprising that significant biological effects occurred in both tissues, although given the extent of accumulation in the stomach it might be expected to have undergone a greater suite of oxidative stress-based effects. Most important however is the fact that effects are occurring in the hepatopancreas. This highlights that these particles are able to breach the filter press and subsequently interact with tissues in the digestive gland.

Significant increases of up to 300% in SOD, CAT and GPx activity for 8 days have been noticed when the hepatopancreas of the mud crab *Scylla olivacea*

was injected with 100nm CdNPs at concentrations of 20mg Cd/kg crab (Kavitha *et al.* 2013). The authors suggested an increased anti-oxidant defence response as the reason for these increases. The wide suite of effects was probably due to the high concentration of CdNPs injected into the hepatopancreas, thereby negating the mediation provided by the stomach, which will limit access to the hepatopancreas.

Despite significant accumulation of Ce, trophic transfer of CeO₂NPs had no effect on oxidative stress or lipid peroxidation in either the respiratory or ionic gills. Although it cannot be directly compared, in the previous aqueous exposure experiment oxidative stress in the gills did not occur until Ce concentrations reached above 200 µg/g dry weight. In this experiment average concentrations were around 40µg/g therefore it is possible that biological effects are not instigated until a higher concentration. It is also possible that NPs in the gill tissue are clumped in haemocytes, podocytes, or even granules, and that this might limit their effects.

4.6 Conclusion

In this chapter it has been shown that the gills, stomach and hepatopancreas of *C. maenas* accumulate nano-CeO₂ to a greater extent than micro-CeO₂ during acute immersed exposure, with the gills accumulating Ce to a much greater extent than the other organs. However total accumulation was less than 5% of the dose, suggesting limited scope for bioaccumulation, and this total is likely to be less if the gill burden is not internalised. Micro-CeO₂ has a transitory anti-oxidant effect, whilst nano-CeO₂ has a transitory pro-oxidant effect.

In emersed trophic transfer experiments *C. maenas* was able to accumulate Ce following consumption of *M. edulis* exposed to CeO₂NPs, however with Trophic Transfer Factors at 0.66 (±1.1) and below, this suggests biomagnification is unlikely, and the TTF is likely to reduce based upon digestive rhythms and removal through faeces. The stomach was the organ of greatest accumulation however some particles were able to reach the gills despite removing

contamination as an avenue of uptake. Biological effects were limited to increased SOD and CAT activity in the hepatopancreas.

It has not been possible to compare the accumulation and effects of CeO₂NPs and micro-CeO₂ from trophic transfer in this experiment, due in part to the unpredictability of crabs actually feeding which led to lack of available suitable size test crabs. Experiments earlier in this thesis showed that micro-CeO₂ did not accumulate to the same extent in *M. edulis* as CeO₂NPs do. As such the total Ce content that could be transferred from mussel to crab will be limited. Given that trophically transferred CeO₂NPs caused no significant biological effects in the gills, and few in the digestive organs, then it is highly unlikely that a reduced intake of micro-CeO₂ would have a greater effect, especially since it generally had an anti-oxidant effect in *M. edulis*. As such it can be proposed that CeO₂NPs have a size-related effect on the biological processes of higher trophic organisms, yet the root of this effect is the reduced uptake of larger particles from lower trophic organisms.

From an environmental release perspective, the limited effects following immersed exposure at the proposed regulatory limit (3mg/l) suggest that current levels of anthropogenic input (< ng/l) will have limited impact on *C. maenas*. Similarly, the trophic transfer exposures occurred at concentrations much higher than the proposed limit with only marginal oxidative stress, so anthropogenic inputs would need to increase many-fold before regulations are needed. Based upon the fact that some biological effects did occur however, the suggested regulatory limit does not feel sufficient to adequately protect Crustacea from anthropogenic Ce in the future. It is therefore proposed that future studies should further examine oxidative stress markers at concentrations below 3mg/l.

Chapter 5: Use of Isotopically-labelled $^{140}\text{CeO}_2\text{NPs}$ in Trophic Transfer Experiments

5.1 Abstract

High natural background concentrations of Ce in both *C. maenas* and *M. edulis*, coupled with low uptake during exposure, have necessitated trophic transfer experiments at concentrations far above environmental relevance. To address this issue, collaboration with Imperial College London has produced non-radioactive, isotopically-labelled $^{140}\text{CeO}_2\text{NPs}$ (2nm), provided in 6K MW dextran (4mg/ml). Artificially increasing the ratio of one isotope allows enhanced concentrations to be measured by measuring the ratios of the isotopes, as opposed to total increases in concentration.

In exposures of 100µg/l of $^{140}\text{CeO}_2\text{NP}$, *M. edulis* accumulated 512ng ^{140}Ce - 1.9% of the dose - over 4 hours. The gills and digestive gland were the major organs of accumulation. In terms of oxidative stress and lipid peroxidation, the dextran coating alone was found to have a greater suite of effects than the $^{140}\text{CeO}_2\text{NPs}$, including significantly increased mantle SOD and significantly depressed digestive gland GST and mantle TBARS activity.

Feeding exposed mussels to *C. maenas* in dry conditions showed the stomach as the major organ of accumulation, yielding Trophic Transfer Factors of 0.12 including, and 0.03 excluding, the stomach. There is evidence of these $^{140}\text{CeO}_2\text{NPs}$ being accumulated in the crab's hepatopancreas. There was evidence of increased ^{140}Ce in the haemolymph which might explain how accumulation in the gills was also significant, despite having no direct connection to the digestive organs. The $^{140}\text{CeO}_2\text{NPs}$ had no statistically significant effect on oxidative stress or lipid peroxidation in any organ following trophic transfer.

5.2 Introduction

In the previous chapter it was discovered that CeO₂NPs can be trophically transferred from the mussel *M. edulis* to the crab *C. maenas*. Due to high background levels and limited accumulation by both predator and prey, it was necessary to use high initial concentrations (20mg/l) that were beyond those that could be deemed either environmentally relevant ($\leq 1\mu\text{g/l}$, Keller & Lazareva 2014) or close to the suggested regulatory limit ($\leq 3\text{mg/l}$, O'Brien & Cummins, 2010).

Results so far have shown that *M. edulis* will accumulate less than 5% of any offered dose of CeO₂NPs (Chapter 3), whilst the gills and hepatopancreas of *C. maenas* accumulated on average only 1.14% of a 20mg CeO₂NPs/l dose following trophic transfer (Chapter 4.5). Of this, only 26.9% was attributed to the hepatopancreas, making the accumulation by the hepatopancreas just 0.0001% of the original dose. Extrapolating from this, a 100 $\mu\text{g/l}$ initial dose – closer to, but still 100-fold higher than the maximum suggested anthropogenic input – would yield concentrations in the hepatopancreas of only 0.1 μg Ce. Given average hepatopancreatic background control values of 0.33 μg Ce (Chapter 4.5), this would render any experimental-based increases in the hepatopancreas as undetectable against background concentrations.

This issue was addressed by Larner & Rehkamper (Larner and Rehkamper 2012) who were looking to expose aquatic organisms to ZnONPs. They highlighted concentration detection can carry a 10% degree of uncertainty, whilst background concentrations of zinc could also vary by 10%. This means that for reliability, ecotoxicology experiments should ideally use concentrations that result in uptake 10-fold greater than background concentrations. In the case of Zn, background levels of around 10 $\mu\text{g/g}$ in soft tissues, and 50-200 $\mu\text{g/g}$ in sediments has resulted in various authors exposing *D. magna* at concentrations of 100mg/l; far exceeding the expected environmental concentrations of 50-500 $\mu\text{g/l}$ and the US EPA limit of 80 $\mu\text{g/l}$. Whilst this may be useful for understanding partitioning of uptake of Zn in soft tissues, in terms of understanding biological effects in real-world scenarios the concentrations used become irrelevant.

It was realised that these problems might be overcome by measuring changes in the isotopic ratios of Zn. Stable isotopes occur in nature in natural ratios, with zinc found as five stable isotopes: ^{64}Zn (49.1%), ^{66}Zn (27.7%), ^{68}Zn (18.5%), ^{67}Zn (4%) and ^{70}Zn (0.6%). By exposing an organism to a nanoparticle crafted exclusively from one isotope, any accumulation would therefore alter its abundance ratio in the organism compared to the other isotopes. The difference between expected and observed ratios would therefore determine how much of that specific isotope has been accumulated. It is worth mentioning that these ratios can differ naturally however depending on a number of factors; in the case of oxygen for example, ^{16}O evaporates at a faster rate than ^{18}O therefore organisms in higher temperature water tend to have a higher percentage of ^{18}O (Miller *et al.* 1987). Similarly ^{15}N is retained by organisms to a greater extent than ^{14}N , thereby allowing researchers to estimate an organism's position in trophic food webs (Hansson *et al.* 1997). As such it is useful to first establish a control baseline of isotopic ratios for the element and organism under study.

Larner & Rehkamper (2012) calculated that manufacturing ZnONPs from the low-cost and widely available ^{68}Zn isotope and comparing its ratio to that of ^{67}Zn would allow for a detectable increase in ^{68}Zn of 5ng/g against a background concentration of 100µg/g zinc. These ^{68}Zn particles were later used in exposures of $^{68}\text{ZnONPs}$, micro- ^{68}ZnO and $^{68}\text{ZnCl}_2$ to the mudshrimp *Corophium volutator* (Larner *et al.* 2012). Use of this technique further allowed the authors to distinguish ^{68}Zn accumulated in the nanoparticulate phase to that accumulated through nanoparticle dissolution. Performing dissolution experiments with the particles yields a specific ratio of enhanced ^{68}Zn in the water column. In subsequent uptake experiments, should the organism yield similar or lower ratios to those of the dissolution experiments, then it is likely that uptake has occurred through the aqueous phase. If the ratio is greater than expected from dissolution, this suggests that the organism has accumulated ^{68}Zn through particulate uptake. This becomes paramount when attempting to distinguish between toxicity caused by dissolution and that caused by direct uptake of the nano-form, and allows for better prediction of uptake and toxicity

in media of differing ionic strength, whereby agglomeration might limit dissolution.

In similar collaboration with Mark Rehkamper at Imperial College London, isotopic nano- $^{140}\text{CeO}_2$ ($^{140}\text{CeO}_2\text{NPs}$) particles have been manufactured, nominally 2nm and coated in dextran (as detailed in Chapter 2.1.2). Of the four stable isotopes of Ce (^{136}Ce , ^{138}Ce , ^{140}Ce , ^{142}Ce), ^{140}Ce is the major isotope accounting for around 88% of all Ce, whilst ^{142}Ce accounts for around 11% (De Laeter *et al.* 1991). Use of pure ^{140}Ce in manufacture of these NPs would therefore skew the ratio of ^{140}Ce : ^{142}Ce . Measuring this change in ratio of Ce in crabs fed NP-exposed mussels gives an accurate value of Ce accumulation even when background levels might mask absolute changes e.g. in the hepatopancreas, gills and haemolymph.

The ratio of 11% ^{142}Ce : 88% ^{140}Ce can be reduced to a ratio of 1:8. In its simplest form, this calculation of change in concentration works as follows:

- Following exposure to ^{140}Ce , an organism contains 9ng ^{142}Ce and 81 ng ^{140}Ce . This is a ratio of 1:9.
- Based on the isotopic ratio of 1:8, it would be expected that a control organism containing 9ng of ^{142}Ce should actually contain 72ng of ^{140}Ce
- The difference between the ^{140}Ce values of the control and exposed organisms thereby dictates how much extra ^{140}Ce the organism has accumulated. In this example, $81\text{ng}-72\text{ng} = 9\text{ng}$ accumulated from the exposure.

Experiments in the previous chapter showed that the gills of *C. maenas* were a major site of CeO_2NP accumulation during air-fed exposures, yet it was not apparent how and why they accumulated there. It is known that crabs have both ionic and non-ionic gills with the ionic gills heavily involved with ion depuration (Crothers 1967), and it is also thought that haemocytes naturally agglomerate in the gills and tight hemal spaces once they engulf particles that have entered the haemolymph (Johnson 1987). The nano-size of these new $^{140}\text{CeO}_2\text{NPs}$ (2nm) means they have more potential to cross tissue and cell barriers and possibly into the haemolymph (Farrell and Nelson 2013). This new

technique of using isotopic ratios will also be able to identify enriched Ce within the haemolymph against what have so far been shown to be highly variable background concentrations. If Ce is entering the haemolymph then this will conclusively explain how organs with no connection to feeding are able to accumulate nanoparticles, and poses interesting questions as to what other organs the NPs may be distributed.

This experiment aims to study trophic transfer of CeO₂NPs from the mussel *M. edulis* to the crab *C. maenas* by use of nanoparticles manufactured from a natural isotope of Ce, ¹⁴⁰Ce, at concentrations towards environmental relevance. Due to the novel nature of the particle, this study will also examine the potential for ¹⁴⁰CeO₂NPs to cause biological effects (oxidative stress, lipid peroxidation) in both predator and prey. In previous studies in this thesis, initial exposure concentrations of 20mg CeO₂NPs/l resulted in only minor oxidative stress in *C. maenas* following trophic transfer. It is therefore predicted that initial exposure concentrations of only 100µg/l are unlikely to instigate any biological effects in *C. maenas*.

The hypotheses of this experiment are that *M. edulis* will accumulate ¹⁴⁰CeO₂NPs, and that these will be trophically transferred to *C. maenas*. These particles will subsequently penetrate the stomach, hepatopancreas, gills and haemolymph of *C. maenas*, but they will cause no significant effects on biological processes in either organism.

5.3 Method

Nanoparticles were manufactured at Imperial College London using ^{140}Ce . Particles measured an average 1.86 ± 0.43 nm (Chapter 2.1.2). $^{140}\text{CeO}_2\text{NPs}$ were provided at a concentration of $150\mu\text{g/ml}$ in a solution containing dextran (6,000 Da molecular weight) at 4mg/ml , and vortexed for 2 minutes before use.

M. edulis (average. 5.5cm. 21g), were exposed as per Chapter 2.3.3. Control mussels (n=18) were exposed to algae only. Exposed mussels (n=18) were exposed to algae and $^{140}\text{CeO}_2\text{NPs}$ at a concentration of $100\mu\text{g CeO}_2/\text{l}$ (i.e. $33.33\mu\text{g}$ total). A dextran-control was used to provide comparison between biological effects caused in *M. edulis* by the $^{140}\text{CeO}_2\text{NPs}$, and those potentially caused by its dispersant. Dextran-control (n=8) mussels received algae and an equivalent dose of dextran only. Exposure time was 4 hours. After this, 8 mussels from each group were dissected for Ce accumulation analysis and biological effects. 10 mussels from each of the control and exposed groups were opened and fed to crabs.

C. maenas (Control average $29.1 \pm 1.9\text{g}$; Exposed average $33.7 \pm 1.7\text{g}$) were acclimated and fed mussels as per the emersed exposure experiment in Chapter 4.5. Each crab was offered either a control or exposed mussel, opened and scraped, and allowed 24 hours to feed in a darkened environment. Following this time crabs, and any waste materials, were removed and dissected for analysis of Ce accumulation and biological effects. 10 crabs were used for each treatment.

Tissues were dissected and freeze-dried as per Chapter 2.2. Acid digestion of tissues and analysis of ^{140}Ce content of tissues was performed by Imperial College, London. Biological effects assays (TBARS, SOD, GST, CAT) were performed on tissue supernatant extracted as per Chapter 2.2.3 and statistical analysis performed as per Chapter 2.2.4.

5.4 Results and Discussion

5.4.1 Accumulation of $^{140}\text{CeO}_2\text{NPs}$ in *M. edulis* and subsequent Biological Effects

Table 5.1 details the extra enriched concentrations of Ce found in the various compartments of *M. edulis* following exposure, and concentrations per gram dry weight. It was intended that 8 mussels were analysed for each treatment, however due to technical problems in the collaborators' laboratory, not all the replicates have yet been analysed. Exposed data is limited to $n=4$ for all tissues, and control data ($n=4$) is only available for the mantle.

Organ	Actual ng Enriched ^{140}Ce		ng Enriched $^{140}\text{Ce/g}$ dry weight	
	Control \pm SE	Exposed \pm SE	Control \pm SE	Exposed \pm SE
Gill (4)	d/d	209.8 \pm 48.8	d/d	2485 \pm 477
Digestive Gland (4)	d/d	291.8 \pm 52.6	d/d	1668 \pm 310
Mantle (4)	0.106 \pm 0.051	10.98 \pm 3.98	0.559 \pm 0.037	43.87 \pm 11.99*
TOTAL	d/d	512.49	d/d	860.1
% Accumulation	-	1.91%		
Pseudofaeces (6)	-	323.8 \pm 91		

Table 5.1: Mean Cerium concentrations in the gill, digestive gland and mantle of *M. edulis* following exposure to 100 $\mu\text{g/l}$ 2nm $^{140}\text{CeO}_2\text{NPs}$. (X) = n-number. d/d = data deficient. (*) = significantly higher than control ($p < 0.05$).

From available data, it was found that exposed mantle tissue contained significantly more enriched Ce than unexposed mantle tissue [Mann-Whitney U-test: $U=0$, $p=0.021$. Control data was found to be non-normal, even following log transformation (Shapiro-Wilk: $p=0.011$), hence a non-parametric test was used].

There was also significant variation between exposed tissues [one-way ANOVA: $F(2,9)=14.315$, $p=0.002$], with mantle tissue containing significantly less ^{140}Ce than either the gill (Tukey's HSD: $p=0.001$) or the digestive gland (Tukey's: $p=0.017$), but no difference between gill and digestive gland concentration (Tukey's: $p=0.237$).

In terms of control data, technically there should be no – or, at worst, negligible – evidence of enriched ^{140}Ce . Given the volume of enriched ^{140}Ce found in the gill and digestive gland then it is entirely likely that *M. edulis* has taken up

significant amounts on $^{140}\text{CeO}_2\text{NPs}$, however this cannot be proved statistically at this time

In terms of concentration, the digestive gland was the major organ of $^{140}\text{CeO}_2\text{NP}$ accumulation (292ng), followed by the gill (210ng) and mantle (11ng). This yielded a total of 512.5ng per mussel, or 860.1ng Ce/g dry weight. Each mussel was exposed to 100 μg $\text{CeO}_2\text{NPs/l}$, equivalent to 33 μg of CeO_2NPs per dose, or 26.87 μg Ce. This results in an assimilation efficiency of 1.91%, slightly lower but similar to the 5% shown in previous chapters for *M. edulis* exposures to CeO_2NPs , and by Montes *et al* (2012). In previous experiments however it is the stomach that has been shown as the major accumulator of CeO_2NPs , responsible for roughly 95% of the total body burden, and similar to values reported by Montes *et al* (2012). Here the value is closer to 57%, with the gill accounting for 40%. Again, this is in contrast to previous experiments where the gill and mantle concentrations were similarly low, yet is similar to the background ratios of Ce in the organism.

Whilst exposed mussels accumulated an average 512ng ^{140}Ce , it was also found that they rejected on average 324ng ^{140}Ce into pseudofaeces, equivalent to around 40% of the total processed. This value is lower than the 95% reported by Montes *et al* (2012) following CeO_2NP exposure, and might be related to the concentrations used. This experiment was performed at 100 $\mu\text{g/l}$ compared to the 1-10 mg/l by Montes *et al* (2012). They posited that at lower concentrations mussel handling ability would be less impaired, with fewer particles sent directly to pseudofaeces since the mussel is not saturated. The reduced accumulation in this experiment would lend weight to this theory, as would the effect of dextran in reducing agglomeration. If these particles do not agglomerate as quickly to a size where they can be captured, then there would be less pseudofaeces production. It would be useful to vary the exposure concentration in future experiments to understand if this has an effect of pseudofaeces production.

Unlike the JRC particles used in the previous chapters, the $^{140}\text{CeO}_2\text{NPs}$ used here have not undergone extensive characterisation, and therefore data such as agglomeration speed, zeta potential and surface charge is unknown. Such

characteristics will determine the methods of interaction of the particles with anything else in the water column. The dextran coating for example might affect their ability to adhere to algal cells, mantle surface, or even the exposure beakers, thereby altering potential availability (Baalousha 2009). Similarly if the particles do not agglomerate quickly, being only 2nm they have more potential to be accumulated during pinocytosis by gill epithelial cells (George *et al.* 1976). Given that the partitioning seen here is depressed in the digestive gland and increased in the gills, it is speculated that the dextran coating has prevented the agglomerative and adhesive properties of the $^{140}\text{CeO}_2\text{NPs}$, thereby reducing their ability to adhere to algal cells or be directly captured as agglomerates. In retaining their small size they can therefore be pinocytosed or endocytosed by epithelial gill cells. However this speculation would require further data which was not available for inclusion in this thesis for technical and procedural reasons.

In terms of biological effects (Fig 5.1), for the mussels exposed to dextran-only a one-way ANOVA [$F(2,21)=3.62$, $p=0.045$] with Tukey's post-hoc test ($p=0.039$) highlighted a significant reduction in TBARS activity in the gill as compared to the control. This was also true of reduced GST activity in the digestive gland [one-way ANOVA: $F(2,21)=3.757$, $p=0.04$; Tukey's HSD: $p=0.041$], and increased SOD activity in the mantle [t -test: $t(14)=-3.424$, $p=0.004$].

For those mussels exposed to $^{140}\text{CeO}_2\text{NPs}$, the trend in biological activity was similar to that of dextran-only and indeed there were no significant differences in biological activity between $^{140}\text{CeO}_2\text{NP}$ -exposed and dextran-only exposed mussels. However there were also no significant differences between those exposed to $^{140}\text{CeO}_2\text{NPs}$ and the control mussels.

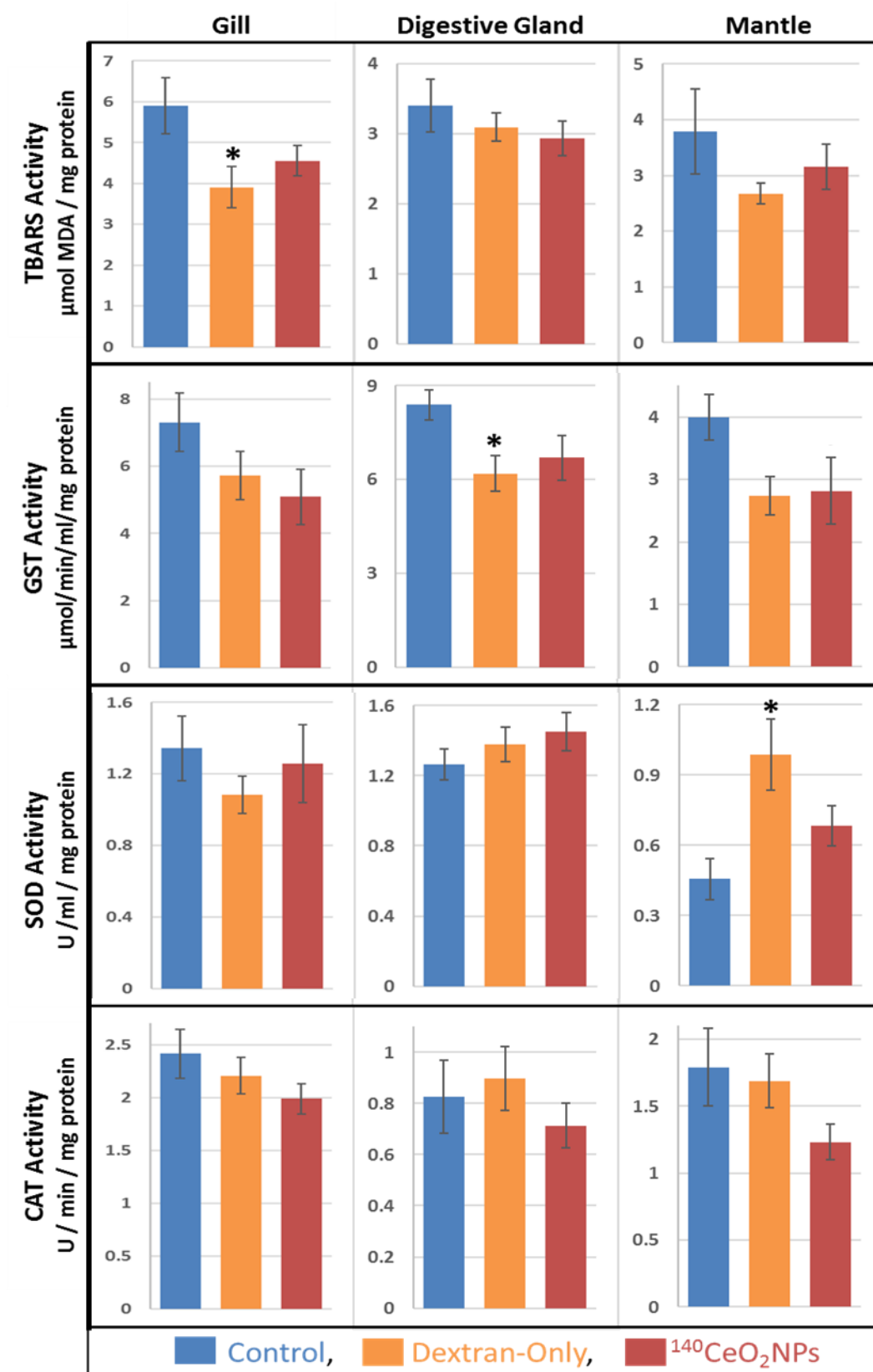


Fig 5.1: Differences in TBARS, SOD, GST and CAT activity (mean \pm SE) between unexposed *M. edulis*, and those exposed to dextran or 2nm ¹⁴⁰CeO₂NPs for four hours (n = 8 per treatment). * = significant difference from control

The significant reduction in TBARS and GST activity might suggest that dextran is having a protective effect against lipid peroxidation, since both assays can be indicative of this (Lovell *et al.* 1998). Alternatively it suggests a negative effect, with GST activity reduced due to either depletion through direct conjugation with, for example, the hydroxyl free radical (Howie *et al.* 1990), or as a side effect of depleted GSH (Carlson *et al.* 2008). The significant increase in SOD activity caused by dextran indicates a pro-oxidative effect (Halliwell and Gutteridge 2007) and suggests that dextran alone is having an adverse effect on *M. edulis*. CeO₂ might act as an anti-oxidant since valence switching at the surface can neutralise, for example, the superoxide free radical (Heckert *et al.* 2008). Here it appears there is some evidence that CeO₂ is able to mediate pro-oxidant effects of dextran, yet further testing is required to conclusively prove the relationship. Dextran-coated CeO₂NPs have previously been shown to be scavengers of ROS (Gupta *et al.* 2016) hence such an anti-oxidant effect is feasible.

Introduction of dextran-coated CeO₂NPs into cultures of cancerous osteosarcoma cells has resulted in significantly decreased cell viability after 24 hours with 0.1M and 0.01M dextran, and with Ce concentrations of 100µg/l (Yazici *et al.* 2015). At day three however only 0.1M dextran significantly and sequentially reduced cell viability at concentrations above 250µg Ce/l, with 0.01M dextran slightly reducing viability at concentrations above 500µg Ce/l. At lower concentrations cell viability actually increased after 3 days. This shows that dextran concentration can change the toxicity of CeO₂NPs. The original purpose of the Yazici (2015) study was to understand if dextran-CeO₂NPs could kill cancer cells, however without a non-cancerous control it is impossible to tell if the particles they used would have similarly affected viability of healthy cells. They also did not use a dextran-only control, therefore it is unknown if the dextran or the nanoform was more responsible for the effect, although they did posit that increased mono-dispersity of the 0.1M dextran-coated particles might have been responsible for the effect.

In a later study (Alpaslan *et al.* 2015) it was found that 0.1M dextran-coated 5nm CeO₂NPs were more effective at killing bone cancer cells at pH 6, with minimal impact on viability of non-cancerous cells. There was less effect on

either cell type at pH 7 or 9. Healthy cells did show reduced viability when treated with CeO₂NPs at concentrations above 250 µg/l, although again viability was still 3-fold higher than cancerous cells. This contrasts with the results presented here which were performed at pH 8.1, with significant effects seen at 100µg/l CeO₂NPs. The digestive gland of *M. edulis* is around pH 6.5 (Langton 1977), yet there is only one significant effect shown regarding reduced GST, and again only with dextran. Alpaslan et al (2015) suggested an 'oxidase-like' activity of their particles at lower pH, perhaps producing, rather than scavenging hydrogen peroxide, to explain pH differences. They also suggested that lower pH increased positive charge on the particles, making them more attractive to negatively-charged cell membranes. In this way the effect of particle surface charge might influence their biological effects. Again, without a dextran-only control for their study, it is unknown if the coating had more impact than the particle.

In support of the work detailed above, the authors showed the ability of their particles to scavenge ROS in human dermal fibroblast cells exposed to H₂O₂ (Alpaslan *et al.* 2016). Cell viability was maintained or increased up to concentrations of 1mM H₂O₂ at concentrations of 500µg CeO₂NPs/l, although higher concentrations of CeO₂NPs actually decreased viability. In particular increased cellular ROS generation was linked to decreased viability. This suggests that reduced GST activity in this study might well be an anti-oxidant effect as the CeO₂NPs scavenge free radicals that might require either GST or GSH conjugation, although reduced SOD activity might also be expected if this were the case.

5.4.2 Trophic Transfer of $^{140}\text{CeO}_2\text{NPs}$ from *M. edulis* to *C. maenas*, and subsequent Biological Effects

Table 5.3 provides a comprehensive list of the enriched ^{140}Ce concentrations available, as found in *C. maenas* following consumption on exposed mussels. Only 1 of the 10 control organisms have been partially analysed and, of the 8 of 10 exposed crabs analysed, data is not available for 7. The available data has been used to estimate assimilation efficiency, and this ranges from 0.44% to 86% including the stomach. Excluding the stomach reduces this from 0% to 15%, depending on the organism. Certain assumptions have been made, including basing calculations on an average amount of Ce fed to each crab, rather than the actual amount based on uptake variability of each mussel.

Table 5.2 details the average concentrations of Ce found in the various compartments of *C. maenas* following consumption of *M. edulis*, and concentrations per gram dry weight. As detailed above, not all data is available for every crab, hence the n-number used for average calculations in each case has also been highlighted.

Organ (<i>n</i> -number: Control, Exposed)	Actual ng Enriched ^{140}Ce		ng $^{140}\text{Ce/g}$ dry weight	
	Control \pm SE	Exposed \pm SE	Control \pm SE	Exposed \pm SE
Stomach (1,8)	1.5	129.7 \pm 48.4	11.85	724 \pm 167
Hepatopancreas (0,1)	d/d	9.53 \pm 6.44	d/d	16.6 \pm 11.2
Respiratory Gill (2,7)	0.006 \pm 0.004	1.11 \pm 0.44	0.28 \pm 0.1	11.55 \pm 4.79*
Ionic Gill (1,6)	0.516	9.5 \pm 6.96	5.92	108.3 \pm 69.8
Haemolymph (0,1)	d/d	0.077	d/d	4.241
TOTAL	-	149.92	-	166.9
AE % (inc/ex stomach)		29.3 / 3.95		

Table 5.2: Mean Cerium concentrations in the stomach, hepatopancreas, gills and haemolymph of *C. maenas* following consumption of *M. edulis* containing c. 512.5ng Ce. (X) = n-number. d/d = data deficient. (*) = significantly higher than control ($p < 0.05$, *t*-test). AE = Assimilation Efficiency. TTF = Trophic Transfer Factor

	Crab*								
	Control 1	Ex 1	Ex 2	Ex 3	Ex 4	Ex 5	Ex 6	Ex 7	Ex 8
Ave Fed		512.49							
Remains	2.00	99.64	206.01	163.04	D	201.89	300.02	D	D
Total Fed		412.85	306.48	349.45	512.49	310.60	212.47	512.49	512.49
Stomach	1.50	81.94	162.73	79.16	22.40	1.22	112.26	137.43	440.71
Hepatopancreas	D	9.53	D	D	D	D	D	D	D
Respiratory Gill	0.01	2.40	2.40	1.08	0.16	0.08	2.47	0.47	D
Ionic Gill	0.52	5.24	43.90	5.94	0.03	0.07	1.83	D	D
Heamolymph	D	0.08	D	D	D	D	D	D	D
Total	2.02	99.19	209.03	86.18	22.59	1.37	116.56	137.90	440.71
AE %	-	24.03	68.20	24.66	4.41	0.44	54.86	26.91	85.99
AE ex Stomach %	-	4.18	15.11	2.01	0.04	0.05	2.02	0.09	0.00

Table 5.3: Actual cerium values (ng) found in *C. maenas* following consumption of *M. edulis* exposed to 100µg/l 4nm ¹⁴⁰CeO₂NPs for 4 hours. AE = Assimilation Efficiency (= ng Fed/ng Recovered). D = Data deficient. *data only available for 1/10 control crabs, and 8/10 exposed crabs.

The results show that ^{140}Ce concentrations in the stomach were significantly higher than both the respiratory gill [t -test: $t(7.009)=4.253$, $p=0.004$ (equal variance not assumed; Levene's: $p=0.017$)] and the ionic gill (Mann-Whitney U-test: $U=5$, $p=0.014$. Ionic gill data found to be not normal even following log transformation, hence use of a non-parametric test). Despite averages in the ionic gill being nearly 10-fold higher than the respiratory gill, there was no significant difference (Mann-Whitney U-test: $U=12$, $p=0.199$). There was also evidence of increased ^{140}Ce in the haemolymph of exposed crabs, giving weight to the theory that the haemolymph is responsible for distributing Ce to non-digestive organs of the crab. Including the stomach, there was an average of 29.3% transfer of Ce from mussel to crab. Excluding the stomach this equates to 3.95% transfer.

From the available data it has only been possible to analyse significant difference between enriched ^{140}Ce concentrations in the control and exposed respiratory gill (control $n=2$, exposed $n=7$), and significantly more ^{140}Ce was found in the respiratory gills of those crabs eating exposed mussels [t -test: $t(6.006)=-2.953$, $p=0.025$ (equal variance not assumed; Levene's: $p=0.03$)]. This highlights that significant trophic transfer of 2nm $^{140}\text{CeO}_2\text{NPs}$ is occurring between *M. edulis* and *C. maenas*, and is penetrating into the gill tissues.

Crabs were fed a mussel containing 860.1ng Ce/g dry weight of mussel. Only one crab has had all four tissues analysed, yielding total concentrations of 106.5ng enriched ^{140}Ce /g including, and 21.6ng/g excluding stomach. Based on this single crab, this equates to Trophic Transfer Factors of 0.12 and 0.03 respectively. Again, these TTFs are far below 1, therefore biomagnification is not expected (Mathews and Fisher 2008).

In terms of biological effects, there was a trend to reduced SOD activity in both gill types, as well as increased SOD and GST, and reduced CAT activity, in the stomach (Fig 5.2). However, none of these trends were significant ($p > 0.05$, t -test, $df=18$) despite an n -number of 10 per treatment. The accumulation data suggests that crabs were in different stages in digestion when sacrificed, therefore the response to biological effects would not be as consistent. This would account for some of the variability in the results.

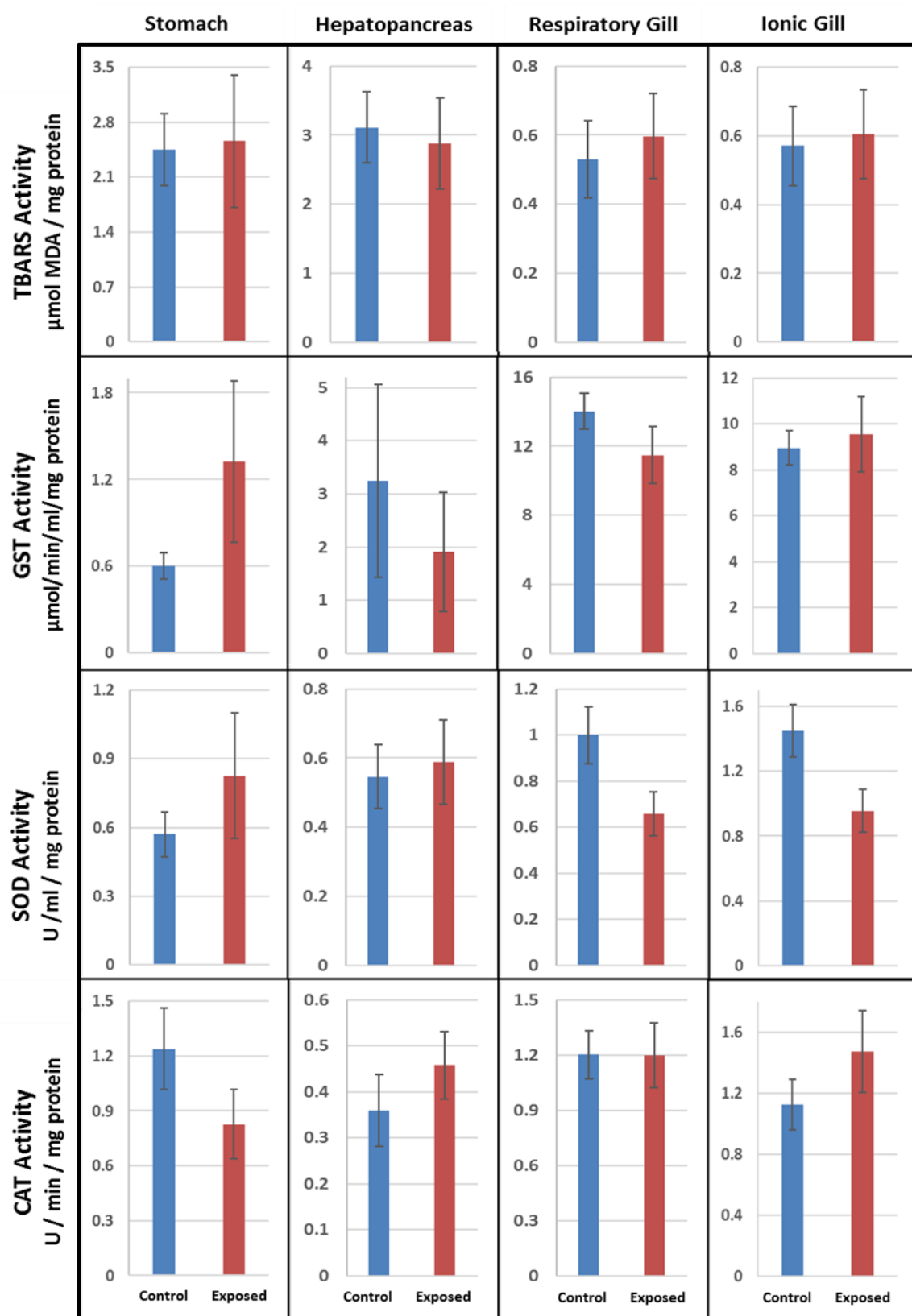


Fig 5.2: Differences in TBARS, SOD, GST and CAT activity in the organs of *C. maenas* following trophic transfer of 2nm $^{140}\text{CeO}_2\text{NPs}$ from *M. edulis* to *C. maenas* (n = 10 per treatment). No significant differences recorded. Blue = Control, Red = Exposed.

Another reason might be that nano-CeO₂ simply does not induce any significant biological effects at such low concentrations. It was shown in the previous chapter that 10nm CeO₂ had a mild pro-oxidative effect in the stomach and hepatopancreas of *C. maenas*, but little in other organs. The concentrations used in this experiment were 200-fold lower than previously used in trophic transfer experiments (100µg/l compared to 20mg/l) therefore it is unsurprising that so few effects have occurred. In terms of environmental relevance, this suggests that current estimated anthropogenic inputs (a minimum of 100-fold lower than the concentrations used here) are not of a level that would cause biological effects following trophic transfer.

5.5 Conclusion

This study is the first to use a metal nanoparticle, manufactured using a stable isotope, to prove trophic transfer between two marine organisms. This novel method allowed detection in organism tissues of increased levels of ¹⁴⁰Ce below natural general background levels, and at concentrations closer towards environmental relevance than have previously been feasible.

The results showed that *M. edulis* was able to accumulate 1.9% of a 33µg dose of 2nm dextran-coated ¹⁴⁰CeO₂NPs following 4 hours' exposure. Exposure to the dextran only had a greater impact on biological processes than the nanoparticles. Consumption of a ¹⁴⁰CeO₂NP-exposed mussel by *C. maenas* yielded a Trophic Transfer Factor of 0.12 including the stomach, and 0.03 excluding the stomach. Lack of data has prevented significant conclusions concerning accumulation, however there is some evidence that these ¹⁴⁰CeO₂NPs entered the gills, hepatopancreas and haemolymph of *C. maenas*, yet had no significant effects on biological processes.

Release of Ce is currently unregulated, hence it was proposed that a maximum limit of 3mg/l should be applied (O'Brien and Cummins 2010), similar to that for other benign materials. Based on the results seen in Chapter 4 concerning oxidative stress it was suggested that 3mg/l might not be sufficient to protect these mussels from oxidative stress following acute exposure. The results in

this chapter have yielded no oxidative stress effects from the $^{140}\text{CeO}_2\text{NPs}$ at only $100\mu\text{g/l}$ in the mussel, despite isolated biological effects following exposure to the dextran-only control. Further investigation is required regarding mussel recovery from acute exposure, as are the effects of longer term chronic exposures however, based on the results seen here, there is no need to suggest a further reduced limit for Ce release.

It is possible to speculate that $^{140}\text{CeO}_2\text{NPs}$ can be trophically transferred. This is important with regards to food webs, however given that the concentrations used were still many orders of magnitude higher than anthropogenic inputs, and that TTFs remained below 0.2 with no impact on biological effects in *C. maenas*, it is unlikely that any significant trophic transfer of CeO_2NPs will occur in the long-term future.

**Chapter 6: Comparisons in the Uptake Efficiency between
Silver Nanoparticles and Silver Nanorods by *M. edulis*, and
subsequent Biological Effects**

6.1 Abstract

The recent use of nano-silver as an antibacterial in commercial products will lead to an increase in silver concentrations entering our oceans. Whilst the likely fate of silver is dissolution and complex formation e.g. AgCl, the dissolution process itself produces H₂O₂ which can cause oxidative stress.

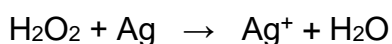
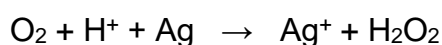
Here a 48-hour time series experiment demonstrated uptake by *M. edulis* of Ag-nanoparticles (AgNPs) and Ag-nanorods (AgNRs) at 10µg/l. Initially AgNPs were taken up mostly into the digestive gland within 8 hours and eliminated over the 48 hours, the mantle following a similar pattern. Gill accumulation was fastest in the first 8 hours, and likely through constant dissolution, however there was scant evidence of AgNPs instigating oxidative stress after 4 or 8 hours. AgNRs accumulated in the digestive gland within 2 hours but were quickly eliminated; despite this there were significant reductions in CAT activity in the digestive gland and mantle after 8 hours suggesting an overwhelmed OS defence.

Uptake and effects of AgNPs and AgNRs were compared to those of AgNO₃ (at 10µg Ag/l) and their nano-dispersants after 24 hours. Both AgNPs and AgNO₃ showed similar significant uptake profiles. AgNR uptake was not significant. AgNO₃ caused the greatest suite of effects on oxidative stress, and at no point were effects caused by either nanoform significantly more damaging than AgNO₃. Particle dispersants also appeared more damaging than either nanoform. The results suggest that in this experiment, silver dissolution is the main driver of Ag-nanoform toxicity however the dispersants might also play an important role.

6.2 General Introduction

Silver has long been used for its antibacterial properties (Jeong *et al.* 2005, Lee *et al.* 2005, Shrivastava *et al.* 2007) and such a characteristic has led to its recent inclusion, in nano-particulate form, in hundreds of consumer products including clothing, deodorant, sticking plasters and household linens (Luoma 2008). Washing these products leads to release of AgNPs into freshwater systems which will ultimately discharge to the marine environment (Benn and Westerhoff 2008). Maximum global production of AgNPs was estimated at over 400 metric tons in 2010 (Keller *et al.* 2013), just 1.2% of the 33,000 metric ton annual worldwide demand for silver (TheSilverInstitute 2016). Of the 400 metric tons of nanosilver, around 15% of this is expected to reach waterways.

The previous chapters in this thesis have focussed on CeO₂NPs as they are negligibly soluble at the neutral pH ranges of natural waters (Dogra *et al.* 2016), and therefore uptake and effects can be attributed, in theory, directly to nano-size, and not due to potential ion dissolution. However in the case of AgNPs they will dissolve to some extent in fresh- and seawater and therefore dissolution potential of Ag⁺ from the AgNP becomes important when assessing toxicity since Ag⁺ is involved in the production of peroxide radicals (Batley *et al.* 2012). Dissolution of silver is possible only with a strong oxidising agent. In the case of aquatic media, this is through dissolved oxygen in the water and therefore dissolved oxygen concentration is a strong mediating factor in silver dissolution. The following equations have been suggested (Liu and Hurt 2010):



In freshwater Ag⁺ will tend to form complexes with sulphur, but with increasing chloride content i.e. in marine waters, Ag⁺ will react with free chloride ions to produce AgCl (Liu *et al.* 2010). This can be useful in locking away free silver ions from direct uptake yet it is also believed that AgCl⁰ can be accumulated via diffusion due to its low polarity, thereby adding a vector for uptake by marine organisms (Luoma *et al.* 1995). Since the dissolution process still produces H₂O₂ as an intermediate, even if free Ag⁺ is quickly complexed there is still

potential for oxidative stress and lipid peroxidation (Liu and Hurt 2010). Dissolved silver may also interact and interfere with thiols, such as glutathione and cysteine, which are necessary for a number of cellular processes, including anti-oxidant defences and protein folding (Liu *et al.* 2010).

Area	ng Ag/l
Eastern Atlantic	0.03 – 1.04
North Atlantic	0.07 – 7.44
North West Atlantic	0.64 – 2.20
Texas Estuaries*	0.54 – 18.34
South Atlantic	0.13 – 3.42
North East Pacific	0.03 – 2.64
San Francisco Bay*	0.65 – 26.21
Southern California (So-Cal) Bight*	0.32 – 33.12
North Pacific (near Japan)	0.45 – 5.05
North Pacific	0.11 – 9.46
Southern Ocean	0.96 – 2.42

Table 6.1: Average Silver concentrations (ng Ag/l) for selected oceans, and (*) areas of known high anthropogenic inputs (Barriada *et al.* 2007)

Table 6.1 shows the concentrations of Ag found in various oceans, and those found in areas of high anthropogenic input. It is worth mentioning that Bay areas i.e. San Francisco and San Diego (in the So-Cal Bight) have limited ocean mixing and the highest anthropogenic inputs, hence nearshore Bay concentrations tend to be much higher. Average Ag concentrations in San Diego Bay have been measured at 20.3 ng/l compared to only 1.8 ng/l in proximal coastal waters just outside the Bay (Sanudo-Wilhelmy and Flegal 1992). Current EPA toxicity guidelines for the acute release of Ag into marine waters are only 1.9 µg/l (EPA 2009), extremely low compared to Zn (90µg/l) and Pb (210µg/l), but very similar to mercury (1.8µg/l), and over fifty times higher than the highest measurements take from the polluted So-Cal Bight.

Previously the 1976 UK Council Directive (76/464/EEC) for the Protection of Aquatic Life set interim guidelines of maximum allowable total dissolved silver in UK coastal waters at 1µg/l (EnvironmentAgency 2011). This was superseded by the EU Water Framework Directive (2000/60/EC) under which 33 Priority Substances (Directive 208/105/EC) were selected for environmental quality standards - including polyaromatic hydrocarbons, biocides and the metals Pb

and Cd - but did not include Ag (EuropeanCommission 2008). Furthermore the UK highlighted 29 other Priority Substances for British waters - including ammonia and arsenic, and the metals Cu, Fe, Ni and Zn – due to their persistence, toxicity and potential accumulation, but again did not include Ag (WFDUK 2013). Instead it was determined that monitoring data indicated low risk from Ag release for which standards were not required, yet highlighted that the increasing use of AgNPs required further monitoring and future review.

Unlike essential metals such as zinc and copper, silver is non-essential and this might explain why it is toxic at such low concentrations (Chiarelli and Roccheri 2014). Exposures of the embryos and adults of the oyster *C. virginica* to AgNPs (15 ± 6nm, citrate-capped, 48 hours) have demonstrated impaired embryonic development at 1.6 µg/l, with a significant dose-dependent lysosomal destabilisation of adult hepatopancreas cells at concentrations above 160 ng/l (Ringwood *et al.* 2010). These concentrations are lower than EPA guidelines and highlight the importance of using environmentally realistic exposure concentrations in order to best understand how organisms will react in real-world scenarios.

If the dissolution of silver is related to toxicity, then dissolution speed may well be the driver behind the magnitude of effects. Increasing particle surface area provides a greater reactive surface and will increase dissolution potential (Baalousha *et al.* 2012). Given that, by weight, smaller NPs have a greater total surface area than larger NPs, it is hypothesised that reducing size will increase toxicity. This has been shown in exposures of alveolar macrophages to 15, 30 and 55nm AgNPs at concentrations from 0-75µg/l. At 10µg/l both 15 and 30nm AgNPs significantly reduced cell viability, whilst 15nm AgNPs also significantly increased ROS production in macrophages and depleted GSH. Both effects were not seen until ≥50µg/l AgNPs for the larger particles, if at all (Carlson *et al.* 2008). The authors suggested that increased surface area of smaller particles at the same dose will increase reactions with GSH thereby depleting it, and that ROS increases are a result of macrophage defensive failure following internalisation.

Surface area is related not just to size, but also to shape. Compared to spheres, the long, thin shape of rods and their sharp points will encourage dissolution, and indeed they may even pierce cell membranes, get lodged in fragile tissues and resist transit through the organism (Baalousha *et al.* 2012). Increased dissolution due to increased surface area was thought to be a reason why Zn-nanorods were more toxic to diatoms than Zn-nanospheres (Peng *et al.* 2011). As such it is important to compare morphological forms of nanosilver in order to fully understand toxicity.

The first study in this chapter compares the uptake of AgNPs and Ag-nanorods (AgNRs) over 48 hours into the gill, digestive gland and mantle of *M. edulis*, and explores their effect on oxidative stress and lipid peroxidation after 4 and 8 hours. This time frame was initially chosen to understand if acute exposure resulted in a rapid and acute response. This would then guide the timescale for further experiments to understand response delay over a longer timescale. In terms of biological activity, the relationship between Ag dissolution and hydrogen peroxide generation makes the CAT assay a viable tool for assessing the impact of AgNPs. Similarly with previous studies recording effects of Ag on GSH, then measuring activity levels of its conjugator - GST - becomes a tangible endpoint of biological effects. Several authors have reported changes in SOD activity (Jiang *et al.* 2014, Cozzari *et al.* 2015) and lipid peroxidation (Gomes *et al.* 2015, Yuan *et al.* 2018) following exposure to AgNPs therefore use of the SOD and TBARS assays becomes pertinent to the investigation. Again the dissociation of H₂O₂ into the hydroxyl free radical, known to affect lipid peroxidation, makes studying GST and TBARS activity highly pertinent.

The second study compares the uptake and inducement of biological effects by AgNPs and AgNRs after 24 hours, as compared to ionic silver and the dispersants used to stabilise the Ag nano-forms. This timescale was chosen based on the results of the first study in this chapter.

6.3. Time Series Uptake of Ag Nanorods and Nanoparticles by *M. edulis* and Differences in Biological Effects following 4 and 8 hours Exposure

6.3.1 Introduction

Previous experiments in this thesis have shown the maximum uptake of CeO₂NPs by *M. edulis* at around 4 hours, and predominantly into the digestive gland, followed by elimination over 48 hours. These experiments involved particles which are regarded as insoluble under the conditions of the assay (Dogra *et al.* 2016). As such the uptake kinetics of soluble particles, such as AgNPs, may differ from those of insoluble particles and it is necessary to investigate the uptake of AgNPs to understand how they might be accumulated by *M. edulis*, and thus affect biological processes.

A recent review into methods of silver toxicity has shown that cellular uptake of silver can be achieved via diffusion, endocytosis, or membrane-bound protein channels. Once internalised they might affect mitochondrial function, generate ROS, cause protein oxidation, or interfere with signalling pathways (McShan *et al.* 2014). Dissolution studies presented in Chapter 2.1.4 showed the dissolution of AgNPs (JRC NM-300K, nominally <20nm) at 50% after 4 hours and 90% after 24 hours, whilst AgNRs (JRC NM-302, nominally 100-200nm x 5-10µm) showed 20% dissolution after 4 hours and 70% after 24 hours. As mentioned previously, the dissolution of Ag⁺ from Ag is accompanied by the production of H₂O₂, and free silver can also affect cellular anti-oxidant defences such as thiols (Carlson *et al.* 2008). Such stressors are predicted to induce a defensive response.

In terms of AgNPs affecting oxidative stress responses, a recent study on exposure of mouse cell lines (RAW264.7) to AgNPs (69nm) found that GSH levels were significantly reduced in a dose-dependent manner from 0.4mg/l onwards, yet the effect was not significant at 0.2mg/l (Park *et al.* 2010). Presence of AgNPs in the cytosol led the authors to believe that toxicity was driven by particle dissolution *in situ* following uptake (a 'Trojan horse'-style effect), especially in the case where the particles had been swallowed by macrophages. These concentrations however are far above environmental

realism, and the dose-dependent reduction suggests damage to cellular production of GSH, rather than a measured response by the cells.

In contrast, another study (Arora *et al.* 2009) involving *in vitro* exposures of mouse fibroblast cells to AgNPs (7-20nm) showed a slight, yet significant 1.2-fold increase in GSH levels and a significant 1.4-fold decrease in lipid peroxidation at a concentration of 30mg/l. Liver cells showed significantly increased SOD (1.4-fold) and GSH (1.1-fold) activity at 225 mg/l. AgNPs were also seen in the mitochondria where they might have interfered with OS defences, yet the authors suggested that the measured response seen was due to an effective OS response. These studies show that response to AgNPs is not universal in all tissues and depends on cell type. Given the high concentrations used (mg/l), they also highlight the resistance of mammalian cells to silver as compared to the EPA guidelines of 1.9µg/l for marine discharge.

Rod and tube-shaped NPs have been associated with frustrated phagocytosis. The average size of a macrophage for example is 10µm, so it is believed they may have trouble engulfing particles greater than this size (Boyles *et al.* 2015). Various authors have highlighted the similarity in impact of nanorods and tubes to that of asbestos fibres. Experiments (generally comparing asbestos fibres to carbon nanotubes) have shown that tubes and fibres less than 20µm in length can cause some morphological changes – similar to those seen with spherical 15nm nano-carbon black (Boyles *et al.* 2015), but do not cause significantly increased inflammation or granuloma response (Poland *et al.* 2008). In contrast longer rods and fibres did increase both of these, with evidence of cell piercing during phagocytosis. Following phagocytosis, phagocytes produce superoxide to digest intra-cellular objects. Whilst nano-carbon black particles did not significantly induce this phagocytic burst in rat lung macrophages, all sizes of nanotube and asbestos fibres did (Boyles *et al.* 2015). Such over-production of superoxide is likely to have an effect on oxidative stress, and therefore measuring SOD activity becomes highly pertinent during Ag-nanoform exposures.

This study will investigate the ability for *M. edulis* to accumulate AgNPs and AgNRs over 48 hours, as well as examine the differences in biological effects induced by AgNPs and AgNRs after 4 and 8 hours. The hypotheses for this study are that all silver nanoforms will accumulate in the digestive gland of *M. edulis* following exposure, that all silver nanoforms will increase oxidative stress within the gill, stomach and mantle of *M. edulis* following exposure, and that AgNPs will cause greater oxidative stress in *M. edulis* than AgNRs through increased dissolution.

6.3.2 Method

A time series study (0, 2, 4, 8, 24, 32, 48 hours) was performed to understand uptake in gill, digestive gland and mantle tissues of *M. edulis* following a single dose of AgNPs (16.8nm) or AgNRs (2676 x 213nm) at 10µg/l. Mussels were exposed as per Chapter 2.3.3. At each timepoint mussels (n=6 per nano-form) were removed and gill, digestive gland and mantle were removed for ICP-MS analysis for silver content as per Chapter 2.3, and for analysis of oxidative stress (SOD & CAT activity) and lipid peroxidation (TBARS & GST activity) as per Chapter 2.2.2. Silver concentration results were pooled to a single sample, per tissue, per nanoform, per timepoint.

6.3.3 Results and Discussion

6.3.3.1 Time Series Uptake of AgNPs and AgNRs by *M. edulis*

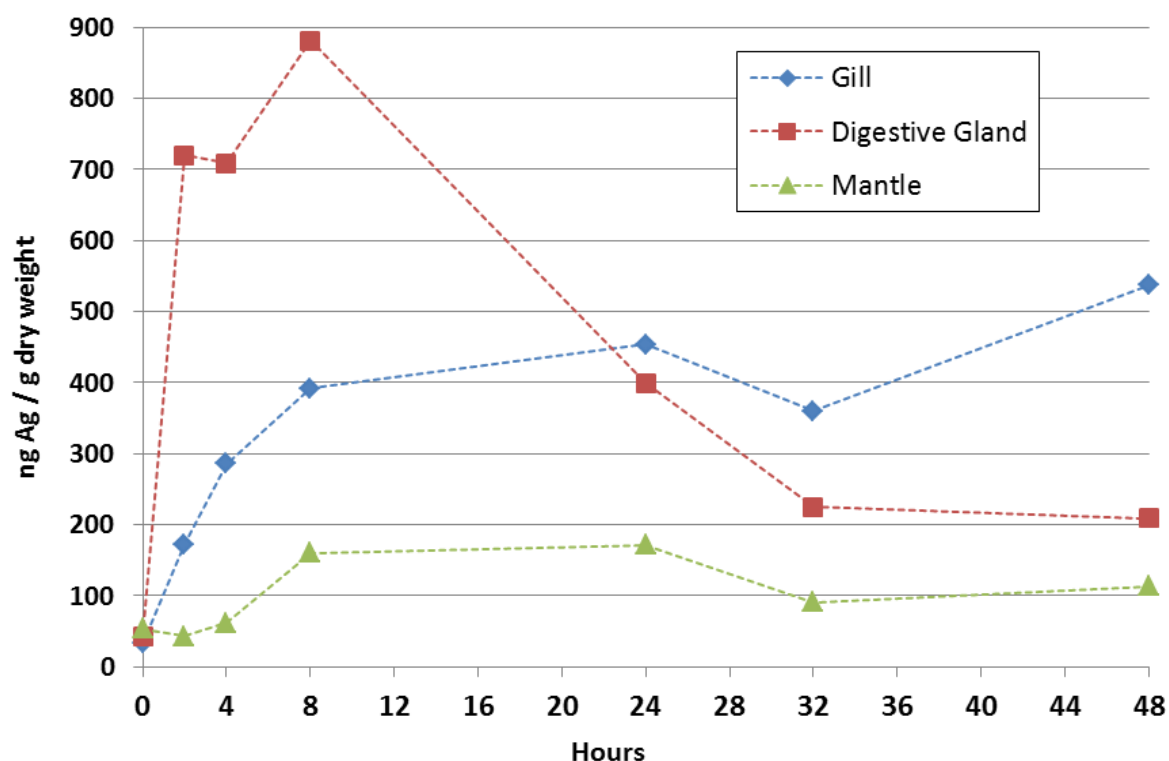


Fig 6.1: Silver concentrations (ng/g dry weight) in the gill, digestive gland and mantle of *M. edulis* following exposure to AgNPs (NM-300K; 10 μ g/l) over 48 hours (samples were pooled from n=6 to n=1, hence statistical analysis has not been performed)

Fig 6.1 shows silver concentrations in the gill, digestive gland and mantle of *M. edulis* following exposure to AgNPs (NM-300K) for 48 hours. Gill concentration generally increases over 48 hours, whilst mantle concentration increases over 24 hours, drops slightly after 32 hours, then slightly increases by 48 hours. Digestive gland concentration increases over 8 hours then drops by 24 hours and is further eliminated towards 48 hours.

As per the uptake of CeO₂NPs seen in Chapter 3, the highest total body silver concentrations are seen between 4 and 8 hours, in the order of digestive gland, gill, then mantle. That these similarities in digestive gland accumulation are highest at 8 hours is not surprising since the particles used here (c. 10-20nm) are of a similar size to the 10nm and 28nm CeO₂NPs used earlier.

Uptake into the digestive gland can be direct, through adsorption to algal cells, or in the water taken in during feeding. The small size of the particles (10-20nm) suggests that direct uptake by becoming trapped in gill filaments with a mesh of around $1.5\mu\text{m}^2$ is unlikely. However the AgNPs were supplied in a dispersant solution (Tween20 + PEG, Chapter 2.2.3), which would become diluted upon introduction to the exposure medium. The high ionic strength of the saltwater would then encourage agglomeration (Wang and Wang 2014), potentially making the particles of a size to be captured direct.

This agglomeration behaviour might explain why gill concentration increases over time as particles become trapped in the filaments. Increases in mantle concentration might result from particle adherence over time. Another possible reason for this pattern is uptake through dissolution. It was shown in Chapter 2.1.4 that 50% of these AgNPs had dissolved within 4 hours, and 90% dissolved after 24-48 hours. Structures such as the gills and mantle would therefore be bathed in dissolved silver, which is likely to influence uptake into these organs. The fact that the digestive gland concentrations show decline after 8 hours suggests that no more physical particles are entering this organ. Dissolution would subject the organism to either free Ag^+ or dissolved AgCl (Liu and Hurt 2010). It is known that external organs, such as gills, are able to accumulate lead and iron through endocytosis – and in one case 100nm polystyrene NPs - however these pathways have been little explored regarding other insoluble metals (Moore 2006, Deb and Fukushima 2007). More likely is that diffusion, protein pumps, and Na^+ channels are the reason for this (McShan *et al.* 2014).

Fig 6.2 shows the uptake profile of AgNRs over 48 hours, and is somewhat different to that of the AgNPs (Fig 6.1). Here maximum uptake is in the digestive gland after 2 hours (at concentrations double those of the NPs), followed by over 80% loss by 4 hours, then slow decrease towards 48 hours. Levels in the mantle never increase greater than the control, whilst levels in the gill increase slightly after 2 hours, but then remain steady over 48 hours. Again, the pooling of samples means these results are guide only, and have not been statistically validated.

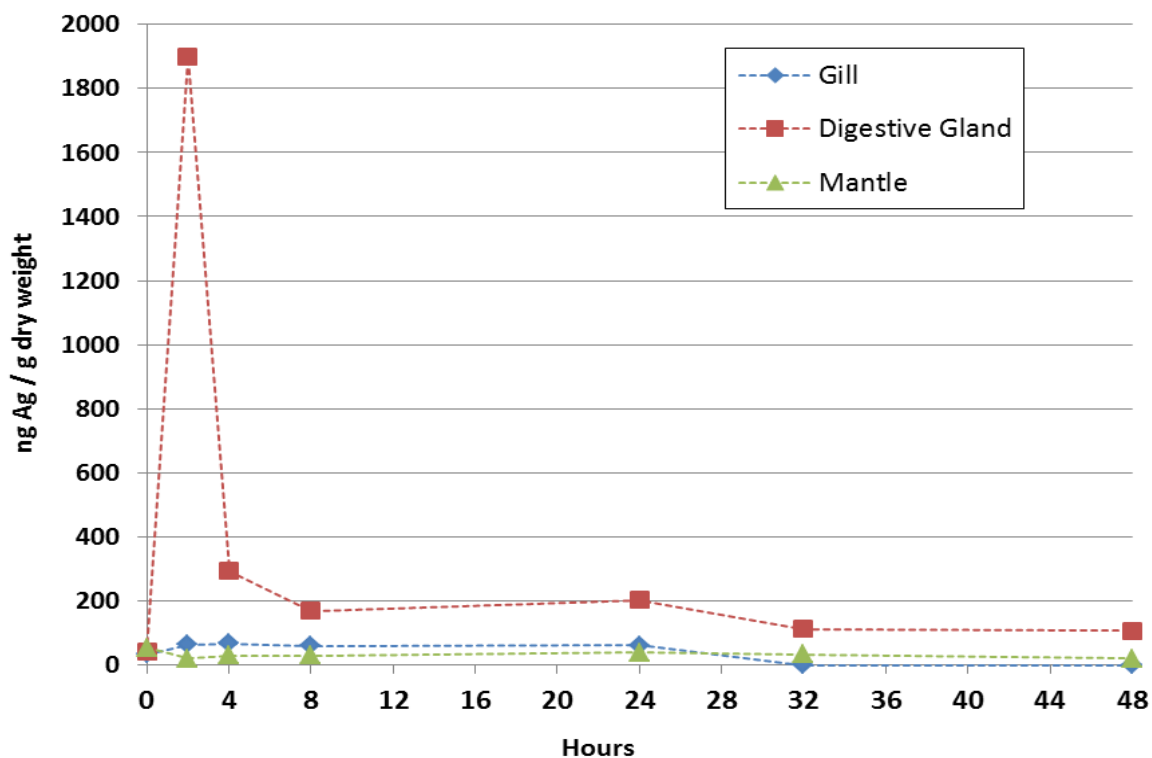


Fig 6.2: Silver concentrations (ng/g dry weight) in the gill, digestive gland, and mantle of *M. edulis* following exposure to AgNRs (NM-302; 10µg/l) over 48 hours (samples were pooled from n=6 to n=1, hence statistical analysis has not been performed)

The average size of the AgNRs used (2676 x 213nm) is larger than the mussel's inter-ciliary mesh. This means they can be captured by the gills without adhesion to algal cells in the water column, however uptake through adhesion is also possible. Since these particles do not need time to agglomerate to a trappable size then uptake is likely to be more rapid. Given their size also, fewer particles are required to make up a concentration of 10µg/l.

	Shape	Ave. Size (nm)	Surface Area (nm ²)	Volume (nm ³)	Mass per particle (ng)
AgNPs NM-300K	Sphere	16.8 Ø	886.68	2.48 x 10 ³	2.6015 x 10 ⁻⁸
AgNRs NM-302	Rod	2676 x 213	1.86 x 10 ⁶	9.54 x 10 ⁷	1.0007 x 10 ⁻³

Table 6.2: Dimensions of the AgNPs and AgNRs used in this experiment

One silver nanorod has a mass some 3.85×10^5 times greater than that of one silver nanoparticle (Table 6.2), therefore if only a few particles are ingested by the organism then there would still be a high increase in silver concentration.

Following maximum uptake, silver concentrations drop in the digestive gland by over 80% within 2 hours. This suggests the majority of AgNRs are removed quickly, most likely into the faeces. Over the next 44 hours the remaining particles are slowly eliminated towards control levels, although since this rate slows then it is possible that there is retention in some form or some intracellular digestion, either of particles or dissolved silver.

With regards to the gill tissue, AgNR exposure barely doubles silver concentration in the first 2 hours then remains stable, unlike the steady increase in gill concentration seen with AgNPs in Fig 6.1. Mantle concentration never increases above the control. It is possible that rapid uptake by the stomach effectively removed most of the particles from the water column thereby leaving few to further interact with the other organs, either directly or through dissolution. Both these organs are similarly used to transporting and removing particles of this size, therefore they might simply not be retained.

Dissolution of these AgNRs in seawater was previously measured at around 20% within 4 hours, rising to 70% after 24 hours (as per the experiments in Chapter 2.1.4). This was slower than that of the AgNPs and might explain why gill and mantle Ag concentrations following AgNR exposure are much lower than those following AgNP exposure, however the dissolution experiments were limited and lacked replication, so further investigation into this issue is necessary.

It is also worth noting that the mussels in exposures to both nanoforms retained some silver after 48 hours, and it might be expected that this would eventually be eliminated. A study involving transfer of oysters from silver-contaminated sites to clean sites showed that after 56 days, *C. gigas* lost 75% of its silver burden and *C. virginica* 23%, before concentrations plateaued (Okazaki and Panietz 1981). It was concluded that some silver must be trapped in the organism, unable to be depurated, and this would ask questions as to the recovery ability of bivalves from long-term silver exposure.

6.3.3.2 Biological Effects of AgNPs and AgNRs on *M. edulis*

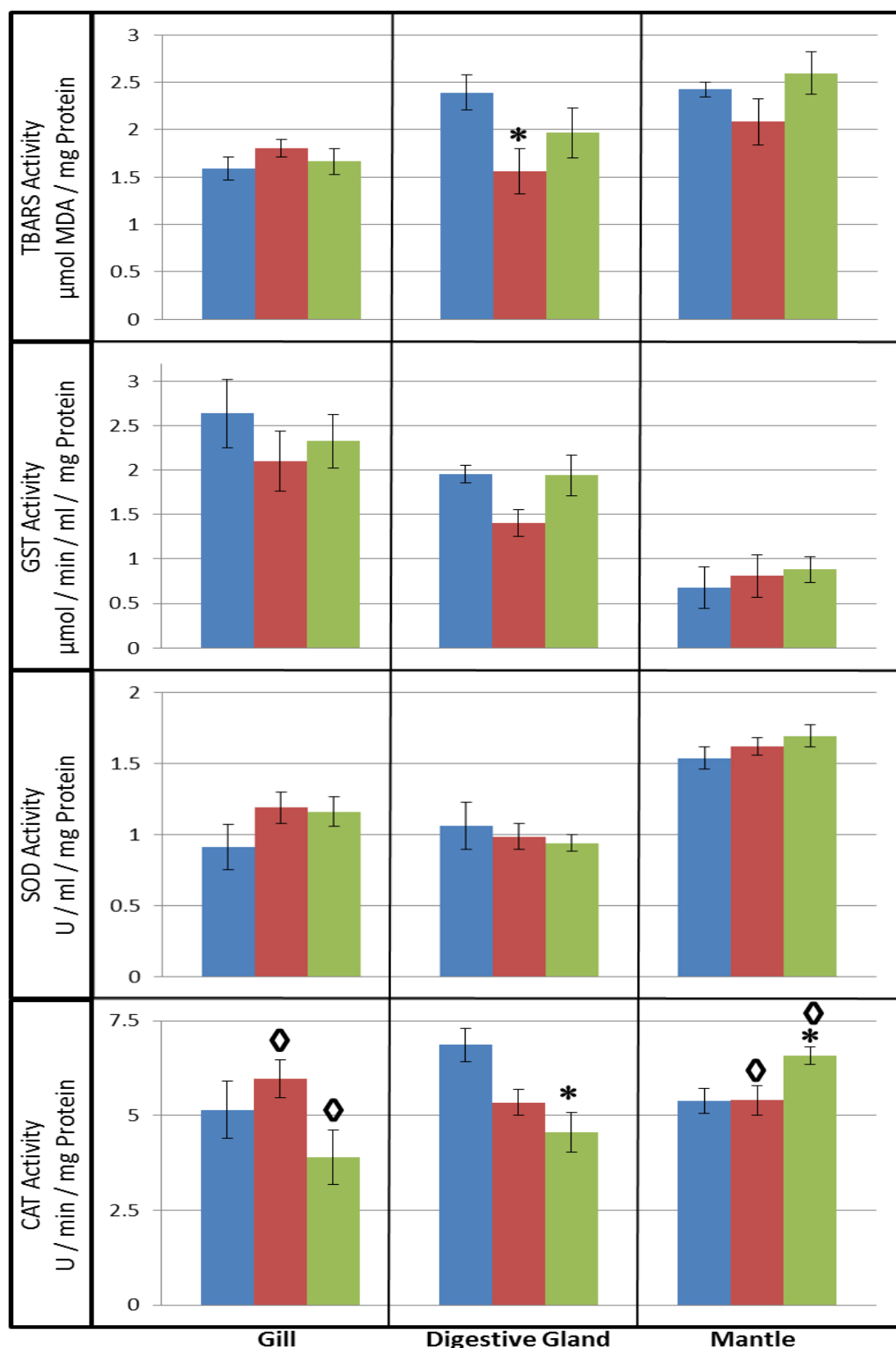


Fig 6.3: Significant differences in induced biological effects in Gill, Digestive Gland and Mantle tissue after **4 hours** following exposure of *M. edulis* to AgNPs and AgNRs (10μg/l). ■ = Control, ■ = AgNPs, ■ = AgNRs. * = significantly different from control. ◇ = Form-related significant difference ($p < 0.05$). $n=8$ per treatment

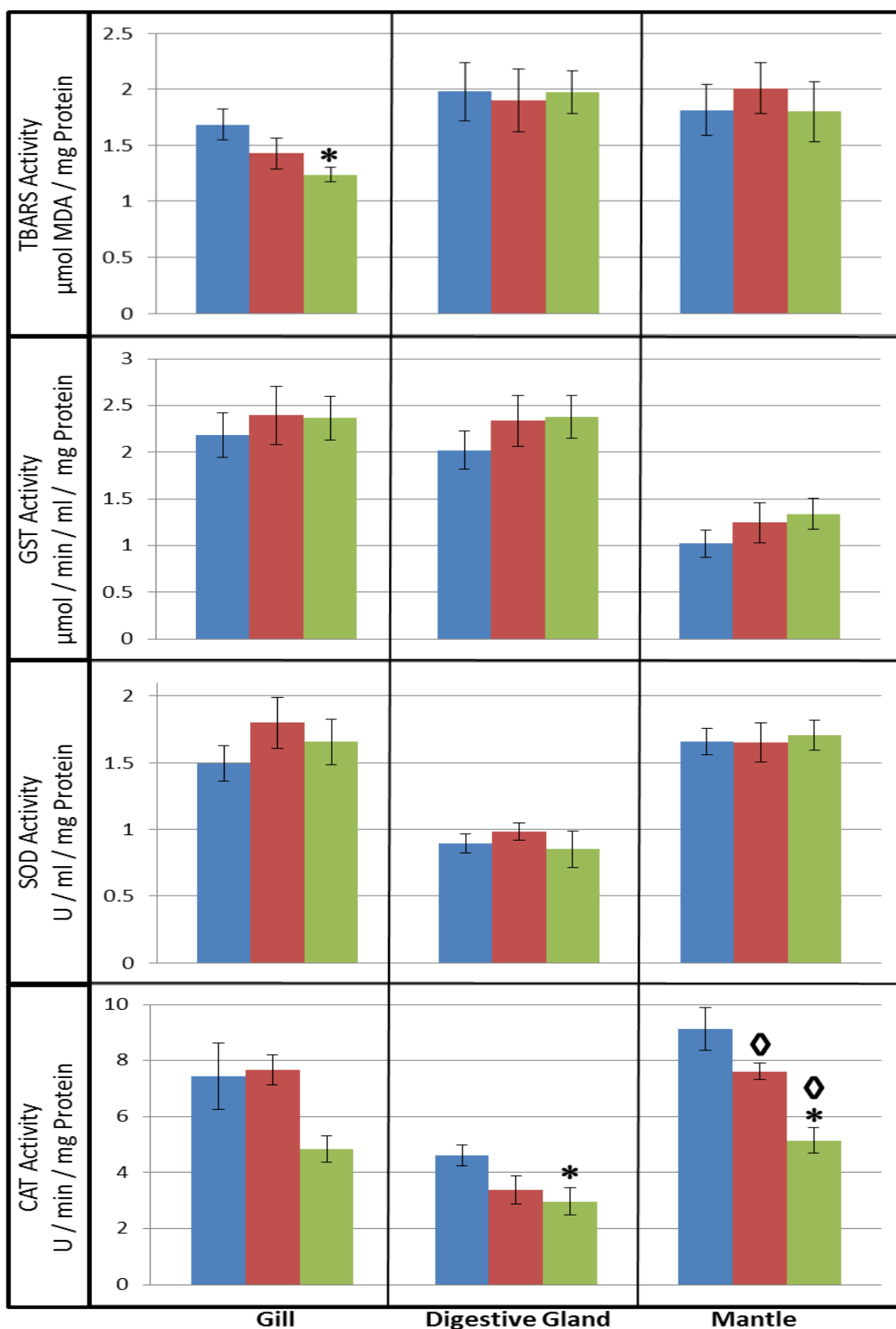


Fig 6.4: Significant differences in induced biological effects in Gill, Digestive Gland and Mantle tissue after **8 hours** following exposure of *M. edulis* to AgNPs and AgNRs (10μg/l). ■ = Control, ■ = AgNPs, ■ = AgNRs. * = significantly different from control. ◊ = Form-related significant difference ($p < 0.05$). $n=8$ per treatment

Figs 6.3-6.4 show the impact of NM-300K AgNPs and NM-302 AgNRs on the biological processes of *M. edulis* after 4 and 8 hours exposure. After 4 hours there was a significant difference in gill CAT activity between AgNP and AgNR exposed mussels (Mann Whitney U-test: $U=13$, $p=0.046$; data not normal even following log transformation, hence a non-parametric test was used), but neither was significantly different to the control. In the digestive gland, there was significant variation in TBARS activity [one-way ANOVA: $F(2,21)=4.217$, $p=0.029$], with a Tukey's HSD highlighting significantly lower activity following AgNP exposure ($p=0.022$). There was also significant variation in CAT activity [one-way ANOVA: $F(2,21)=7.112$, $p=0.004$], with a Tukey's HSD highlighting significantly lower activity following AgNR exposure ($p=0.004$). There was also significant variation in the mantle CAT activity [one-way ANOVA: $F(2,21)=4.519$, $p=0.023$], with Tukey's HSD highlighting activity significantly higher following AgNR exposure as compared to both the control ($p=0.04$) and AgNPs ($p=0.044$)

After 8 hours there was significant variation in gill TBARS activity [one-way ANOVA: $F(2,21)=3.553$, $p=0.047$] with Tukey's HSD indicating significantly lower activity following AgNR exposure ($p=0.038$). There was also significant variation in gill CAT activity [one-way ANOVA: $F(2,21)=3.745$, $p=0.041$], but Tukey's HSD highlighted no specific significant differences ($p>0.05$). There was also significant variation in digestive gland CAT activity [one-way ANOVA: $F(2,21)=4.009$, $p=0.034$; data log transformed], with Tukey's HSD highlighting significantly reduced ($p=0.03$) activity following AgNR exposure as compared to the control. In the mantle, again CAT activity was significantly varied [one-way ANOVA: $F(2,21)=13.783$, $p=0$], with Tukey's HSD highlighting activity following AgNR exposure as significantly lower than both the control ($p=0$) and AgNPs ($p=0.011$).

Maximum uptake of AgNRs was at 2 hours in all tissues, with the majority being found in the digestive gland. As such significant effects on CAT activity in this organ are not surprising; it is known that the dissolution of AgNRs leads to the production of H_2O_2 , which would require increased production of CAT to neutralise. The fact that CAT activity significantly declines is indicative of an overwhelmed anti-oxidant defence. Such a trend is reflected in the mantle,

whereby significant increases in CAT activity after 4 hours turn into significant decreases after 8 hours.

Such an effect was noticed in chronic exposures of *M. galloprovincialis* to 10µg/l CuONPs (Gomes *et al.* 2011). After 7 days exposure, CuONPs caused significantly increased CAT activity as compared to both the control and ionic copper, yet by day 15 CAT activity was significantly lower than ionic copper and the control. The authors suggested the antioxidant defences of the organism had been overwhelmed by this point. Copper is an essential metal, therefore some exposure is no doubt beneficial to the organism hence it would be able to regulate its uptake. Silver however is not essential, therefore it is possible that exposure to silver is overwhelming its defensive capacity at an earlier timeframe.

Despite steady accumulation in the gills over 56 hours, AgNPs caused no biological effects in this tissue that were significantly different to the control. Indeed, the only effect of AgNPs is in reducing TBARS activity after 4 hours in the digestive gland. It was found that 4-8 hours was the point of maximum accumulation of the AgNPs in the digestive gland so it might be expected that such an effect might last over 8 hours, yet this was not the case, indicating the organism has recovered well. Interestingly, exposure to AgNRs also caused significantly reduced TBARS activity in the gill after 8 hours, but not 4, suggesting an onset of this effect with time.

Most authors have reported increases in lipid peroxidation following exposure to nano-silver (Piao *et al.* 2011, Zhornik *et al.* 2014). However a 21-day study exposing *M. edulis* and the oyster *C. gigas* to 20µg soluble Ag/l every 48 hours suggested that reduced lipid peroxidation in *C. gigas* was related to increased metallothionein (MT) production. Essentially by increasing MT production the oyster was attempting to quickly bind the metals before they could form damaging ROS. This in turn would limit the number of ROS interacting with lipids, thereby decreasing lipid peroxidation and MDA formation (Géret 2002). In the same experiments the mussel *M. edulis* did not follow this pattern, and instead both MT and MDA production were shown to have increased after 21 days. It is possible that the chronic timescale of the Géret (2002) study might

have been responsible for the increased MDA levels seen in *M. edulis*, whereas the drop in MDA levels seen in this study might be due to the short timescale (4 & 8 hours), and over the longer term increased lipid peroxidation may occur. In future experiments it would be worth examining the relationship between MDA and MT levels in order to draw better conclusions from this.

In Chapter 3 reductions in TBARS, CAT and GST activity were associated with a protective, anti-oxidant effect of micron-size CeO₂. Indeed, in a recent experiment AgNPs have also been shown to act as an anti-oxidant in the carp *Catla catla* by mitigating oxidative stress caused by both cadmium and the bacterium *Aeromonas hydrophila* (Reddy et al. 2014). However it is believed that pre-induction of MT e.g. exposing the organism to one metal before exposing it to another, helps the organism deal with the secondary toxicant. In this way, the opposite has also been shown, with pre-induction of cadmium reducing lipid peroxidation caused by silver (Shinogi and Maeizumi 1993). This further highlights that reductions of TBARS and CAT activity in this experiment are not likely to be related to a protective effect of the Ag-nanoforms. Piao *et al.* (2011) went a step further to suggest that some reduced oxidative defence activities might be due to apoptosis, originated from mitochondrial disruption caused by AgNP-generated ROS. Essentially reduced activity would then be symptomatic of a reduced number of functioning cells.

Interestingly there is no significant impact by either particle on SOD activity in any organ at any time scale. It was thought that increased superoxide production as a result of increased phagocytic burst from frustrated phagocytosis of AgNRs could result in increased SOD activity (Brown *et al.* 2007), but there is no evidence of this. The average length of the AgNRs in this experiment was less than 3µm, far below the value of 15µm often associated with frustrated phagocytosis (Boyles *et al.* 2015).

An exposure of zebrafish *D. rerio* to 30-120mg Ag/l for 24 hours recorded no significant difference in SOD1 activity, yet dose-dependent reductions in CAT and glutathione peroxidase 1a activity, however this was accompanied by significant increases in lipid peroxidation and GSH levels (Choi *et al.* 2010). The authors have cited this as evidence for oxidative stress and DNA damage

with the organism struggling to cope with over-production of H_2O_2 , and again provides further evidence that the significant decreases seen in this experiment are from highly damaging mechanisms.

The first hypothesis of these studies was that all silver nanoforms would accumulate most readily in the digestive gland of *M. edulis*. It is true that the digestive gland initially accumulated the most silver, however much of this was eliminated over 48 hours. In the case of AgNPs the gill, and to a lesser extent, the mantle, showed steady accumulation over time, likely through dissolution.

It was also hypothesised that all silver nanoforms would increase oxidative stress within the gill, stomach and mantle of *M. edulis* following exposure, and that AgNPs would cause greater oxidative stress in *M. edulis* than AgNRs through increased dissolution. In fact AgNPs and AgNRs caused different effects at different times, with AgNPs having a single, isolated effect on TBARS activity in the digestive gland after 4 hours, and AgNRs mostly affecting CAT activity in all three organs. The differences in these effects are likely related to uptake kinetics, particle rejection, and particle dissolution.

This study provides an overview to the uptake of Ag-nanoforms over 48 hours, and their subsequent biological effects after 4 and 8 hours. Particle dissolution has been highlighted as a reason for biological effects, however no comparison was made between the nanoforms and ionic silver. The next study in this chapter will focus on this comparison in order to better understand how Ag-nanoforms instigate biological effects.

These acute dosing experiments were performed at $10\mu\text{g Ag/l}$, five times the US regulatory limit, and 100-fold higher than current anthropogenic inputs. The effects on oxidative stress were both inconsistent and transitory, with organs appearing to recover well, and it is suspected that the regulatory limit is sufficient to protect *M. edulis* from acute oxidative stress. However chronic dosing should be investigated to further understand the effects of long-term, low-level anthropogenic inputs.

6.4. Comparing AgNPs to AgNRs, their Dispersants, and Ionic Silver: Accumulation and Biological Effects in *M. edulis* following 24 Hours Exposure

6.4.1 Introduction

The previous experiment in this chapter compared the uptake of AgNPs to AgNRs over 48 hours, as well as the suite of biological effects induced by both nanoforms after 4 and 8 hours. As highlighted in Chapter 1, currently under discussion is whether nano-silver is more or less damaging to organisms than ionic (dissolved) silver, for example, due to properties such as *in situ* dissolution of the nanoform.

Growth inhibition IC_{50} values for the diatom *P. tricornutum* have been recorded at 400 μ g/l for $AgNO_3$, but 6-fold higher for citrate-capped AgNPs (14nm) and 9-fold higher for 15nm PVP-capped AgNPs (Angel *et al.* 2013). Comparing this to dissolution rate showed equivalent free silver concentrations at each IC_{50} value, showing that dissolution was the driver of toxicity. Similarly, ionic silver reduced macro-algal photosystem yield at only 2.5 μ g/l, compared to 55 μ g/l for AgNPs (Turner *et al.* 2012). In the case of the annelid *N. diversicolor*, exposure to both AgNPs and micron-size Ag caused more DNA damage than exposure to ionic silver, positing a nano-effect not related to dissolution (Cong *et al.* 2011). Exposure of the oyster *C. virginica* to both AgNPs and $AgNO_3$ reduced phagocytosis to a similar extent in the haemolymph (Abbott Chalew *et al.* 2012) and caused analogous haemocyte damage (Gomes *et al.* 2013a), yet the different forms caused damage to different proteins, highlighting that the nanoform may be responsible for a different method of toxicity.

To better understand how silver form affects toxicity, this experiment will compare the uptake and effects of AgNPs and AgNRs to those of ionic silver (in the form of $AgNO_3$). It is also necessary to compare the effects of the nanoform to its dispersant to ensure that the nanoform itself is the sole cause of any biological effects. Due to the transient and inconclusive nature of the biological effects seen at 4 and 8 hours, mussels will instead be exposed for 24 hours, which will also give some perspective on longer term exposure.

The hypotheses for this experiment are that *M. edulis* will accumulate ionic silver to a greater extent than nano-silver, that ionic silver will induce a greater suite of biological effects than nano-silver, and that the nano-silver dispersants alone will have little effect on biological processes in *M. edulis*.

6.4.2 Method

Mussels (n=8) were exposed to AgNPs (NM-300K), AgNRs (NM-302) and ionic silver (AgNO₃) at 10µg/l, as well as their respective silver-free nano-dispersants (NM-300D, NM-302D) for 24 hours as per Chapter 2.3.3. Gill, digestive gland and mantle tissue were removed for ICP-MS analysis for silver content as per Chapter 2.2.1, and for analysis of oxidative stress (SOD & CAT activity) and lipid peroxidation (TBARS & GST activity) as per Chapter 2.2. Pseudofaeces and faeces were also collected by filtering the water the mussels were in (post-exposure) through a 40µm filter, freeze-drying, then dissolving in 2ml HNO₃ on a hotplate at 60°C. These samples were also analysed by ICP-MS as per Chapter 2.2.

6.4.3 Results and Discussion

6.4.3.1 Accumulation

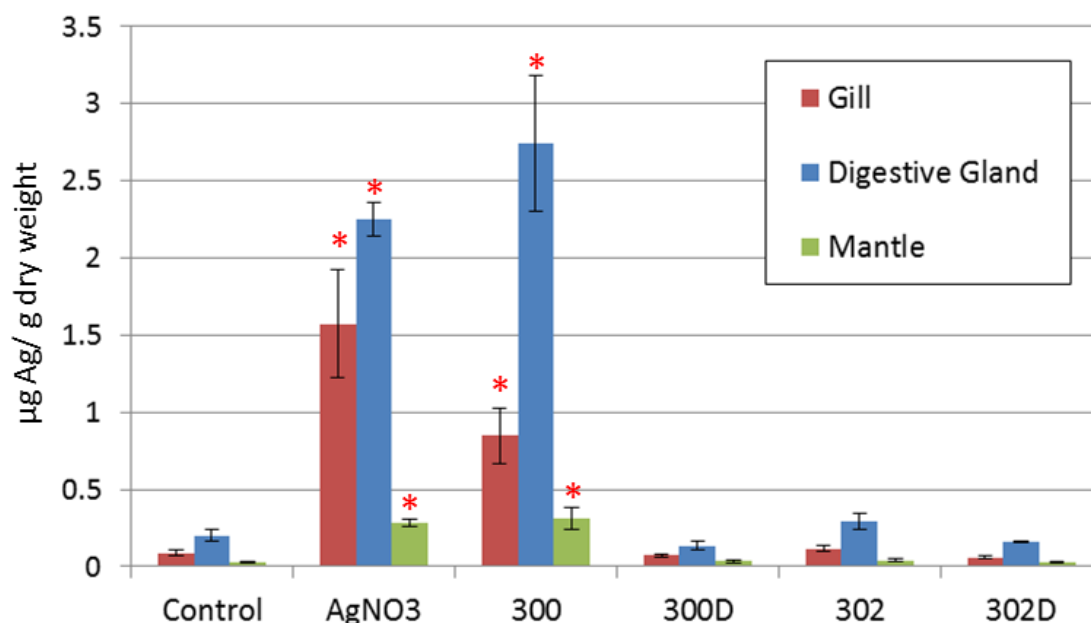


Fig 6.5: Mean Silver concentration ($\mu\text{g/g}$ dry weight) in the gill, digestive gland and mantle of *M. edulis* following exposure to AgNO_3 , the AgNP NM-300K, its dispersant NM-300D, the AgNR NM-302, and its dispersant NM-302D, at a concentration of $10 \mu\text{g Ag/l}$ for 24 hours. $n = 4$ per treatment (pooled from $n=8$). * = significantly higher than control ($p < 0.05$, one-way ANOVA)

Fig 6.5 shows silver concentrations in the gill, digestive gland and mantle of *M. edulis* following 24 hours exposure ($10 \mu\text{g Ag/l}$) to AgNO_3 , AgNPs, AgNRs, and their associated silver-free dispersants. There was significant variation in Ag concentrations in the gills [one-way ANOVA: $F(5,18)=14.183$, $p=0$], with a Tukey's HSD showing both AgNO_3 and AgNPs as significantly higher ($p < 0.05$) than both the control any other treatment, including AgNRs. Gill concentrations also differed significantly between AgNO_3 and AgNP treatments (Tukey's HSD $p=0.049$). There was no significant difference between the control and AgNR-exposed concentrations.

There was also significant variation in Ag concentrations in the digestive gland [one-way ANOVA: $F(5,18)=41.071$, $p=0$] and mantle [one-way ANOVA: $F(5,18)=18.484$, $p=0$]. Again, Ag concentrations in both AgNO_3 and AgNP-exposed mussels was significantly higher than the control and every other

treatment (Tukey's HSD, $p < 0.05$), but in this instance they were not significantly different from each other in either tissue (Tukey's HSD: digestive gland $p = 0.461$; mantle $p = 0.994$). Again there was no significant increase in Ag concentration from AgNR exposure as compared to the control (Tukey's HSD: $p = 1$ in both cases).

These results echo those of the previous time series experiment whereby *M. edulis* exposed to AgNRs showed almost complete elimination by 24 hours. As expected there is also no significant difference in Ag concentration between control tissues and those in exposures to the silver-free dispersants alone, nor was there any difference between Ag concentrations following AgNR exposure and exposure to the dispersants (Tukey's HSD: $p \geq 0.99$ in all comparisons).

Uptake profiles of both AgNPs and AgNO₃ are similar; uptake in all organs in both treatments is significantly higher than the control (Table 6.3), and the only significant difference in silver concentration between AgNO₃ and AgNP exposure is in the gills, with silver concentrations following AgNO₃ exposure being significantly higher. In the previous experiment it was thought that the continuous increase of silver concentrations in the gills following exposure to AgNPs was related to dissolution of Ag⁺. Earlier dissolution experiments (Chapter 2.1.4) showed that 50% of these AgNPs would dissolve in 4 hours rising to 90% after 24 hours. Mussel gills can accumulate ionic silver through ion-mediated channels in the gill epithelium (McShan *et al.* 2014). This provides strong evidence that AgNP dissolution is the reason for accumulation; the significant difference in concentration being from the time taken for AgNPs to dissolve before uptake by the gills. Dissolution would also explain why levels in the mantle are similar between AgNO₃ and AgNPs with these free-floating organs being bathed in Ag⁺ following dissolution.

As shown in Chapter 2.1.4, AgNRs exhibited 20% dissolution in 4 hours, rising to 70% after 24 hours. These values suggest that dissolution could occur, however maximum AgNR uptake by the mussel was shown at 2 hours in the previous experiment, with rapid removal. It is likely that the AgNRs are removed from the water column and isolated before they have a chance to

dissolve. In contrast the maximum uptake of AgNPs at 8 hours gives them time to dissolve before they are cleared from the water column.

It was also previously suggested that AgNPs had only accumulated in the digestive gland due to adsorption to algal feed. There is evidence here of accumulation of ionic silver in the digestive gland, therefore it is possible that in AgNP exposures any dissolved silver can also be accumulated independently of the AgNP. AgCl can adsorb to phytoplankton (Tappin *et al.* 2010), and dissolved AgCl can be accumulated via diffusion, therefore AgCl formation from either an ionic or nano-source, and subsequent adsorption to algal feed, could increase delivery to the digestive gland as could simple diffusion, and ingestion of water with dissolved silver in it.

Table 6.3 shows the average actual micrograms of silver found in each tissue after 24 hours exposure, as well as concentrations recovered from faeces and pseudofaeces i.e. processed particles, either rejected or undigested. Total silver recovered in unexposed assays (Control, 300D, 302D) is similar falling between 0.06-0.09µg and providing a useful background concentration. In each case levels of AgNO₃ and AgNP-originated silver are some 10-fold higher than control organisms, and similar regarding the gill and mantle. This again gives weight to the concept that ion uptake is responsible for most accumulation, with organs being bathed in dissolved silver.

	Control	AgNO ₃	AgNP (300K)	300D	AgNR (302)	302D
Gill	0.0208	0.3270	0.1973	0.0165	0.0237	0.0133
Digestive Gland	0.0444	0.6037	0.4829	0.0238	0.0693	0.0287
Mantle	0.0187	0.2071	0.1909	0.0164	0.0227	0.0190
Soft Tissue Total	0.0839	1.1378	0.8711	0.0567	0.1157	0.0610
Faeces/Pseudofaeces	0.0082	0.1104	0.4090	0.0037	0.4316	0.0064
Total Recovered	0.0922	1.2482	1.2802	0.0605	0.5474	0.0674

Table 6.3: Average total silver content (µg) found in gill, digestive gland and mantle tissues of individual *M. edulis* (n=8, pooled to n=1) following 24hrs exposure to 3.33µg Ag (10µg/l) through AgNPs (300K), AgNRs (302K) or AgNO₃, or to the equivalent concentration of their nano-dispersants (300D, 302D) alone (silver-exposed totals in **bold**)

At 0.547µg, total recovered silver concentrations following AgNR exposures appear much higher than those of the control (0.092µg), yet 0.431µg of this is from faeces and pseudofaeces, with soft tissue Ag concentrations (0.116µg) much closer to the control. This suggests that the organism is eliminating or rejecting, with nearly 80% of the silver it had so far processed as unnecessary. The faeces and pseudofaeces recovered from AgNP exposures contain a similar 0.409µg Ag, again highlighting elimination or rejection, yet the soft tissues contained 0.871µg, 68% of the total recovered, and eight times that found in the AgNR exposures. A study involving exposure of *M. galloprovincialis* to CeO₂NPs or ZnONPs (at 1-10mg/l) showed the mussel transforming some 99% of CeO₂NPs into pseudofaeces, and some 50-90% of the ZnONPs depending on concentration (Montes *et al.* 2012). As such the high concentrations seen in this experiment are not unexpected.

Of interest is that only 0.11µg Ag are to be found in the faeces and pseudofaeces of AgNO₃-exposed mussels, with 91% of the total recovered silver accumulated by the soft tissues. A similar result was shown with oysters exposed to 2µg/l ionic silver for 4 hours, with their faeces not containing significantly more Ag than the control (Abbe and Sanders 1990). In comparison, faeces from oysters fed algal cells pre-treated with silver contained significantly more silver than the control. Dissolved silver could have been accumulated across the mantle, gill and gut without feeding. In the experiments in this Chapter it was not determined whether silver was internalised, or simply adsorbed to the surface of the organs. Exposures of the periwinkle *L. littorea* to 58nm AgNPs (20µg/l) for example have shown no internal accumulation, however some did stick to the gills and head (Li *et al.* 2012). There was silver in the faeces, suggesting that the periwinkle may have fed on silver adsorbed to debris, yet none of the silver was retained.

Table 6.3 attempts to provide a mass balance for the fate of silver based upon an initial exposure dose of 3.33µg Ag (i.e. 10µg/l). From this data alone it is not possible to mass balance back to the original 3.33µg dose. This suggests four things: the first is that not all the faeces and pseudofaeces were recovered following the exposure, the second is that free ions and undissolved particles remained in the water column post-exposure, the third that adsorption of

particles to the mussel's shell or the exposure beakers would have essentially locked this silver away from potential uptake, and the fourth that silver was taken up by other parts of the organism not examined - the foot, the adductor muscle and the valves for example.

6.4.3.2 Biological Effects

GILL

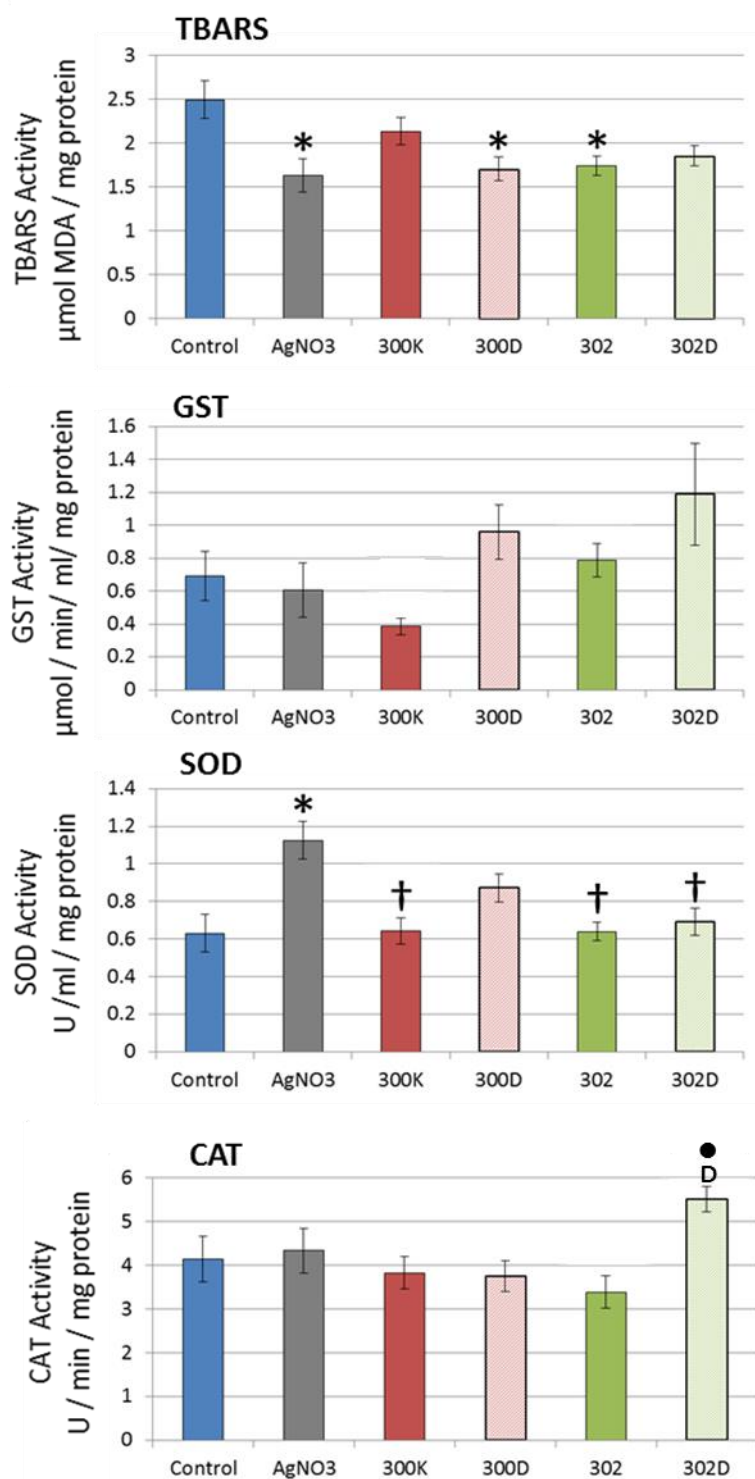


Fig 6.6: Differences in **Gill** TBARS, SOD, GST and CAT activity between control mussels and those subjected to AgNO₃, AgNPs (300K), AgNRs (302), and their respective dispersants (300D, 302D) following 24 hours exposure at 10μg/l Ag. n=8 per treatment. Symbols indicate significant difference ($p < 0.05$, one-way ANOVA with Tukey's HSD): * = from Control; † = from AgNO₃; D = between dispersants; • = between nanoform and its own dispersant

DIGESTIVE GLAND

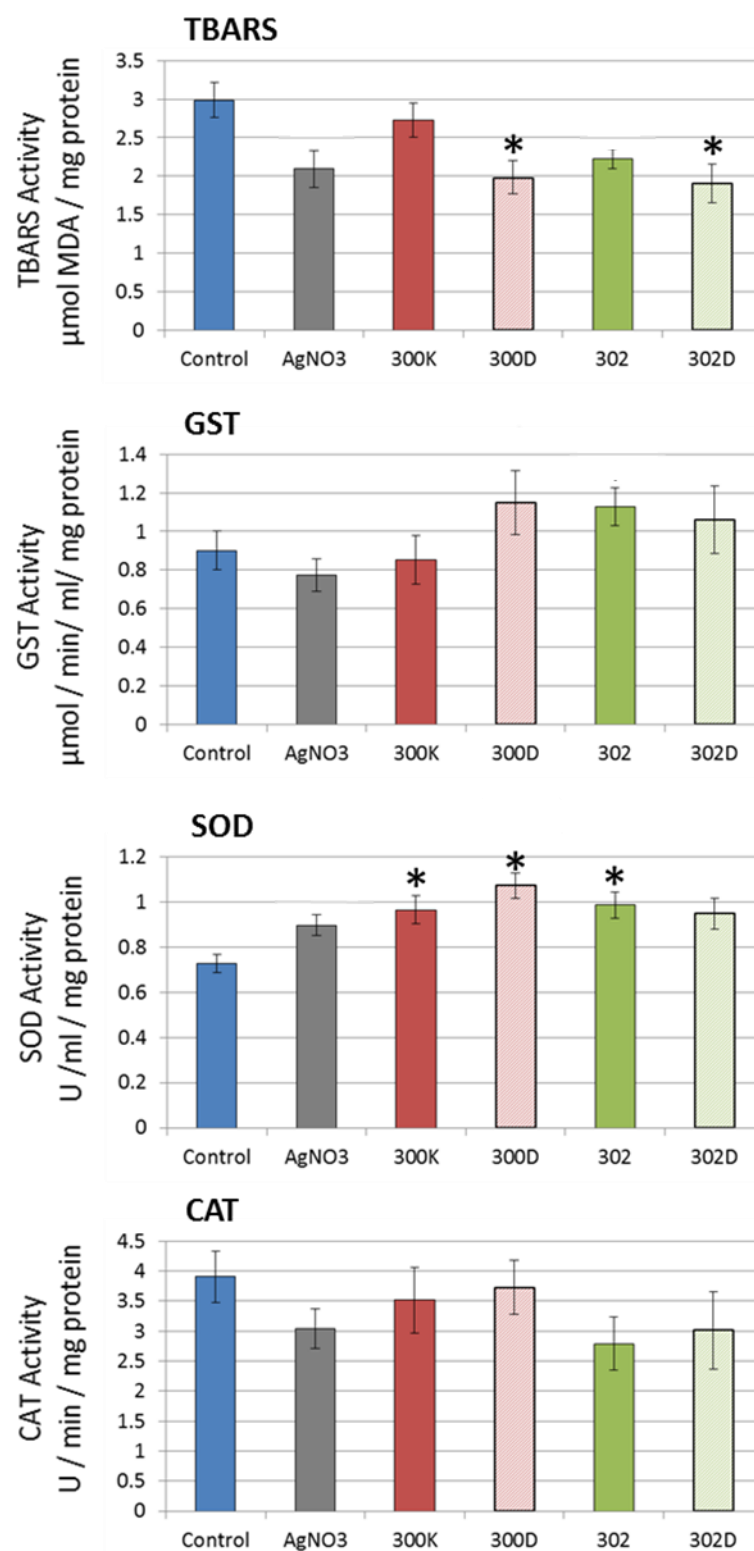


Fig 6.7: Differences in **Digestive Gland** TBARS, SOD, GST and CAT activity between control mussels and those subjected to AgNO₃, AgNPs (300K), AgNRs (302), and their respective dispersants (300D, 302D) following 24 hours exposure at 10μg Ag/l. n=8 per treatment. * = Significant difference from Control ($p < 0.05$, one-way ANOVA with Tukey's HSD)

MANTLE

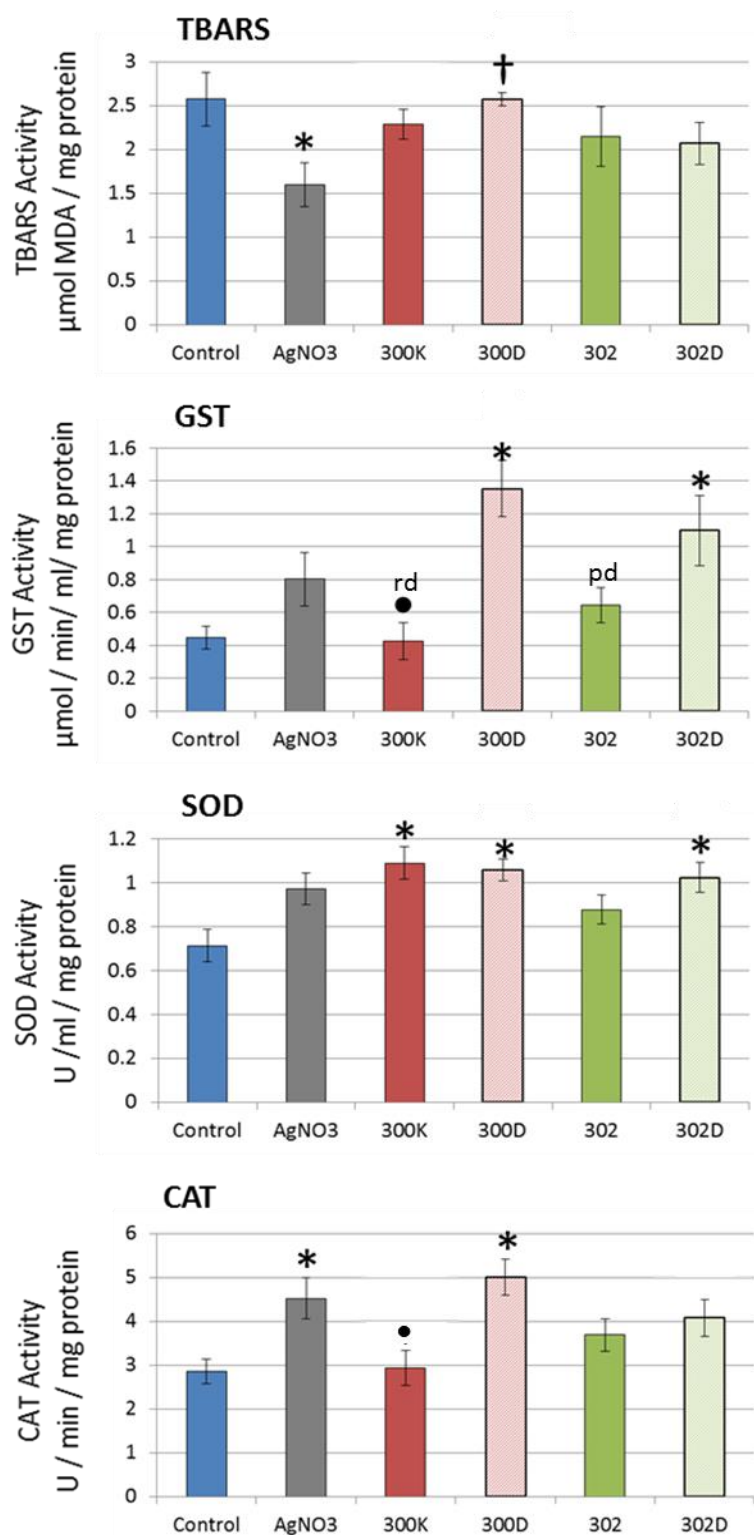


Fig 6.8: Differences in **Mantle** TBARS, SOD, GST and CAT activity between control mussels and those subjected to AgNO₃, AgNPs (300K), AgNRs (302), and their respective dispersants (300D, 302D) following 24 hours exposure at 10μg Ag/l. n=8 per treatment. Symbols indicate significant difference ($p < 0.05$, one-way ANOVA with Tukey's HSD): * = from Control; † = from AgNO₃; • = between nanoform and its own dispersant; rd = from rod dispersant 302D; pd = from particle dispersant 300D

Figs 6.6-6.8 show significant differences in biological effects in *M. edulis* caused by AgNO₃, AgNPs (NM-300K), AgNRs (NM-302) and their associated dispersants (300D, 302D) following 24 hours exposure. In the gill there was significant variation between groups with regards to TBARS activity [one-way ANOVA, $F(5,42)=15.183$, $p=0$]. In particular, activity following exposure to AgNO₃, AgNP-dispersant 300D and AgNRs was significantly lower than the control (Tukey's HSD: $p=0.05$, 0.013 & 0.02 respectively). Despite these effects on lipid peroxidation there was no significant difference in GST activity [one-way ANOVA, $F(5,42)=2.345$, $p=0.59$].

There was also significant variation regarding gill SOD activity [one-way ANOVA, $F(5,42)=6.054$, $p=0$], with activity following AgNO₃ exposure significantly higher than the control (Tukey's HSD: $p=0.001$), AgNPs ($p=0.002$), AgNRs ($p=0.001$) and the AgNR-dispersant 302D ($p=0.005$). Regarding CAT activity, there was significant group variation [one-way ANOVA, $F(5,42)=3.287$, $p=0.014$], with activity following exposure to the AgNR-dispersant 302D being significantly higher than to AgNRs alone (Tukey's HSD: $p=0.008$) and to the AgNP-Dispersant 300D ($p=0.041$)

In the digestive gland, there was significant variation in TBARS activity [one-way ANOVA, $F(5,42)=4.101$, $p=0.004$] with activity following exposure to both dispersants 300D (Tukey's HSD: $p=0.023$) and 302D ($p=0.012$) being significantly lower than the control. Again there was no significant difference in GST activity [one-way ANOVA, $F(5,42)=1.416$, $p=0.239$]. There was significant variation in digestive gland SOD activity [one-way ANOVA, $F(5,42)=4.304$, $p=0.03$] with significantly higher activity following exposure to AgNPs (Tukey's HSD: $p=0.047$), the AgNP-dispersant 300D ($p=0.001$) and AgNRs ($p=0.024$). There was however no significant difference in CAT activity [one-way ANOVA, $F(5,42)=1.124$, $p=0.363$].

With regards to the mantle, there was significant variation in TBARS activity [one-way ANOVA, $F(5,42)=3.12$, $p=0.017$ (data log transformed)] with activity following exposure to AgNO₃ significantly lower than the control (Tukey's HSD: $p=0.029$) and the AgNP-dispersant 300D ($p=0.015$). There was significant

variation in GST activity [one-way ANOVA, $F(5,42)=6.334$, $p=0$] with activity following exposure to AgNP-dispersant 300D significantly higher than the control (Tukey's HSD: $p=0.001$), AgNPs ($p=0.001$) and AgNRs ($p=0.017$). Activity following exposure to the AgNR-dispersant 302D was also significantly higher than the control (Tukey's HSD: $p=0.035$) and AgNPs ($p=0.026$), but not AgNRs ($p=0.266$).

There was significant variation in mantle SOD activity [one-way ANOVA, $F(5,42)=4.34$, $p=0.003$], with activity significantly higher than the control following exposure to AgNPs (Tukey's HSD: $p=0.004$), AgNP-dispersant 300D ($p=0.01$) and AgNR-dispersant 302D ($p=0.025$). There was also significant variation in CAT activity [one-way ANOVA, $F(5,42)=4.755$, $p=0.002$] with activity significantly higher than the control following exposure to AgNO₃ (Tukey's HSD: $p=0.049$) and the AgNP-dispersant 300D ($p=0.005$). Exposure to 300D alone also resulted in significantly greater activity than exposure to the AgNPs themselves ($p=0.007$).

In terms of TBARS activity, where significant effects occur, they are lower than the control. One reason TBARS activity might be reduced is due to the organism increasing MT production in an attempt to quench free silver ions before they can cause lipid peroxidation (Géret 2002), and this has been shown in exposure of *C. virginica* oyster embryos to AgNPs, which resulted in increased MT production (Ringwood *et al.* 2010). It has also been previously shown that Cu/Zn-SOD can conjugate silver, thereby providing another detoxification method (Ciriolo *et al.* 1994). These results show that decreased TBARS activity is sometimes accompanied by increased SOD activity (AgNO₃ in the gill, 300D in the mantle). This suggests that the organism is increasing SOD production to quench silver, which may then have a knock-on effect of preventing lipid peroxidation. In the case of AgNO₃ and the mantle, decreased TBARS occurs with increased CAT activity; since increases in CAT are often a result of increased SOD activity producing excess H₂O₂ (Halliwell and Gutteridge 2007) this relationship again seems pertinent. It would be useful to examine changes in MT levels in future exposures in order to better understand these mechanisms of protection and the interaction between TBARS, SOD and CAT activity.

Both AgNPs and AgNRs are linked to increased SOD activity in the digestive gland, and this is likely due to it being the organ of greatest silver accumulation. Increased SOD production to facilitate the conjugation of Cu/Zn-SOD with silver is one reason for this, as would be the need for SOD to counteract ROS formation by quenching the superoxide free radical. Phagocytosis of particles is accompanied by a phagocytic burst whereby the phagocyte attempts to neutralise the consumed particle by degrading it with superoxide (Brown *et al.* 2007). Rod shapes have been shown to cause frustrated phagocytosis whereby the phagocyte is unable to properly engulf it, leading to increased phagocytic burst, with rods greater than 15µm length causing significant damage (Boyles *et al.* 2015). The AgNRs characterised for use in this experiment had an average length of less than 3µm, and a maximum length of less than 11µm (Chapter 2.2.3) therefore it is unlikely they caused frustrated phagocytosis. Some particles however had 90° bends in them (Fig 2.5); increasing the complexity of the shape could feasibly lead to frustrated phagocytosis, and at least some contribution to the increased SOD activity. Future investigation should include microscopy to determine if phagocytosis is inhibited by these AgNRs.

Whilst the significant effects of AgNPs and AgNRs differ slightly as compared to the control, at no point is there a significant difference in effect between the two nanoforms. This is also generally true when comparing effects of AgNO₃ to those of the nanoform, with the only significant difference being significantly increased SOD activity in the gill following AgNO₃ exposure. Taken together, this suggests that ion dissolution is the main driver of toxicity. Previous studies have shown that the toxicity of the same NM-300K AgNPs to the bacteria *Pseudomonas putida* was driven by silver ion release, even at low dissolution rates, and that AgNO₃ was at least an order of magnitude more toxic than the nanoform, although this was at concentrations of 780µg/l and above (Mallevre *et al.* 2014). Studies using AgNPs of different size and coating similarly concluded that the dissolution was the main driver of toxicity to *C. elegans*, and that the AgNPs were not as toxic as a the same concentration of free silver at around 100µg/l (Yang *et al.* 2012). Experiments with the earthworm *Enchytraeus crypticus*, NM-300K and AgNO₃ (45-60 mg Ag/kg soil) have also

resulted in increased oxidative stress, including induction of MT from the nanoform, with the authors concluding that differences in effects were due to slow dissolution from the AgNP, but thought that a nano-scale effect might still exist (Ribeiro *et al.* 2015).

Exposures of the oyster *C. virginica* to AgNO₃ and citrate-coated AgNPs (20-30nm) for 48 hours have highlighted both differences in target organ and oxidative response between the two forms (McCarthy *et al.* 2013). In particular AgNO₃ significantly increased lipid peroxidation in the gills from 0.2µg/l and the hepatopancreas at 20µg/l, whilst AgNPs only increased LPx in the hepatopancreas from 0.2µg/l and, although they caused a reduction in LPx at all concentrations, this was not deemed significant. This is similar to the results in this experiment whereby LPx was generally depressed in the gill and digestive gland by Ag-nanoforms, although AgNO₃ also depressed LPx.

In the McCarthy *et al.* (2013) study AgNO₃ (at 0.2µg/l) also significantly decreased GSH in the gills and increased it in the hepatopancreas, whereas AgNPs only increased GSH in the hepatopancreas at 20µg/l. The results presented here show no significant changes in GST activity in either the gill or digestive gland, but a significant increase in the mantle from the dispersants. This suggests a measured response in the mantle to oxidative stress, since depressions in GST activity would correspond to depleted GSH, which is a sign of imbalance in anti-oxidant defences.

In terms of CAT activity, the McCarthy *et al.* (2013) study reported AgNPs causing significant increases in the gills from 0.2-2µg/l and significant reductions in the hepatopancreas, whilst AgNO₃ had no effect. The results here report only significant CAT increases in the mantle following exposure to AgNO₃ and the dispersant 300D. The discrepancies between these results might be due to significant increases in hepatopancreatic protein content reported by McCarthy, which would skew the ratio of Protein:CAT activity, thereby causing reductions. Either way the similarity of response between SOD and CAT reported in these results highlights the inter-twined relationship of these two enzymes.

Exposures of *M. galloprovincialis* to AgNPs and AgNO₃ have shown the gills to be a target for free/dissolved silver, with the digestive gland more susceptible to AgNPs (Gomes *et al.* 2014). In that experiment Ag⁺ and AgNPs caused different responses with regards to SOD, CAT and GPx activity, therefore the authors could not conclusively determine if silver toxicity was solely related to dissolution, however their earlier work noted AgNPs and Ag⁺ had similar effects on heat shock protein expression, GST, energy metabolism (Gomes *et al.* 2013b) and DNA damage in haemolymph cells (Gomes *et al.* 2013a).

Experiments with the freshwater mussel *Elliptio complanata* also showed AgNPs and Ag⁺ increasing lipid peroxidation and MT levels (Gagne *et al.* 2013), however it was believed that due to differences in DNA damage from LPx and MT that the mechanisms of toxicity to induce such responses were in fact different, and therefore reduced LPx cannot always be linked to increased MT.

The general lack of detrimental effects after 24 hours exposure in this study supports another study whereby peak levels of ROS were induced in less than 6 hours in *M. galloprovincialis*, and generally returned to control levels by 24 hours, even at concentrations three times higher than those used in this chapter (Katsumiti *et al.* 2015). Another study involving 28 day exposures of *M. edulis* to 5µg/l AgNPs (2 day re-dose) also showed no effect on either phagocyte activity or efficiency, despite Ag-burden increasing by 200% (Côté *et al.* 2014). This highlights that 24 hours might be sufficient for recovery, and that feeding and re-dosing schedules should closely approximate real-world scenarios. In that essence, more frequent feeding under chronic exposure conditions could prevent mussel recovery and impact organism health to a greater extent.

Differences in effects, even when using the same AgNPs, might be linked to aging. It has been shown that citrate and PVP-stabilised AgNPs still show slight dissolution over time, even before dispersal, such that exposures involving older particles will contain more free silver than new particles (Kittler *et al.* 2010). The production date of each nanoform could then affect levels of free silver in the exposures, such that results appear closer to those seen with ionic exposures, and not nanoform exposures. Dissolution of AgNRs is thought to cause weak points in the structure, and therefore potential for them to break into smaller,

squarer particles which could actually reduce the possibility of frustrated phagocytosis (Donaldson *et al.* 2011) and further increase dissolution speed.

There was no difference in silver content between the controls and AgNR exposures, yet despite this AgNRs still induced some significant biological effects. The previous experiment in this chapter showed AgNRs significantly reducing CAT activity after 4 and 8 hours. In this experiment there was some reduced TBARS and increased SOD activity, but no difference in CAT activity. It appears then that the effects seen after 24 hours are simply lasting effects from uptake at an earlier timepoint. Interestingly, gill TBARS activity is constantly suppressed from 8 hours on, and that SOD activity only increases at the 24 hour mark. A similar relationship is seen with AgNPs in the digestive gland, with significantly reduced TBARS activity recorded after 4 hours in the previous experiment, and significantly increased SOD activity seen after 24 hours. This makes it possible to speculate that the initial defence mechanism of *M. edulis* against silver exposure is metallothionein, yet to prove this would require measurement of MT induction, and this should be considered in future exposures.

Interestingly, the dispersant for the AgNP NM-300K, NM-300D, not only causes the same effects as its nanoform, but actually causes a greater suite of significant effects and, in particular, caused significantly greater GST and CAT activity in the mantle as compared to the nanoform. The dispersant itself contains Tween-20 and PEG. Research into Tween-20 has shown that it has some antioxidant capacity by reducing ROS production in human white blood cells (Perez-Roses *et al.* 2015), however the concentrations used (1mg/l-1g/l) were far above those used in this experiment. Conversely, Tween-20 has been shown to inhibit egg-laying in cattle ticks (Ravindran *et al.* 2011), but again this was at concentrations of 10g/l. Research into PEG has also shown anti-oxidant properties by conjugating with SOD (Veronese *et al.* 2002), whilst PEG-coatings on iron nanoparticles have been shown to reduce toxicity compared to uncoated particles by blocking nanoparticles from directly interacting with reactive oxygen species (Yu *et al.* 2012). On its own then, this dispersant should demonstrate a greater range of anti-oxidant effects, but the exact opposite of this is seen. It might be that in combination with the AgNP, the dispersant is able to act as an

anti-oxidant, thereby reducing effects of the AgNPs on *M. edulis* by reducing the burden on its defences. This still does not fully explain why the dispersant alone is more toxic, although from the examples given above (human v tick) it appears that Tween-20 could be more toxic to invertebrates than vertebrates.

A recent study on toxicity of NM-300K to *Daphnia* species showed that the dispersant alone (NM-300D) had no significant effects on organism survival or population increase (Volker *et al.* 2013) at the same concentration as used in this experiment. However in the same study the AgNPs themselves only impacted these parameters at concentrations of 10µg/l, and even then not until the 4th generation in the case of *Daphnia magna*. Since the Volker study only reports survival, it is impossible to determine if the dispersant caused some sub-lethal, oxidative stress response in the organism that might not necessarily impact on survival.

In terms of the AgNR dispersant NM-302D, the AgNRs and NM-302D do cause different significant effects in different tissues as compared to the control. Compared to each other, there is no significant difference except in gill CAT activity, whereby the dispersant is responsible for significantly increased activity. This suggests then that the dispersant is more prone to causing OS-related effects than the particle. Research by the NPL (Robinson *et al.* 2014) has shown that the dispersant, containing polycarboxylate ether and PVP, is photocatalytic and able to generate ROS to the same extent as the AgNR NM-302. This may explain how 302D is able to have such a significant effect on biological processes in *M. edulis* even without a nanoparticle present. However this does not fully explain why the presence of both AgNPs and AgNRs appear to protect the organism from their dispersants.

The presence of natural organic matter and humic acids has been shown to prevent the dissolution of silver (Liu and Hurt 2010). The exposures performed in this chapter used neither NOM nor humic acids, although the addition of algal cells could be classed as an organic component. In real-world scenarios the potential for dissolution is likely to decrease, with agglomerates more likely as the dominant form presented to the organism. Even if dissolution occurs, free silver could easily conjugate with other particles in the water column.

It was originally hypothesised for this experiment that *M. edulis* would accumulate ionic silver to a greater extent than nano-silver and that ionic silver would induce a greater suite of biological effects than nano-silver. It was seen that even though AgNPs and AgNO₃ accumulated to the same extent, AgNO₃ proved more toxic than either nanoform. It was also hypothesised that the nano-silver dispersants alone will have little effect on biological processes in *M. edulis*. The fact that the dispersants caused a greater suite of biological effects than the nanoforms actually casts doubt on the toxicity of the nanoforms themselves, although the dispersants may have helped mitigate toxicity. Future studies should compare capped and uncapped particles to help understand how dispersants affect toxicity.

6.5 Conclusion

The experiments in this chapter have concerned the uptake of two nanoforms of silver, and the ways in which they affect oxidative stress and lipid peroxidation in the gills, digestive gland and mantle of *M. edulis*. In time series exposures to AgNPs the digestive gland initially accumulated the most silver (within 8 hours), yet this was continuously eliminated over the next 36 hours. In contrast the gills continuously accumulated silver over 48 hours. There was only one isolated biological effect; that of reduced TBARS activity in the gills after 8 hours.

AgNRs were mostly accumulated within 2 hours in the digestive gland of *M. edulis*, but were quickly and continuously eliminated over the following 46 hours. There was an isolated effect after 8 hours on gill TBARS activity, with most effects concerning significant changes in CAT activity after 4 and 8 hours. Despite being quickly eliminated, effects appear to be longer lasting.

A 24 hour exposure of *M. edulis* to AgNO₃, AgNPs, AgNRs, and their respective dispersants, showed that AgNO₃ and AgNP accumulation at this time was both significant and significantly similar in all tissues, whilst earlier dissolution studies suggested that AgNP dissolution was the main driver of accumulation in the gills. AgNR accumulation was not significantly different to unexposed samples.

Early processing of AgNRs as either faces of pseudofaeces might lock them away and prevent further dissolution, in turn affecting uptake ability.

In terms of biological effects, AgNPs and AgNRs had different significant effects on different organs, showing that particle shape can influence different types of toxicity. The dispersants showed greater effects on biological processes than the particles, begging the question as to whether the dispersants are mediating the toxicity of nanoform, or the nanoform mediates the toxicity of the dispersants.

Despite these effects, none of them were significantly different to those caused by AgNO₃, and indeed AgNO₃ had more effect on biological processes in general. As such it cannot be concluded that Ag-nanoforms have any greater impact on organisms than ionic silver.

The reduced suite of oxidative stress effects over time suggests that *M. edulis* is able to recover from acute exposure to AgNPs and AgNRs at concentrations of 10µg/l. This concentration is 5-fold higher than acute release guidelines set by the EPA, and 300-fold higher than the highest nearshore concentrations recorded in industrialised areas of the USA. Currently silver nanoform production comprises less than 2% of worldwide silver production, and as such it is unlikely that Ag-nanoforms will have any great impact on *M. edulis* in the near future, however it would be worth examining the impact of chronic exposure in future studies.

Chapter 7: Conclusion

The aim of this thesis was to evaluate the bioaccumulation and biological effects of Me(O)NPs in a simple marine food chain at concentrations around the regulatory limit. Within this aim there were a number of objectives, namely:

- To assess the accumulation potential of Me(O)NPs by the mussel *M. edulis*
- To assess the biological effects of Me(O)NPs on the mussel *M. edulis*
- To assess the potential for trophic transfer of Me(O)NPs between *M. edulis* and *C. maenas*
- To assess the biological effects of Me(O)NPs on *C. maenas* following trophic transfer

In terms of accumulation potential, maximum accumulation of commercially available JRC NM-Series CeO₂NPs (10nm and 28nm) by *M. edulis* was roughly 5% of the dose after 4 hours' exposure, and the digestive gland was the organ of maximum uptake (95%). Smaller particles were accumulated to a greater extent, whilst increasing the concentration appeared to reduce the efficiency of uptake. This supports the work of Montes et al. (2012), Tedesco et al. (2010) and Hull et al (2013) who also suggested bivalves accumulate roughly 5% of an NP dose, and that increasing concentration reduces relative uptake. In terms of biological activity, CeO₂NPs had no significant pro-oxidant effects, whilst micron-size CeO₂ had some anti-oxidant effects. Based on this it was suggested that the proposed regulatory limit of 3mg/l (O'Brien and Cummins 2010) was likely sufficient to protect *M. edulis* from acute oxidative stress associated with exposure to CeO₂NPs.

Exposure of *M. edulis* to 100µg/l 2nm dextran-dispersed ¹⁴⁰CeO₂NPs yielded slightly different results, with uptake limited to 2% of the dose, and the gills and digestive gland showing similar levels of accumulation. This supports the literature that reducing particle size below that of the prey size reduces uptake efficiency in *M. edulis* (Ward and Kach 2009). Since dextran is known to reduce aggregation and agglomeration, this also supports the idea that particle clumping behaviour will influence both uptake and retention. In terms of biological activity, the ¹⁴⁰CeO₂NPs caused no effects suggesting the safety of these particles in the environment at this concentration. The dextran-only

control however had several significant biological effects, raising further questions as to whether the particle dispersants are more damaging than the particles themselves, and highlighting a point to address in future nanotoxicology studies.

In exposures of *M. edulis* to JRC NM-Series AgNRs and AgNPs at 10µg/l, it was found that the gills steadily accumulated silver from AgNP exposures over 48 hours, whilst levels in the digestive gland and mantle peaked between 8 and 24 hours before being eliminated. AgNRs were accumulated mainly in the digestive gland within 2 hours, then quickly eliminated. Biological effects were isolated, and generally related to significantly reduced CAT activity.

In a comparative 24 hours' exposure with AgNO₃, the similarity of uptake between AgNO₃ and AgNPs suggested dissolution as the main driver of AgNP accumulation, although AgNO₃ was responsible for greater Ag accumulation, especially in the gills. This supports much of the literature that has highlighted ionic forms of silver accumulating more readily than Ag-nanoforms. In terms of biological effects, there was a trend towards significantly reduced gill TBARS activity, and significantly increased SOD activity in the digestive gland and mantle, yet at no time did either nanoform cause an effect that was significantly more damaging than ionic silver. Some authors have found AgNO₃ as more toxic than the nanoforms and highlighted dissolution as the driver of this (Turner *et al.* 2012, Angel *et al.* 2013), whilst others have noticed a nano-scale effect (Cong *et al.* 2011, Gomes *et al.* 2014) and posited a Trojan-horse style approach (Park *et al.* 2010) whereby *in situ* dissolution might target different biological processes in different ways. To this end it would be worth examining different endpoints such as GSH levels, haemocyte damage, MT levels and phagocytosis impairment in future studies to best understand the full extent of effects of Ag-nanoforms. The experiments were conducted above the US EPA regulatory limit of 1.9µg/l therefore it is likely effects will be further limited at the regulatory concentration.

It was again found that the dispersants for the AgNPs (Tween 20 + PEG) and the AgNRs (polycarboxylate ether + PVP) alone caused a greater suite of damaging biological effects than when with their particle (similar to the results

with $^{140}\text{CeO}_2\text{NPs}$), and this highlights that different dispersants can affect toxicity and therefore thorough investigation is required to understand how varying particle coatings affect accumulation and biological effects.

With both the tested CeO_2NPs and Ag-nanoforms, single dose exposure up to 24 hours at or around the regulatory limit appears to cause some biological stress to *M. edulis*, yet they can recover well and this is possibly not surprising for an organism whose lifestyle is based around filter-feeding larger volumes of water which will contain a wide variety of essential, non-essential, and toxic substances. However it is this period of recovery that is most pertinent – chronic exposure would see the mussel continuously subjected to these nanoparticles, which might then remove the element of recovery. Future research should examine such effects over a number of days or weeks in order to better understand mussel health.

In both CeO_2NP and Ag-nanoform exposures it was found that the mussel was biotransforming a quantity of these particles into pseudofaeces: 40% in the case of $^{140}\text{CeO}_2\text{NPs}$ and 80% in the case of AgNRs. The rejection of these back into the water column thereby provides a sink of NPs that becomes available to other marine organisms such as coprophages. These animals are likely to be smaller, and the effects of feeding on a highly dense source of nanoparticles are therefore likely to be greater. This is also true of normal faecal matter which, given the digestive rhythms and uptake patterns of the mussel, is also likely to result in faeces dense with NPs.

Acute aqueous accumulation of 10nm JRC CeO_2NPs by the shore crab *C. maenas* showed that the gills were a major site of uptake and significant biological effects, although it was believed that significant biological effects were speculated to have originated from damage to bacteria found on the gill cuticle. To this end further investigation is required as to whether aqueous exposure of CeO_2NPs to crabs has any further effects on the gill ultrastructure or the gill function, such as limiting gas and ion exchange by coating the diffusive surface, an issue investigated previously using microplastics (Watts *et al.* 2016). Gill damage would lead to increased ventilation rate, which leads to increased

energy expenditure; in essence a cascade of effects that might impact, for example, locomotion, reproduction and recovery (Hebel *et al.* 1997).

It was not possible in these experiments to mass balance accumulation with the original dose, suggesting that NPs have adsorbed to exposure apparatus or to other parts of the organism. In natural conditions NPs will adsorb to a variety of substrates, including bacterial assemblages, making these particles potentially available to grazers (Li *et al.* 2012). Mussel and crab shells are also known to provide substrate for epibionts such as barnacles therefore it is possible that such settlement might be affected by shells coated in a layer of NPs. Again, this requires further research to fully understand the fate of NPs in complex marine ecosystems.

In trophic transfer experiments 10nm JRC CeO₂NPs were shown to transfer from *M. edulis* to *C. maenas*. The stomach of the crab was seen as a site of major accumulation, however an inverse relationship between stomach and faecal Ce content highlighted that this was likely transitory. Trophic Transfer Factors were calculated at 0.66 (± 1.1), including stomach content, which suggests biomagnification is unlikely. Of more interest was that the CeO₂NPs were accumulated in the hepatopancreas since it is guarded by a filter press designed to restrict access to objects > 100nm. Once in the hepatopancreas the particles will have a longer residence time than those rejected from the stomach to the gut, and future research should attempt to understand this impact in the longer term. Oxidative stress effects were limited to the hepatopancreas and stomach. An elevated Ce presence in the gills was surprising since there is no direct connection between the gills and digestive organs, although their presence did not instigate any significant effects on oxidative stress or lipid peroxidation. It was hypothesised that the particles might be entering the haemolymph, thereby providing routes of transit around the organism, with engulfment by haemocytes leading to clumping in tight hemal spaces, and this would be an area for future investigation. Unfortunately variable background concentrations of Ce in the haemolymph prevented this from being conclusively shown.

It an attempt to resolve the matter of variable background concentrations, dextran-coated CeO₂NPs were crafted exclusively for the stable isotope ¹⁴⁰Ce. By analysing changes in the isotopic ratios between ¹⁴⁰Ce and ¹⁴²Ce following exposure, this technique allowed for more accurate identification and quantification of Ce that originated purely from an enriched source. As expected there was evidence of enriched Ce in the stomach and hepatopancreas, however there was also evidence of accumulation in the respiratory gill and haemolymph. This shows that CeO₂NPs can enter the circulatory system of the crab this might provide a route for translocation to other tissues. Trophic Transfer Factors were low, at only 0.12 including the stomach and 0.03 excluding stomach content. Following initial mussel exposure concentrations of 100µg/l, there were no significant oxidative stress or lipid peroxidation effects to be seen in any measured crab tissues.

It would appear from the results presented here, whereby *C. maenas* accumulated less than 0.05% of the dose fed to *M. edulis*, that any trophic transfer of CeO₂NPs further than two steps in the food chain (i.e. to a predator's predator; not including primary producers) is likely to be beyond the limits of detection when using environmentally realistic concentrations. Similar results have been recorded in a terrestrial food chain, where no significantly higher Ce concentrations were found in spiders that were fed on crickets that themselves had been fed on Ce-exposed zucchini (Hawthorne *et al.* 2014). This is encouraging for risk assessment, especially since the results here used exposure concentrations orders of magnitude greater than natural anthropogenic inputs, and at these concentrations the ¹⁴⁰CeO₂NPs had no significant biological effect on the crabs.

Prior to this thesis there was no information concerning the short-term impact of Me(O)NPs on higher marine invertebrates. Here it is shown that despite rapid accumulation following short-term exposure, organisms can effectively eliminate CeO₂NPs and AgNPs from their bodies with limited impact on oxidative stress. There was also a lack of information concerning trophic transfer between marine invertebrates. Here it is shown that trophic transfer did not lead to biomagnification. Together this information is important as it shows that not only are these particles relatively safe in the environment, but also that their

release will not impact up through the food chain. Previous debate has also focussed on whether nanoforms are more damaging than ionic counterparts. This thesis shows that, in the case of Ag, the ionic form accumulated more readily and was more damaging than the nanoform. This shows that current regulations concerning environmental release of ionic silver are likely sufficient for nanosilver also.

In measuring the oxidative stress response as an indicator of threat to population stability, this thesis provides the first step to broadly understanding how Me(O)NPs might biologically impact on organisms. This information can then be used to tailor future experiments; for example, general increases in SOD activity would then lead to specific research into the expression of certain SOD genes. Without this first step a great deal of time could be wasted on examining genes that have no response.

Changes in ROS levels can lead to impacts on cell regulation and cause cellular damage, eventually leading to apoptosis. If more energy is put into maintaining the balance of ROS, then this will leave less available for foraging, mating, gamete production and predator avoidance, for example (Scott and Sloman 2004). As such even though exposure to these toxicants might be classed as sub-lethal, the combined effect of a number of stressors that include Me(O)NPs will impact on both organism health and therefore long-term population stability.

There were several limitations to this research. Firstly, a lack of previous research into the subject meant that the specifics of organism uptake and biological response to Me(O)NPs were unknown and had to be investigated before more detailed experiments could be performed. Combining this with budgetary limitations, it was therefore considered more relevant to pool samples on range-finding i.e. time series accumulation studies in order to reduce the cost of analysis, and as such these accumulation experiments are essentially pilot studies. However this time series data could then be used to identify the most pertinent timepoints to investigate more thoroughly, and therefore the best way to maximize more significant output from the available financial resources.

Secondly, exposing *M. edulis* in pristine artificial seawater meant organic components were lacking. The presence of humic and fulvic acids (Bhatt and Tripathi 2011) for example can affect the agglomeration potential of Me(O)NPs, thereby in real-world scenarios the extent to which these particles become visible to the mussel will vary. Exposure of marine diatoms to AgNPs for example has highlighted loss of biomass in lab experiments, yet this could not be replicated in field experiments (Lodeiro *et al.* 2017). The presence of other micro- and macro-organisms in normal waters would likely further reduce the concentration of Me(O)NPs to which mussels would be subjected. A prime example would be shell epibionts such as barnacles, which also filter feed, and are therefore also like to accumulate some of the Me(O)NPs in proximity of the mussel. Habitat complexity will similarly provide alternate substrate to Me(O)NPs to adhere to with increasing substrate complexity likely to reduce particle number in the water column. Tidal rhythms and depth will also affect mussel accumulation. During low tide any mussels out of the water would not be subject to further exposure, however mussels are known to hold water in their shells if they find themselves dry. Any Me(O)NPs in the water would therefore be retained when the mussel is closed (Zuykov *et al.* 2011) rather than being filtered or ingested/rejected, and this could have a bearing on both type of effect and target organ. As such it should be necessary in future exposures to as closely mimic natural conditions as possible to understand the true dynamics of interaction.

With regards to *C. maenas*, the crabs moult stage dictates whether it is more present in-shore or off-shore. Since anthropogenic inputs are more likely to be in-shore point discharges, moult-stage could therefore determine the extent of the crab's exposure. In terms of aqueous accumulation, issues highlighted for *M. edulis* concerning substrate complexity, tidal rhythm and presence of other organisms will similarly apply to *C. maenas*. In terms of trophic transfer, in reality the crab is more likely to feed underwater, which in turn would make sloppy feeding – and therefore release of NP-laden mussel flesh into the water column - a more realistic variable. Again however the presence of other scavengers or crabs also feeding on the same Me(O)NP-laden prey would likely limit the release of Me(O)NPs back into the water column, as well as reduce the

amount trophically transferred at any one sitting. Accurately applying digestive rhythms to experimental procedure (Hopkin and Nott 2009) would therefore increase the accuracy of any results obtained during trophic transfer.

This thesis has focussed on trophic transfer between two macro-organisms, a mussel and a crab. In marine ecosystems there are a plethora of different organisms, all with a variety of size, feeding method and lifestyle. As filterers of water and therefore most likely to encounter particles in the water column, there is a need to understand the impact of NPs on mussel health as their filtering ability will benefit other organisms in their habitat. However there is also a very real need to further study impacts of these NPs on other micro-organisms and, in particular, larval forms. Agglomerates of ZnONPs have been shown to limit the movement of the nauplii of the copepod *T. japonicus*, and the larvae were also observed feeding on the agglomerates (Wong *et al.* 2010). It is feasible that agglomeration of CeO₂NPs could have a similar effect. Similarly, both AgNO₃ and AgNPs have been shown to impact on settlement of the larvae of the barnacle *Balanus amphitrite* and the polychaete *Hydroides elegans*, yet *H. elegans* accumulated more silver from the nanoform (Chan and Chiu 2015). This shows that accumulation and effects of Me(O)NPs can be organism specific, and therefore makes it harder to implement cohesive policy regarding the safety of these toxicants in the environment. These studies also highlight that understanding at which stage in their life cycle these organisms are most affected is incredibly important as studying effects on adult organisms has little relevance if Me(O)NPs are affecting juvenile mortality to a point that impacts both recruitment and survival. Since larvae are also a food source then adverse effects on food supply early in the food chain could have a massive impact on higher trophic organisms.

Bivalves have long been used as bio-indicators of marine health due to their ubiquitous presence; other species recommended include phytoplankton due to its base position in the food chain (Zhuang and Gao 2014) and zooplankton since they scavenge on detritus and are often the link between phytoplankton and higher predators (Parmar *et al.* 2016). Matranga & Corsi (2012) highlighted sediment dwellers and benthic species as good model organisms since NPs are likely to agglomerate and sink. There is great value in understanding effects of

Me(O)NPs on specific organisms yet there is also a wider need to understand the true fate of Me(O)NPs in complex ecosystems. It may have been found that crab gills are particularly susceptible to aqueous exposures of Me(O)NPs, but if bivalves are removing the particles before they reach the crabs then in real terms the severity of the threat becomes diminished. This has been touched upon by other authors (Ferry *et al.* 2009) using AuNPs whereby biofilms were highlighted as major accumulators, yet more studies are required given the biological and habitat diversity of marine ecosystems.

There is also a case for a multi-factorial approach to understanding the impact of Me(O)NPs. Experiments with ZnONPs on larvae of the sea urchin *Tripneustes gratilla* showed that growth was stunted with increasing temperature since temperature affected metabolic processes (Mos *et al.* 2017). Similarly, adaptation of mussels to cold weather sees increases of unsaturated fatty acids in cell membranes to promote membrane fluidity; however these unsaturated fatty acids are known to be more prone to lipid peroxidation (Montserrat *et al.* 2007) therefore temperature and seasonality will again play a role in the extent of Me(O)NP-instigated oxidative stress. Differences in salinity will also play a part; experiments here were conducted at full salinity; mussels and crabs often live in coastal areas subject to salinity fluctuations from freshwater inputs i.e. rivers. Low salinity will reduce chloride complexation (of, for example, free silver ions), whilst simultaneously increasing ion pumping rate of the organism thereby providing more routes for toxicant entry (Lushchak 2011). As such there may well be different responses to NP exposure depending on salinity.

To date, research in nano-toxicology has generally focussed on using pristine reference materials available from the JRC, or Me(O)NPs synthesised from single metals. Indeed this thesis has focussed on the effects of pristine CeO₂NPs and AgNPs. Whilst the insolubility of CeO₂NPs makes them useful as a tracking particle, there is very little demand for such particles in that condition. Similarly the likelihood is that, barring any direct spill scenarios, organisms will be subjected to weathered particles. It has been suggested that ecotox studies should address exposures using nano-products, however there are issues in how exactly this should occur, especially given the wide variety of

products that includes NPs i.e. from clothes to plastics. Current methods for product weathering, such as cryo-milling and sanding, produce heterogeneous NPs making it difficult to tease out whether it is shape, size, or the composition of products themselves (Scott-Fordsmand *et al.* 2017) that accounts for the effects. However, is this truly an issue? The desire to test homogeneous products is unlikely to match real-world scenarios where any number of factors can influence particle characteristics. The most sensible step towards future nano research would be firstly to understand the fate of NPs. Once you know this, then designing appropriate eco-toxicity studies becomes even more relevant, regardless of whether the NPs remain nano-sized.

There is a new trend towards the production of nanocomposites in which nanomaterials are added to, for example, ceramic matrices to increase hardness, or to polymers to change catalytic, magnetic and electrical properties (Camargo *et al.* 2009). However gathering information concerning exactly what is being made in what volumes and how they are being used is tricky due to non-disclosure from manufacturers. Combined with this the low production volumes and concentrations of NPs used in commercial products often mean they are not subject to usual regulations; no safety information is required for products containing less than 0.1% NPs, and the US EPA provides an exemption for materials produced in volumes less than 10 tons per year (Lai *et al.* 2018). It has been suggested then that the output of future nano research should focus on providing information to companies that helps them choose NPs for product inclusion more carefully, thereby helping mitigate potential issues before manufacture, with a goal to limiting the variety of NPs that might enter ecosystems.

In summary, the acute accumulation and effects of CeO₂NPs on *M. edulis* appear temporary and recoverable. Trophic transfer experiments showed *C. maenas* accumulating only 5% of a fed dose of CeO₂NPs, with low TTFs indicating biomagnification is unlikely and, most importantly, with no significant effect on biological processes. Anthropogenic use of Ce is unlikely to increase in near future to a level whereby regulatory limits need to be set, however chronic exposure experiments should be performed to confirm this. The case study presented in this thesis showed dissolution drives longer-term

accumulation of Ag-nanoforms, but these nanoforms had less impact on biological effects than exposure to ionic silver. This is important since Ag-nanoform production is likely to increase, yet the results show that current regulatory limits concerning Ag release feel sufficient to protect marine organisms from this emerging market.

Appendix A: Conferences, Publications & Grants

Conferences

- Office of Environmental Nano Safety (OENS) 7th International Conference on the Environmental Effects of Nanoparticles and Nanomaterials (ICEENN), 2012, Banff, Canada: Poster Presentation
- SETAC North America 33rd Annual Meeting, 2012, Los Angeles, USA: Poster Presentation
- Ecotoxicology Research and Innovation Centre (ERIC)/SETAC Joint Meeting, 2013, Plymouth, UK: Poster Presentation
- OENS 9th ICEENN, 2014, South Carolina, USA: Speaker

Publications

- Baker TJ, Tyler CR & Galloway TS (2014) Impacts of metal and metal oxide nanoparticles on marine organisms, Environmental Pollution (186) 257-271 DOI: 10.1016/j.envpol.2013.11.014 ([attached post-references](#))

Grants

- NERC-awarded Competitive Grant at the Facility for Environmental Nanoscience Analysis and Characterisation (FENAC), Birmingham: Value £24,000

References

- Abbe, G. R. and J. G. Sanders (1990). "Pathways of silver uptake and accumulation by the American oyster (*Crassostrea virginica*) in Chesapeake Bay." Estuarine, Coastal and Shelf Science **31**(2): 113-123.
- Abbott Chalew, T. E., J. F. Galloway and T. K. Graczyk (2012). "Pilot study on effects of nanoparticle exposure on *Crassostrea virginica* hemocyte phagocytosis." Mar Pollut Bull **64**(10): 2251-2253.
- Acworth, I. N. and B. Bailey (1995). The Handbook of Oxidative Metabolism. Chelmsford, Massachussets, ESA.
- Alishahi, A., A. Mirvaghefi, M. R. Tehrani, H. Farahmand, S. Koshio, F. A. Dorkoosh and M. Z. Elsabee (2011). "Chitosan nanoparticle to carry vitamin C through the gastrointestinal tract and induce the non-specific immunity system of rainbow trout (*Oncorhynchus mykiss*)."
Carbohydrate Polymers **86**(1): 142-146.
- Alpaslan, E., C. Xu, H. Yazici, A. Roy and T. Webster (2016). "pH and time dependent antioxidant activity of dextran coated cerium oxide nanoparticles." Frontiers in Bioengineering and Biotechnology **4**.
- Alpaslan, E., H. Yazici, N. H. Golshan, K. S. Ziemer and T. J. Webster (2015). "pH-Dependent Activity of Dextran-Coated Cerium Oxide Nanoparticles on Prohibiting Osteosarcoma Cell Proliferation." ACS Biomaterials Science & Engineering **1**(11): 1096-1103.
- Amin, K. A., M. S. Hassan, S. T. Awad el and K. S. Hashem (2011). "The protective effects of cerium oxide nanoparticles against hepatic oxidative damage induced by monocrotaline." Int J Nanomedicine **6**: 143-149.
- Angel, B. M., G. E. Batley, C. V. Jarolimek and N. J. Rogers (2013). "The impact of size on the fate and toxicity of nanoparticulate silver in aquatic systems." Chemosphere **93**(2): 359-365.
- Appeltans, W., P. Bouchet, G. Boxshall, C. De Broyer, N. de Voogd, D. Gordon, B. Hoeksema, T. Horton, M. Kennedy, J. Mees, G. Poore, G. Read, S. Stöhr, T. Walter and M. Costello. (2012). "World Register of Marine Species." Retrieved 8th April 2013, from <http://www.marinespecies.org/aphia.php?p=browser>.
- Arora, S., J. Jain, J. M. Rajwade and K. M. Paknikar (2009). "Interactions of silver nanoparticles with primary mouse fibroblasts and liver cells." Toxicol Appl Pharmacol **236**(3): 310-318.
- Asghari, S., S. A. Johari, J. H. Lee, Y. S. Kim, Y. B. Jeon, H. J. Choi, M. C. Moon and I. J. Yu (2012). "Toxicity of various silver nanoparticles compared to silver ions in *Daphnia magna*." J Nanobiotechnology **10**: 14.
- Ayala, A., M. F. Munoz and S. Arguelles (2014). "Lipid peroxidation: production, metabolism, and signaling mechanisms of malondialdehyde and 4-hydroxy-2-nonenal." Oxid Med Cell Longev **2014**: 360438.
- Baalousha, M. (2009). "Aggregation and disaggregation of iron oxide nanoparticles: Influence of particle concentration, pH and natural organic matter." Sci Total Environ **407**(6): 2093-2101.
- Baalousha, M., Y. Ju-Nam, P. A. Cole, B. Gaiser, T. F. Fernandes, J. A. Hriljac, M. A. Jepson, V. Stone, C. R. Tyler and J. R. Lead (2012). "Characterization of cerium oxide nanoparticles-part 1: size measurements." Environ Toxicol Chem **31**(5): 983-993.
- Baalousha, M., Y. Ju-Nam, P. A. Cole, J. A. Hriljac, I. P. Jones, C. R. Tyler, V. Stone, T. F. Fernandes, M. A. Jepson and J. R. Lead (2012). "Characterization of cerium oxide nanoparticles-part 2: nonsize measurements." Environ Toxicol Chem **31**(5): 994-1003.
- Babu, K. S., M. Anandkumar, T. Y. Tsai, T. H. Kao, B. S. Inbaraj and B. H. Chen (2014). "Cytotoxicity and antibacterial activity of gold-supported cerium oxide nanoparticles." Int J Nanomedicine **9**: 5515-5531.
- Baker, T. J., C. R. Tyler and T. S. Galloway (2013). "Impacts of metal and metal oxide nanoparticles on marine organisms." Environ Pollut.

Barmo, C., C. Ciacci, B. Canonico, R. Fabbri, K. Cortese, T. Balbi, A. Marcomini, G. Pojana, G. Gallo and L. Canesi (2013). "In vivo effects of n-TiO₂ on digestive gland and immune function of the marine bivalve *Mytilus galloprovincialis*." Aquat Toxicol **132-133**: 9-18.

Barnes, R. S. K., P. P. Calow, P. J. W. Olive, D. W. Golding and J. I. Spicer (2001). The Invertebrates: A Synthesis. Oxford, UK, Blackwell Science Ltd.

Barrento, S., I. Lupatsch, A. Keay and G. Christophersen (2013). "Metabolic rate of blue mussels (*Mytilus edulis*) under varying post-harvest holding conditions." Aquatic Living Resources **26(3)**: 241-247.

Barriada, J. L., A. D. Tappin, E. H. Evans and E. P. Achterberg (2007). "Dissolved silver measurements in seawater." TrAC Trends in Analytical Chemistry **26(8)**: 809-817.

Batley, G. E., J. K. Kirby and M. J. McLaughlin (2012). "Fate and Risks of Nanomaterials in Aquatic and Terrestrial Environments." Acc Chem Res.

Beers Jnr, R. F. and I. W. Sizer (1952). "A spectrophotometric method for measuring the breakdown of hydrogen peroxide by catalase." Journal of Biological Chemistry **195(1)**: 133-140.

Beninger, P. G., A. Veniot and Y. Poussart (1999). "Principles of pseudofeces rejection on the bivalve mantle: integration in particle processing." Marine Ecology Progress Series **178**: 259-269.

Benn, T. M. and P. Westerhoff (2008). "Nanoparticle Silver Released into Water from Commercially Available Sock Fabrics." Environ Sci Technol **42(11)**: 4133-4139.

Bernhardt, E. S., B. P. Colman, M. F. Hochella, B. J. Cardinale, R. M. Nisbet, C. J. Richardson and L. Yin (2010). "An Ecological Perspective on Nanomaterial Impacts in the Environment." Journal of Environment Quality **39(6)**: 1954.

Bhatt, I. and B. N. Tripathi (2011). "Interaction of engineered nanoparticles with various components of the environment and possible strategies for their risk assessment." Chemosphere **82(3)**: 308-317.

Bielmyer, G. K., M. Grosell and K. V. Brix (2006). "Toxicity of Silver, Zinc, Copper, and Nickel to the Copepod *Acartia tonsa* Exposed via a Phytoplankton Diet." Environ Sci Technol **40(6)**: 2063-2068.

Blaser, S. A., M. Scheringer, M. Macleod and K. Hungerbühler (2008). "Estimation of cumulative aquatic exposure and risk due to silver: contribution of nano-functionalized plastics and textiles." Sci Total Environ **390(2-3)**: 396-409.

Boyles, M. S., L. Young, D. M. Brown, L. MacCalman, H. Cowie, A. Moisala, F. Smail, P. J. Smith, L. Proudfoot, A. H. Windle and V. Stone (2015). "Multi-walled carbon nanotube induced frustrated phagocytosis, cytotoxicity and pro-inflammatory conditions in macrophages are length dependent and greater than that of asbestos." Toxicol In Vitro **29(7)**: 1513-1528.

Bradford, A., R. D. Handy, J. W. Readman, A. Atfield and M. Mühling (2009). "Impact of Silver Nanoparticle Contamination on the Genetic Diversity of Natural Bacterial Assemblages in Estuarine Sediments." Environ Sci Technol **43(12)**: 4530-4536.

Bradford, M. M. (1976). "A rapid and sensitive method for the quantitation of microgram quantities of protein utilizing the principle of protein-dye binding." Analytical Biochemistry **72(1-2)**: 248-254.

Brennecke, D., E. C. Ferreira, T. M. Costa, D. Appel, B. A. da Gama and M. Lenz (2015). "Ingested microplastics (>100 µm) are translocated to organs of the tropical fiddler crab *Uca rapax*." Mar Pollut Bull **96(1-2)**: 491-495.

Brown, D. M., I. A. Kinloch, U. Bangert, A. H. Windle, D. M. Walter, G. S. Walker, C. A. Scotchford, K. Donaldson and V. Stone (2007). "An in vitro study of the potential of carbon nanotubes and nanofibres to induce inflammatory mediators and frustrated phagocytosis." Carbon **45(9)**: 1743-1756.

Browne, M. A., A. Dissanayake, T. S. Galloway, D. M. Lowe and R. C. Thompson (2008). "Ingested Microscopic Plastic Translocates to the Circulatory System of the Mussel, *Mytilus edulis* (L.)." Environ Sci Technol **42(13)**: 5026-5031.

Browne, M. A., A. Dissanayake, T. S. Galloway, D. M. Lowe and R. C. Thompson (2008). "Ingested Microscopic Plastic Translocates to the Circulatory System of the Mussel, *Mytilus edulis*(L.)." Environmental Science & Technology **42**(13): 5026-5031.

Bryan, G. W. (1971). "The Effects of Heavy Metals (other than Mercury) on Marine and Estuarine Organisms." Proceedings of the Royal Society B: Biological Sciences **177**(1048): 389-410.

Bryan, G. W. (2009). "Concentrations of zinc and copper in the tissues of decapod crustaceans." Journal of the Marine Biological Association of the United Kingdom **48**(02): 303.

Bryan, G. W. (2009). "Concentrations of zinc and copper in the tissues of decapod crustaceans." J Mar Biol Assoc UK **48**(02): 303.

Buffet, P. E., C. Amiard-Triquet, A. Dybowska, C. Risso-de Faverney, M. Guibbolini, E. Valsami-Jones and C. Mouneyrac (2012). "Fate of isotopically labeled zinc oxide nanoparticles in sediment and effects on two endobenthic species, the clam *Scrobicularia plana* and the ragworm *Hediste diversicolor*." Ecotoxicol Environ Saf **84**: 191-198.

Buffet, P. E., J. F. Pan, L. Poirier, C. Amiard-Triquet, J. C. Amiard, P. Gaudin, C. Risso-de Faverney, M. Guibbolini, D. Gilliland, E. Valsami-Jones and C. Mouneyrac (2013). "Biochemical and behavioural responses of the endobenthic bivalve *Scrobicularia plana* to silver nanoparticles in seawater and microalgal food." Ecotoxicol Environ Saf **89**: 117-124.

Buffet, P. E., O. F. Tankoua, J. F. Pan, D. Berhanu, C. Herrenknecht, L. Poirier, C. Amiard-Triquet, J. C. Amiard, J. B. Berard, C. Risso, M. Guibbolini, M. Romeo, P. Reip, E. Valsami-Jones and C. Mouneyrac (2011). "Behavioural and biochemical responses of two marine invertebrates *Scrobicularia plana* and *Hediste diversicolor* to copper oxide nanoparticles." Chemosphere **84**(1): 166-174.

Burrell, S., T. Gunnarsson, K. Gunnarsson, D. Clarke and A. D. Turner (2013). "First detection of paralytic shellfish poisoning (PSP) toxins in Icelandic mussels (*Mytilus edulis*): Links to causative phytoplankton species." Food Control **31**(2): 295-301.

Bustamante, P. and P. Miramand (2005). "Subcellular and body distributions of 17 trace elements in the variegated scallop *Chlamys varia* from the French coast of the Bay of Biscay." Sci Total Environ **337**(1-3): 59-73.

Camargo, P. H. C., K. G. Satyanarayana and F. Wypych (2009). "Nanocomposites: synthesis, structure, properties and new application opportunities." Materials Research **12**(1).

Canesi, L., C. Ciacci, R. Fabbri, A. Marcomini, G. Pojana and G. Gallo (2012). "Bivalve molluscs as a unique target group for nanoparticle toxicity." Mar Environ Res **76**: 16-21.

Canesi, L., R. Fabbri, G. Gallo, D. Vallotto, A. Marcomini and G. Pojana (2010). "Biomarkers in *Mytilus galloprovincialis* exposed to suspensions of selected nanoparticles (Nano carbon black, C60 fullerene, Nano-TiO₂, Nano-SiO₂)." Aquat Toxicol **100**(2): 168-177.

Carlson, C., S. M. Hussain, A. M. Schrand, L. K. Braydich-Stolle, K. L. Hess, R. L. Jones and J. J. Schlager (2008). "Unique cellular interaction of silver nanoparticles: size-dependent generation of reactive oxygen species." J Phys Chem B **112**(43): 13608-13619.

Chan, C. Y. and J. M. Chiu (2015). "Chronic Effects of Coated Silver Nanoparticles on Marine Invertebrate Larvae: A Proof of Concept Study." PLoS One **10**(7): e0132457.

Chiarelli, R. and M. C. Roccheri (2014). "Marine Invertebrates as Bioindicators of Heavy Metal Pollution." Open Journal of Metal **04**(04): 93-106.

Choi, J. E., S. Kim, J. H. Ahn, P. Youn, J. S. Kang, K. Park, J. Yi and D. Y. Ryu (2010). "Induction of oxidative stress and apoptosis by silver nanoparticles in the liver of adult zebrafish." Aquat Toxicol **100**(2): 151-159.

Choi, O., T. E. Clevenger, B. Deng, R. Y. Surampalli, L. Ross, Jr. and Z. Hu (2009). "Role of sulfide and ligand strength in controlling nanosilver toxicity." Water Res **43**(7): 1879-1886.

Ciriolo, M. R., P. Civitareale, M. T. Carri, A. De Martino, F. Galiazzo and G. Rotilio (1994). "Purification and characterization of Ag,Zn-superoxide dismutase from *Saccharomyces cerevisiae* exposed to silver." Journal of Biological Chemistry **269**(41): 25783-25787.

Cleveland, D., S. E. Long, P. L. Pennington, E. Cooper, M. H. Fulton, G. I. Scott, T. Brewer, J. Davis, E. J. Petersen and L. Wood (2012). "Pilot estuarine mesocosm study on the environmental fate of Silver nanomaterials leached from consumer products." Sci Total Environ **421-422**: 267-272.

Comero, S., C. Klein, B. Stahlmecke, J. Romazanov, T. Kuhlbusch, E. Van Doren, P. Wick, G. Locoro, W. Koerdel, B. Gawlik, J. Mast, H. F. Krug, K. Hund-Rinke, S. Friedrichs, G. Maier, J. Werner and T. Linsinger (2011). NM-300 Silver Characterisation, Stability, Homogeneity, Joint Research Centre Institute: 95.

Cong, Y., G. T. Banta, H. Selck, D. Berhanu, E. Valsami-Jones and V. E. Forbes (2011). "Toxic effects and bioaccumulation of nano-, micron- and ionic-Ag in the polychaete, *Nereis diversicolor*." Aquat Toxicol **105**(3-4): 403-411.

Conway, J. R., S. K. Hanna, H. S. Lenihan and A. A. Keller (2014). "Effects and implications of trophic transfer and accumulation of CeO₂ nanoparticles in a marine mussel." Environ Sci Technol **48**(3): 1517-1524.

Cornelis, G., J. K. Kirby, D. Beak, D. Chittleborough and M. J. McLaughlin (2010). "A method for determination of retention of silver and cerium oxide manufactured nanoparticles in soils." Environmental Chemistry **7**(3): 298.

Côté, C., K. Lemarchand, I. Desbiens, M. Barthes, K. Osterheld, M. Millour, É. Pelletier, M. Fournier and P. Brousseau (2014). "Immunotoxicity of silver nanoparticles in blue mussel (*Mytilus edulis*)." Journal of Xenobiotics **4**(2).

Cozzari, M., A. C. Elia, N. Pacini, B. D. Smith, D. Boyle, P. S. Rainbow and F. R. Khan (2015). "Bioaccumulation and oxidative stress responses measured in the estuarine ragworm (*Nereis diversicolor*) exposed to dissolved, nano- and bulk-sized silver." Environ Pollut **198**: 32-40.

Croteau, M. N., A. D. Dybowska, S. N. Luoma and E. Valsami-Jones (2011). "A novel approach reveals that zinc oxide nanoparticles are bioavailable and toxic after dietary exposures." Nanotoxicology **5**(1): 79-90.

Croteau, M. N., S. K. Misra, S. N. Luoma and E. Valsami-Jones (2011). "Silver bioaccumulation dynamics in a freshwater invertebrate after aqueous and dietary exposures to nanosized and ionic Ag." Environ Sci Technol **45**(15): 6600-6607.

Crothers, J. H. (1967). "The biology of the shore crab *Carcinus maenas* (L.) 1. The background, anatomy, growth and life history." Field Studies Journal **2**(4): 407-434.

Dall, W. and D. J. W. Moriarty (1983). Functional Aspects of Nutrition and Digestion. London, Academic Press.

Danovaro, R., L. Bongiorno, C. Corinaldesi, D. Giovannelli, E. Damiani, P. Astolfi, L. Greci and A. Pusceddu (2008). "Sunscreens cause coral bleaching by promoting viral infections." Environ Health Perspect **116**(4): 441-447.

Davies, R. L. and S. F. Etris (1997). "The development and functions of silver in water purification and disease control." Catalysis Today **36**(1): 107-114.

de Laeter, J. R., J. K. Böhlke, P. De Bièvre, H. Hidaka, H. S. Peiser, K. J. R. Rosman and P. D. P. Taylor (2003). "Atomic weights of the elements. Review 2000 (IUPAC Technical Report)." Pure and Applied Chemistry **75**(6).

De Laeter, J. R., K. G. Heumann and K. J. R. Rosman (1991). "Isotopic Compositions of the Elements 1989." Journal of Physical and Chemical Reference Data **20**(6): 1327.

Deb, S. C. and T. Fukushima (2007). "Metals in aquatic ecosystems: mechanisms of uptake, accumulation and release-Ecotoxicological perspectives." International Journal of Environmental Studies **56**(3): 385-417.

DeForest, D. K., K. V. Brix and W. J. Adams (2007). "Assessing metal bioaccumulation in aquatic environments: the inverse relationship between bioaccumulation factors, trophic transfer factors and exposure concentration." Aquat Toxicol **84**(2): 236-246.

Demchick, P. and A. L. Koch (1996). "The permeability of the wall fabric of *Escherichia coli* and *Bacillus subtilis*." J Bacteriol **178**(3): 768-773.

Dogra, Y., K. P. Arkill, C. Elgy, B. Stolpe, J. Lead, E. Valsami-Jones, C. R. Tyler and T. S. Galloway (2016). "Cerium oxide nanoparticles induce oxidative stress in the sediment-dwelling amphipod *Corophium volutator*." *Nanotoxicology* **10**(4): 480-487.

Doiron, K., E. Pelletier and K. Lemarchand (2012). "Impact of polymer-coated silver nanoparticles on marine microbial communities: a microcosm study." *Aquat Toxicol* **124-125**: 22-27.

Domingos, R. F., M. A. Baalousha, Y. Ju-Nam, M. M. Reid, N. Tufenkji, J. R. Lead, G. G. Leppard and K. J. Wilkinson (2009). "Characterizing Manufactured Nanoparticles in the Environment: Multimethod Determination of Particle Sizes." *Environ Sci Technol* **43**(19): 7277-7284.

Donaldson, K., F. Murphy, A. Schinwald, R. Duffin and C. A. Poland (2011). "Identifying the pulmonary hazard of high aspect ratio nanoparticles to enable their safety-by-design." *Nanomedicine (Lond)* **6**(1): 143-156.

Ellis, T., R. Gardiner, M. Gubbins, A. Reese and D. Smith (2015). Aquaculture statistics for the UK, with a focus on England and Wales 2012. F. a. A. S. Centre for Environment. Weymouth, CEFAS.

EnvironmentAgency. (2011). "Chemical Standards Report: Silver." 2017, from <http://evidence.environment-agency.gov.uk/ChemicalStandards/report.aspx?cid=105>.

EPA (2009). Toxicological Review of Cerium Oxide and Cerium Compounds EPA/635/R-08/002F.

EPA, U. (2009). "National Recommended Water Quality Criteria." Retrieved 16th Jan 2012, 2013, from <http://water.epa.gov/scitech/swguidance/standards/criteria/current/index.cfm>.

EuropeanCommission. (2008). "Priority Substances and Certain Other Pollutants according to Annex II of Directive 2008/105/EC." from http://ec.europa.eu/environment/water/water-framework/priority_substances.htm.

Evelo, C. T., R. P. Bos and P. J. Borm (1993). "Decreased glutathione content and glutathione S-transferase activity in red blood cells of coal miners with early stages of pneumoconiosis." *Occupational and Environmental Medicine* **50**(7): 633-636.

Fabrega, J., S. R. Fawcett, J. C. Renshaw and J. R. Lead (2009). "Silver Nanoparticle Impact on Bacterial Growth: Effect of pH, Concentration, and Organic Matter." *Environ Sci Technol* **43**(19): 7285-7290.

Fabrega, J., J. C. Renshaw and J. R. Lead (2009). "Interactions of silver nanoparticles with *Pseudomonas putida* biofilms." *Environ Sci Technol* **43**(23): 9004-9009.

Fabrega, J., R. Tantra, A. Amer, B. Stolpe, J. Tomkins, T. Fry, J. R. Lead, C. R. Tyler and T. S. Galloway (2012). "Sequestration of zinc from zinc oxide nanoparticles and life cycle effects in the sediment dweller amphipod *Corophium volutator*." *Environ Sci Technol* **46**(2): 1128-1135.

Fabrega, J., R. Zhang, J. C. Renshaw, W. T. Liu and J. R. Lead (2011). "Impact of silver nanoparticles on natural marine biofilm bacteria." *Chemosphere* **85**(6): 961-966.

Fairbairn, E. A., A. A. Keller, L. Madler, D. Zhou, S. Pokhrel and G. N. Cherr (2011). "Metal oxide nanomaterials in seawater: linking physicochemical characteristics with biological response in sea urchin development." *J Hazard Mater* **192**(3): 1565-1571.

Falugi, C., M. G. Aluigi, M. C. Chiantore, D. Privitera, P. Ramoino, M. A. Gatti, A. Fabrizi, A. Pinsino and V. Matranga (2012). "Toxicity of metal oxide nanoparticles in immune cells of the sea urchin." *Mar Environ Res* **76**: 114-121.

Farrell, P. and K. Nelson (2013). "Trophic level transfer of microplastic: *Mytilus edulis* (L.) to *Carcinus maenas* (L.)." *Environ Pollut* **177**: 1-3.

Ferguson, J. C. and C. W. Walker (1991). "Cytology and function of the madreporite systems of the starfish *Henricia Sanguinolenta* and *Asterias Vulgaris*." *Journal of Morphology* **210**(1): 1-11.

Fernández-Reiriz, M. J., P. Range, X. A. Álvarez-Salgado, J. Espinosa and U. Labarta (2012). "Tolerance of juvenile *Mytilus galloprovincialis* to experimental seawater acidification." *Marine Ecology Progress Series* **454**: 65-74.

Ferry, J. L., P. Craig, C. Hexel, P. Sisco, R. Frey, P. L. Pennington, M. H. Fulton, I. G. Scott, A. W. Decho, S. Kashiwada, C. J. Murphy and T. J. Shaw (2009). "Transfer of gold nanoparticles from the water column to the estuarine food web." *Nat Nanotechnol* **4**(7): 441-444.

FOREGS. (2005). "Statistical Data of Analytical Results." Retrieved 4th February 2013, 2013, from <http://weppi.gtk.fi/publ/foregsatlas/article.php?id=15>.

Fortibuoni, T., S. Noventa, F. Rampazzo, C. Gion, M. Formalewicz, D. Berto and S. Raicevich (2013). "Evidence of butyltin biomagnification along the Northern Adriatic food-web (Mediterranean Sea) elucidated by stable isotope ratios." *Environ Sci Technol* **47**(7): 3370-3377.

Fu, P. P., Q. Xia, H. M. Hwang, P. C. Ray and H. Yu (2014). "Mechanisms of nanotoxicity: generation of reactive oxygen species." *J Food Drug Anal* **22**(1): 64-75.

Gagne, F., J. Auclair, P. Turcotte and C. Gagnon (2013). "Sublethal effects of silver nanoparticles and dissolved silver in freshwater mussels." *J Toxicol Environ Health A* **76**(8): 479-490.

Gagnon, J. and K. M. Fromm (2015). "Toxicity and Protective Effects of Cerium Oxide Nanoparticles (Nanoceria) Depending on Their Preparation Method, Particle Size, Cell Type, and Exposure Route." *European Journal of Inorganic Chemistry* **2015**(27): 4510-4517.

Gambardella, C., L. Gallus, A. M. Gatti, M. Faimali, S. Carbone, L. V. Antisari, C. Falugi and S. Ferrando (2014). "Toxicity and transfer of metal oxide nanoparticles from microalgae to sea urchin larvae." *Chemistry and Ecology* **30**(4): 308-316.

Garcia-Alonso, J., F. R. Khan, S. K. Misra, M. Turmaine, B. D. Smith, P. S. Rainbow, S. N. Luoma and E. Valsami-Jones (2011). "Cellular internalization of silver nanoparticles in gut epithelia of the estuarine polychaete *Nereis diversicolor*." *Environ Sci Technol* **45**(10): 4630-4636.

Garcia-Negrete, C. A., J. Blasco, M. Volland, T. C. Rojas, M. Hampel, A. Lapresta-Fernandez, M. C. Jimenez de Haro, M. Soto and A. Fernandez (2013). "Behaviour of Au-citrate nanoparticles in seawater and accumulation in bivalves at environmentally relevant concentrations." *Environ Pollut* **174**: 134-141.

Gazeau, F., L. M. Parker, S. Comeau, J.-P. Gattuso, W. A. O'Connor, S. Martin, H.-O. Pörtner and P. M. Ross (2013). "Impacts of ocean acidification on marine shelled molluscs." *Marine Biology* **160**(8): 2207-2245.

George, S. G., B. J. S. Pirie and T. L. Coombs (1976). "The kinetics of accumulation and excretion of ferric hydroxide in *Mytilus edulis* (L.) and its distribution in the tissues." *Journal of Experimental Marine Biology and Ecology* **23**(1): 71-84.

George, S. G., B. J. S. Pirie and T. L. Coombs (1980). "Isolation and elemental analysis of metal-rich granules from the kidney of the scallop, *Pecten maximus* (L.)." *Journal of Experimental Marine Biology and Ecology* **42**(2): 143-156.

Géret, F. (2002). "Influence of metal exposure on metallothionein synthesis and lipid peroxidation in two bivalve mollusks: the oyster (*Crassostrea gigas*) and the mussel (*Mytilus edulis*)." *Aquatic Living Resources* **15**(1): 61-66.

Ghaznavi, H., R. Najafi, S. Mehrzadi, A. Hosseini, N. Tekyemaroof, A. Shakeri-Zadeh, M. Rezayat and A. M. Sharifi (2015). "Neuro-protective effects of cerium and yttrium oxide nanoparticles on high glucose-induced oxidative stress and apoptosis in undifferentiated PC12 cells." *Neurol Res* **37**(7): 624-632.

Gomes, S. I., D. Hansen, J. J. Scott-Fordsmand and M. J. Amorim (2015). "Effects of silver nanoparticles to soil invertebrates: oxidative stress biomarkers in *Eisenia fetida*." *Environ Pollut* **199**: 49-55.

Gomes, T., O. Araujo, R. Pereira, A. C. Almeida, A. Cravo and M. J. Bebianno (2013a). "Genotoxicity of copper oxide and silver nanoparticles in the mussel *Mytilus galloprovincialis*." *Mar Environ Res* **84**: 51-59.

Gomes, T., C. G. Pereira, C. Cardoso and M. J. Bebianno (2013b). "Differential protein expression in mussels *Mytilus galloprovincialis* exposed to nano and ionic Ag." *Aquat Toxicol* **136-137**: 79-90.

Gomes, T., C. G. Pereira, C. Cardoso, J. P. Pinheiro, I. Cancio and M. J. Bebianno (2012). "Accumulation and toxicity of copper oxide nanoparticles in the digestive gland of *Mytilus galloprovincialis*." *Aquat Toxicol* **118-119**: 72-79.

Gomes, T., C. G. Pereira, C. Cardoso, V. S. Sousa, M. R. Teixeira, J. P. Pinheiro and M. J. Bebianno (2014). "Effects of silver nanoparticles exposure in the mussel *Mytilus galloprovincialis*." *Mar Environ Res* **101**: 208-214.

Gomes, T., J. P. Pinheiro, I. Cancio, C. G. Pereira, C. Cardoso and M. J. Bebianno (2011). "Effects of copper nanoparticles exposure in the mussel *Mytilus galloprovincialis*." *Environ Sci Technol* **45**(21): 9356-9362.

Goodman, S. H. and M. J. Cavey (1990). "Organization of a phyllobranchiate gill from the green shore crab *Carcinus maenas* (Crustacea, Decapoda)." *Cell and Tissue Research* **260**(3): 495-505.

Gottschalk, F., T. Sonderer, R. W. Scholz and B. Nowack (2009). "Modeled environmental concentrations of engineered nanomaterials (TiO₂, ZnO, Ag, CNT, Fullerenes) for different regions." *Environ Sci Technol* **43**(24): 9216-9222.

Gottschalk, F., T. Sun and B. Nowack (2013). "Environmental concentrations of engineered nanomaterials: review of modeling and analytical studies." *Environ Pollut* **181**: 287-300.

Gupta, A., S. Das, C. J. Neal and S. Seal (2016). "Controlling the surface chemistry of cerium oxide nanoparticles for biological applications." *J. Mater. Chem. B* **4**(19): 3195-3202.

Hach (2009). Nitrogen, Ammonia (0 to 0.50mg/L NH₃-N), Salicylate method: 5.

Halliwell, B. (1991). "Reactive oxygen species in living systems: Source, biochemistry, and role in human disease." *The American Journal of Medicine* **91**(3): S14-S22.

Halliwell, B. and J. M. C. Gutteridge (2007). *Free Radicals in Biology and Medicine*. Oxford, UK, Oxford University Press.

Handy, R. D., F. von der Kammer, J. R. Lead, M. Hasselov, R. Owen and M. Crane (2008). "The ecotoxicology and chemistry of manufactured nanoparticles." *Ecotoxicology* **17**(4): 287-314.

Hanna, S. K., R. J. Miller, D. Zhou, A. A. Keller and H. S. Lenihan (2013). "Accumulation and toxicity of metal oxide nanoparticles in a soft-sediment estuarine amphipod." *Aquat Toxicol* **142-143**: 441-446.

Hansson, S., J. E. Hobbie, R. Elmgren, U. Larsson, B. Fry and S. Johansson (1997). "The Stable Nitrogen Isotope Ratio as a Marker of Food-Web Interactions and Fish Migration." *Ecology* **78**(7): 2249-2257.

Hawthorne, J., R. De la Torre Roche, B. Xing, L. A. Newman, X. Ma, S. Majumdar, J. Gardea-Torresdey and J. C. White (2014). "Particle-size dependent accumulation and trophic transfer of cerium oxide through a terrestrial food chain." *Environ Sci Technol* **48**(22): 13102-13109.

Hebel, D. K., M. B. Jones and M. H. Depledge (1997). "Responses of Crustaceans to Contaminant Exposure: a Holistic Approach." *Estuarine, Coastal and Shelf Science* **44**(2): 177-184.

Hebel, D. K., M. B. Jones, R. M. Moate and M. H. Depledge (1999). "Differing sensitivities of respiratory and osmoregulatory gill tissue of *Carcinus maenas* (Crustacea: Decapoda) to water-borne copper." *Marine Biology* **133**(4): 675-681.

Heckert, E. G., A. S. Karakoti, S. Seal and W. T. Self (2008). "The role of cerium redox state in the SOD mimetic activity of nanoceria." *Biomaterials* **29**(18): 2705-2709.

Heckert, E. G., S. Seal and W. T. Self (2008). "Fenton-Like Reaction Catalyzed by the Rare Earth Inner Transition Metal Cerium." *Environmental Science & Technology* **42**(13): 5014-5019.

Henry, R. P., Č. Lucu, H. Onken and D. Weihrauch (2012). "Multiple functions of the crustacean gill: osmotic/ionic regulation, acid-base balance, ammonia excretion, and bioaccumulation of toxic metals." *Frontiers in Physiology* **3**.

Hoecke, K. V., J. T. K. Quik, J. Mankiewicz-Boczek, K. A. C. D. Schamphelaere, A. Elsaesser, P. V. d. Meeren, C. Barnes, G. McKerr, C. V. Howard, D. V. D. Meent, K. Rydzyński, K. A. Dawson, A. Salvati, A. Lesniak, I. Lynch, G. Silversmit, B. r. D. Samber, L. Vincze and C. R. Janssen (2009). "Fate and Effects of CeO₂ Nanoparticles in Aquatic Ecotoxicity Tests." *Environmental Science & Technology* **43**(12): 4537-4546.

Holbrook, R. D., K. E. Murphy, J. B. Morrow and K. D. Cole (2008). "Trophic transfer of nanoparticles in a simplified invertebrate food web." *Nat Nanotechnol* **3**(6): 352-355.

Hopkin, S. P. and J. A. Nott (2009). "Some observations on concentrically structured, intracellular granules in the hepatopancreas of the shore crab *Carcinus maenas* (L.)." Journal of the Marine Biological Association of the United Kingdom **59**(04): 867.

Hopkin, S. P. and J. A. Nott (2009). "Studies on the digestive cycle of the shore crab *Carcinus maenas* (L.) with special reference to the b cells in the hepatopancreas." Journal of the Marine Biological Association of the United Kingdom **60**(04): 891.

Hotze, E. M., T. Phenrat and G. V. Lowry (2010). "Nanoparticle Aggregation: Challenges to Understanding Transport and Reactivity in the Environment." Journal of Environment Quality **39**(6): 1909.

Howie, A. F., L. M. Forrester, M. J. Glancey, J. J. Schlager, G. Powis, G. J. Beckett, J. D. Hayes and C. R. Wolf (1990). "Glutathione S-transferase and glutathione peroxidase expression in normal and tumour human tissues." Carcinogenesis **11**(3): 451-458.

Hu, M., L. Li, Y. Sui, J. Li, Y. Wang, W. Lu and S. Dupont (2015). "Effect of pH and temperature on antioxidant responses of the thick shell mussel *Mytilus coruscus*." Fish Shellfish Immunol **46**(2): 573-583.

Hu, W., S. Culloty, G. Darmody, S. Lynch, J. Davenport, S. Ramirez-Garcia, K. A. Dawson, I. Lynch, J. Blasco and D. Sheehan (2014). "Toxicity of copper oxide nanoparticles in the blue mussel, *Mytilus edulis*: a redox proteomic investigation." Chemosphere **108**: 289-299.

Hull, M. S., P. J. Vikesland and I. R. Schultz (2013). "Uptake and retention of metallic nanoparticles in the Mediterranean mussel (*Mytilus galloprovincialis*)." Aquat Toxicol **140-141**: 89-97.

Jennings, J. R. and P. S. Rainbow (1979). "Studies on the uptake of cadmium by the crab *Carcinus maenas* in the laboratory. I. Accumulation from seawater and a food source." Marine Biology **50**(2): 131-139.

Jeong, S. H., Y. H. Hwang and S. C. Yi (2005). "Antibacterial properties of padded PP/PE nonwovens incorporating nano-sized silver colloids." Journal of Materials Science **40**(20): 5413-5418.

Jiang, H. S., X. N. Qiu, G. B. Li, W. Li and L. Y. Yin (2014). "Silver nanoparticles induced accumulation of reactive oxygen species and alteration of antioxidant systems in the aquatic plant *Spirodela polyrrhiza*." Environ Toxicol Chem **33**(6): 1398-1405.

Johnson, A. C. and B. Park (2012). "Predicting contamination by the fuel additive cerium oxide engineered nanoparticles within the United Kingdom and the associated risks." Environ Toxicol Chem **31**(11): 2582-2587.

Johnson, P. T. (1987). "A review of fixed phagocytic and pinocytotic cells of decapod crustaceans, with remarks on hemocytes." Developmental & Comparative Immunology **11**(4): 679-704.

Jones, H. D., O. G. Richards and T. A. Southern (1992). "Gill dimensions, water pumping rate and body size in the mussel *Mytilus edulis* L." Journal of Experimental Marine Biology and Ecology **155**(2): 213-237.

Jørgensen, C. B. (1974). "On gill function in the mussel *Mytilus Edulis* L." Ophelia **13**(1-2): 187-232.

Joshi, S., E. A. Kulp, W. G. Fahrenholtz and M. J. O'Keefe (2012). "Dissolution of cerium from cerium-based conversion coatings on Al 7075-T6 in 0.1M NaCl solutions." Corrosion Science **60**: 290-295.

JRC-IRMM (2011). Zinc Oxide NM-110, NM-111, NM-112, NM-113 Characterisation and Test Item Preparation NM-Series of Representative Manufactured Nanomaterials.

JRC (2011). List of Materials in the JRC Nanomaterials (NM) Repository.

JRC (2014). Towards a review of the EC Recommendation for a definition of the term "nanomaterial". Part 2: Assessment of collected information concerning the experience with the definition G. Roebben and H. Rauscher. Luxembourg, JRC. **EUR 26744 EN**: 89.

Kach, D. J. and J. E. Ward (2008). "The role of marine aggregates in the ingestion of picoplankton-size particles by suspension-feeding molluscs." Mar Biol **153**(5): 797-805.

Kadar, E., D. M. Lowe, M. Sole, A. S. Fisher, A. N. Jha, J. W. Readman and T. H. Hutchinson (2010). "Uptake and biological responses to nano-Fe versus soluble FeCl₃ in excised mussel gills." *Anal Bioanal Chem* **396**(2): 657-666.

Kadar, E., F. Simmance, O. Martin, N. Voulvoulis, S. Widdicombe, S. Mitov, J. R. Lead and J. W. Readman (2010). "The influence of engineered Fe₂O₃ nanoparticles and soluble (FeCl₃) iron on the developmental toxicity caused by CO₂-induced seawater acidification." *Environ Pollut* **158**(12): 3490-3497.

Kandasamy, K., N. M. Alikunhi, G. Manickaswami, A. Nabikhan and G. Ayyavu (2012). "Synthesis of silver nanoparticles by coastal plant *Prosopis chilensis* (L.) and their efficacy in controlling vibriosis in shrimp *Penaeus monodon*." *Applied Nanoscience*.

Katsumiti, A., D. Gilliland, I. Arostegui and M. P. Cajaraville (2015). "Mechanisms of Toxicity of Ag Nanoparticles in Comparison to Bulk and Ionic Ag on Mussel Hemocytes and Gill Cells." *PLoS One* **10**(6): e0129039.

Kavitha, R., S. Deepa Rani, S. Sivagnanam and M. Padmaja (2013). "Cadmium Nanoparticle Induced Histological and Biochemical changes in Hepatopancreas of Mud Crab *Scylla olivacea* (Herbst, 1796)." *Journal of Academia and Industrial Research* **2**(3): 205-209.

Kehrer, J. P. (2000). "The Haber–Weiss reaction and mechanisms of toxicity." *Toxicology* **149**(1): 43-50.

Keller, A. A. and A. Lazareva (2014). "Predicted Releases of Engineered Nanomaterials: From Global to Regional to Local." *Environmental Science & Technology Letters* **1**(1): 65-70.

Keller, A. A., S. McFerran, A. Lazareva and S. Suh (2013). "Global life cycle releases of engineered nanomaterials." *Journal of Nanoparticle Research* **15**(6).

Keller, A. A., H. Wang, D. Zhou, H. S. Lenihan, G. Cherr, B. J. Cardinale, R. Miller and Z. Ji (2010). "Stability and aggregation of metal oxide nanoparticles in natural aqueous matrices." *Environ Sci Technol* **44**(6): 1962-1967.

Khodashenas, B. and H. R. Ghorbani (2015). "Synthesis of silver nanoparticles with different shapes." *Arabian Journal of Chemistry*.

Kittler, S., C. Greulich, J. Diendorf, M. Köller and M. Eppele (2010). "Toxicity of Silver Nanoparticles Increases during Storage Because of Slow Dissolution under Release of Silver Ions." *Chemistry of Materials* **22**(16): 4548-4554.

Koehler, A., U. Marx, K. Broeg, S. Bahns and J. Bressling (2008). "Effects of nanoparticles in *Mytilus edulis* gills and hepatopancreas - a new threat to marine life?" *Mar Environ Res* **66**(1): 12-14.

Korsvik, C., S. Patil, S. Seal and W. T. Self (2007). "Superoxide dismutase mimetic properties exhibited by vacancy engineered ceria nanoparticles." *Chem Commun (Camb)*(10): 1056-1058.

Lai, R. W. S., K. W. Y. Yeung, M. M. N. Yung, A. B. Djuricic, J. P. Giesy and K. M. Y. Leung (2018). "Regulation of engineered nanomaterials: current challenges, insights and future directions." *Environ Sci Pollut Res Int* **25**(4): 3060-3077.

Langton, R. W. (1977). "Digestive rhythms in the mussel *Mytilus edulis*." *Marine Biology* **41**(1): 53-58.

Larner, F., Y. Dogra, A. Dybowska, J. Fabrega, B. Stolpe, L. J. Bridgestock, R. Goodhead, D. J. Weiss, J. Moger, J. R. Lead, E. Valsami-Jones, C. R. Tyler, T. S. Galloway and M. Rehkamper (2012). "Tracing bioavailability of ZnO nanoparticles using stable isotope labeling." *Environ Sci Technol* **46**(21): 12137-12145.

Larner, F. and M. Rehkamper (2012). "Evaluation of stable isotope tracing for ZnO nanomaterials--new constraints from high precision isotope analyses and modeling." *Environ Sci Technol* **46**(7): 4149-4158.

Laughlin, R. B., W. French and H. E. Guard (1986). "Accumulation of bis(tributyltin) oxide by the marine mussel *Mytilus edulis*." *Environ Sci Technol* **20**(9): 884-890.

Lee, D., R. E. Cohen and M. F. Rubner (2005). "Antibacterial properties of Ag nanoparticle loaded multilayers and formation of magnetically directed antibacterial microparticles." *Langmuir* **21**(21): 9651-9659.

Lewinski, N. A., H. Zhu, C. R. Ouyang, G. P. Conner, D. S. Wagner, V. L. Colvin and R. A. Drezek (2011). "Trophic transfer of amphiphilic polymer coated CdSe/ZnS quantum dots to *Danio rerio*." Nanoscale **3**(8): 3080-3083.

Li, B., J. E. Ward and B. A. Holohan (2008). "Transparent exopolymer particles (TEP) from marine suspension feeders enhance particle aggregation." Marine Ecology Progress Series **357**: 67-77.

Li, H., A. Turner and M. T. Brown (2012). "Accumulation of Aqueous and Nanoparticulate Silver by the Marine Gastropod *Littorina littorea*." Water, Air, & Soil Pollution **224**(1).

Li, P., Q. Peng and Y. Li (2011). "Controlled synthesis and self-assembly of highly monodisperse Ag and Ag₂S nanocrystals." Chemistry **17**(3): 941-946.

Lima, I., S. M. Moreira, J. R. Osten, A. M. Soares and L. Guilhermino (2007). "Biochemical responses of the marine mussel *Mytilus galloprovincialis* to petrochemical environmental contamination along the North-western coast of Portugal." Chemosphere **66**(7): 1230-1242.

Liu, J. and R. H. Hurt (2010). "Ion release kinetics and particle persistence in aqueous nano-silver colloids." Environ Sci Technol **44**(6): 2169-2175.

Liu, J., D. A. Sonshine, S. Shervani and R. H. Hurt (2010). "Controlled release of biologically active silver from nanosilver surfaces." ACS Nano **4**(11): 6903-6913.

Livingstone, D. R., F. Lips, P. G. Martinez and R. K. Pipe (1992). "Antioxidant enzymes in the digestive gland of the common mussel *Mytilus edulis*." Marine Biology **112**(2): 265-276.

Livingstone, I. (1995). "Basic features of a generalized mollusc showing the internal anatomy " Retrieved 7th March 2018, 2018, from http://biodidac.bio.uottawa.ca/thumbnails/filedet.htm/File_name/gast003b/File_type/gif.

Lodeiro, P., T. J. Browning, E. P. Achterberg, A. Guillou and M. S. El-Shahawi (2017). "Mechanisms of silver nanoparticle toxicity to the coastal marine diatom *Chaetoceros curvisetus*." Sci Rep **7**(1): 10777.

Lovell, M. A., C. Xie and W. R. Markesbery (1998). "Decreased glutathione transferase activity in brain and ventricular fluid in Alzheimer's disease." Neurology **51**(6): 1562-1566.

Lubick, N. (2008). "Nanosilver toxicity: ions, nanoparticles • or both?" Environmental Science & Technology **42**(23): 8617-8617.

Luoma, S. N. (2008). PEN 15 - Silver Nanotechnologies and the Environment: Old Problems or New Challenges?

Luoma, S. N., Y. B. Ho and G. W. Bryan (1995). "Fate, bioavailability and toxicity of silver in estuarine environments." Marine Pollution Bulletin **31**(1-3): 44-54.

Lushchak, V. I. (2011). "Environmentally induced oxidative stress in aquatic animals." Aquat Toxicol **101**(1): 13-30.

Malleve, F., T. F. Fernandes and T. J. Aspray (2014). "Silver, zinc oxide and titanium dioxide nanoparticle ecotoxicity to bioluminescent *Pseudomonas putida* in laboratory medium and artificial wastewater." Environ Pollut **195**: 218-225.

Manzo, S., M. L. Miglietta, G. Rametta, S. Buono and G. Di Francia (2013). "Toxic effects of ZnO nanoparticles towards marine algae *Dunaliella tertiolecta*." Sci Total Environ **445-446**: 371-376.

Marigomez, I., M. Soto, M. P. Cajaraville, E. Angulo and L. Giamberini (2002). "Cellular and subcellular distribution of metals in molluscs." Microsc Res Tech **56**(5): 358-392.

Marnett, L. J. (1999). "Lipid peroxidation—DNA damage by malondialdehyde." Mutation Research/Fundamental and Molecular Mechanisms of Mutagenesis **424**(1-2): 83-95.

Martin, J. L. M. (1973). "Iron metabolism in *Cancer irroratus* (crustacea decapoda) during the intermoult cycle, with special reference to iron in the gills." Comparative Biochemistry and Physiology Part A: Physiology **46**(1): 123-129.

Mathews, T. and N. S. Fisher (2008). "Evaluating the trophic transfer of cadmium, polonium, and methylmercury in an estuarine food chain." Environ Toxicol Chem **27**(5): 1093-1101.

Matranga, V. and I. Corsi (2012). "Toxic effects of engineered nanoparticles in the marine environment: model organisms and molecular approaches." Mar Environ Res **76**: 32-40.

McCarthy, M. P., D. L. Carroll and A. H. Ringwood (2013). "Tissue specific responses of oysters, *Crassostrea virginica*, to silver nanoparticles." Aquat Toxicol **138-139**: 123-128.

McCumber, L. J. and L. W. Clem (1977). "Recognition of viruses and xenogeneic proteins by the blue crab, *Callinectes sapidus*. I. Clearance and organ concentration." Developmental & Comparative Immunology **1**(1): 5-14.

McLaughlin, P. A. (1980). Comparative Morphology of Recent Crustacea. San Francisco, W. H. Freeman & Co.

McQuillan, J. S., H. G. Infante, E. Stokes and A. M. Shaw (2012). "Silver nanoparticle enhanced silver ion stress response in *Escherichia coli* K12." Nanotoxicology **6**: 857-866.

McShan, D., P. C. Ray and H. Yu (2014). "Molecular toxicity mechanism of nanosilver." J Food Drug Anal **22**(1): 116-127.

Meister, A. and M. E. Anderson (1983). "Glutathione." Annu Rev Biochem **52**: 711-760.

Mermillod-Blondin, F. and R. Rosenberg (2006). "Ecosystem engineering: the impact of bioturbation on biogeochemical processes in marine and freshwater benthic habitats." Aquatic Sciences **68**(4): 434-442.

Meyhöfer, E. (1985). "Comparative Pumping Rates in Suspension-Feeding Bivalves." Mar Biol **85**(2): 137-142.

Miao, A. J., K. A. Schwehr, C. Xu, S. J. Zhang, Z. Luo, A. Quigg and P. H. Santschi (2009). "The algal toxicity of silver engineered nanoparticles and detoxification by exopolymeric substances." Environ Pollut **157**(11): 3034-3041.

MilestoneSRL. (2013). "Apps Form Request." from http://www.milestonesrl.com/en/various/library-request.html?method_request=HPR-FO-30%20Oyster%20tissue.

Miller, A. F. (2012). "Superoxide dismutases: ancient enzymes and new insights." FEBS Lett **586**(5): 585-595.

Miller, K. G., R. G. Fairbanks and G. S. Mountain (1987). "Tertiary oxygen isotope synthesis, sea level history, and continental margin erosion." Paleoceanography **2**(1): 1-19.

Miller, R. J., H. S. Lenihan, E. B. Muller, N. Tseng, S. K. Hanna and A. A. Keller (2010). "Impacts of metal oxide nanoparticles on marine phytoplankton." Environ Sci Technol **44**(19): 7329-7334.

Møhlenberg, F. and H. U. Riisgård (1978). "Efficiency of particle retention in 13 species of suspension feeding bivalves." Ophelia **17**(2): 239-246.

Monserat, J. M., P. E. Martinez, L. A. Geracitano, L. L. Amado, C. M. Martins, G. L. Pinho, I. S. Chaves, M. Ferreira-Cravo, J. Ventura-Lima and A. Bianchini (2007). "Pollution biomarkers in estuarine animals: critical review and new perspectives." Comp Biochem Physiol C Toxicol Pharmacol **146**(1-2): 221-234.

Montes, M. O., S. K. Hanna, H. S. Lenihan and A. A. Keller (2012). "Uptake, accumulation, and biotransformation of metal oxide nanoparticles by a marine suspension-feeder." J Hazard Mater **225-226**: 139-145.

Moore, M. N. (2006). "Do nanoparticles present ecotoxicological risks for the health of the aquatic environment?" Environ Int **32**(8): 967-976.

Morris, R. J. and E. Tentori (1985). "The lipid composition of the foregut wall of *Carcinus maenas* and its relationship to observed permeability." Comparative Biochemistry and Physiology Part B: Comparative Biochemistry **82**(4): 695-697.

Mos, B., K. L. Kaposi, A. L. Rose, B. Kelaher and S. A. Dworjanyn (2017). "Moderate ocean warming mitigates, but more extreme warming exacerbates the impacts of zinc from engineered nanoparticles on a marine larva." Environ Pollut **228**: 190-200.

Murai, R., A. Sugimoto, S. Tanabe and I. Takeuchi (2008). "Biomagnification profiles of tributyltin (TBT) and triphenyltin (TPT) in Japanese coastal food webs elucidated by stable nitrogen isotope ratios." Chemosphere **73**(11): 1749-1756.

Nicolini, V., E. Gambuzzi, G. Malavasi, L. Menabue, M. C. Menziani, G. Lusvardi, A. Pedone, F. Benedetti, P. Luches, S. D'Addato and S. Valeri (2015). "Evidence of catalase mimetic activity in Ce(3+)/Ce(4+) doped bioactive glasses." J Phys Chem B **119**(10): 4009-4019.

Nimse, S. B. and D. Pal (2015). "Free radicals, natural antioxidants, and their reaction mechanisms." RSC Advances **5**(35): 27986-28006.

Niu, J., A. Azfer, L. M. Rogers, X. Wang and P. E. Kolattukudy (2007). "Cardioprotective effects of cerium oxide nanoparticles in a transgenic murine model of cardiomyopathy." Cardiovasc Res **73**(3): 549-559.

O'Brien, N. and E. Cummins (2010). "Ranking initial environmental and human health risk resulting from environmentally relevant nanomaterials." J Environ Sci Health A Tox Hazard Subst Environ Eng **45**(8): 992-1007.

OECD (2009). "Nanotechnology: An Overview Based on Indicators and Statistics [DSTI/DOC(2009)7 - JT03267289]."

Okazaki, R. K. and M. H. Panietz (1981). "Depuration of twelve trace metals in tissues of the oysters *Crassostrea gigas* and *C. virginica*." Marine Biology **63**(2): 113-120.

Oral, R., P. Bustamante, M. Warnau, A. D'Ambra, M. Guida and G. Pagano (2010). "Cytogenetic and developmental toxicity of cerium and lanthanum to sea urchin embryos." Chemosphere **81**(2): 194-198.

Pan, J. F., P. E. Buffet, L. Poirier, C. Amiard-Triquet, D. Gilliland, Y. Joubert, P. Pilet, M. Guibolini, C. Risso de Faverney, M. Romeo, E. Valsami-Jones and C. Mouneyrac (2012). "Size dependent bioaccumulation and ecotoxicity of gold nanoparticles in an endobenthic invertebrate: the Tellinid clam *Scrobicularia plana*." Environ Pollut **168**: 37-43.

Park, B., K. Donaldson, R. Duffin, L. Tran, F. Kelly, I. Mudway, J. P. Morin, R. Guest, P. Jenkinson, Z. Samaras, M. Giannouli, H. Kouridis and P. Martin (2008). "Hazard and risk assessment of a nanoparticulate cerium oxide-based diesel fuel additive - a case study." Inhal Toxicol **20**(6): 547-566.

Park, E. J., J. Yi, Y. Kim, K. Choi and K. Park (2010). "Silver nanoparticles induce cytotoxicity by a Trojan-horse type mechanism." Toxicol In Vitro **24**(3): 872-878.

Parmar, T. K., D. Rawtani and Y. K. Agrawal (2016). "Bioindicators: the natural indicator of environmental pollution." Frontiers in Life Science **9**(2): 110-118.

PEN (2012). "Silver Nanotechnology: A Database of Silver Nanotechnology in Commercial Products."

Peng, X., S. Palma, N. S. Fisher and S. S. Wong (2011). "Effect of morphology of ZnO nanostructures on their toxicity to marine algae." Aquat Toxicol **102**(3-4): 186-196.

Perez-Roses, R., E. Risco, R. Vila, P. Penalver and S. Canigual (2015). "Antioxidant activity of Tween-20 and Tween-80 evaluated through different in-vitro tests." J Pharm Pharmacol **67**(5): 666-672.

Perkins, E. J. (1967). "Some aspects of the biology of *Carcinus maenas* (L.)." Trans J Proc Dumfries Galloway nat Hist Antiq Soc **44**: 47-56.

Perneger, T. V. (1998). "What's wrong with Bonferroni adjustments?" British Medical Journal **316**(7139): 1236-1238.

Petersen, E. J., T. B. Henry, J. Zhao, R. I. MacCuspie, T. L. Kirschling, M. A. Dobrovolskaia, V. Hackley, B. Xing and J. C. White (2014). "Identification and avoidance of potential artifacts and misinterpretations in nanomaterial ecotoxicity measurements." Environ Sci Technol **48**(8): 4226-4246.

Piao, M. J., K. A. Kang, I. K. Lee, H. S. Kim, S. Kim, J. Y. Choi, J. Choi and J. W. Hyun (2011). "Silver nanoparticles induce oxidative cell damage in human liver cells through inhibition of reduced glutathione and induction of mitochondria-involved apoptosis." Toxicol Lett **201**(1): 92-100.

Pipe, R. K., C. Porte and D. R. Livingstone (1993). "Antioxidant enzymes associated with the blood cells and haemolymph of the mussel *Mytilus edulis*." Fish & Shellfish Immunology **3**(3): 221-233.

Pirmohamed, T., J. M. Dowding, S. Singh, B. Wasserman, E. Heckert, A. S. Karakoti, J. E. King, S. Seal and W. T. Self (2010). "Nanoceria exhibit redox state-dependent catalase mimetic activity." *Chem Commun (Camb)* **46**(16): 2736-2738.

Poland, C. A., R. Duffin, I. Kinloch, A. Maynard, W. A. Wallace, A. Seaton, V. Stone, S. Brown, W. Macnee and K. Donaldson (2008). "Carbon nanotubes introduced into the abdominal cavity of mice show asbestos-like pathogenicity in a pilot study." *Nat Nanotechnol* **3**(7): 423-428.

PROSPeCT (2010). Protocol for Nanoparticle Dispersion. *Ecotoxicology Test Protocols for Representative Nanomaterials in Support of the OECD Sponsorship Programme*, Nanotechnology Industries Association: 10.

Pulido-Reyes, G., I. Rodea-Palomares, S. Das, T. S. Sakthivel, F. Leganes, R. Rosal, S. Seal and F. Fernandez-Pinas (2015). "Untangling the biological effects of cerium oxide nanoparticles: the role of surface valence states." *Sci Rep* **5**: 15613.

Quik, J. T., I. Lynch, K. Van Hoecke, C. J. Miermans, K. A. De Schamphelaere, C. R. Janssen, K. A. Dawson, M. A. Stuart and D. Van De Meent (2010). "Effect of natural organic matter on cerium dioxide nanoparticles settling in model fresh water." *Chemosphere* **81**(6): 711-715.

Radenac, G., D. Fichet and P. Miramand (2001). "Bioaccumulation and toxicity of four dissolved metals in *Paracentrotus lividus* sea-urchin embryo." *Mar Environ Res* **51**: 151-166.

Rainbow, P. S. (2009). "Trace Metal Accumulation in Marine Invertebrates: Marine Biology or Marine Chemistry?" *Journal of the Marine Biological Association of the United Kingdom* **77**(01): 195.

Rasband, W. S. (1997-2015). "ImageJ v1.48." from <http://imagej.nih.gov/ij/>.

Ravindran, R., S. Juliet, A. K. Gopalan, A. K. Kavalimakkil, S. A. Ramankutty, S. N. Nair, P. M. Narayanan and S. Ghosh (2011). "Toxicity of DMSO, Triton X 100 and Tween 20 against *Rhipicephalus (Boophilus) annulatus*." *J Parasit Dis* **35**(2): 237-239.

REACH. (2015). "Nanomaterials." Retrieved 25th November, 2015, from http://ec.europa.eu/growth/sectors/chemicals/reach/nanomaterials/index_en.htm.

Reddy, N. A. and N. R. Menon (1979). "Effects of Ammonia and Ammonium on Tolerance and Byssogenesis in *Perna viridis*." *Marine Ecology Progress Series* **1**: 315-321.

Reddy, T. K., T. N. V. K. V. Prasad and S. J. Reddy (2014). "Studies on combined effect of *Aeromonas hydrophila* and cadmium on lipid peroxidation and antioxidant status in selected tissues of Indian freshwater major carp, *Catla catla*: role of silver nanoparticles." *IOSR Journal of Pharmacy (IOSRPHR)* **4**(10): 01-07.

Reid, D. G., P. Abelló, M. J. Kaiser and C. G. Warman (1997). "Carapace Colour, Inter-moult Duration and the Behavioural and Physiological Ecology of the Shore Crab *Carcinus maenas*." *Estuarine, Coastal and Shelf Science* **44**(2): 203-211.

Ribeiro, M. J., V. L. Maria, J. J. Scott-Fordsmand and M. J. Amorim (2015). "Oxidative Stress Mechanisms Caused by Ag Nanoparticles (NM300K) are Different from Those of AgNO₃: Effects in the Soil Invertebrate *Enchytraeus crypticus*." *Int J Environ Res Public Health* **12**(8): 9589-9602.

Riisgård, H. U., P. P. Egede and I. Barreiro Saavedra (2011). "Feeding Behaviour of the Mussel, *Mytilus edulis*: New Observations, with a Minireview of Current Knowledge." *Journal of Marine Biology* **2011**: 1-13.

Riisgård, H. U., P. Funch and P. S. Larsen (2014). "The mussel filter-pump - present understanding, with a re-examination of gill preparations." *Acta Zoologica*: n/a-n/a.

Riisgård, H. U., P. S. Larsen and N. F. Nielsen (1996). "Particle capture in the mussel *Mytilus edulis*: The role of latero-frontal cirri." *Marine Biology* **127**(2): 259-266.

Ringwood, A. H., M. McCarthy, T. C. Bates and D. L. Carroll (2010). "The effects of silver nanoparticles on oyster embryos." *Mar Environ Res* **69** Suppl: S49-51.

Robinson, K. N., R. F. Tantra, A. T. , D. Sarantaridis, D. D. Gohil, C. R. G. Allen, P. Quincey and C. Minelli (2014). Global NanoMapp report: physico-chemical properties of NM 302 nano-silver reference material., National Physical Laboratory, Hampton Road, Teddington, Middlesex, TW11 0LW: 23.

Rosa, M., J. E. Ward, S. E. Shumway, G. H. Wikfors, E. Pales-Espinosa and B. Allam (2013). "Effects of particle surface properties on feeding selectivity in the eastern oyster *Crassostrea virginica* and the blue mussel *Mytilus edulis*." Journal of Experimental Marine Biology and Ecology **446**: 320-327.

Rosenkranz, P., Q. Chaudhry, V. Stone and T. F. Fernandes (2009). "A comparison of nanoparticle and fine particle uptake by *Daphnia magna*." Environ Toxicol Chem **28**(10): 2142-2149.

Sadok, S., R. Uglow and S. Haswell (1995). "Fluxes of haemolymph ammonia and free amino acids in *Mytilus edulis* exposed to ammonia." Marine Ecology Progress Series **129**: 177-187.

Salminen, R. e. (2005). "Geochemical Atlas of Europe. Part 1: Background Information, Methodology and Maps. Espoo: Geological Survey of Finland." from <http://weppi.gtk.fi/publ/foregsatlas/>.

Sánchez-Marín, P., J. I. Lorenzo, R. Blust and R. Beiras (2007). "Humic Acids Increase Dissolved Lead Bioavailability for Marine Invertebrates." Environ Sci Technol **41**(16): 5679-5684.

Sanudo-Wilhelmy, S. A. and A. R. Flegal (1992). "Anthropogenic silver in the Southern California Bight: a new tracer of sewage in coastal waters." Environmental Science & Technology **26**(11): 2147-2151.

Schubert, D., R. Dargusch, J. Raitano and S. W. Chan (2006). "Cerium and yttrium oxide nanoparticles are neuroprotective." Biochem Biophys Res Commun **342**(1): 86-91.

Scott-Fordsmand, J. J., J. M. Navas, K. Hund-Rinke, B. Nowack and M. J. B. Amorim (2017). "Nanomaterials to microplastics: Swings and roundabouts." Nano Today **17**: 7-10.

Scott, G. R. and K. A. Sloman (2004). "The effects of environmental pollutants on complex fish behaviour: integrating behavioural and physiological indicators of toxicity." Aquat Toxicol **68**(4): 369-392.

Scown, T. M., E. M. Santos, B. D. Johnston, B. Gaiser, M. Baalousha, S. Mitov, J. R. Lead, V. Stone, T. F. Fernandes, M. Jepson, R. van Aerle and C. R. Tyler (2010). "Effects of aqueous exposure to silver nanoparticles of different sizes in rainbow trout." Toxicol Sci **115**(2): 521-534.

SEPA (2005). Hydrogeological Risk Assessment for Landfills and the Derivation of Control and Trigger Levels, Version 2.12. SEPA Technical Guidance NOte.

Shanks, A. L. and E. W. Edmondson (1989). "Laboratory-Made Artificial Marine Snow - a Biological Model of the Real Thing." Mar Biol **101**(4): 463-470.

Shaw, B. J., G. Al-Bairuty and R. D. Handy (2012). "Effects of waterborne copper nanoparticles and copper sulphate on rainbow trout, (*Oncorhynchus mykiss*): physiology and accumulation." Aquat Toxicol **116-117**: 90-101.

Sherratt, P. J. and J. D. Hayes (2001). Enzyme Systems that Metabolise Drugs and Other Xenobiotics, John Wiley & Sons.

Shinogi, M. and S. Maeizumi (1993). "Effect of preinduction of metallothionein on tissue distribution of silver and hepatic lipid peroxidation." Biol Pharm Bull **16**(4): 3.

Shrivastava, S., T. Bera, A. Roy, G. Singh, P. Ramachandrarao and D. Dash (2007). "Characterization of enhanced antibacterial effects of novel silver nanoparticles." Nanotechnology **18**(22): 225103.

Silvester, N. R. and M. A. Sleight (1984). "Hydrodynamic aspects of particle capture by *Mytilus*." Journal of the Marine Biological Association of the United Kingdom **64**(04): 859.

Simmons, J., K. Simkiss, M. G. Taylor and K. E. Jarvis (1996). "Crab biominerals as environmental monitors." BULLETIN-INSTITUT OCEANOGRAPHIQUE MONACO-NUMERO SPECIAL: 225-232.

Singh, C., S. Friedrichs, G. Ceccone, P. Gibson, K. A. Jensen, M. Levin, H. Goenaga Infante, D. Carlander and K. Rasmussen (2014). Cerium Dioxide, NM-211, NM-212, NM-213. Characterisation and test item preparation, Publications Office of the European Union. **2015**.

Smith, J. D. (1942). "A Note on the Morphology and Cytology of the Branchiae of *Carcinus Maenas*." Proceedings of the Royal Irish Academy. Section B: Biological, Geological, and Chemical Science **48**: 105-118.

Smith, V. J. and N. A. Ratcliffe (1980). "Cellular defense reactions of the shore crab, *Carcinus maenas*: in vivo hemocytic and histopathological responses to injected bacteria." Journal of Invertebrate Pathology **35**(1): 65-74.

Snell, T. W. and D. G. Hicks (2011). "Assessing toxicity of nanoparticles using *Brachionus manjavacas* (Rotifera)." Environ Toxicol **26**(2): 146-152.

Studart, A. R., E. Amstad and L. J. Gauckler (2007). "Colloidal stabilization of nanoparticles in concentrated suspensions." Langmuir **23**(3): 1081-1090.

Styrishave, B., A. Agaard and O. Andersen (1999). "In situ studies on physiology and behaviour in two colour forms of the shore crab *Carcinus maenas* in relation to season." Marine Ecology Progress Series **189**: 221-231.

Suresh, A. K., D. A. Pelletier, W. Wang, J. W. Moon, B. Gu, N. P. Mortensen, D. P. Allison, D. C. Joy, T. J. Phelps and M. J. Doktycz (2010). "Silver nanocrystallites: biofabrication using *Shewanella oneidensis*, and an evaluation of their comparative toxicity on gram-negative and gram-positive bacteria." Environ Sci Technol **44**(13): 5210-5215.

Tappin, A. D., J. L. Barriada, C. B. Braungardt, E. H. Evans, M. D. Patey and E. P. Achterberg (2010). "Dissolved silver in European estuarine and coastal waters." Water Res **44**(14): 4204-4216.

Taylor, A. C. (1976). "The respiratory responses of *Carcinus maenas* to declining oxygen tension." Journal of Experimental Biology **65**: 309-322.

Taylor, E. W. and P. J. Butler (1973). "The behaviour and physiological responses of the shore crab *Carcinus maenas* during changes in environmental oxygen tension." Netherlands Journal of Sea Research **7**: 496-505.

Tedesco, S., H. Doyle, J. Blasco, G. Redmond and D. Sheehan (2010). "Exposure of the blue mussel, *Mytilus edulis*, to gold nanoparticles and the pro-oxidant menadione." Comp Biochem Physiol C Toxicol Pharmacol **151**(2): 167-174.

Tedesco, S., H. Doyle, J. Blasco, G. Redmond and D. Sheehan (2010). "Oxidative stress and toxicity of gold nanoparticles in *Mytilus edulis*." Aquat Toxicol **100**(2): 178-186.

Tedesco, S., H. Doyle, G. Redmond and D. Sheehan (2008). "Gold nanoparticles and oxidative stress in *Mytilus edulis*." Mar Environ Res **66**(1): 131-133.

TheSilverInstitute (2016). World Silver Survey 2016: A Summary. T. S. I. T. Reuters: 12.

Thill, A., O. Zeyons, O. Spalla, F. Chauvat, J. Rose, M. Auffan and A. M. Flank (2006). "Cytotoxicity of CeO₂ Nanoparticles for *Escherichia coli*. Physico-Chemical Insight of the Cytotoxicity Mechanism." Environmental Science & Technology **40**(19): 6151-6156.

Tian, J. and J. Yu (2011). "Poly(lactic-co-glycolic acid) nanoparticles as candidate DNA vaccine carrier for oral immunization of Japanese flounder (*Paralichthys olivaceus*) against lymphocystis disease virus." Fish Shellfish Immunol **30**(1): 109-117.

Turner, A., D. Brice and M. T. Brown (2012). "Interactions of silver nanoparticles with the marine macroalga, *Ulva lactuca*." Ecotoxicology **21**(1): 148-154.

Tyler-Walters, H. (2008). "*Mytilus edulis* Common mussel." Marine Life Information Network: Biology and Sensitivity Key Information Reviews Retrieved 23rd February 2016, 2016, from <http://www.marlin.ac.uk/species/detail/1421>.

Um, N., M. Miyake and T. Hirato (2011). "Dissolution of Cerium Oxide in Sulfuric Acid." 165-170.

Vahl, O. (1973). "Pumping and oxygen consumption rates of *Mytilus edulis* L. of different sizes." Ophelia **12**(1-2): 45-52.

Veronese, F. M., P. Caliceti, O. Schiavon and M. Sergi (2002). "Polyethylene glycol-superoxide dismutase, a conjugate in search of exploitation." Advanced Drug Delivery Reviews **54**(4): 587-606.

Vidal-Linan, L., J. Bellas, J. A. Campillo and R. Beiras (2010). "Integrated use of antioxidant enzymes in mussels, *Mytilus galloprovincialis*, for monitoring pollution in highly productive coastal areas of Galicia (NW Spain)." Chemosphere **78**(3): 265-272.

Vig, E. and J. Nemcsok (1989). "The effects of hypoxia and paraquat on the superoxide dismutase activity in different organs of carp, *Cyprinus carpio* L." Journal of Fish Biology **35**(1): 23-25.

Vogt, G. and E. T. Qunitio (1994). "Accumulation and excretion of metal granules in the prawn, *Penaeus monodon*, exposed to water-borne copper, lead, iron and calcium." Aquatic Toxicology **28**(3-4): 223-241.

Volker, C., C. Boedicker, J. Daubenthaler, M. Oetken and J. Oehlmann (2013). "Comparative toxicity assessment of nanosilver on three *Daphnia* species in acute, chronic and multi-generation experiments." PLoS One **8**(10): e75026.

von Moos, N., P. Burkhardt-Holm and A. Kohler (2012). "Uptake and effects of microplastics on cells and tissue of the blue mussel *Mytilus edulis* L. after an experimental exposure." Environ Sci Technol **46**(20): 11327-11335.

Wahie, S., J. J. Lloyd and P. M. Farr (2007). "Sunscreen ingredients and labelling: a survey of products available in the UK." Clin Exp Dermatol **32**(4): 359-364.

Wang, J. and W. X. Wang (2014). "Salinity influences on the uptake of silver nanoparticles and silver nitrate by marine medaka (*Oryzias melastigma*)." Environ Toxicol Chem **33**(3): 632-640.

Wang, T., J. Bai, X. Jiang and G. U. Nienhaus (2012). "Cellular Uptake of Nanoparticles by Membrane Penetration: A Study Combining Confocal Microscopy with FTIR Spectroelectrochemistry." ACS Nano **6**(2): 1251-1259.

Wang, W.-X. (2001). "Comparison of metal uptake rate and absorption efficiency in marine bivalves." Environmental Toxicology and Chemistry **20**(6): 1367-1373.

Ward, E. J. and S. E. Shumway (2004). "Separating the grain from the chaff: particle selection in suspension- and deposit-feeding bivalves." Journal of Experimental Marine Biology and Ecology **300**(1-2): 83-130.

Ward, J. E. and D. J. Kach (2009). "Marine aggregates facilitate ingestion of nanoparticles by suspension-feeding bivalves." Mar Environ Res **68**(3): 137-142.

Watts, A. J., C. Lewis, R. M. Goodhead, S. J. Beckett, J. Moger, C. R. Tyler and T. S. Galloway (2014). "Uptake and retention of microplastics by the shore crab *Carcinus maenas*." Environ Sci Technol **48**(15): 8823-8830.

Watts, A. J., M. A. Urbina, R. Goodhead, J. Moger, C. Lewis and T. S. Galloway (2016). "Effect of Microplastic on the Gills of the Shore Crab *Carcinus maenas*." Environ Sci Technol **50**(10): 5364-5369.

Wegner, A., E. Besseling, E. M. Foekema, P. Kamermans and A. A. Koelmans (2012). "Effects of nanopolystyrene on the feeding behavior of the blue mussel (*Mytilus edulis* L.)." Environ Toxicol Chem **31**(11): 2490-2497.

Wen, L. S., P. H. Santschi, G. A. Gill and D. G. Tang (2002). "Silver concentrations in Colorado, USA, watersheds using improved methodology." Environ Toxicol Chem **21**(10): 2040-2051.

WFDUK (2013). Updated Recommendations on Environmental Standards: River Basin Management (2015-21). UKTAG Environmental Standards Phase 3. U. T. A. G. o. t. W. F. Directive, WFDUK: 80.

Wong, S. W., P. T. Leung, A. B. Djuricic and K. M. Leung (2010). "Toxicities of nano zinc oxide to five marine organisms: influences of aggregate size and ion solubility." Anal Bioanal Chem **396**(2): 609-618.

Wotton, R. S. (2004). "The ubiquity and many roles of exopolymers (EPS) in aquatic systems." Scientia Marina **68**(S1): 13-21.

Xue, Y., Q. Luan, D. Yang, X. Yao and K. Zhou (2011). "Direct Evidence for Hydroxyl Radical Scavenging Activity of Cerium Oxide Nanoparticles." The Journal of Physical Chemistry C **115**(11): 4433-4438.

Yang, X., A. P. Gondikas, S. M. Marinakos, M. Auffan, J. Liu, H. Hsu-Kim and J. N. Meyer (2012). "Mechanism of silver nanoparticle toxicity is dependent on dissolved silver and surface coating in *Caenorhabditis elegans*." *Environ Sci Technol* **46**(2): 1119-1127.

Yazici, H., E. Alpaslan and T. J. Webster (2015). "The Role of Dextran Coatings on the Cytotoxicity Properties of Ceria Nanoparticles Toward Bone Cancer Cells." *Jom* **67**(4): 804-810.

Yu, M., S. Huang, K. J. Yu and A. M. Clyne (2012). "Dextran and polymer polyethylene glycol (PEG) coating reduce both 5 and 30 nm iron oxide nanoparticle cytotoxicity in 2D and 3D cell culture." *Int J Mol Sci* **13**(5): 5554-5570.

Yuan, L., C. J. Richardson, M. Ho, C. W. Willis, B. P. Colman and M. R. Wiesner (2018). "Stress Responses of Aquatic Plants to Silver Nanoparticles." *Environ Sci Technol* **52**(5): 2558-2565.

Zhang, H., Z. Ji, T. Xia, H. Meng, C. Low-Kam, R. Liu, S. Pokhrel, S. Lin, X. Wang, Y. P. Liao, M. Wang, L. Li, R. Rallo, R. Damoiseaux, D. Telesca, L. Madler, Y. Cohen, J. I. Zink and A. E. Nel (2012). "Use of metal oxide nanoparticle band gap to develop a predictive paradigm for oxidative stress and acute pulmonary inflammation." *ACS Nano* **6**(5): 4349-4368.

Zhang, Q., J. Q. Huang, M. Q. Zhao, W. Z. Qian and F. Wei (2011). "Carbon nanotube mass production: principles and processes." *ChemSusChem* **4**(7): 864-889.

Zhang, Y., Y. Chen, P. Westerhoff and J. Crittenden (2009). "Impact of natural organic matter and divalent cations on the stability of aqueous nanoparticles." *Water Res* **43**(17): 4249-4257.

Zhao, C. M. and W. X. Wang (2011). "Comparison of acute and chronic toxicity of silver nanoparticles and silver nitrate to *Daphnia magna*." *Environ Toxicol Chem* **30**(4): 885-892.

Zhornik, E. V., L. A. Baranova, E. S. Drozd, M. S. Sudas, N. H. Chau, N. Q. Buu, T. T. N. Dung, S. A. Chizhik and I. D. Volotovskii (2014). "Silver nanoparticles induce lipid peroxidation and morphological changes in human lymphocytes surface." *Biophysics* **59**(3): 380-386.

Zhu, X., J. Wang, X. Zhang, Y. Chang and Y. Chen (2010). "Trophic transfer of TiO₂ nanoparticles from *Daphnia* to zebrafish in a simplified freshwater food chain." *Chemosphere* **79**(9): 928-933.

Zhu, X., J. Zhou and Z. Cai (2011). "The toxicity and oxidative stress of TiO₂ nanoparticles in marine abalone (*Haliotis diversicolor supertexta*)." *Mar Pollut Bull* **63**(5-12): 334-338.

Zhuang, W. and X. Gao (2014). "Methods, Mechanisms and Typical Bio-Indicators of Engineered Nanoparticle Ecotoxicology: An Overview." *CLEAN - Soil, Air, Water* **42**(4): 377-385.

Zuykov, M., E. Pelletier and S. Demers (2011). "Colloidal complexed silver and silver nanoparticles in extrapallial fluid of *Mytilus edulis*." *Mar Environ Res* **71**(1): 17-21.